USE OF MEMBRANE PROTEINS AS ANTIFUNGAL DRUG TARGETS

Doctor of Philosophy

ASTON
UNIVERSITY

SEPTEMBER 2022

Thesis abstract

Membrane proteins as antifungal drug targets

Alexis Lode
Doctor of Philosophy
Aston University
September 2022

Fungal infections represent a much-overlooked threat that has yet to receive its due consideration. Their invasive branch has an underestimated impact on human morbidity and mortality. Despite this, research on antifungal therapies has been stalling for almost two decades now, while resistant strains have emerged on essentially every class of drugs that has been commercially available.

Therefore, developing ways to counteract this emerging resistance is of paramount importance if we wish to remain capable of treating invasive fungal infections. New classes of drugs using new mechanisms of action would be highly desirable, especially if they are targeting fungal markers that have not been identified as potential targets before.

This thesis project has been carried out in partnership with F2G Ltd, Manchester, UK, regarding the expression of new potential drug targets for antifungal treatments. It focuses on membrane proteins, which are a crucial gateway to the cell and an important source of untargeted markers that could represent very promising alternatives. Two main targets, both enzymatic membrane proteins, have been expressed in *Pichia Pastoris* yeast cells and solubilised using poly (styrene-co-maleic acid) lipid particles or SMALPs, which enables to retain the membrane protein with its surrounding lipids so that the protein stays in its native conformation. This allowed the protein to remain functional, so that a functional assay could be developed later on in order to test its activity. The final step was to test potential antifungal compounds developed by F2G to inhibit the enzymatic reaction, which was the key for the antifungal activity detected in earlier studies by F2G.

Because membrane proteins are much harder to work with than soluble ones, they can sometimes be more difficult to obtain in sufficient amount and purity. Therefore, an attempt at engineering a contaminant-free *P. pastoris* cell line was carried out, with the goal of removing the main contaminant found during membrane protein production and purification.

Keywords: membrane proteins, drug development, SMALPs, functional assay, contaminant elimination

Acknowledgements

First and foremost, I would like to thank my supervisor Dr. Alice Rothnie for having given me the opportunity to pursue my career in a research environment, her continuous help and support during those three years and her involvement in this project.

I would also like to thank my associate supervisors Dr. Alan Goddard and Pr. Roslyn Bill for all the precious advice they have provided throughout my PhD. Their thoughts and ideas have been the corner stone of the achievements I have been able to make.

A special thank you to the examiners for reading my thesis in such a short while and for taking the time to allow me to defend it.

Thank you to Pr. Corinne Spickett and Sarah Smith for the much-required help in mass spectrometry, from sample preparation to data analysis.

Thank you to our collaborators at F2G, and in particular to Jason Oliver, for all the material that was provided as well as the advice that was given throughout this project.

A massive thank you to all the lab members in MB 331, as well as in MB 347, for all the experience shared during these years and the amazing working environment. A particular thank you to Luke Broadbent for the help in my first month with handling yeast cultures. Another particular thank you to Dr. Philip Kitchen and Thanos Kesidis for the help with various questions and techniques about yeast I have been asking throughout my project.

Thank you also to all the office members for making each day brighter, and especially to all the Memtrainees as well as Ellen for all the support and assistance that you have all provided.

A very special thank you to my colleague and friend Annaïg, for making this whole journey so much more enjoyable, for all the mental support and for all the things we have shared during those three years and all the years we have known each other before that.

I would like to thank my parents, brother and sister for always believing in me and pushing me to pursue my dreams, even when I think they may not be reachable. Of course, thank you to my partner Ervan for making up with my bad moods whenever I would come back

from work frustrated from unsuccessful experiments, and for trying to understand all the incomprehensible science I would try to explain.

Finally, I would like to thank the European Union for the funding that allowed this project to exist in the first place, within the Horizon 2020 research and innovation programme under the Marie Sklodowska-Curie grant agreement No 847419.

Table of Contents

List of figures

Chapter 1: Introduction

Chapter 3: SdeA

Chapter 4: Removal of stubborn contaminant

Chapter 5: Activity assays

Chapter 6: DHODH

Chapter 7: Discussion

List of tables

Chapter 6: DHODH

List of abbreviations

ABC = ATP-binding cassette
AIDS = Acquired immune deficiency syndrome
AOX = Alcohol oxidase
APS = Ammonium persulfate
ATP = Adenosine triphosphate
BCA = Bicinchoninic acid
BMGY = Buffered glycerol complex medium
BMMY = Buffered methanol complex medium
BSA = Bovine serum albumin
CAI = Codon adaptation index
CD = Cluster of differentiation
CDC = Centers for disease control and prevention (USA)
CMC = Critical micelle concentration
CoA = Coenzyme A
COVID = Coronavirus disease
CS = Cutsmart
CytbrR = cytochrome b5 reductase or dehydrogenase
DDM = Dodecyl-β-D-maltoside
DG = n-dodecyl-β-D-glucopyranoside
DIBMA = Diisobutylene-maleic acid
DLS = Dynamic light scattering
DNA = deoxyribonucleic acid
DHODH = Dihydroorotate dehydrogenase
DTT = Dithiothreitol
EDTA = Ethylene diamine tetraacetic acid
EGTA = Ethylene glycol tetraacetic acid
ER = Endoplasmic reticulum
FAD = Flavin adenine dinucleotide
FMN = Flavin mononucleotide
FT = Flow-through
GPCR = G-protein coupled receptor
GRAVY = Grand average of hydropathy
HEPES = 4-(2-hydroxyethyl)-1-piperazineethanesulfonic acid

HPLC = High-performance liquid chromatography
HSCT = Hematopoietic stem cell transplant
HRP = Horseradish peroxidase
IA = Invasive aspergillosis
IAA = Iodoacetamide
IC50 = Half maximal inhibitory concentration
IPTG = Isopropyl β-D-1-thiogalactopyranoside
IFI = Invasive fungal infections
LB = Lysogeny broth
LC/MS = Liquid chromatography/Mass spectrometry
LMNG-CHS = lauryl maltose neopentyl glycol with cholesteryl hemisuccinate
mADH = mitochondrial alcohol dehydrogenase isoenzyme III
MALDI = Matrix-assisted laser desorption/ionization
MDR = Multidrug resistance
MIC = Minimum inhibitory concentration
MFS = Major facilitator superfamily
MGY = Minimal glycerol medium
MOPS = (3-(N-morpholino)propanesulfonic acid)
NAD = Nicotinamide adenine dinucleotide
NF-κB = Nuclear factor kappa-light-chain-enhancer of activated B cells
Ni-NTA = Nickel nitrilotriacetic acid
(d)NTP= (Deoxy)nucleoside triphosphate
OD = Optical density
OG = n-octyl-β-D-glucopyranoside
ORNG = Oxidative release of natural glycans
PAGE = Polyacrylamide gel electrophoresis
PCR = Polymerase chain reaction
PDB = Protein data bank
PDR = Pleiotropic drug resistance
pH = potential for hydrogen
pI = Isoelectric point
PVDF = Polyvinylidene fluoride
RNA = Ribonucleic acid
ROS = Reactive oxygen species
SCD1 = Stearoyl-CoA desaturase 1
SdeA = Stearoyl-CoA desaturase
SDS = Sodium dodecyl sulphate

SEC = Size exclusion chromatography

SMA = Styrene maleic acid

SMALP = Styrene maleic acid lipid particle

SOB = Super optimal broth

TAE = Tris acetate-EDTA

TBS = Tris-buffered saline

TBS-T = Tris-buffered saline with Tween

TCA = Trichloroacetic acid

TEMED = Tetramethylethylenediamine

TM = Transmembrane

TNF = Tumour necrosis factor

TOF = Time of flight

v/v = volume / volume

w/v = weight / volume

WB = Western blot

WHO = World Health Organization

YNB = Yeast nitrogen base

YPD or YEPD = Yeast extract peptone dextrose

YPDS = Yeast extract peptone dextrose with sorbitol

1. Introduction

1.1 General fungal infection

1.1.1 Epidemiology

Fungal infections are a type of disease caused by eukaryotic microorganisms called fungi. They range from superficial infection of the skin and nails (25% of the population affected worldwide (Brown *et al.* 2012)) to invasive fungal infections (IFI). The latter is much less common than the previous category, but it is a much higher concern since it is associated with a surprisingly high mortality rate. Indeed, an estimated one and a half to two million people die each year from these diseases, which would mean they are at least as much, if not more lethal infections than malaria or tuberculosis (Brown *et al.* 2012), the latter being ranked in the top 10 of the deadliest diseases in the world (WHO 2020). Most of these deaths can be imputed to four different families of fungi: *Cryptococcus*, *Candida*, *Aspergillosis* and *Pneumocystis* (Denning and Bromley 2015). The incidence of fungi-related diseases has largely increased in the past decades due to the rise of patients showing immunodeficiency, which can be caused by direct intervention (during organ transplants) or not (diseases like AIDS, certain types of cancer) (Brown *et al.* 2012). In 2014, *Candida spp.* alone were found to be the 4th most common isolate of bloodstream infections in many countries (Oren and Paul 2014). Invasive aspergillosis are the second most common type of IFI (Oren and Paul 2014), but can be even more frequent than invasive candidiasis in some conditions (Pagano *et al.* 2006). Recently, many cases of mucormycosis have been observed in patients previously diagnosed with COVID-19, and who were also suffering from diabetes (Hoenigl *et al.* 2022). This is an example of the fact that IFIs are particularly dangerous for people already showing health conditions.

1.1.2 Existing treatments

Three main classes of drugs have been developed against these different IFIs. The azoles are heterocyclic compounds containing two to three atoms of nitrogen (Table 1.1). They were discovered in the late 1960s and developed in the 1980s. The first azoles developed contained an imidazole ring (two atoms of nitrogen) but showed concerning liver toxicity as well as other drug-specific toxicities, which is why they were formulated only for topical use (Ostrosky-Zeichner *et al.* 2010). The second class of azoles developed were the triazoles (three atoms of nitrogen), during the 1990s, for which there was an improvement in both

efficiency and lower toxicity of the drugs. They present a good oral absorption but are also available for intravenous use (Waller 2018).

Fluconazole	Posaconazole
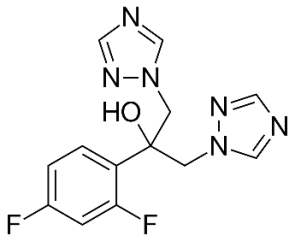	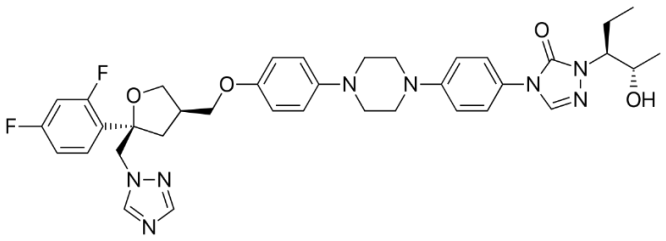
Voriconazole	Ketoconazole
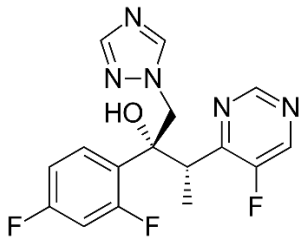	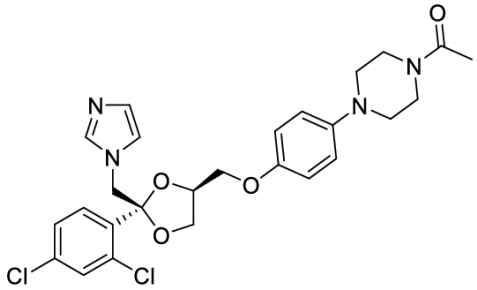

Table 1.1: Chemical structures of widely used azole drugs. *Fluconazole, posaconazole and voriconazole are triazoles used to treat IFIs such as candidiasis, aspergillosis or cryptococcosis. Ketoconazole is an imidazole-based drug used to treat local fungal skin infections. The triazole group is preferred to the imidazole one because it enhances the specificity for the fungal version of the target. The extra methyl group in voriconazole enhances the hydrophobic interaction with the target. Similarly, the difluorophenyl substituent is also now preferred to the dichlorophenyl one.*

Azoles function by inhibition of ergosterol synthesis, which is the major sterol found in fungal membranes instead of cholesterol (Figure 1.1A), thus leading to membrane lysis and the death of the fungal organism. Its presence in fungi and absence in human cells make ergosterol a very interesting drug target for specificity. Thanks to their azole ring which forms a stoichiometric complex with the haem iron of lanosterol 14α-demethylase (Hitchcock 1991), a form of cytochrome P-450 called cyp51a, triazoles are specifically targeting this 14α-demethylase which is the enzyme that catalyses the demethylation of lanosterol into a major precursor for many sterols in fungi, including ergosterol (Figure 1.1B) (Lepesheva and Waterman 2007). The accumulation of 14α-methyl-sterols may disrupt the close packing of acyl chains of phospholipids, but it can also impair the function of some membrane-bound proteins such as ATPases and enzymes from the respiratory chain on the mitochondrial membrane, thus leading to an arrest of the growth (Brunton, Lazo, and Parker 2005).

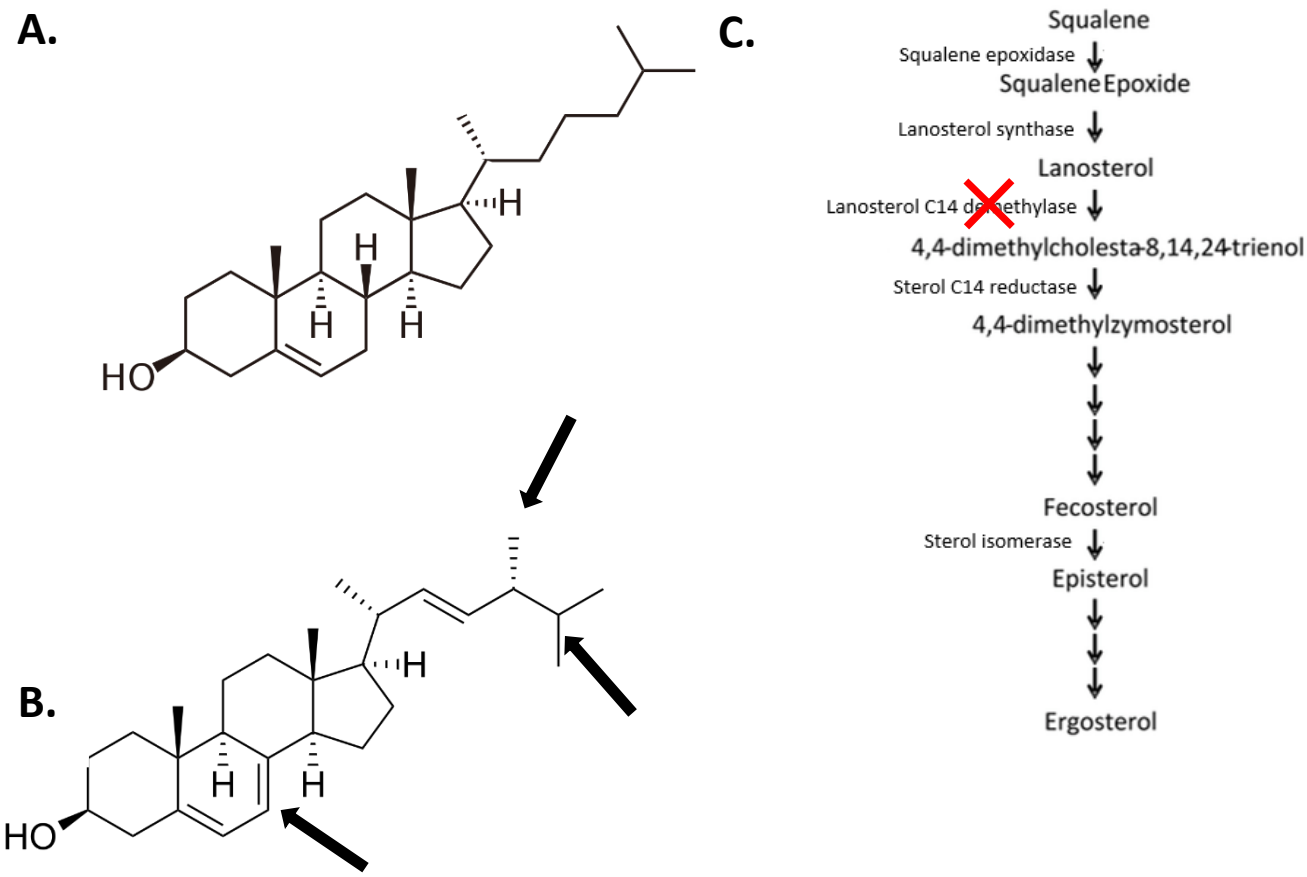

Figure 1.1: A. and B. Comparison of the structures of cholesterol (A.) and ergosterol (B.). *Their biggest structural differences are the presence of two extra double bonds and one methyl group on the ergosterol structure (black arrows). C. Representation of the action of azoles on the ergosterol synthesis pathway.*

This happens via the metabolism of these methylsterols into a 14α-methyl-3,6-diol compound, via a Δ5-6 desaturase, that will have the toxic effects in the cell (Hu *et al.* 2018). Moreover, the fungal plasma membrane depleted from ergosterol is more likely to be subject to further damage on several membrane bound enzymes, including nutrient transport or chitin synthesis enzymes (Barrett-Bee, Newboult, and Pinder 1991) as well as growth and proliferation enzymes (Nes *et al.* 1993). During human treatment, adverse effects usually occur during prolonged exposure to high doses of the drug. They usually range from nausea and vomiting towards hepatic dysfunctions (Brunton, Lazo, and Parker 2005). Most adverse effects are dose-dependent and reversible (Zonios and Bennett 2008).

The second class of antifungal drugs is the polyenes, amongst which can be found amphotericin B, nystatin or natamycin (Table 1.2).

Amphotericin B	
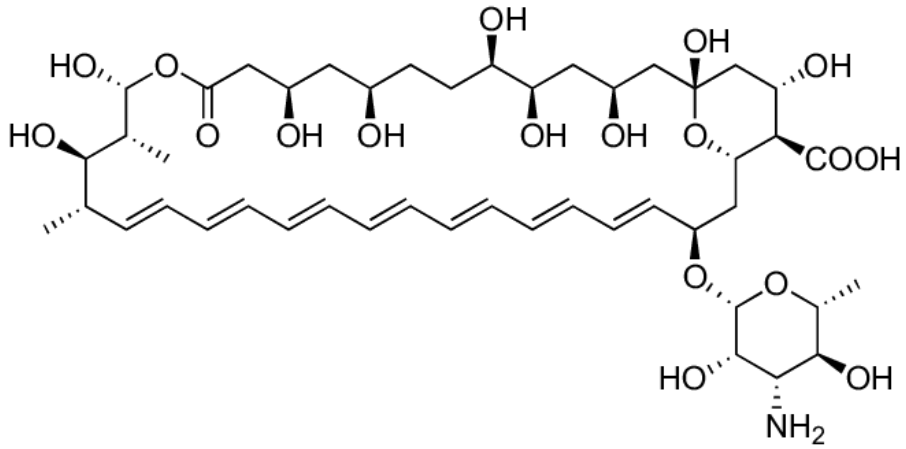	
Nystatin	Natamycin
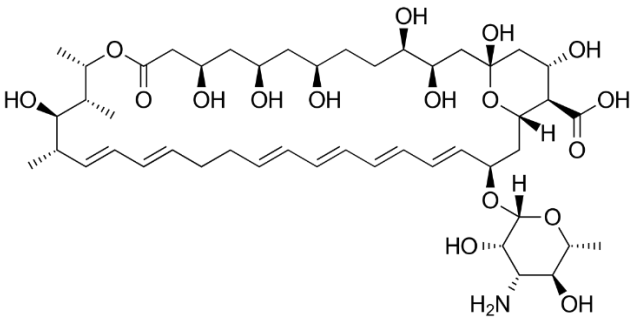	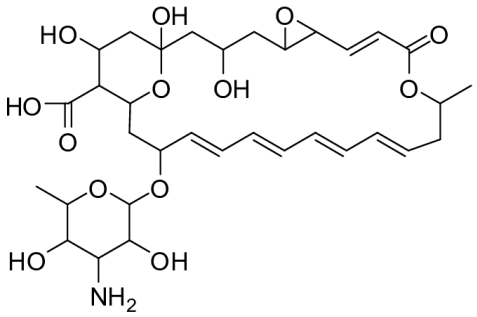

Table 1.2: Chemical structure of three of the most widely used polyene drugs. *They are characterised by one hydrophilic and one hydrophobic side, and an aminosugar residue.*

Amphotericin B is the main drug of the polyene family and was first developed in 1959. It acts by binding strongly to the ergosterol in the fungal membrane and leads to the formation of hydrophilic pores (Gruszecki *et al.* 2003) that will eventually cause a loss of monovalent cations, a disruption of the active membrane transport dependent on membrane potential, a depolarisation of the cell and its death . Moreover, amphotericin B leads to an increase in macrophage activity, leading to the fungal cells clearance, by inducing the formation of reactive oxygen species (Wilson, Thorson, and Speert 1991) and thus oxidative stress within the membrane. It also stimulates the phagocytic activity nearby by stimulating the production

of cytokines such as interleukin 1 or tumour necrosis factor alpha (TNF-α) (Noor and Preuss 2020; Chia and McManus 1990; Tokuda *et al.* 1993). The local upregulation of the immune system can however lead the patient to experience fever periods. Other antifungal drugs from the polyene family include nystatin (which was the first treatment developed against IFIs in the early 1950s) and natamycin, which can be used to treat respectively mucous membrane infections or eye infections. They are both used topically only as their side effects are too severe (Waller 2018). Indeed, polyenes are capable of binding cholesterol as well as ergosterol, meaning they are capable of destroying the host cells very easily, particularly in the kidneys. This can be explained through their affinity for lipids, which means that they can be incorporated in plasma low density lipoproteins (Brajtburg *et al.* 1984) that will be collected by renal epithelial cells, hence the increased damage on this organ. Their greater affinity for ergosterol compared to cholesterol only comes from the presence of a double bond on carbon 22 of ergosterol (Figure 1.1a) (Cybulska *et al.* 1986). Amphotericin B is the only polyene drug used systemically as it is the only one that was formulated in nanoparticular complexes such as liposomal spheres, in the 1990s (Hamill 2013). This new type of formulation greatly decreased the nephrotoxic effects traditionally observed upon the use of this family of drugs, and enabled an increase in the concentration of drug used for a better efficiency (Seyedmousavi *et al.* 2013). The lipids used in those formulations are usually phospholipids rather than sterols, in order to prevent the drug release via disruption of the sterol membrane (Barratt and Bretagne 2007).

Finally, a fourth class of antifungal drugs developed is composed of echinocandins (caspofungin, micafungin, anidulafungin) that were discovered in the 1970s (Table 1.3), first as fermentation products from pneumocandins. They were later modified in order to improve their properties into the three molecules that we now know (Patil and Majumdar 2017). These three molecules noncompetitively inhibit the β-(1,3)-D-glucan synthase, which is an essential component of the cell wall synthesizing β-glucan, which plays an important role in the resistance against osmotic forces. Its absence thus leads to osmotic instability and cell lysis (Beauvais and Latge 2001; Brunton, Lazo, and Parker 2005; Wiederhold and Lewis 2003).

Caspofungin	Micafungin
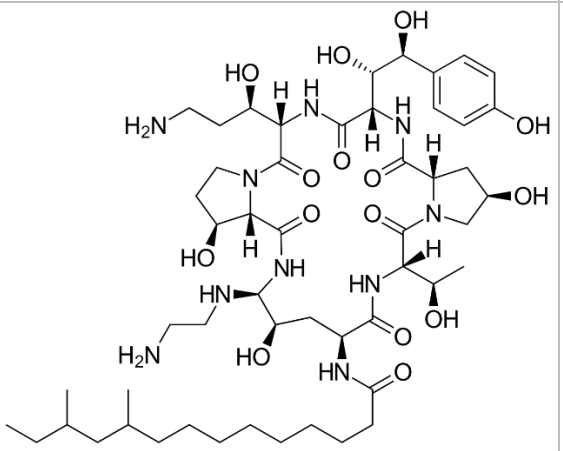	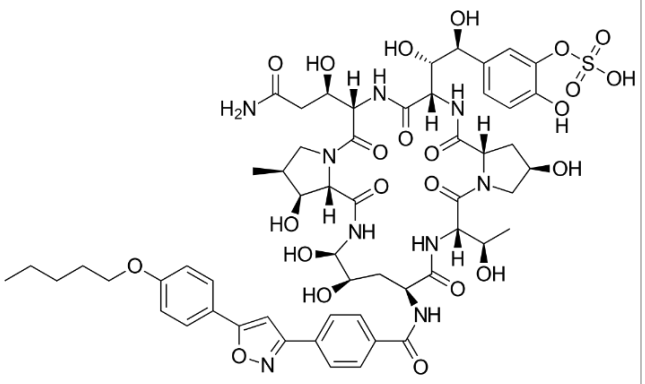
Anidulafungin	
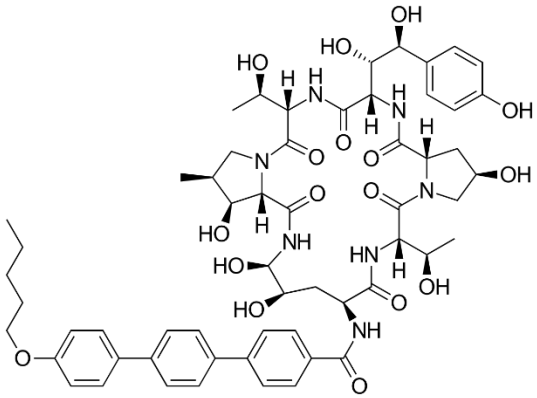	

Table 1.3: Chemical structures of the three main drugs developed in the family of echinocandins. *Their structure is overall very similar, with a cyclic peptidic core and a lipid chain in the bottom. They only differ by their hydrophobic tail, slightly different hydroxylation patterns and a few different functions added (amine, amide or sulphate).*

β-(1,3)-D-glucan synthase is an attractive target as it is not present in the mammalian cells (Morris and Villmann 2006). The interesting point of this target is that, opposite to sterols for the previous drugs, there is no human equivalent for this protein, as cell wall is absent from mammalian cells. It is also known that any disruption in the cell wall's organisation or metabolism significantly affects growth (Debono and Gordee 1994). Fewer adverse effects are reported for this class of drugs and mostly originate from the mode of injection. Indeed, histamine-mediated reactions were spotted during the infusion of the drug, which quickly disappeared after stopping the infusion. There is also a risk of liver toxicity (Morris and Villmann 2006). Echinocandins were shown to have an efficiency comparable to that of triazoles (Wang, Xue, *et al.* 2015) or polyenes (Mora-Duarte *et al.* 2002), with anidulafungin

being sometimes even more efficient. One of the biggest disadvantages of this class of drugs resides in their cost (Neoh *et al.* 2011), which limits their use to patients who show resistance to other drug families (Morris and Villmann 2006). Anidulafungin was, however, shown as cost-effective by several studies (Grau *et al.* 2013; Neoh *et al.* 2017). Another issue is their absence of oral bioavailability, mostly due to their large molecular weight and their cyclic peptidic core, which means they are quickly degraded in the gastrointestinal tract. Therefore, they can only be administered via intravenous injection (Chang, Slavin, and Chen 2017).

A fourth class of drugs called pyrimidine analogues can be described. These molecules can be incorporated in RNA and DNA sequences, therefore destabilizing their structure and leading to growth arrest (Sanglard 2016). They are used as pro-drugs (such as flucytosine) that only fungal organisms are able to metabolise into pyrimidine analogues (such as 5-fluorouracil, which in turn will compete with uracil for their incorporation into fungal RNA for example) (Figure 1.2). Indeed, the enzyme catalysing this reaction is a cytosine deaminase. It is present in both fungi and bacteria but is absent from mammalian cells (Szary, Missol, and Szala 1998). Still, pyrimidine analogues may have side effects on the bone marrow, leading to leukopenia or thrombocytopenia (Brunton, Lazo, and Parker 2005). Due to the rapid emergence of resistance, it is primarily used in combination therapy, often with amphotericin B (Spitzer, Robbins, and Wright 2017; Oliver *et al.* 2016).

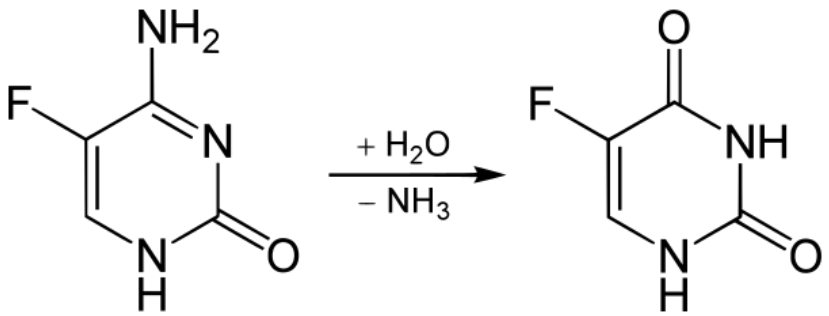

Figure 1.2: Conversion of 5-fluorocytosine (flucytosine) into 5-fluorouracil.

1.1.3 Issues with the antifungal drug development pipeline

There has not been any major new class of antifungal drugs developed in the last two decades, and not a single new molecule was added to the therapeutic arsenal in the last 15 years (Figure 1.3).

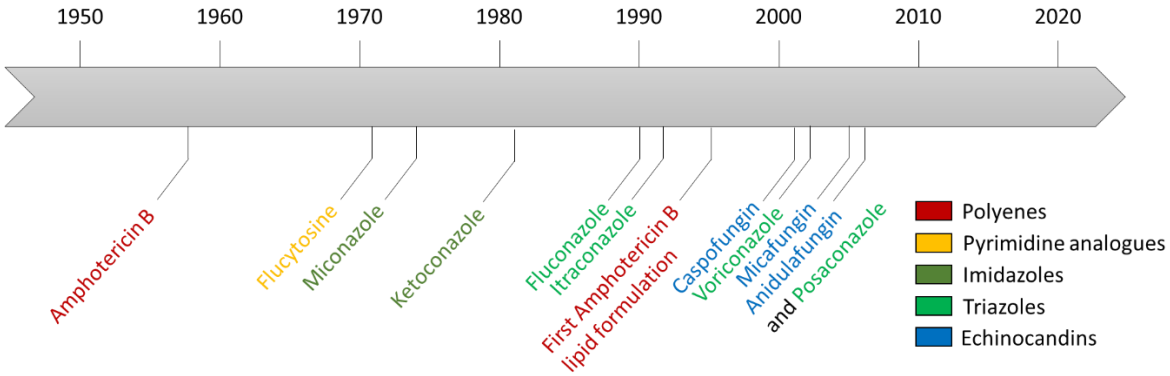

Figure 1.3: Availability dates of the main antifungal treatments still in use today. *A clear acceleration of the discovery process can be observed from the 1990s but there has been no significant improvement of the situation since 2006.*

The important prevalence of invasive fungal infections in developing countries, compared to developed countries, can explain why the efforts of drug discovery research have not been up to the challenge in this field. As an example, *Pneumocystis jirovecii* pneumonia is mostly found in countries in Africa, Central and South America or Asia (Table 1.4). Therefore, pharmaceutical industries are less willing to spend tremendous amounts of money on research to cure diseases mostly in countries that cannot afford them.

Another important problem comes from the lack of *in vitro-in vivo* correlation during drug development for antifungals (Lakhani, Patil, and Majumdar 2019). Indeed, many fungal strains can be responsible for the same IFIs, and it can be difficult to develop antifungals that provide a good potency against each of them. Susceptibility testing often suffers from small sample size, non-uniformity of data reported on MIC (minimum inhibitory concentration) or focus on one particular species (Maharana *et al.* 2016).

Country (Reference)	Burden	Rate/100,000	Assumptions
Nigeria [62]	74,595	48.2	40% of new AIDS cases in children and 10% in adults
Kenya [75]	17,000	43.0	10% in HIV with CD4 < 200
Trinidad and Tobago [79]	400	30.0	80% of HIV patients with CD < 200
Tanzania [78]	9600	22.0	10.4% of adults living with HIV
Ukraine [80]	6152	13.5	60% of HIV patients
Jamaica [74]	350	13.0	255 in HIV HAART naïve
Senegal [133]	1149	8.2	22% of new AIDS
Uzbekistan [63]	165	5.37	60% of HIV with CD < 200
Guatemala [73]	722	4.7	4.7% in HIV patients
Peru [77]	1447	4.6	13% in AIDS
Mexico [76]	5130	4.5	24% in HIV
Chile [67]	766	4.3	35% of new HIV cases
Nepal [121]	990	3.6	16.7% of new AIDS case in children and 22.4% of adults

Table 1.4: Estimated burden of Pneumocystis jirovecii pneumonia according to countries. *Table taken from (Bongomin* et al. *2017).*

Discovering new drug targets is quite a challenge because fungi are eukaryotic organisms, thus genetically much closer to human than bacteria or viruses (Figure 1.4). Therefore, it is much more difficult to find a potential target that will not have an equivalent in human cells that could lead to side effects (Ibrahim *et al.* 2020; Chanumolu, Rout, and Chauhan 2012). The research is partly focused on finding new targets that will be specific to fungal cells. This is especially the case for the fungal cell wall, which is easily accessible, but also some metabolic pathways, including the glyoxylate pathway, the pyrimidine biosynthesis pathway or the cytochrome P450 enzymes amongst others (McCarthy *et al.* 2017).

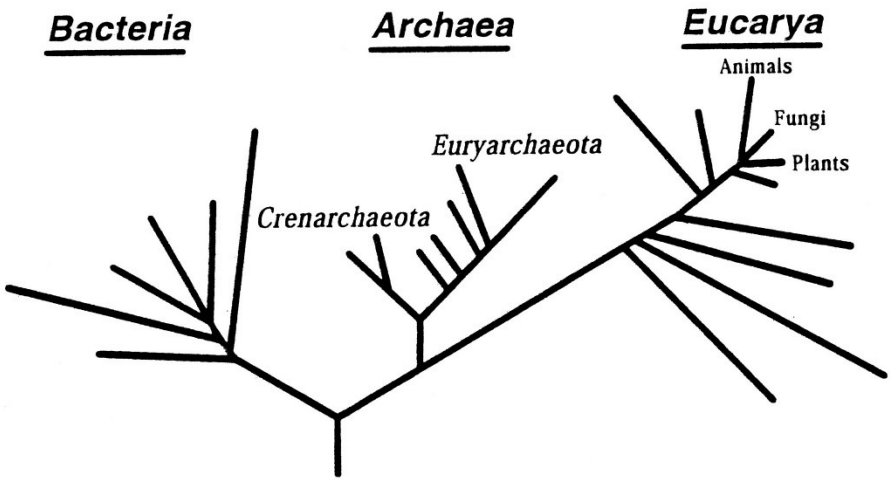

Figure 1.4: Phylogenetic tree of life classified according to ribosomal RNA sequences (Woese 2000).

1.1.4 Resistance

These three classes of drugs showed interesting outcomes when they were first developed but the research in this field has greatly slowed down since the 1990s, with no interesting therapeutic alternative developed since. Furthermore, all of them show drug- or class-specific toxicities as well as increasingly widespread resistance (Sanglard 2016; McCarthy *et al.* 2017). Indeed, some strains of fungi have a natural resistance for certain drugs, such as the *Aspergilli spp.* for fluconazole (Leonardelli *et al.* 2016; CDC). Resistance can also be acquired during prolonged treatment in proper or improper use (Shah *et al.* 2012; Lortholary *et al.* 2011). Moreover, there are already some strains today that are showing resistance to all three main classes of drugs, as seen in *C. auris* (Ostrowsky *et al.* 2020; Rhodes and Fisher 2019) or *A. fumigatus* (Verweij *et al.* 2020).

Fungal organisms develop resistance through three main mechanisms: decrease of effective drug concentration, drug target alterations or metabolic bypasses (Figure 1.5) (Sanglard 2016; Fisher *et al.* 2022; Berman and Krysan 2020).

(1) The decrease of effective drug concentration happens via four different methods:

a. The expulsion of the drug from the cell using active efflux transporters involves two major families in fungal organisms: the ATP-binding cassette (ABC) transporters and the major facilitator superfamily (MFS) transporters. Both actively eject antifungal drugs out of the cells, using respectively ATP hydrolysis energy or the electrochemical proton-motive force. More specifically, within the ABC transporters family, the pleiotropic drug resistance (PDR) transporters are the ones involved in azole treatment resistance (James *et al.* 2021; Whaley *et al.* 2018).

b. The overexpression of the drug target is a second possible method, making it impossible for the drug to saturate its target without tremendously increasing the drug intake. In this particular case, as seen before, drug toxicities related to their concentration prevent the investigation of this option. This type of resistance is particularly observed in azole-resistant strains, and is suspected to derive from the extensive use of azoles in agriculture (Vermeulen, Lagrou, and Verweij 2013).

c. The decrease of effective drug target concentration can be a consequence of the sequestration of the drug in extracellular compartments, made from biofilms. Fungal organisms, and particularly *Candida* and *Aspergillus* species, are capable of producing biofilms in the extracellular matrix (Mitchell *et al.* 2015). This type of resistance has been observed for azoles, polyenes and pyrimidine analogues (Desai, Mitchell, and Andes 2014).

d. Finally, the decrease of effective drug concentration can happen when the pro-drug is not metabolised into an active drug. This is particularly the case for pyrimidine

analogues, which are produced as pro-drugs to decrease their toxicity for the host's cells. It can happen when there is a mutation in the fungal enzyme supposed to metabolise the pro-drug into an active drug (Hope *et al.* 2004).

(2) The second type of mechanism for antifungal resistance relies on alterations of the drug target. The target will still be able to perform its function, although its affinity for the drug is largely decreased. This mechanism applies to enzyme targets such as lanosterol 14α-demethylase (Lamb *et al.* 2000) and β-(1,3)-D-glucan synthase (Morris and Villmann 2006). While the former seems to affect differently each type of azole drugs, with posaconazole being less affected than fluconazole (Sanglard and Coste 2016), the latter seems to affect all of the echinocandins. This kind of resistance can be due to enzymes that present a natural polymorphism enabling decreased affinity for the drugs (Cowen *et al.* 2014; Macedo *et al.* 2021), or to potential acquired mutations, e.g. R467K in lanosterol 14α-demethylase (Lamb *et al.* 2000).

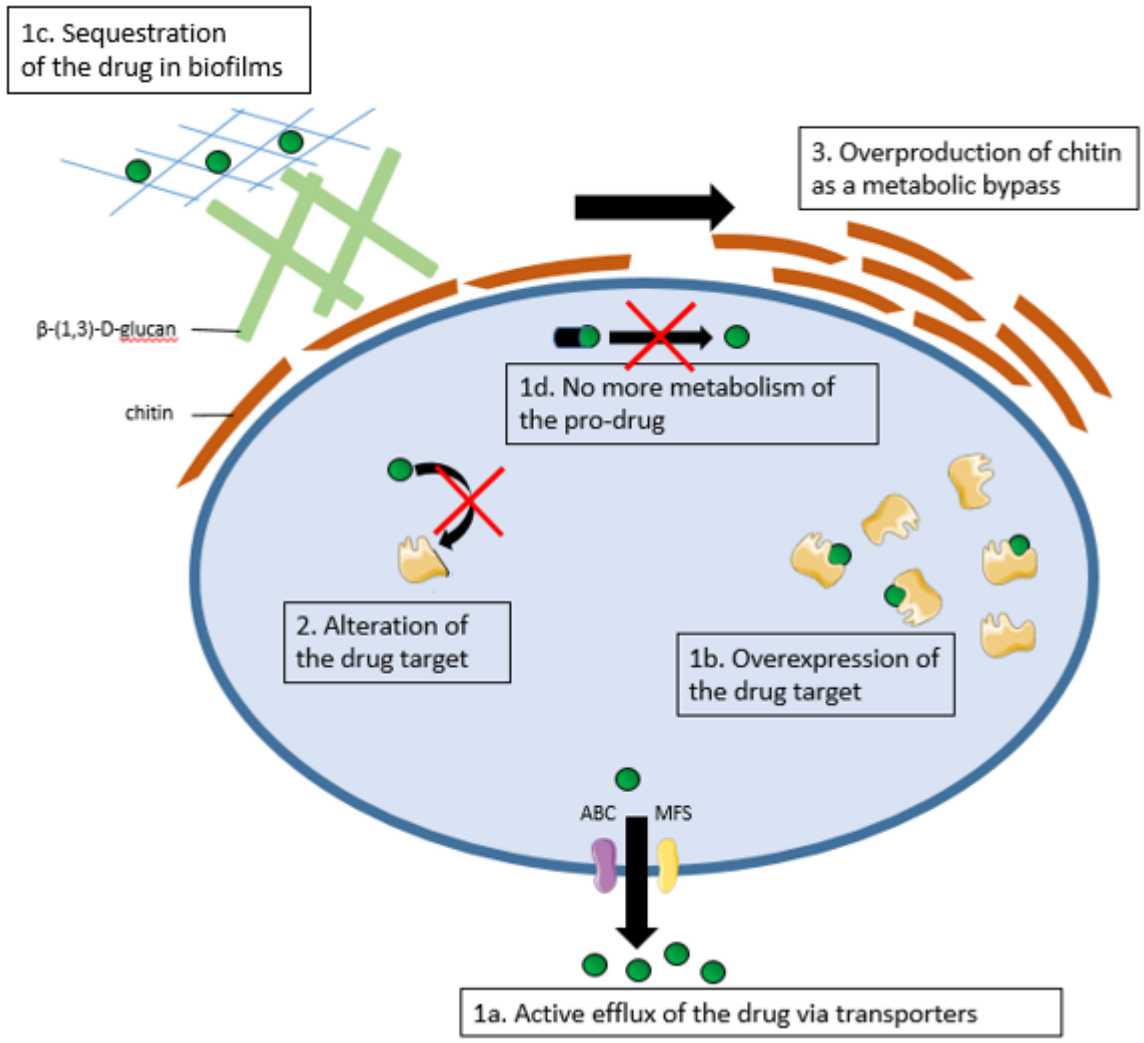

Figure 1.5: Representation of the mechanisms of resistance exhibited by fungal cells in order to overcome antifungal treatment.

(3) Finally, the last mechanism for antifungal resistance resides in the use of metabolic bypasses. They consist in compensatory mechanisms in order to decrease the consequences of the drug's activity. During polyene treatment, a synthetic production of alternative sterols that will replace ergosterol within the membrane can happen, leading to the loss of toxic effects from polyene treatment (Waller 2018). For echinocandins, overexpression of other cell wall components such as chitin can take place in order to counterbalance the lack of β-(1,3)-D-glucan (Walker, Gow, and Munro 2010). Finally, in azoles, a loss-of-function mutation can occur in the enzyme that converts the 14α-methylsterols into 14α-methyl-3,6-diol, leading to the absence of the toxic effects of this compound on the fungal cell (Kelly *et al.* 1995).

In order to overcome the issue of resistance-developing fungal strains, new strategies are being developed during drug development processes. They include systems of drug delivery allowing higher local drug concentrations, the calculation of potential resistance emergence as well as the use of chronic aspergillosis and acute candidiasis models or *in vitro* systems that better replicate the *in vivo* environment (Fisher *et al.* 2022). These leads are the main drivers for tackling the emergence of resistant fungal strains nowadays.

1.2 *Aspergillus fumigatus*

A. fumigatus is a saprotrophic fungal organism. It is the most common aerial fungal pathogen to cause diseases, including the fatal invasive aspergillosis in individuals with immunodeficiency (Fang and Latge 2018). It is mostly found in soil and decaying organic matter, where it plays an important role in carbon and nitrogen recycling (Fang and Latge 2018).

1.2.1 Virulence factors

It is a strong pathogen with a high thermoresistance, as growth was observed between 12 and 65 ˚C (Kozakiewicz and Smith 1994). It is also resistant to a wide range of pH between 2.1 and 8.8 (Jensen 1931). This resistance to harsh environmental conditions makes it one of the most importantly found fungal organism in self-heating composts and heaps of decaying matter (Jensen 1931). It also presents more defence mechanisms such as ABC transporter efflux pumps than other closely related fungi (Nierman *et al.* 2005), as well as oxidation stress response thanks to the presence of glutathione transferases (Burns *et al.* 2005), catalases and superoxide dismutases (Abad *et al.* 2010).

A. fumigatus replicates via sporulation, and its spores (known as conidia) are even more thermoresistant than the organism itself (Kwon-Chung and Sugui 2013). They are found everywhere in the environment, which is why it is believed everybody inhales several hundred spores every day. These spores are highly dispersible thanks to an important hydrophobicity and are protected from ultraviolet irradiation through the presence of a melanin-derived pigment in their cell wall (Brakhage and Liebmann 2005). The gene responsible for the production of this pigment would also be involved in the pathogen's evasion to the immune system, as a mutant strain producing pigmentless conidia has been shown to be far more sensitive to reactive oxygen species (ROS) and to damage by macrophages (Brakhage and Liebmann 2005). This would be due to the pigment being able to scavenge ROS (Jahn *et al.* 1997; Langfelder *et al.* 1998). The spores are capable of reaching lower airways in the lungs thanks to their small size (Kwon-Chung and Sugui 2013), and they are more likely to adhere to extracellular matrix proteins (presumably fibronectin) in the lung thanks to a large amount of negatively charged carbohydrates on their surface (such as sialic acid) (Wasylnka, Simmer, and Moore 2001). Nutrients are believed to be taken from destroyed cells of the host through the release of a proapoptotic mycotoxin called gliotoxin, found in the sera of infected patients and targeting the NF-κB pathway (Sugui *et al.* 2007; Hof and Kupfahl 2009). This toxin is a small, hydrophobic nonribosomal dipeptide that belongs to the epipolythiodioxopiperazines family. It exerts toxicity on cells from the immune system, particularly phagocytic cells and T-lymphocytes (Bruns *et al.* 2010) by preventing the production of superoxide compounds from immune cells that help destroy infecting microorganisms, thus slowing down the immune reaction. However, its primary function is to allow the fungal organism to compete with other microorganisms in its ecological niche (Gardiner, Waring, and Howlett 2005). Other examples of mycotoxins produced by *A. fumigatus* include fumiglacavine C, aurasperon C, helvolic acid or fumagillin (Rementeria *et al.* 2005).

The pathogenic features of this microorganism are also believed to be found in the production of a number of indolic alkaloids with antimitotic properties. This has also led to the development of a class of anticancer drugs known as tryptostatins (Cui, Kakeya, and Osada 1996).

Altogether, many virulence factors can explain the important mortality triggered by *A. fumigatus*. Although it generally cannot overcome the action of the immune system in healthy patients, it is more likely to become pathogenic in patients showing immunodeficiency, causing a wide range of pulmonary infections known as aspergillosis, such as allergic bronchopulmonary aspergillosis, aspergilloma or invasive aspergillosis (IA), the latter being the leading cause of death from infections related to this microorganism.

1.2.2 Pathophysiology of invasive aspergillosis

IA is the main form of complication of fungal *Aspergilli spp*. infections. As the number of immunosuppressed people is constantly increasing, more people are at risk of developing such infections. Furthermore, IA is a disease difficult to diagnose, particularly in early stages (Latge 1999), and with limited therapy options (Kontoyiannis and Bodey 2002). Four types of IA have been described according to the organ that is infected: acute or chronic pulmonary aspergillosis (most common one), tracheobronchitis, acute invasive rhinosinusitis and disseminated disease involving other organs. The clinical features of the disease depend on the organ that is infected, although they mostly involve respiratory consequences. More specifically, pulmonary aspergillosis is characterized by hyphal invasion and destruction of pulmonary tissue. Other symptoms can include pleuritic chest pain, high-grade fever (depending on the patient's immune system's viability), haemoptysis or pulmonary infiltrates. They have been reviewed by several papers twenty years ago (Denning 1998; Oren and Goldstein 2002), or more recently (Ledoux *et al.* 2020). The variability of these symptoms, as well as the lack of an efficient method for diagnosis, make IA a difficult disease to tackle. The best method for diagnosis is the combination of different methods, including computed tomography or antigen detection (Latge 1999). As it is often confused with bacterial infection, fever resistant to antibiotic can also be a good indicator for IA (Ledoux *et al.* 2020). Other methods exist but they all show inaccuracies, including the failure of detection of early-stage infiltrates in radiography or the wrong results of biopsy tissue cultures. This can be due to either the culture being contaminated by the environment in false positives, or the fungal organism not growing in culture because of the presence of antifungal drugs in the host's organism in false negatives (Oren and Goldstein 2002; Latge 1999).

More recently, invasive pulmonary aspergillosis has been observed in patients suffering from COVID-19, after they had been treated with azithromycin, which has an established immunomodulatory effect (Delliere *et al.* 2020). Increased mortality was observed in patients who developed IA.

1.2.3 Epidemiology of *A. fumigatus*

Most of the time, the microorganism is quickly eliminated by the immune system. However, as immunocompromised patients are more at risk, and as immunosuppressive treatments are increasingly used to cure diseases such as autoimmune ones, more and more patients are susceptible to be infected by this microorganism. It is estimated to cause over

600,000 deaths annually, with a mortality rate ranging between 25 and 90% (Brown *et al.* 2012; Gsaller *et al.* 2016; Denning and Bromley 2015). *Aspergillus* infections are the most common microbial infections in hematopoietic stem cell transplant (HSCT) recipients (Kontoyiannis *et al.* 2010).

1.2.4 Resistance mechanisms in *A. fumigatus*

This organism shows several of the resistance mechanisms described before. Amongst them can be found the overexpression of drugs efflux transporters, as the genome of *A. fumigatus* was predicted to contain at least 49 ABC and 278 MFS transporter genes (Lamping *et al.* 2010; Kovalchuk and Driessen 2010; Chamilos and Kontoyiannis 2005). Several specific transporters were shown to be upregulated in azole-resistant strains such as ABC transporters AtrF (Slaven *et al.* 2002) and AfuMDR4 (Nascimento *et al.* 2003), or MFS transporter AfuMDR3 (Nascimento *et al.* 2003). *A. fumigatus*' resistance mechanisms are also developed through the overexpression of the target protein in azole resistance, via the duplication of promoter elements, together with the L98H point mutation in the *cyp*51A gene (Snelders, Melchers, and Verweij 2011), which is the gene encoding for the azole drug target in *A. fumigatus*. This protein is a central enzyme in the ergosterol biosynthesis pathway in fungi, presenting the lanosterol 14α-demethylase activity previously mentioned. This is another mechanism decreasing the affinity of the drug for the target. This particular mutation conferred a resistance to all azole molecules used (Snelders *et al.* 2008). Several other mutations have been described in the *cyp*51A gene (Hagiwara, Watanabe, and Kamei 2016), having a different impact on the affinity of each of the azole drugs used (Snelders, Melchers, and Verweij 2011). Another mechanism for alteration of the drug target was studied in Fks1p, the gene encoding for the major subunit of glucan synthase (Rocha *et al.* 2007). It was found that the S678P substitution has a detrimental impact on the affinity of echinocandins for the target.

A. fumigatus finally shows intrinsic resistance to fluconazole, derived from the weak binding of the molecule to one of the isoenzymes corresponding to the target (lanosterol 14α-demethylase) (Warrilow *et al.* 2010).

1.3 Novel antifungal drug development

This project is a collaboration with F2G Ltd, based in Manchester, United Kingdom. The company is working on several leads for novel antifungal development, which are promising

compounds that may lead to the development of new drugs. They tested several different series of compounds on a panel of fungal organisms and identified series known as F3, F6 and F2, which have a wide antifungal activity.

1.3.1 Dihydroorotate dehydrogenase (DHODH)

A first series of compounds known as F3 has been identified as having an antifungal activity on several *Aspergillus* spp. The target of interest was identified as dihydroorotate dehydrogenase (DHODH), which takes part in the pyrimidine production process. Such identification could be performed by addition of exogenous pyrimidines that reverted the antifungal effect (Oliver *et al.* 2016). Interestingly, relatively high levels of pyrimidines were necessary to revert this effect (5 mM minimum), and several species of fungi presenting a disruption of their pyrimidine biosynthesis pathway were showing attenuated virulence in animal models of infection (Noble and Johnson 2005; D'Enfert *et al.* 1996; de Gontijo *et al.* 2014; Retallack *et al.* 1999). This indicated that targeting this pathway was a valid antifungal strategy.

DHODH is an inner membrane mitochondrial enzyme that weighs approximately 56.7 kDa. The human version of the protein is already a target in other types of disease such as in oncology (Christian *et al.* 2019), multiple sclerosis (Miller 2017), rheumatoid arthritis (Breedveld and Dayer 2000) or malaria (Hoelz *et al.* 2018). F2G has already developed a drug reversibly inhibiting DHODH (Figure 1.6), which is currently in clinical trials. This drug, called olorofim or F901318 by F2G, belongs to a new class of antifungal compounds called orotomides. F2G has already shown an interesting fungistatic effect on *A. fumigatus* (du Pre *et al.* 2018). Olorofim has also shown interesting antifungal potency on azole-resistant strains (Oliver *et al.* 2016). It does not show any antifungal activity on *Candida* spp, which is why it was not discovered earlier as antifungal screens usually use them as a primary target for antifungal activity. Mutations on the *C. albicans* gene of two residues (namely Phe162 and Val171) to the residues predicted to occupy the same location in *A. fumigatus* created a mutant that could be inhibited by olorofim (Oliver *et al.* 2016).

In order to find out the inhibitory mechanism, a genetic screen was performed to identify genes that, when present in multiple copies, provided resistance to olorofim (Oliver *et al.* 2016). In this study, resistant strains were selected and their genome was compared in order to find similarities that could identify one specific gene, thus identifying the gene corresponding to DHODH. Structurally, several residues have been identified as essential for drug binding by F2G (namely V200 and M209), which would imply that orotomides bind in the quinone channel of the protein, where ubiquinone enters the enzyme from the inner

mitochondrial membrane, preventing the reoxidation of the cofactor $FMNH_2$ (Oliver *et al.* 2016). While there is normally a process called pyrmidine salvage pathway in fungi, whereby fungal organisms are capable of bypassing the inhibition of pyrmidine synthesis by uptaking them from the extracellular environment, this mechanism appears to be inefficient in *A. fumigatus* (Oliver *et al.* 2016).

Although there is not much known about adverse effects yet, the important difference in IC50 (during *in vitro* assays) between the fungal version of DHODH and its human homologue (>2200-fold difference) means that it is unlikely for this drug to have detrimental consequences on this human homologue. During the first phases of clinical trials, olorofim has been shown to be well tolerated both orally and intravenously (Wiederhold 2020). It is also showing a very interesting efficiency against several *Aspergillus spp.*, both azole-susceptible and resistant, as well as other non-aspergillus moulds (Georgacopoulos *et al.* 2021).

So far, F2G has been working on both whole organisms and purified protein. However, for the purified protein assays, they have been working on a truncated version of the protein lacking the membrane-spanning helix anchor. Drug affinity or fungistatic assays have been performed on this version of the protein, which is why it would be interesting to express both truncated (DHODH-TR) and full-length (DHODH-FL) versions of the protein to make sure olorofim's activity is not impaired by the absence of the membrane part.

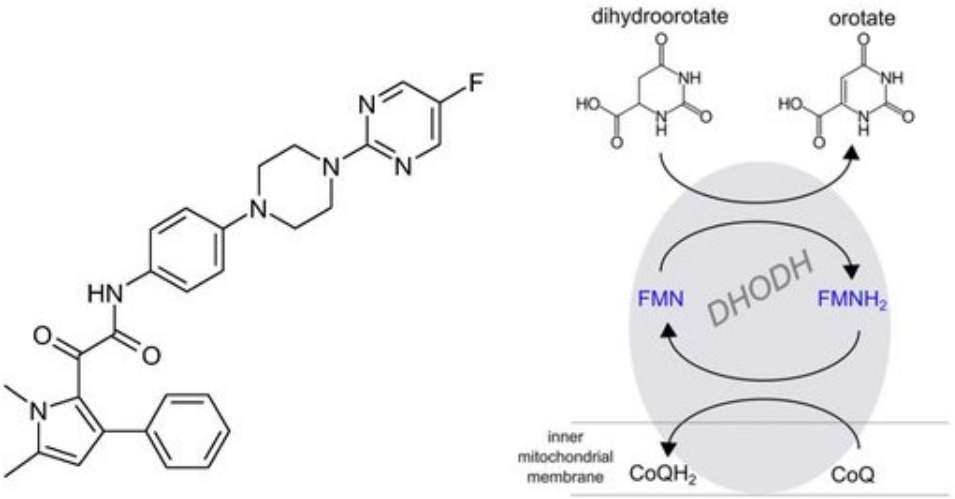

Figure 1.6 (from F2G Ltd): representation of the olorofim drug developed by F2G and its target (DHODH). *The inhibitory activity of this compound on DHODH stops the pyrimidine production pathway in the fungus.*

1.3.2 Stearoyl-CoA desaturase (SdeA)

A second series of compounds called F6 has been identified for having an antifungal activity on *A. fumigatus*. F2G performed a haploinsufficiency test that identified stearoyl-CoA desaturase (SdeA) as a hit, wherein one of the copies of the gene is deleted or mutated (inducing a loss of function), therefore preventing the normal function of the protein encoded by this gene.

SdeA is a 51.9 kDa (according to its sequence and a molecular weight calculator (Expasy)) enzyme found in the membrane of the endoplasmic reticulum (ER) of *A. fumigatus* cells. It is also known as Ole1 in *S. cerevisiae*. Its human homologue is called SCD1 for stearoyl-CoA desaturase 1, which crystal structure was determined a few years ago (Wang, Klein, *et al.* 2015). The crystal structure for *A. fumigatus* protein's structure has not been determined yet however. It has a desaturating activity on lipids, particularly on 18:0 stearic acid, turning it into Δ9 oleic acid. This enzyme works jointly with cytochrome b_5 dehydrogenase (containing FAD), which is going to bring the electrons necessary for the desaturation reaction through the oxidation of NADH (Figure 1.7). The electrons captured by cytochrome b_5 dehydrogenase (or reductase) are transferred to two iron ions. They switch from the ferric to the ferrous state by giving these electrons to the desaturase enzyme. Together with oxygen, they will participate in the desaturation reaction forming a Δ9 18:1 (cis) oleic acid. This reaction is of paramount importance in filamentous fungi as oleic acid is used as a precursor for a range of secondary metabolites. Indeed, *Aspergillus* species are reported to synthesise polyunsaturated fatty acids thanks to a Δ12 desaturase using the Δ9 product previously synthesised (Wilson *et al.* 2004).

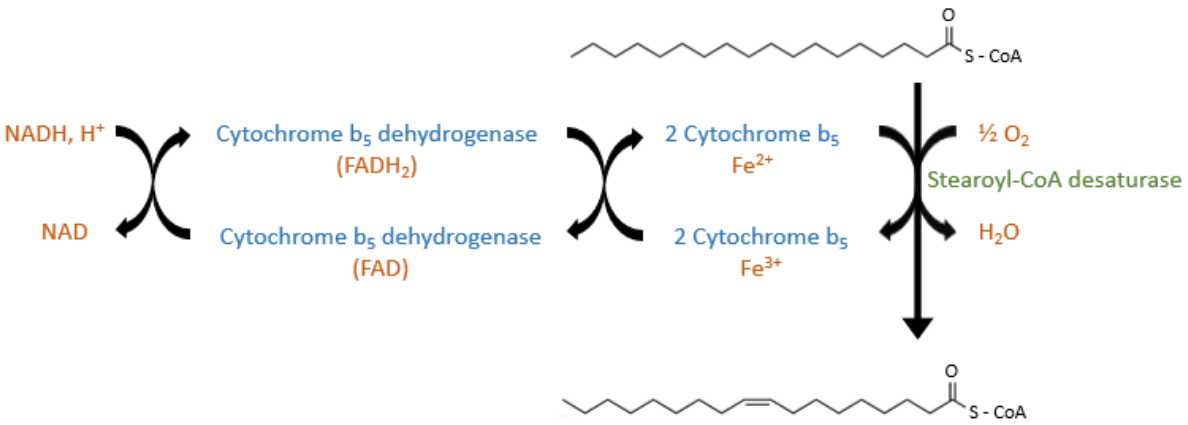

Figure 1.7: Chemical reaction leading to the desaturation of fatty acids using stearoyl-CoA desaturase (SdeA) as the enzyme. *The oxidation of NADH,H⁺ provides electrons that are transported to the enzyme via an iron ion.*

Therefore, oleic acid can be further desaturated into linoleic acid, which is the precursor of psi factors, which are involved in asexual spore production in different *Aspergillus* species (Calvo *et al.* 1999). Linoleic acid is also believed to be a supporter of some mycotoxins production in *Aspergillus* species, such as aflatoxin (Calvo *et al.* 2002). Overall, production of unsaturated fatty acids is vital for filamentous fungi and targeting the enzyme responsible for this reaction can be an interesting lead for the development of antifungal drugs.

During the haploinsufficiency test performed by F2G, the ratio of saturated to unsaturated fatty acids was increased upon exposure to an F6 compound. Furthermore, the antifungal activity of the series was reversed by addition of unsaturated fatty acids but not saturated fatty acids, implicating a desaturation step. This showed that SdeA was the target of interest for this series of compounds.

In order to test specifically each molecule from the F6 series, and to try to improve the drugs by medicinal chemistry approaches, the target enzyme needs to be expressed and purified, and an in vitro activity assay developed.

1.3.3 Target 3

A third series of compounds called F2 has been identified as having an antifungal activity. Very preliminary studies have suggested the target of this series to be another membrane protein involved in the glycosylation process. F2G is planning on developing future studies about this potential third membrane target.

Therefore, three different membrane protein targets have been identified as potential new anti-fungal drugs. This project will focus on two of them, with a particular emphasis on SdeA. However, membrane proteins provide several challenges that need to be addressed.

1.4 General introduction on membranes and proteins

1.4.1 Membranes

Membranes are the main tool for compartment separation in cells. They provide a separation between the external environment and the cytosol in every cell through the plasma membrane, but also separation between different compartments (called organelles, such as

nucleus or mitochondrion) within eukaryotic cells. They are of paramount importance as the plasma membrane helps protecting cells from their surrounding environment, while internal organelle membranes are important for maintaining homeostasis within them, which is crucial for them to function properly. As an example, a loss of ions or pH homeostasis in the Golgi apparatus can induce a loss of function for protein sorting and membrane trafficking, thus leading to diseases such as *Cutis laxa* or *Hailey-Hailey* disease (Kellokumpu 2019). This homeostasis property is also found in the plasma membrane for maintaining the electrochemical gradient on each side of the membrane, crucial for proper neuron functioning for example.

Membranes are mainly made of lipids and proteins. The lipid part comprises phospholipids and sterols, which spontaneously form bilayers through their amphiphilic properties. Each of these layers generally have a different composition, with some phospholipids found mostly if not exclusively in one leaflet rather than the other. Their structural diversity is very wide, especially in mammals, which demonstrates their multiple physiological functions (Harayama and Riezman 2018). Further to its barrier role, the plasma membrane also has a decisive role in the movement of different ions and molecules in and out of the cell and organelles (Yang and Hinner 2015), through several different pathways (passive permeation, active transport…). It also plays an important role in the cell structure, via the anchoring of the cytoskeleton to this plasma membrane (Denker and Barber 2002).

1.4.2 Membrane proteins

1.4.2.1 Importance of working with membrane proteins

Membrane proteins represent the entry point of the cell for many compounds. They display a whole range of essential functions, ranging from signalling mechanisms to transport through the membrane or enzymatic activity (Figure 1.8). Membrane proteins play a crucial role in drug discovery as they account for 60 % of drug targets (Overington, Al-Lazikani, and Hopkins 2006; Santos *et al.* 2017) while representing only around 23 % of the human proteome (Uhlen *et al.* 2015). Several types of targets can be of interest, whether they are enzymes, ion channels, membrane receptors or transporters, but some of them are quite overrepresented. As an example, receptors make up 44 % of human drug targets, including 19 % for GPCRs (Rask-Andersen, Almen, and Schioth 2011). Furthermore, GPCRs and ion channels alone represent 50 % of small-molecule drugs targets (Santos *et al.* 2017). They can often be more attractive than cytosolic or nuclear targets because they are directly accessible at the surface of the target cell and do not require transportation through the

membrane. Despite a shift of interest from ion channels to some phosphotransferases and ligands as drug targets, membrane proteins remain one of the major components of ongoing clinical trials (Rask-Andersen, Masuram, and Schioth 2014).

Even more importantly, recent papers have highlighted the importance of the interactions of membrane proteins with their lipid environment for proper function (Chen *et al.* 2022; Xu *et al.* 2021; Sander *et al.* 2021), emphasizing the relevance of taking into account those interactions in order to work with appropriately functioning membrane proteins.

However, due to the level of complexity of the interactions taking place in the membrane, it can be quite challenging to reproduce this environment *in vitro*, therefore hindering reproducibility of drug potency in a natural environment. Some attempts have been made at recreating a native environment for studying drug-protein interaction, using 3D models of cell culture to mimic the complexity of living tissue (Langhans 2018; Ravi *et al.* 2015; Pampaloni, Reynaud, and Stelzer 2007).

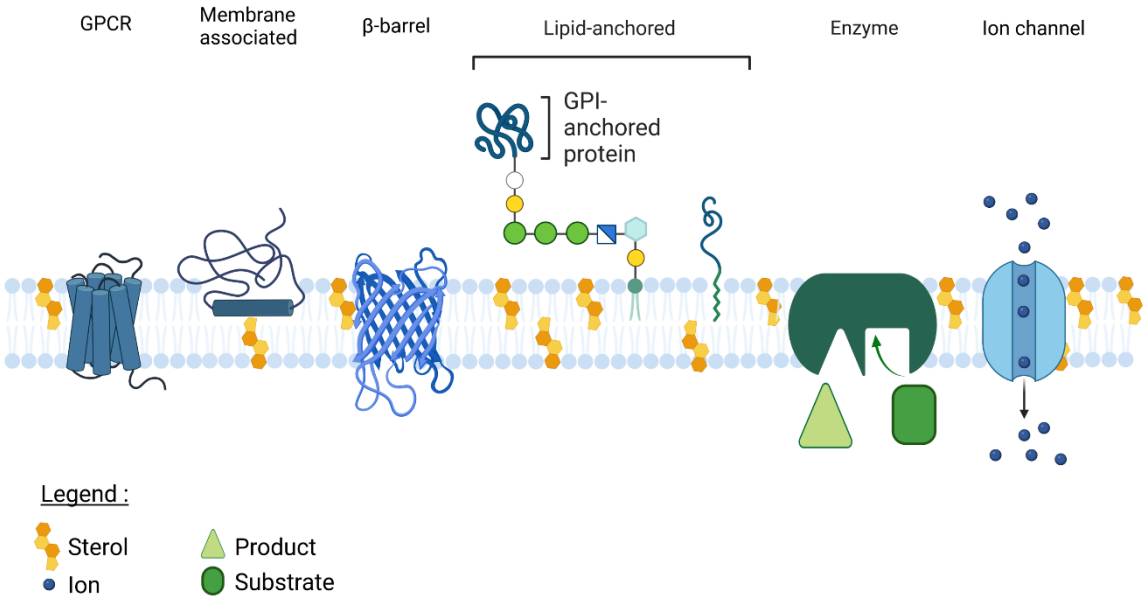

Figure 1.8: Representation of a membrane with different types of membrane proteins. *GPCRs are receptors that will bind ligands in order to induce downstream pathways activation. Membrane-associated and lipid-anchored proteins can play a role in cellular communication or cell anchorage within the tissue or with the cytoskeleton. β-barrels and ion channels are involved in the transport of molecules to and from the cell, while enzymes catalyse a chemical reaction to transform a reagent into a product. Figure created using Biorender.*

1.4.2.2 Membrane protein folding and orientation

Membrane proteins not only need to be correctly folded for functioning properly, but they also need to be in the correct orientation. Taking place in the Endoplasmic Reticulum (ER), appropriate folding is essential for active sites to be in the right position, affecting its ability to interact with other proteins and compounds (Figure 1.9). Misfolded proteins are believed to be responsible for many neurodegenerative pathologies (Chaudhuri and Paul 2006) or type 2 diabetes mellitus (Nevone, Merlini, and Nuvolone 2020) amongst other examples. They are generally grouped under the term amyloidosis.

Protein orientation within the membrane is also essential for several reasons: misorientated proteins can be wrongly assigned to a specific trafficking pathway, or lack post-translational modifications essential for their function such as glycosylation, which is only happening on the non-cytosolic side of the membrane. Often, membrane proteins will interact with specific lipids in the membrane bilayer, which may not be found from one leaflet to the other, thus preventing correct membrane-lipids interactions when the protein is in the wrong orientation. All these issues can lead to the protein not passing the ER's quality checks, and ending up degraded in the best-case scenario, or accumulating in the cytosol as aggregates, leading up to diseases.

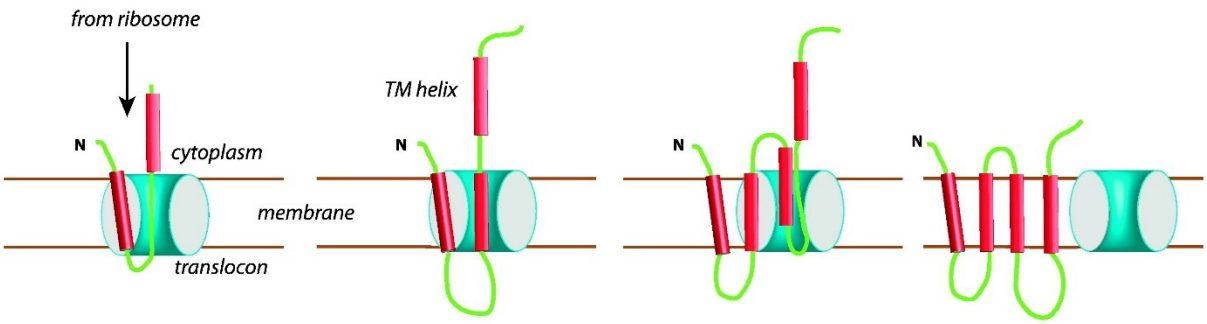

Figure 1.9: Generally accepted mechanism for the insertion of multi-spanning membrane proteins into membranes (Cymer, von Heijne, and White 2015). *The protein coming out of the ribosome goes through the membrane via the translocon. Transmembrane domains are recognised and partitioned into the membrane.*

1.5 Challenges of the expression of recombinant membrane proteins – Selection of expression hosts

This project thus focuses on the overexpression and purification of membrane proteins. Indeed, while it is possible to study membrane proteins in whole cells or in membrane fractions (without the need to purify them), it can be tricky to assess their activity, especially when assessing enzymatic activity, due to the presence of other compounds that could cross-react. The desired enzymatic activity that should be observed in this case must correspond to the protein of interest's activity only for the proper development of a functional assay and inhibition assay. However, overexpressing and purifying membrane proteins is still quite a challenge as membrane proteins have always been more difficult to express than soluble ones, with a yield most likely to be smaller. It can be more difficult to produce high amounts of membrane proteins due to the reduced area available in the membrane, in comparison to cytosolic proteins. Furthermore, membrane protein production can be limited by the inactive state of the protein produced, whether it is due to non-native folding, incorrect post-translational modifications or selection of the wrong expression system.

1.5.1 Selection of the host

The selection of the expression system is important with the main choices available being bacteria, yeast, insect and mammalian hosts. Each host's assets and weaknesses are detailed in a recent review (Kesidis *et al.* 2020). While bacteria showed several advantages including the cost effectiveness, the short time of production and an important ease of manipulation, they can lack the folding and post-translational modifications required for the production of eukaryotic membrane proteins. Yeast systems are also, in a lesser extent, easy to manipulate, they show an interesting economy of use (Cereghino *et al.* 2002) and relatively rapid expression times (Byrne 2015). They are also capable of reaching a high cell density and produce active eukaryotic membrane proteins. Finally, insect and mammalian systems are more expensive and time-consuming, but they are optimal for the production of large eukaryotic proteins with complex post-translational modifications.

It was proposed to use a yeast system for expression of fungal targets, since it is genetically closer to the original fungal organism producing both membrane proteins of interest (SdeA and DHODH-FL) and is capable of expressing post-translational modifications, such as glycosylation (Cereghino *et al.* 2002). Choosing a system that resembles the original organism has traditionally shown the best results, owing to similar folding environments and

cofactors as well as access to related trafficking and post-translational modifications (Gulezian *et al.* 2021).

In yeast systems, two main hosts show the best features for classical membrane protein expression: *Saccharomyces cerevisiae* and *Pichia pastoris*. The methylotrophic *P. pastoris* is capable of using a strong inducible promoter such as p*aox1*, from the alcohol oxidase encoding gene (*aox1*), which is tightly repressed by glucose or glycerol and strongly induced by the addition of methanol as a carbon source (Hartner and Glieder 2006). There are also inducible promoters that can be used in *S. cerevisiae*, such as the tet-on/tet-off system, the galactose (GAL) one or DDI2 (Lin *et al.* 2018), but also constitutive ones such as PMA1. They can however show deficiencies sometimes (such as the need to remove all glucose from the culture media in the GAL system for example).

Saccharomyces cerevisiae presents a comprehensive strain collection, from which suitable expression hosts can be selected, according to one's specific research needs, and supported by information in the *Saccharomyces* Genome Database (http://www.yeastgenome.org/). The yeast deletion collections comprise over 21,000 mutant strains that carry precise start-to-stop deletions of approximately 6000 *S. cerevisiae* ORFs (Giaever and Nislow 2014).

On the other hand, *P. pastoris* is capable of reaching very high cell densities, which is why it was chosen for the production of these proteins of interest. While it can go up to more than 100 g/L of dry cell weight (corresponding to more than 500 OD_{600} units/mL) under tightly regulated conditions, including the use of bioreactors, it is likely to find more average values for membrane protein production processes (approximately 100 OD_{600} units/mL) (Byrne 2015). These very high cell densities can however become detrimental if some cases, leading to proteolysis (Jahic *et al.* 2003) and cellular stress (Mattanovich *et al.* 2004).

Two strains of *P. pastoris* were favoured during this protein production processes, which are X-33 and GS115. They differ by a mutation on their *his4* gene, which is inactivated in GS115, making it a histidine auxotroph, therefore allowing selection of cells having included the gene. On the other hand, X-33 possesses an active *his4* gene, making it a histidine prototroph (Brady *et al.* 2020). It usually requires an antibiotic resistance gene for plasmid integration selection. Both strains were used during this project.

For the partner protein cytochrome b_5 dehydrogenase, it was decided to express it in *Escherichia coli*, as it had already been expressed by F2G in this host with good yields. Since it is a very small – the expressed, truncated, version of the protein is estimated to weigh 34.4 kDa with its tags– and simple protein, there was no major obstacle for its production in bacteria.

Finally, it was also decided to express DHODH-TR in *E. coli*, also because F2G has already done so with success previously. With the membrane part being removed, the remaining soluble protein becomes much easier to express.

While *P. pastoris* possesses a gene with homologous function to that of SdeA (Fad9A and B) (Yu *et al.* 2012), it is somewhat less clear for DHODH. A hypothetical protein can be identified in the Kyoto Encyclopedia of Genes and Genomes corresponding to DHODH but the protein itself does not seem to have been clearly identified.

1.5.2 Purification of membrane proteins

One of the biggest issues with the production of membrane proteins remains the extraction of an active protein from the membrane during the purification. The extraction is essential because the membrane is highly complex, with many different proteins. In order to avoid big chunks of membranes being purified altogether, which would first impair the purification efficiency by blocking the resin pores, and second prevent downstream studies because of the presence of numerous membrane components, it is important to solubilise membrane proteins and separate them from the rest of the membrane.

Traditionally, detergents, also called surfactants, were used to solubilise the protein before it could be purified. They are made of a hydrophilic head and a hydrophobic tail and are capable of inserting in the cell membranes, disrupting the membrane structure (Figure 1.10a). They also interact with the membrane protein, forming micelles that will hide the hydrophobic part of the protein normally inside the membrane (Figure 1.11a).

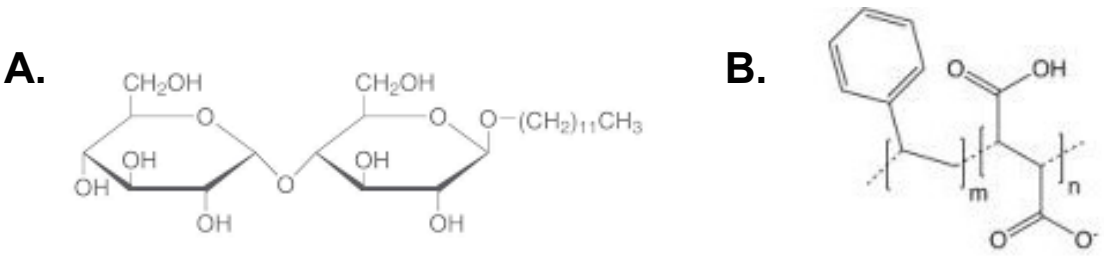

Figure 1.10: Chemical representation of DDM (Dodecyl-β-D-maltoside) (A.) and SMA (Styrene-Maleic Acid copolymer) (B.). *A. In DDM, the cycles loaded with hydroxyl groups represent the hydrophilic moiety of the detergent, while the long saturated carbon chain is the hydrophobic one. B. In SMA, the styrene groups are the hydrophobic moiety while the maleic acid ones are hydrophilic. The letters m and n represent the ratio of each moiety, which can differ from one polymer to the other, providing each polymer with a specific (S:MA) ratio.*

This method has proven to be successful in the purification of membrane proteins, and many different detergents have been developed, depending on the downstream applications that are planned (Arnold and Linke 2008). However, these detergents show significant setbacks as they often denature the protein (Yang, Wang, *et al.* 2014), thus limiting the possible studies performed on the protein afterwards. Indeed, the use of detergents can often lead to protein instability and eventually a loss of activity for the protein, excluding any potential functional study later on (Lee 2005; Rothnie 2016). This loss of activity can be due to the absence of annular lipids or to the loss of lateral pressure found in the membrane environment.

Other methods for studying membrane proteins include their reconstitution into a lipid environment (lipid particles). This kind of method incudes reconstitution into nanodiscs such as amphipols, or into lipid-detergent micelles such as proteoliposomes. These methods allow the protein to be reconstituted into a more native environment, more suitable for a correct three-dimensional folding of the protein of interest, therefore enhancing its functional activity. It is however difficult to mimic as best as possible the native lipid environment of the protein, due to the level of complexity of native membranes and the different lipid composition of each kind of host, which in turn can lead to the protein's loss of activity. More specifically, properties of the hydrophobic groups (length and saturation of the tail) or hydrophilic groups (charges on the head group) have a non-negligible impact on the interaction of the lipid with the membrane protein (Shen, Lithgow, and Martin 2013). Lipidomic studies or bibliographic research should be performed in order to investigate the best way to copy this environment.

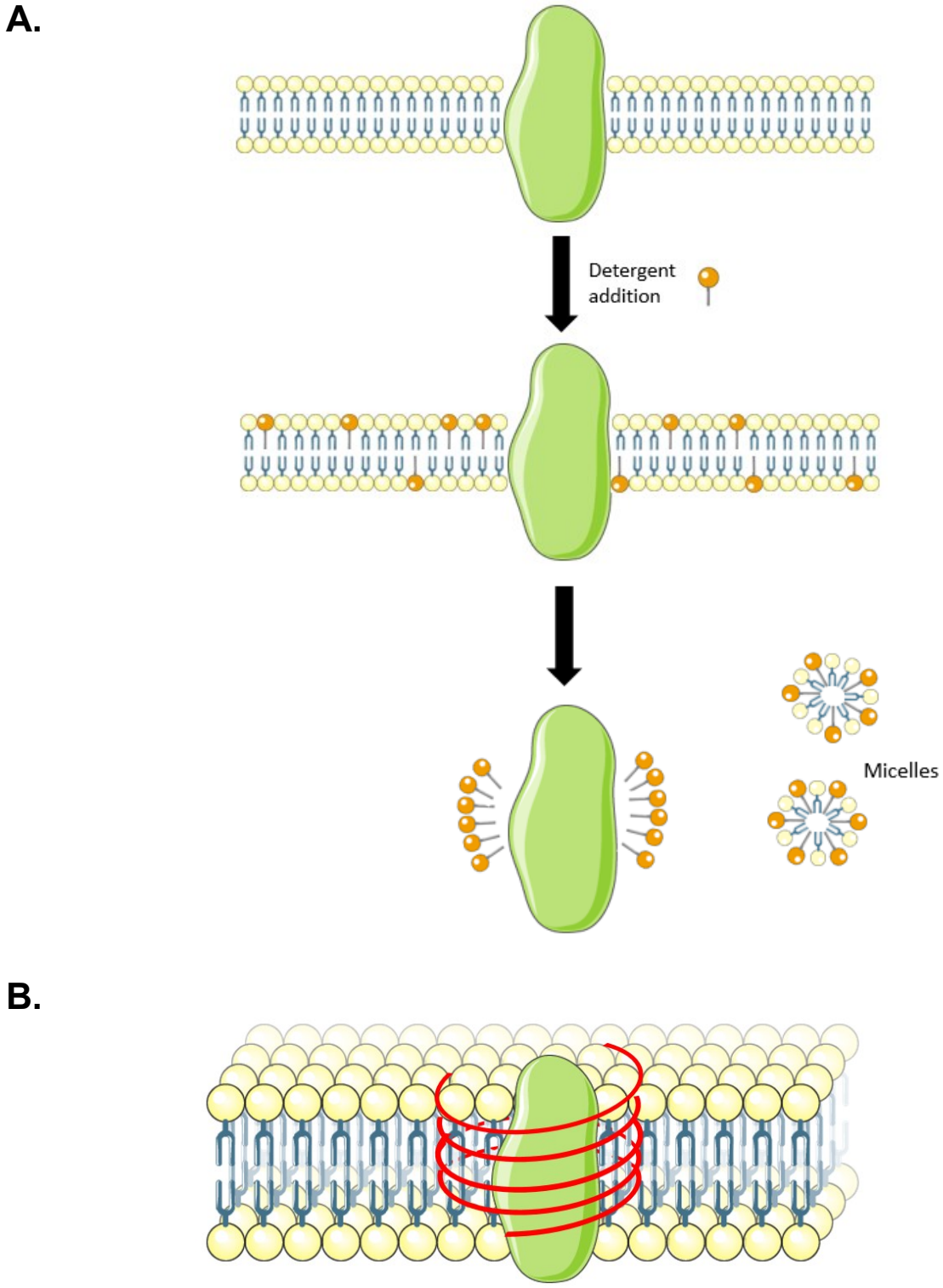

Figure 1.11: Representation of the extraction of a protein from a membrane using detergent (A.) or SMA (B.). *A. With detergent, the protein loses all connection to the surrounding lipids, which can be a cause for the loss of function and native folding often observed using detergents. The hydrophobic tails of the detergent will surround the part of the protein normally hidden within the membrane, thus protecting it from the environment. The phospholipids from the membrane form micelles with the detergent, also protecting their hydrophobic tails in the core of the micelle. B. Representation of the extraction of a protein from a membrane using SMA polymer (red). The lipids closest to the protein will be kept in the structure, leaving the protein structurally intact and functional.*

A different technique relying on SMA (Styrene Maleic Acid) polymers can also be used. SMA is a styrene-maleic acid co-polymer (Figure 1.10b) capable of inserting in the membranes in order to form disc-like structures called SMALPs (Styrene Maleic Acid Lipid Particles), containing lipids from the membrane and proteins (Figure 1.11b). This is possible thanks to the presence of a hydrophobic moiety (styrene) and a hydrophilic one (maleic acid) (Postis *et al.* 2015). This method has already been used for the study of membrane proteins (Jamshad *et al.* 2011; Knowles *et al.* 2009) and is particularly advantageous for their purification, as it leads to the conservation of the native lipid environment surrounding the protein, in order to keep the protein's distinctive features.

Moreover, the conservation of the protein's conformation in the membrane using SMA usually allows it to be fully functional (Stroud, Hall, and Dafforn 2018), and is very interesting for the perspective of the later performed functional assay in this study. SMA extraction is also an attractive option by being capable of extracting membrane proteins from various hosts, including yeast (Gulati *et al.* 2014). Indeed, SMA polymers are thought not to be specific to any particular lipid type, meaning that they can encapsulate membrane proteins from various hosts (Cuevas Arenas *et al.* 2016; Dominguez Pardo *et al.* 2017). It should be noted that this point is still quite controversial as some studies are showing no difference between the lipid composition found in SMALPs and that of the original *E. coli* membrane (Teo *et al.* 2019), whereas others found slight differences in terms of lipid polarity between SMALPs and the original *P. pastoris* membrane (Ayub *et al.* 2020). SMA's propensity towards certain types of membranes rather than others is another discussion point, with one study finding that plasma membrane solubilisation can be slower than organelles' (Dorr *et al.* 2017). A possible explanation for this could rely on the presence of high sterol and sphingolipids contents in the plasma membrane relatively to the organelles (van Meer, Voelker, and Feigenson 2008). These lipids can form highly ordered structures in membranes known as lipid rafts, which are known to be less fluid than other membranes and quite insoluble to detergents such as Triton X-100 (Simons and Ikonen 1997; Schroeder, London, and Brown 1994). Despite the fact that these examples are mentioning detergents, it is likely that this can also be applicable to SMA, and this was indeed shown more recently in model heterogenous phase-separated bilayers (Dominguez Pardo *et al.* 2017). In this study, SMA was shown to have a strong preference for solubilisation of lipids in fluid phase rather than liquid-ordered phase.

In terms of polymer length and dispersity, the main S:MA ratios used (3:1 and 2:1) both present a molecular weight M_w of approximately 10 kDa. They can differ in number-average molecular weight M_n, which is defined as the total weight of polymer divided by the total number of molecules. This gives an indication on the polymer length and makes a difference

on the solubilisation properties of the polymer. For example, short-size polymers have been shown to be faster and more efficient at solubilising membrane proteins but long-chain ones are more stable over time (Dominguez Pardo *et al.* 2018). The polydispersity index (PDI) corresponds to the ratio M_w/M_n and measures the distribution of molecular weights. A high PDI makes it more difficult to characterise the complex formed by the polymer and the membrane, but this did not affect this project as there was no characterisation step planned.

In any way, SMA2000 polymer was chosen as a starting point as it has been shown it is generally the most effective for yield, purity, stability and function of the produced protein (Morrison *et al.* 2016), although it can be quite dependent on the target studied or on the downstream applications considered (Swainsbury *et al.* 2017; Gulamhussein *et al.* 2020). SMA2000 contains a (2:1) S:MA (styrene to maleic acid) ratio. Several other polymers are commercially available, with different variations in the hydrophobic and hydrophilic moieties. While some just have variations in the S:MA ratio (3:1 for example), others have completely different structures, such as DIBMA, which contains diisobutylene in place of the styrene part. Different tools are also available such as bicelles and amphipols (Dorr *et al.* 2016), or their improved version called cyclapols (Marconnet *et al.* 2020), which can become quite promising in the future.

Solubilisation with SMA-like polymers does come with some limitations. One of the most important ones being its sensitivity to divalent cations (especially Mg^{2+}) that makes the polymer precipitate out of a solution above a certain concentration (Dorr *et al.* 2016; Gulati *et al.* 2014). It can become quite problematic for certain proteins, which need those divalent cations as cofactors (such as ATP-dependent ABC transporters during ATP hydrolysis). Furthermore, the discs formed by SMALP measure about 10 nm, which can sometimes be a bit too small for the extraction of some large membrane proteins (Bell, Frankel, and Bricker 2015). It seems to have become less of a problem more recently, with quite large protein complexes of up to 464 kDa and 48 transmembrane α-helices being solubilised with SMA (Sun *et al.* 2018). Finally, another issue possibly encountered while using SMA polymers comes from its sensitivity to low pH, because of the maleic acid moiety becoming protonated. As the styrene groups are quite hydrophobic, the negative charges present on the maleic acids are necessary to balance this hydrophobicity, in order to keep the aqueous solubility of the polymer as well as the interactions between SMA and lipid membranes (Scheidelaar *et al.* 2015). The protonation of the maleic acid seems to occur in a pH lower than 6 (Scheidelaar *et al.* 2016). SMA polymers also tend to polymerise in acidic pH and in high salt concentrations (Scheidelaar *et al.* 2016).

Multiple studies of membrane proteins solubilised with SMA polymers from yeast membranes have already been performed (Voskoboynikova *et al.* 2021; Smirnova *et al.* 2016; Skaar *et al.* 2015; Jamshad *et al.* 2015), which is why this method prevailed in this project.

1.6 Aims and objectives

The overall aim of this project was to study several membrane proteins as antifungal drug targets, in order to help develop new antifungal drugs. Specifically the objectives were:

- Production of target proteins free of contaminant
    - SdeA
    - Cytochrome b5 dehydrogenase
    - DHODH-FL (full length protein with TM region)
    - DHODH-TR (truncated version without TM region)
- Solubilisation and purification of target proteins
    - SMA
    - Other polymers
    - Conventional detergent (for comparison)
- Development of functional assays (enzymatic assays requiring the production of fully functional proteins)
- Test of novel drug candidates

While the objectives were not entirely well defined, as we did not know what would be achievable yet in terms of quality and quantity of produced proteins, we wanted to be able to produce enough of them to be able to run functional assays using spectrophotometry, which is an easy method to scale down for large screens.

2. Materials and methods

The *P. pastoris* strains used during this project were kindly provided by Prof. Bill's group, as were the empty yeast vectors used (pPICZ). The strains used were *P. pastoris* X-33 and GS115.

The plasmids used were provided by F2G Ltd (for SdeA, DHODH-TR and Cytb5R), or bought from GenScript (DHODH-FL) or Eurofins (SdeA). The primers used during the molecular biology work that was performed were bought from Eurofins.

The zeocin antibiotic was obtained from Invivogen, while kanamycin came from Melford and ampicillin from Sigma-Aldrich.

Every protein expressed contained a poly-histidine tag for purification purposes (6 residues).

The antibody anti-his was bought from R&D systems (reference MAB050), and the secondary anti-mouse HRP (Horseradish peroxidase) antibody from Cell signalling. The anti-c-Myc-tag magnetic beads were purchased from Fisher Scientific.

The protease inhibitor used during yeast cell breaking was an EDTA-free EASYpack protease inhibitor purchased from Roche.

Miniprep, gel extraction and PCR DNA clean up were performed using kits obtained from New England Biolabs. A gel extraction kit from Qiagen was also tested.

The remaining classic reagents were bought from either Sigma-Aldrich, Fisher Scientific or Melford Ltd.

2.1 Production and purification of SdeA

Pichia pastoris membrane protein production methods were based upon Bill *et al.* (Bill 2012) and EasySelect™ Pichia expression kit.

2.1.1 Stock solution preparation

Stock solution	Composition
10X YNB	Yeast nitrogen base with ammonium phosphate (13.4% w/v)
500X Biotin	Biotin (0.02% w/v)
10X Dextrose	D-glucose (20% w/v)
10X Methanol	Methanol (5% v/v)
10X Glycerol	Glycerol (10% v/v)
1M Potassium phosphate buffer pH 6.0	132 mL of 1M K_2HPO_4 with 868 mL of 1M H_2KPO_4. pH adjusted to 6.0 if necessary
YPD	Yeast extract (1% w/v), peptone (2% w/v) and dextrose (2% w/v). If making plates, agar (2% w/v) was added.
YPDS	Same composition as previous YPD supplemented with sorbitol 1M
BMGY	Yeast extract (1% w/v), peptone (2% w/v), potassium phosphate buffer (0.1M), YNB (1X), biotin (1X) and glycerol (1X)
BMMY	Yeast extract (1% w/v), peptone (2% w/v), potassium phosphate buffer (0.1M), YNB (1X), biotin (1X) and methanol (1X)

Table 2.1: Stock solution preparation for* P. pastoris *cell culture.

2.1.2 Transformation of *P. pastoris* cells

2.1.2.1 Electroporation

Electroporation was used to integrate plasmid pPICZαA-SdeA or DHODH-FL into the *P. pastoris* genome (Rosenfeld 1999). Transformation of *P. pastoris* is generally less efficient

than other types of hosts but some improvements can be made to the process in order to improve the transformation efficiency (Wu and Letchworth 2004). A single colony of the desired *P. pastoris* strain (X-33) was cultured overnight in 5 mL of YPD at 30 ˚C and 220 rpm in a sterile 50 mL tube. The next day, 500 mL of fresh YPD medium in a sterile 2L flask were inoculated with 0.1 to 0.5 mL of the overnight preculture and left to grow overnight at 30 ˚C and 220 rpm again, to an OD_{600} of 1.3 to 1.5. The cells were then centrifuged at 1,500 xg for 5 minutes at 4 ˚C. The pellet was resuspended in 500 mL of sterile ice-cold water and centrifuged again the same way. This time, the pellet was resuspended in 250 mL of sterile, ice-cold water before being spun again the same way and resuspended in 20 mL of ice-cold, sterile 1M sorbitol. A final centrifugation was performed with the same parameters before the cells were this time resuspended in 1 mL of ice-cold, sterile 1M sorbitol. The cells were kept on ice for transformation and were not stored. 80 µL of them were mixed with 5-10 µg of linearised plasmid (or 50-100 µg of circular plasmid) and transferred to an ice-cold 0.2 cm electroporation cuvette. The cuvette was incubated on ice for 5 minutes and the cells were pulsed at 1.8 kV in an electroporator (Eppendorf Eporator), before immediately adding 1 mL of ice-cold, sterile 1M sorbitol to the cuvette. The cuvette contents were then transferred to a 15 mL sterile tube and left to incubate at 30 ˚C without shaking for 1-2 hours. 10, 25, 50, 100 and 200 µL were then plated on separate YPDS plates containing 100 µg/mL of zeocin. The plates were left to incubate at 30 ˚C for 3 to 10 days until colonies formed. Some of the colonies were then put into YPD culture to prepare glycerol stocks, using 1 volume of culture and 1 volume of 50% glycerol and frozen at - 80 ˚C.

2.1.2.2 Chemical transformation

As an alternative method for transformation of plasmids into *P. pastoris*, chemical transformation could also be performed. A single colony of the desired *P. pastoris* strain (X-33) was cultured overnight in 5mL of YPD at 30 ˚C and 220 rpm in a sterile 50 mL tube. The next day, 50 mL of fresh YPD medium in a 220 mL sterile flask were inoculated with approximately 0.3 mL of the overnight preculture, in order to reach an OD of 0.1, and left to grow for several hours at 30 ˚C and 200 rpm again, to an OD_{600} of 0.8 to 1.0. The cells were then centrifuged at 1,500 xg for 5 minutes at room temperature and washed three times with 25 mL of sterile distilled water. The cells were finally harvested with a centrifugation at 1,500 xg for 10 minutes at room temperature. An aliquot of cells (< 2 mL) was transferred into a sterile microcentrifuge tube to be washed again with 1 mL of sterile distilled water, followed by another wash with 1 mL of lithium chloride (LiCl) 1M. It was then resuspended again in 1 mL of LiCl 1M and incubated for 1 hour at 30 ˚C. A full speed (around 16,000 xg)

centrifugation was then performed for a few minutes and the pellet was resuspended in 400 µL of LiCl 1M. 50 µL of competent cells were transferred into a new centrifuge tube and spun at full speed again. In this order, the following compounds were added to the pellet: 240 µL of 50% PEG (polyethylene glycol), 36 µL of LiCL, 25 µL of 2 mg/mL ssDNA (salmon sperm) and approximately 10 µg of linearised plasmid DNA. The mixture was vortexed for 1 minute and incubated at 30 ˚C for 30 minutes, before being heat shocked at 42 ˚C for 30 minutes. The cells were pelleted at 4,000 xg for a few minutes and the pellet was resuspended in 1 mL YPD media and incubated at 30 ˚C and 200 rpm for 2 to 4 hours. Different amounts of cells (50, 100, 200 µL) were finally spread on YPD agar plates supplemented with zeocin (100 µg/mL) and incubated for 2 to 4 days at 30 ˚C or until colonies formed.

2.1.3 Cell culture

2.1.3.1 Plates

YPD-agar plates were prepared using melted YPD-agar in plastic Petri dishes. The antibiotic zeocin was added at a concentration of 100 µg/mL. 25 mL were poured in each plate using a pipette, avoiding bubbles, and the agar was left to solidify. The cells were added on the agar using a sterile loop and spread on the surface. The plates were incubated at 30 ˚C for three days.

2.1.3.2 Flasks

Sterile flasks (size 200 mL, one per plate) were filled with 50 mL of BMGY containing zeocin (100 µg/mL). A colony was picked from the plates using a sterile tip and added in the media. The culture was left shaking at 200 rpm and 30 ˚C for 48 hours. 500 mL sterile flasks (one per 200 mL flask) were filled with 200 mL BMGY and 5 mL from the previous culture were added without adding zeocin this time. The flasks were left shaking at 200 rpm and 30 ˚C for 24 hours. 50 mL from each culture flask were collected and centrifuged 10 minutes at 3,000 xg. The supernatant was taken out and the pellets were resuspended in 20 mL BMMY. 5 mL of these resuspended pellets were added with 500 mL of BMMY into sterile 2 L flasks (one per 500 mL flask). They were left shaking at 200 rpm and 30 ˚C for 24 hours. Methanol (final concentration 1% v/v) was added and the flasks were once again left shaking at 200 rpm and 30 ˚C for 24 hours. Finally, all cultures were centrifuged at 3,000 xg for 20 minutes. The pellets were frozen at -80 ˚C.

2.1.4 Cell lysis

Yeast hosts are cells that are typically more resistant to lysis than other types of bacterial, insect or mammalian organisms, principally due to the presence of the cell wall outside of the membrane. Several methods exist to try to break open those cells in order to harvest the desired membranes, which include high pressure (Emulsiflex-C3 and French Press) and homogenization (using glass beads) (Jamshad and Darby 2012). C3 is traditionally recognised as one of the most efficient ways to break any type of cells (Schleicher *et al.* 2020), but there is always a minimum volume lost during the procedure, making it suitable only for large-scale cell disruption. The other two methods are more suitable for small-scale membrane harvesting and were therefore preferred in these conditions.

Preparation of buffers

Sodium phosphate buffer (1 M) was made of monobasic sodium phosphate (0.392 M) and dibasic sodium phosphate (0.608 M). The pH was adjusted to 7.4 if necessary.

Breaking buffer was made of glycerol (5%), EDTA (2 mM), NaCl (100 mM) and sodium phosphate buffer pH 7.4 (50 mM), with addition of protease inhibitor.

Resuspension buffer was made of HEPES (20 mM), NaCl (50 mM) and glycerol (10%). The pH was adjusted to 8.0.

2.1.4.1 Emulsiflex-C3

Resuspension

The pellets obtained and frozen in the previous step were resuspended in breaking buffer. The volume of buffer had to be at least three times the mass of the pellets. One protease inhibitor tablet was added per 50 mL of solution. The mix was stirred in a cold room (4 ˚C) for 15 minutes.

Breaking

A C3 was used to break the cells with the sample kept on ice during the whole process using working conditions detailed by someone previously in the lab (Jamshad and Darby 2012). The homogenization pressure reached was about 30,000 psi, and each sample was run a minimum of three times in the homogenizer, in order to have an optimal amount of broken cells. Once finished, the sample was spun down for 10 minutes at 3,000 xg and 4 ˚C. The supernatant was taken and centrifuged for 45 minutes at 100,000 xg and 4 ˚C. The supernatant was removed and the pellets were weighed in the tubes. They were then

resuspended in resuspension buffer in order to make samples with a concentration of roughly 180 mg/mL, using a Potter homogenizer. The membranes obtained were frozen at -80 ˚C.

2.1.4.2 French press

French Press was used with culture volumes up to 50 mL. Each run was performed with up to 25 mL of culture. The pressure used to lyse cells was equivalent to approximately 30,000 psi (Jamshad and Darby 2012).

Each sample was run three times on the press to maximise the cell breaking efficiency. Full cell lysates were then centrifuged at 3,000 xg for 10 minutes at 4 ˚C. The pelleted unbroken cells were eliminated while the supernatant was centrifuged again at 100,000 xg for 45 minutes at 4 ˚C. The membranes were collected in the pellet and resuspended in resuspension buffer at 180 mg/mL using a Potter homogenizer.

2.1.4.3 Glass beads

The acid-washed glass beads used were obtained from Sigma-Aldrich. Their size was 425-600 µm.

The cells were first washed with sterile water and harvested at 1,500 xg for 5 minutes. The pellet was weighed and the cells were resuspended in breaking buffer at approximately 0.3 g/mL. An equal volume of acid-washed glass beads (size 0.5 mm) was added and the mixture was vortexed 30 seconds and incubated on ice for 1 minute. This cycle was repeated between 10 and 16 times. The glass beads were removed by centrifugation at 4,000 xg for 10 minutes at 4 ˚C. The supernatant was transferred to a microcentrifuge tube and spun down at 10,000 xg for 10 to 30 minutes in order to remove cell debris and intact cells. The supernatant was retained and the membranes were isolated by high-speed centrifugation at 100,000 xg for 45 minutes at 4 ˚C. The pellet was weighed and re-dissolved in resuspension buffer at a concentration of 180 mg/mL using a Potter homogenizer. The membrane preparation was then stored at -80 ˚C.

2.1.5 Protein solubilisation - Purification

2.1.5.1 SMA polymer preparation

The SMA polymer preparation protocol was inspired by a book chapter from 2016 (Rothnie 2016). The polymer was bought from Cray Valley in its anhydride version. It needed to be hydrolysed to form styrene-maleic acid. First, 25 g of SMA2000 powder were dissolved in 250 mL 1 M NaOH overnight at room temperature using a magnetic stirrer and a round-bottomed flask. The reflux step was then replaced with three 16 minutes, 120 ˚C, cycles of autoclave (Broadbent *et al.* 2022; Kopf *et al.* 2019). The polymer solution was divided between four 250 mL centrifuge tubes and concentrated HCl was gradually added to each of them under a fume hood, mixing well, to precipitate the polymer. 100 mL of distilled water was then added to each tube and they were mixed well, before being centrifuged at 10,000 xg for 10 minutes at room temperature and removing the supernatant. 150 mL of distilled water were added to each tube and the polymer was resuspended by shaking, before being centrifuged again the same way as previously and removing the supernatant. This washing process was repeated four more times. Finally, the polymer was dissolved by adding 60 mL 0.6 M NaOH to each tube and either shaking or stirring for several hours. The pH was checked and adjusted to pH 8. The SMA co-polymer was eventually freeze-dried and stored at room temperature.

2.1.5.2 Sample preparation

SMA extraction protocol was inspired from the same paper (Rothnie 2016). 0.25 g (2.5 % (w/v)) of SMA 2000 polymer were mixed with 5 mL of the 180 mg/mL membrane sample and 5 mL of purification buffer, which was made of NaCl (150 mM) and Tris pH 8.0 (20 mM). The mix was left on a shaking plate at room temperature at least an hour. It was then centrifuged at 100,000 xg and 4 ˚C for 20 minutes. The supernatant was harvested and samples taken for SDS-PAGE and western blot analysis. The pellet was resuspended in purification buffer supplemented with 2% (w/v) SDS and samples were also taken for analysis.

2.1.5.3 Detergent solubilisation

Detergent solubilisation was also carried out, using four different detergents (final concentration for solubilisation added in percentage):

- DDM (1% w/v) (n-dodecyl β-D-maltoside)
- OG (2% w/v) (n-octyl-β-D-glucopyranoside)

- DG (1% w/v) (n-dodecyl-β-D-glucopyranoside)
- LMNG – CHS (1% w/v) (lauryl maltose neopentyl glycol with cholesteryl hemisuccinate 10:1)

Each of the detergents was mixed with a solution made of purification buffer and 180 mg/mL membrane sample (ratio 1:1 so the membranes were at 90 mg/mL). The mixture was mixed at 4 ˚C for two hours and then centrifuged the same way as for SMA solubilisation. Samples were taken from total solubilisation before centrifugation, soluble part and insoluble part after centrifugation.

2.1.5.4 Resin preparation

Ni-NTA agarose resin (1 mL of bed volume, which corresponded to 2 mL of slurry) was used for the 10 mL of solubilised protein previously prepared in buffer. It was centrifuged at 500 xg for 10 min, before the liquid supernatant part was removed and the remaining supernatant from the sample preparation was added on the resin. The mix was left on a shaking plate at 4 ˚C overnight.

2.1.5.5 Column

The next day, the sample with the resin was poured in a purification column and the flow-through was collected. The sample tube was rinsed with this flow-through a couple of times. The column was washed with 5x10 bed volumes (here 1 mL) of purification buffer with 20 mM imidazole. The column was washed with 2x10 bed volumes of purification buffer with 40 mM imidazole. The protein was finally eluted with 6x½ bed volume of purification buffer with 200 mM imidazole. Once finished, the column was rinsed with distilled water several times, EDTA (0.5 M, pH 8.0) was added to remove the nickel + imidazole, which turned the resin white. The column was washed again several times with dH_2O before $NiSO_4$ (100mM) was added in order to reload the nickel on the resin. The column was finally rinsed again with dH_2O several times. The exit of the column was blocked with parafilm and the resin was resuspended in 20 % (v/v) ethanol before being collected in a tube and stored at 4 ˚C for later use.

2.1.5.6 Myc-tag purification

A purification using the second tag present in the protein sequence called Myc-tag could be performed. In this procedure, an immunoprecipitation was performed using an antibody directed against this Myc-tag. Pierce anti-c-Myc antibody coupled to magnetic beads were

ordered from Fisher Scientific. The protocol for manual immunoprecipitation was obtained from the Thermoscientific website. 25-100 µL of the antibody and magnetic beads were placed in a microfuge tube before adding 175 µL of TBS-T (25 mM Tris, 0.15 M NaCl, 0.05 % (v/v) Tween-20 detergent) and gently vortexing. The tube was then placed on a magnetic stand to remove the supernatant while keeping the beads. 1 mL of TBS-T was added to the tube before it was inverted several times for a minute. The beads were collected on the magnetic stand while the supernatant was removed and discarded. The protein sample (which had already been purified through a Ni-NTA column) was then added to the pre-washed magnetic beads, together with 400 µL of TBS-T and the tube was incubated at room temperature for 30 minutes with mixing. The beads were collected while the unbound sample was removed and saved for analysis. 5 times more concentrated TBS-T was then used for washing (125 mM Tris, 0.75 mM NaCl, 0.25 % (v/v) Tween-20 detergent) and 300 µL were added to the tube before gently mixing. The beads were collected while the supernatant was removed and discarded. This washing step was repeated twice. Finally, 300 µL of ultrapure water were added to the beads and gently mixed. The beads were again collected while the supernatant was removed and discarded.

The elution of c-Myc-tagged SdeA could be performed through different protocols: if the protein was to be used in a functional assay later, a gentle elution protocol could be used, relying on a Pierce c-Myc peptide at 0.5 mg/mL in TBS. 100 µL of this solution were added to the beads before gently mixing. The sample was incubated at 37 ˚C on a rotator for 5-10 minutes. The beads were separated from the target protein on a magnetic stand before the latter was collected and saved. The elution step could be repeated to increase the yield.

A simpler, but denaturing method could also be used for analysing the efficiency of this method, via using NaOH elution. 100 µL of 50 mM NaOH were added to the beads and the tube was gently mixed and incubated at room temperature on a moving shelf for 5 minutes. The beads were magnetically separated and the supernatant was collected and saved. To neutralize the sample, 50 µL of 1 M Tris, pH 8.5 for each 100 µL of eluate were added.

2.1.6 SDS-PAGE

2.1.6.1 Preparation of buffers

Separating buffer was made of 1.5 M Tris at pH 8.8. Stacking buffer was made of 0.5 M Tris at pH 6.0. 10X SDS-PAGE was made of Tris-base (0.25 M), glycine (1.92 M) and SDS (1 % w/v). Running buffer was made of SDS-PAGE diluted 10 times with distilled water.

Laemmli buffer 5x was made of Tris (0.1 M) pH 6.5, SDS (5 % w/v), glycerol (30 % v/v), β-mercaptoethanol (5% v/v) and bromophenol blue (0.005 % w/v).

2.1.6.2 Preparation of samples

For each sample, 20 µL were mixed with 5 µL of Laemmli buffer 5x.

2.1.6.3 Preparation of the gels

Gels with 12 % polyacrylamide were made for every protein detection as they were all small enough. The acrylamide used was made of a solution of acrylamide and bis-acrylamide at a ratio of 37.5:1 with a concentration of 40 %. For two gels, each phase was made according to the following recipe:

Component	Separating phase	Stacking phase
H_2O	4.4 mL	2.4 mL
Buffer	2.5 mL	1 mL
Acrylamide	3.0 mL	500 µL
10 % (w/v) SDS	100 µL	40 µL
10 % (w/v) APS	100 µL	40 µL
TEMED	10 µL	5 µL

Table 2.2: Composition of the different phases of the 12% polyacrylamide gels prepared for SDS-PAGE.

The prepared gels were 1.0 mm thick. They were placed in a tank with running buffer before being loaded with the different samples tested.

2.1.6.4 Gel running

The gel was run against a Pierce unstained molecular weight marker in the tank containing running buffer at 110 V through the stacking phase and 150 V through the separating phase. The gel was stained using InstantBlue (Abcam).

2.1.7 Western blot

2.1.7.1 Preparation

Western blot buffer 10x was made of Tris-base (0.25 M) and glycine (1.92 M).

Running buffer was then made of WB buffer (1X) and methanol (20 % v/v). A SDS-PAGE gel was run the same way as for the previous step, except a Pierce prestained molecular weight marker was used instead of the unstained one. A PVDF membrane was cut and activated by soaking in methanol 100 %. It was then rinsed with distilled water. The western blot cassettes were assembled as following: foam pad, filter paper, PVDF membrane, filter paper, foam pad and soaked in running buffer. The gel was then added on the cathodic side of the nitrocellulose membrane and the western blot was run for one hour at 100 V.

2.1.7.2 Antibody binding

After the transfer, the membrane was left in a block solution overnight on a moving shelf. This block solution was made of BSA (5 % w/v) and sodium azide (0.1 % w/v) into 20 mL TBS-T, which itself was made of Tris pH 7.4 (20 mM), NaCl (150 mM) and tween-20 (0.05 % v/v). On the next day, the block solution was collected and stored at 4 ˚C for later use. The primary antibody used was a mouse anti-His antibody that was added on the membrane at a dilution of 1:500 in 5 % (w/v) BSA and 0.1 % (w/v) sodium azide in TBS-T. The mixture was left one hour on a moving shelf before the membrane was washed in TBS-T three times, during five minutes each time. The secondary anti-mouse HRP (horseradish peroxidase)-linked antibody was added to the membrane at a dilution of 1:5000 in TBS-T. The membrane was left on a moving shelf for one hour before being washed in TBS-T five times, during five minutes each time. The western blot was developed by chemiluminescence, where HRP substrate is added to the membrane, and imaging is performed by measuring the luminescent product made by the HRP enzyme, using a C-DiGit scanner from Li-Cor and the Image Studio software.

2.1.8 Protein quantification

The amount of membrane protein produced was calculated using a densitometry analysis, via a BSA standard gel, in which several known amounts of BSA were added. The amounts of BSA used were 0.125-0.25-0.5-0.75-1-1.25 µg. For each standard, 15 µL were mixed with 4 µL of Laemmli buffer 5x and loaded on the gel alongside 15 µL of the purified protein sample with 4 µL of Laemmli buffer 5x. The gel was run again at 110 V through the stacking phase and 150 V through the separating phase. After imaging, the pictures of the gel were opened on the software ImageJ. Each lane was measured and turned into peaks. The area under curve was measured through densitometry in order to establish a standard curve for the known BSA concentrations. The sample concentrations were then calculated using this curve.

Another method used relied on colourimetric kits such as DC Protein assay from BioRad and micro-BCA from Thermofisher. They were both used according to the manufacturer's guidelines.

2.1.9 TCA precipitation

If the protein samples were not concentrated enough for the quantification, they were concentrated using the TCA precipitation method. For 1 volume of sample, 1/10th volume of 0.15 % (w/v), deoxycholate was added and the mixture was mixed well. Another 1/10th volume of 72 % (v/v) trichloroacetic acid was added and the mixture was mixed well again, before being centrifuged at 16,000 xg for 10 minutes. The supernatant was removed, leaving a small white pellet that was resuspended in 15 µL of resuspension buffer made of SDS (4% w/v), Tris pH 10 (0.2 M) and NaCl (0.15 M). The protein quantification experiment could then be run the same way as previously.

2.2 mADH contamination

2.2.1 Mass spectrometry analysis

2.2.1.1 Sample preparation with in-gel trypsin digestion

The samples were run on a SDS-PAGE gel and the bands to be analysed were cut out into small pieces. They were then washed with 500 µL of 100 mM ammonium bicarbonate for 30 minutes to 1 hour on a shaker. The wash was discarded and the pieces were washed a

second time with 500 µL of 50 % acetonitrile / 50 % 100 mM ammonium bicarbonate for 30 minutes to 1 hour on a shaker. The wash was discarded. The protein's disulphide bonds were then reduced by adding 150 µL of 100 mM ammonium bicarbonate and 10 µL of 45 mM dithiothreitol (DTT). The mix was kept at 60 °C for 30 minutes in a heating block. Cysteine alkylation was performed by letting the sample cool down to room temperature before adding 10 µL of 100 mM iodoacetamide (IAA) and incubating it in the dark for 30 minutes. The solvent was discarded and the gel pieces were washed in 500 µL of 50 % acetonitrile / 50 % 100 mM ammonium bicarbonate for 30 minutes to 1 hour on a shaker. The wash was discarded and the gel pieces were shrunk by adding 50 µL of acetonitrile. After 5-10 minutes, the solvent was removed and the gel pieces were dried completely in a centrifugal evaporator for 10 minutes at 30 °C. The gel pieces were then rehydrated using 20 µL of trypsin. If this was not sufficient to fully rehydrate gel pieces, 10 µL of extra trypsin were added at a time to fully rehydrate and swell them to previous size. Sufficient 25 mM ammonium bicarbonate was added to cover over the gel pieces. The digestion was left overnight at 37 °C. The next day, the gel pieces were pelleted by a brief short speed centrifugation and the supernatant was transferred to clean Eppendorf tubes. Further extraction from the gel pieces was performed by adding 20 µL of 5 % formic acid to the gel pieces before incubating them for 20 minutes at 37 °C. 40 µL of acetonitrile were added before performing the same incubation step. The gel pieces were pelleted a second time and the supernatant was combined with the supernatant from the previous extraction. They were dried down together in the Speedvac at 30 °C for approximately 1 hour (until it is fully dried), before being resuspended in a volume up to 50 µL of 98 % H_2O, 2 % acetonitrile, 0.1 % formic acid (HPLC solvent A) and loaded into screw top glass autosampler vials (Chromacol, Speck and Burke analytical, Clackmannanshire, UK).

2.2.1.2 Liquid Chromatography – Mass Spectrometry (LC-MS) (Verrastro *et al.* 2018)

Peptides were separated and analysed using an Ultimate 3000 system (Thermo, Heemel Hempstead, UK) coupled to a 5600 TripleTOF (Sciex, Warrington, UK) controlled by Chromeleon Xpress and Analyst software (TF1.5.1, Sciex, Warrington, UK). Enrichment and desalting of the peptides were achieved using a C18 precolumn (C18 PepMap™, 5 µm, 5 mm × 0.3 mm i.d. Dionex, Bellefonte, PA) washing for 4 min with aq 2% acetonitrile, 0.1 % formic acid at 30 µL/min. The peptides were then separated on a C18 nano-HPLC column (C18 PepMap™, 5, 75 µm i.d. × 150 mm, Dionex, Dionex, Camberley, UK) at 300 nL/min using a gradient elution running from 2% to 45% aqueous acetonitrile (0.1% formic acid) over 45 min followed by a washing gradient from 45 % to 90 % aq acetonitrile (0.1% formic

acid) in 1 min. The system was washed with 90 % aq acetonitrile (0.1% formic acid) for 5 min and then re-equilibrated to the starting solvent. Ionisation of the peptides was achieved with spray voltage set at 2.5 kV, a source temperature of 150 °C, declustering potential of 50 V and a curtain gas setting of 15. Survey scans were collected in positive mode from 350 to 1250 Da for 200 ms using the high resolution TOF-MS mode. Information-dependent acquisition (IDA) was used to collect MS/MS data using the following criteria: the 10 most intense ions with +2 to +5 charge states and a minimum of intensity of 200 cps were chosen for analysis, using dynamic exclusion for 12 s, and standard rolling collision energy setting.

The final results were analysed on Mascot Daemon software (Table 2.3).

Setting	Parameters Chosen
Taxonomy	Other Fungi
Database	NCBIprot
Fixed Modifications	Carbamidomethyl (C)
Variable Modifications	Oxidation (M)
Enzyme	Trypsin
Maximum Missed Cleavages	1
Peptide Charge	+2, +3, +4
Peptide Tolerance	± 0.5 Da
MS/MS Ions Search	✓
Data Format	Mascot generic
MS/MS Tolerance	± 0.5 Da

Table 2.3: Parameters used for Mascot software analysis of the mass spectrometry results.

For confidence, the ion score cut off is 40 prior to final calculations on sequence coverage and overall ion score for the proteins.

2.2.2 Urea/alkali membrane washing

SdeA-containing membranes (180 mg/mL) collected from *P. pastoris* cell culture were washed in order to remove potential sticking contaminants from them by centrifuging them as follows (Zhuang *et al.* 1999):

- once with 8 mL of 4 M urea, 10 mM Tris-HCl pH 9.5, 5 mM EGTA,

- twice with 8 mL of 20 mM NaOH,
- once with 8 mL of 5 mM Tris-HCl pH 8.0, 2 mM EDTA, 2 mM EGTA and 100 mM NaCl.

Each washing step was followed by a centrifugation at 226,000 xg for 40 minutes at 4 °C. From this treatment, peripheral proteins and membrane-sticking contaminants were expected to be removed.

2.2.3 Gene knockout

2.2.3.1 Genomic DNA extraction

A Qiagen genomic DNA extraction kit was used following partly the instructions provided by the kit. The DNA was extracted from *P. pastoris* X-33 for the His4 gene, and from *P. pastoris* GS115 for the mADH gene.

The yeast culture was grown overnight in YPD medium at 30 °C and 200 rpm. The next morning, cells were harvested at an OD_{600} between 0.2 and 0.3. They were centrifuged at room temperature for 10 minutes at 1,500 xg and the supernatant was discarded. The pellet was resuspended in 10 mL of sterile distilled water. Cells were spun down again the same way and resuspended in 10 mL of fresh 1M sorbitol, 25 mM EDTA pH 8.0 and 50 mM DTT. A new centrifugation was performed with the same parameters and the cells were reuspsended in 10 mL of 1 M sorbitol this time, before being centrifuged the same way again. Following this step, the cells were resuspended again in 10 mL of 1 M sorbitol, 1 mM EDTA and 10 mM sodium citrate buffer pH 5.8. 13 µL of zymolyase enzyme (400 U/mL, which corresponds to 5.2 U in this reaction) were added to the mixture before it was incubated at 30 °C for 1 hour. The newly formed spheroplasts were centrifuged 10 minutes at 300 xg thereafter, before being resuspended in 180 µL of buffer ATL (provided by the Qiagen kit). 20 µL of proteinase K were added to the mix, which was vortexed and incubated at 56 °C until everything was lysed, either on a shaking water bath or shaking them manually 2-3 times an hour. 200 µL of buffer AL were then added and thoroughly mixed by vortex. 200 µL of ethanol 100 % were added before mixing thoroughly again. The mixture was added to the DNeasy mini spin column (provided by the kit) and centrifuged at 6,000 xg for 1 minute, before being washed with 500 µL of buffer AW1 and spun again. A second wash was performed with 500 µL of buffer AW2 with a centrifugation of 20,000 xg for 3 minutes. Finally, the DNA was eluted using 200 µL of buffer AE after having incubated it at room temperature for 1 minute and centrifuged it at 6,000 xg.

A second kit was also used for genomic DNA extraction from ThermoFisher called Yeast DNA extraction kit. As it was specialised for yeast cells, the kit was simpler to use. This kit was used exactly according to the manufacturer's guidelines.

2.2.3.2 PCR

Polymerase chain reactions were performed using Phusion polymerase (Thermoscientific) according to the manufacturer's guidelines. A mastermix containing the polymerase, GC buffer, 3 mM of $MgCl_2$ and dNTPs (400 µM of each dNTP) was used. Primers were used at different concentrations in order to optimise the reaction. The amount of starting material was also optimised to each reaction, as well as the annealing temperature during the reaction. These optimisation steps are developed in the results section. The PCR reaction used followed the guidelines indicated on the Thermofisher website with 30 to 35 cycles each time.

2.2.3.3 Agarose gel

Agarose gels 1 % (w/v) was made of 1 g of agarose fully dissolved into 100 mL of TAE buffer by heating in a microwave. After letting it cool down at room temperature or under cold tap water, 10 µL of redsafe staining was added and the mixture was vigorously shaken.

Each PCR sample (10 µL), supplemented with 2 µL of loading dye (New England Biolabs 6X Purple gel loading dye), were added in each well and the gel was run at 100 volts for approximately 35 minutes.

The pictures for each gel were taken in a GelDoc imager from Bio-Rad or in a Gbox (Syngene).

2.2.3.4 Gene extraction from gel

The gene extraction was performed using a gel extraction kit from New England Biolabs, following the instructions provided by the manufacturer.

2.2.3.5 Digestion of DNA using restriction enzymes

Digestions were prepared on ice using four different restriction enzymes (*Bam*HI, *Pfo*I, *Eco*RI and *Hind*III) (Table 2.4).

Double digestion with *Bam*HI and *Pfo*I	
DNA	1 µg
10X FastDigest buffer (Fisher)	5 µL
*Pfo*I	1.0 µL (10 units)
*Bam*HI	0.5 µL (10 units)
Nuclease-free water	Up to 50 µL
Double digestion with *Eco*RI and *Hind*III	
DNA	1 µg
10X NEB buffer 3.1	5 µL
*Hind*III	1.0 µL (20 units)
*Eco*RI	1.0 µL (20 units)
Nuclease-free water	Up to 50 µL

Table 2.4: Digestion conditions using two restriction enzymes. *The digestion experiment was left to incubate at 37 ºC for one hour.*

2.2.3.6 Ligation

Ligations were prepared on ice using T4 DNA ligase (New England Biolabs) (Table 2.5).

10X T4 DNA ligase buffer (Fisher)	2 µL
Vector DNA	50 ng
Insert DNA	44.82 ng
T4 DNA ligase	1 µL (400 units)
Nuclease-free water	Up to 20 µL

Table 2.5: Ligation conditions using T4 DNA ligase upon mADH gene ligation. *This reaction was performed with a pGEX-2T vector (4863 bp) and the mADH gene insert (1453 bp). The reaction was left to incubate 10 minutes at room temperature or at 16 ºC overnight.*

A 3:1 molar ratio of insert:vector DNA was used to perform the ligation, which was kept for the later ligation using pGEX-2T-mADH and His4. Mass of insert DNA added was calculated using NEB ligation calculator. The mixture was pipetted up and down and incubated either 10 minutes at room temperature or at 16 °C overnight. The plasmid was then introduced into competent DH5α cells, before being precultured and extracted using a miniprep kit, following the protocols shown in paragraph 3.3.1.

2.2.3.7 Sequencing

The obtained plasmid was sent to Eurofins for sequencing, with a set of primers covering the area of the integrated genes.

2.2.3.8 Preparation of RDB (Regeneration Dextrose) plates and MGY (Minimal Glycerol) medium

A pre-warmed (45 °C) mixture was prepared, containing 100 mL of 10X dextrose (2 % w/v), 100 mL of 10X YNB (1.34 %), 2 mL of 500X biotin (4.10^{-5} %), 10 mL of 100X amino-acids (0.005 %) and 88 mL of sterile water. The 100X amino-acids preparation was made of 500 mg each of L-glutamic acid, L-lysine, L-leucine, L-isoleucine, L-methionine in 100 mL of water, before being filter sterilised and stored at 4 °C for a year maximum. Sorbitol (186 g, final concentration 1 M) were dissolved into 700 mL of water, supplemented with 20 g of agar, before being autoclaved. The solution was placed in a 60 °C water bath prior to addition of the 300 mL of previously prepared pre-warmed mixture. The plates were then immediately poured and stored at 4 °C.

Minimal glycerol medium was prepared by aseptically combining YNB (1.34 %), glycerol (1 %) and biotin (4.10^{-5} %) in autoclaved water. The mixture could be kept at 4 °C for two months.

Neither RBD nor MGY media contained any histidine as the selection was going to be performed on the presence of the His4 gene.

2.2.3.9 Transformation into yeast

The plasmid was integrated into a *P. pastoris* GS115 cell line following an electroporation protocol. 5 mL of the cell line were first grown in YPD at 30 °C overnight, before 0.1 to 0.5 mL of this preculture were inoculated in 500 mL of fresh YPD in a 2L flask, overnight at

30 ºC again, to an OD_{600} of 1.3 to 1.5. The cells were then centrifuged at 1,500 xg for 5 minutes at 4 ºC, and resuspended into 500 mL of ice-cold, sterile water. The same centrifugation step was carried out before resuspending the cells in 250 mL of ice-cold, sterile water. Again, the cells were centrifuged the same way and resuspended in 20 mL of ice-cold, sterile 1 M sorbitol. A final centrifugation step was carried out in order to eventually resuspend the cells in 1 mL of ice-cold, sterile 1 M sorbitol, in order to make a final volume of approximately 1.5 mL. From this cell suspension, 80 µL were then mixed with 5-10 µg of linearised DNA (or 50-100 µg of circular DNA), and transferred to an ice-cold 0.2 cm electroporation cuvette. The cuvette was incubated with the cells on ice for 5 minutes, before they were pulsed with an electroporation device (Eppendorf Eporator) at 1.8 kV. 1 mL of ice-cold 1 M sorbitol was immediately added to the cuvette before transferring the contents to a sterile 15 mL tube, and incubating it at 30 ºC without shaking for 1 to 2 hours. Different volumes of cells were spread out on RBD plates (10, 25, 50, 100 and 200 µL) and incubated at 30 ºC for several days until growth was observed.

Once colonies were grown on the RBD plates, several of them were picked up and put into 5 mL MGY cultures overnight at 30 ºC. Glycerol stocks were prepared for each of the colonies.

2.2.3.10 PCR testing for mADH

The presence of mADH and His4 in the transformed colonies was investigated using colony PCR. 100-200 µL of liquid culture were mixed with 100 µL of a solution containing 200 mM lithium acetate and 1 % SDS, before incubating it at 70 ˚C for 5 minutes. 300 µL of 100 % ethanol were added before vortexing the mixture. The DNA was then spun down at 16,000 xg and the supernatant was discarded. The pellet was washed with 70% ethanol before being resuspended in 100 µL of water. The cell debris was removed by centrifugation at 16,000 xg for 15 seconds. 5 µL of the supernatant was used as DNA template for PCR.

The PCR was performed using the same conditions as previously described, using mADH or His4 primers.

2.2.3.11 mADH expression assay

The selected colonies were put into 50 mL MGY culture at 30 ˚C and 200 rpm, with another culture corresponding to an X-33 wild type strain (already containing both mADH and His4). After each culture had reached an OD_{600} of 2, they were centrifuged 10 minutes at 3,000 xg

and at 4 ˚C before discarding the culture medium. They were then resuspended in 500 mL BMMY in an autoclaved 2 L flask and left to grow at 30 ˚C and 200 rpm. Methanol (final concentration 1 %) was added to the culture every 24 hours, for 5 days.

At different time points, 1 mL was taken from each and the cells were spun down, before the culture medium was discarded and they were frozen at -80 ˚C.

SDS gels were run on each of the cell pellets to check the presence of the mADH band at different time points.

2.2.3.12 Cell breaking and purification

Cell cultures were broken using a French Press, as the culture volumes used were smaller.

After this step, the membranes from different time points were either directly loaded on SDS-PAGE gels, or submitted to SMA membrane extraction before purification the same way as when SdeA is present in the membrane. Washings and elutions were loaded on SDS-PAGE 12 % gels.

2.3 Production and purification of soluble proteins cytochrome b5 dehydrogenase and DHODH-TR

Due to their lower levels of complexity, soluble proteins were produced in a bacterial host throughout this project. *E. coli* DH5α and BL21(DE3) were the two strains used, with the former well known for its propensity to produce high amounts of plasmid, while the latter is mostly used for protein production. DH5α cells are characterised by three mutations: in recA1 and endA1 to promote plasmid insert stability and improve the quality of plasmid prepared in miniprep, and in lacZΔM15 to enable blue/white screening. More specifically, the recA1 mutation reduces deletion formation and plasmid multimerisation. The endA1 mutation inactivates an endonuclease, while the blue/white screening technique allows for a rapid identification of recombinant bacteria.

BL21(DE3) presents an inactivation of proteases (namely lon and ompT), which allow the increased levels of protein production by inactivating the protein degradation mechanism. It also contains a DE3 prophage derived from a bacteriophage λ. This prophage carries the T7 DNA polymerase gene that will be activated by the IPTG induction.

2.3.1 DH5α transformation and culture

2.3.1.1 Preparation of competent DH5α cells

RF1 buffer was made of rubidium chloride (2.4 g), manganese chloride tetrahydrate (1.98 g), potassium acetate (0.589 g), calcium chloride dihydrate (0.3 g) and glycerol (30 g). It was then filled up to 200 mL with dH_2O after the pH was adjusted to 5.8 with acetic acid. Finally, the mix was filter sterilised.

RF2 buffer was made of MOPS (3-(N-morpholino)propanesulfonic acid) (0.209 g), rubidium chloride (0.12 g), calcium chloride dihydrate (1.10 g) and glycerol (15 g). It was then filled up to 100 mL with dH_2O after the pH was adjusted to 6.8 with sodium hydroxide. Finally, the mix was filter sterilised.

SOB (Super Optimal Broth) media was made of bacto tryptone (peptone) (5 g), yeast extract (1.25 g), NaCl 5M (0.5 mL), KCl 1M (0.625 mL), $MgCl_2$ 1M (2.5 mL), $MgSO_4$ 1M (2.5 mL) and filled up to 250 mL with dH_2O before being autoclaved.

Competent cells were prepared using a rubidium chloride competent cells preparation method as following. A DH5α cell culture (one aliquot, which corresponds to 50 to 200 µL) was incubated at 37 ºC in 20 mL of SOB overnight. The next day, 2 mL of this culture were transferred into 200 mL SOB and grown at 37ºC until OD_{550} reached 0.45. It was then incubated on ice for 30 minutes before being spun at 750 xg and 4 ºC for 15 minutes. The pellet was then resuspended in 66 mL of RF1 and incubated on ice for 60 minutes, before being spun again with the same conditions as previously. The pellet was resuspended again in 16 mL of RF2 and incubated on ice for 15 minutes. It was then aliquoted and frozen on dry ice with methanol.

2.3.1.2 Transformation in DH5α cells

An aliquot of 100 µL of competent cells was thawed on ice. 1-2 µL of the provided pET30-CBR (for cytochrome b5 reductase) plasmid were then added and the tube was flicked gently a few times. It was then left on ice for 20 minutes before being heat shocked at 42 ˚C for 30 seconds and eventually put back on ice for two minutes. LB media (500 µL) was then added and the culture was incubated one hour at 37 ˚C and 180 rpm. During this time, agar plates were prepared using LB agar with the addition of kanamycin 100 µg/mL. After the incubation, the cells were spread onto the agar plates and left to dry. When dry, they were incubated overnight at 37 ˚C.

2.3.1.3 Cell preculture

On the next day, a preculture was set up with one colony from the plates in 5 mL of LB media and kanamycin 100 µg/mL. The preculture was then incubated at 37 ˚C and 180 rpm for 12-16 hours.

2.3.1.4 Miniprep

A miniprep kit from Monarch® was used according to the manufacturer's guidelines**.** The 5 mL preculture was first centrifuged at 4,700 xg for two minutes and the supernatant was discarded. The pellet was resuspended in 250 µL of resuspension buffer from the miniprep kit. The resuspension must be thoroughly performed by vortexing and pipetting up and down. Lysis solution (250 µL) from the miniprep kit were added and the tube was inverted 4-6 times in order to mix it. Neutralization solution (350 µL) from the miniprep kit were added and the tube was inverted 4-6 times, turning the solution cloudy. It was then centrifuged at 12,000 xg for 5 minutes and the supernatant was transferred on a spin column with a filter. This column was centrifuged 1 minute at 12,000 xg and the flow-through was discarded. 500 µL of wash solution were added and the column was centrifuged a second time at 12,000 xg for 30 to 60 seconds before discarding the flow-through. This last step was repeated a second time. A final 12,000 xg centrifugation was performed for 1 minute in order to remove residual solution before changing the collection tube. Elution buffer (50 µL, the elution buffer used here was distilled water) were eventually added and left to incubate at room temperature before a last 12,000 xg centrifugation for 2 minutes. The plasmids were collected from the collection tube and their concentration was measured on nanodrop. The plasmids were stored at -20 ˚C.

2.3.2 BL21(DE3) transformation and culture

2.3.2.1 Preparation of competent BL21(DE3) cells

The protocol for preparation of competent cells used was the same as the one used for the preparation of DH5α cells, except the cells used were BL21 (DE3).

2.3.2.2 Transformation in BL21 (DE3) cells

The transformation protocol used was the same as the one used for the transformation of DH5α cells, except the competent cells used were BL21 (DE3).

2.3.2.3 Cell preculture

Three precultures were set up with a different single colony put in three tubes, in 7 mL of LB media and kanamycin 100 µg/mL. They were incubated at 37 ˚C and 180 rpm overnight. After this step, glycerol stocks were prepared.

2.3.2.4 Cell culture

A large culture was then prepared using 1 L of LB media supplemented with 100 µg/mL kanamycin and 4 mL of the precultures. They were incubated at 37 ˚C and 180 rpm. The absorbance at 600 nm was monitored every hour until it reached 0.6. When this was achieved, the gene expression was induced by adding 0.5 mM IPTG and the culture was left to grow for 3 hours at 37 ˚C and 180 rpm. The cells were harvested by centrifugation at 5,524 xg for 10 minutes and resuspended in 20-30 mL of purification buffer

2.3.2.5 Cell lysis

The cell lysis was performed using sonication, after addition of protease inhibitor (1 µM pepstatin, 1.3 µM benzamidine, 1.8 µM leupeptin). The sonicator used was from Fisherbrand, model 120. The sample was kept on ice at all times in order to prevent overheating. Cycles of 40 seconds sonication and 20 seconds resting were repeated during approximately 15 minutes for a 50 mL sample. The amplitude used was 70 %. After sonication, the sample was centrifuged at 43,667 xg and 4 ˚C for 20 minutes. The supernatant was collected.

2.3.3 Protein purification and SDS-PAGE

As these two proteins were soluble, there was no need for an SMA extraction. However, it was purified on a Ni-NTA agarose resin the same way as for the previous protein (section 2.1.5.5). The same purification buffer was used as in section 2.1.5.2. 1 mL of bed volume resin was used per 10 mL of cell extract. The concentrations of imidazole required for the

elution of the protein from the column were the same. SDS gels were also made with 12% of acrylamide. Because higher levels of produced proteins were sometimes reached, higher numbers of elutions could be performed by visually evaluating the amount of protein in the column through its colour. In this case, up to 8 mL of elution buffer were run through the column in order to detach all of the protein of interest.

2.3.4 Protein quantification

The amount of soluble protein produced was measured using a DC (detergent compatible) protein assay kit (BioRad). Increasing concentrations of BSA were prepared (0, 0.025, 0.125, 0.25, 0.5, 0.75, 1, 1.5 and 2 mg/mL) in order to make a standard curve, as well as different dilutions of the protein of interest (1:1, 1:2, 1:5). 5 µL of each standard and sample were pipetted into microplate wells in triplicates. 25 µL of reagent A (an alkaline copper tartrate solution) were added, before eventually adding 200 µL of reagent B (a dilute Folin reagent). The plate was gently agitated and left at room temperature for 15 minutes. Absorbance at 750 nm was finally read on a plate reader.

2.4 Protein absorbance spectrum

SdeA and cytb5R's absorbance spectra measurement were performed according to what was found in the literature (Wahl *et al.* 2010). The cuvettes used had a path length of 1.0 cm. The protein concentration was approximately 200 µg/mL for SdeA and 5 mg/mL for cytb5R. They were both in purification buffer. The oxidised version of the spectrum was measured using the purified protein, while the reduced version was measured after treatment with sodium dithionite at different concentrations (2, 4 and 6 mM). The protein sample was incubated with the reducing reagent for a few minutes before measuring the absorbance spectrum.

2.5 Functional assay

The activity of the proteins SdeA and cytb5R was assayed together using $NADH,H^+$ and stearoyl-CoA, the substrates of the unsaturation reaction, with the two proteins. As $NADH,H^+$ absorbs strongly at 340 nm, while NAD^+ does not, the decrease of absorbance related to the consumption of $NADH,H^+$ was measured over time in a spectrophotometer. The $NADH,H^+$ concentration used for this assay was generally around 0.05 mM, which corresponded to an

OD_{340} of 0.456. The same concentration of FAD was used with 0.05 mM. The concentration of SdeA generally obtained after purification was around 0.2 mg/mL, which corresponds to 3.7 µM. As 750 µL were added, out of a total volume of 1 mL of reaction, the final concentration for SdeA was around 2.8 µM. The concentration of cytochrome b5 dehydrogenase used was more variable, as it was one of the main factors of the reaction speed. It was used at concentrations between 5 and 50 µM, generally at 16 µM. Finally, stearoyl-CoA was used at an excess concentration of a hundred times more than SdeA.

Stearoyl-CoA, $NADH,H^+$ and FAD were added to the eluted SdeA protein and the absorbance measurement was started. After a few minutes, the second protein cytochrome b5 dehydrogenase was added to the mixture and the absorbance at 340 nm was measured for approximately 30 minutes.

2.6 Antifungal drug testing

The inhibition of the desaturation reaction was measured using the same conditions as in the functional assay, but the reaction mixture was supplemented with different concentrations of the potential antifungal drug, starting with an excess concentration of 50 µM and decreasing towards the minimum inhibitory concentration (MIC) measured by F2G at 0.8 µM.

2.7 Bioinformatics

Protein and gene sequences were obtained from KEGG or Uniprot. Transmembrane domains predictions were performed via TMHMM software and CCTOP software. Sequence alignments were performed on BLAST. Conserved regions from each proteins were analysed in Interpro.

3. SdeA

3.1 Membrane protein production prediction

In order to predict if the production of these membrane proteins in yeast was going to be successful, several parameters could be considered. They have been compiled in a paper for expression and solubilisation in yeast (White *et al.* 2007). Size and hydrophobicity can be the two main factors one can think for the successful expression of a membrane protein, but it gets a little more complex than this. Optimal conditions can be found with properties for both DHODH and SdeA in the following table.

Parameter	Optimal conditions in yeast for a minimum of 40% of proteins highly expressed	DHODH (+tags)	SdeA (+tags)
Size (kDa)	< 60 kDa	61.55	57.12
GRAVY score	< 0.2	-0.37	-0.24
Codon Adaptation Index	> 0.15	0.70	0.66
pI range	< 8	8.35	8.44
% of aromatic residues	< 14 %	5.2 %	11 %
Number of TM domains	< 6	1	4
% of protein in TM domains	< 20 %	3.3 %	18.3 %
% of hydrophobic residues in TM segments	> 70 %	79 %	84 %
% of charged and polar residues in TM segments	< 12 %	0 %	5.7 %

Table 3.1: Prediction of the successful production of both SdeA and DHODH according to several parameters. *Both proteins match every single parameter's optimal conditions, with the exception of protein size and pI range. The difference with optimal conditions is however minimal.*

Gravy score stands for grand average of hydropathy, and is calculated from the sum of hydropathy values of each amino acid constituting the protein sequence, in order to provide a general score of hydropathy for the protein, usually between -2 and 2. Positive values mean higher level of hydrophobicity. A correlation between higher hydrophilicity and higher levels of expression was already observed for proteins in general (Goh *et al.* 2004), but this can be a bit more counter-intuitive for membrane proteins. It was also shown to be the case by White *et al.* as lower GRAVY scores were shown to increase high-expression probability. An online tool was used to calculate DHODH and SdeA's scores (http://www.gravy-calculator.de/).

The Codon Adaptation Index (CAI) is an effective measure of synonymous codon usage bias. It is the ratio of usage of each codon, to that of the most abundant codon for a given amino acid. It may give an approximate indication of the likely success of the heterologous gene expression. An online tool (https://www.biologicscorp.com/tools/CAICalculator/) calculates CAI according to the relative synonymous codon usage of a reference sequence or existing expression host organisms (in this case, *Pichia pastoris*).

The pI or isoelectric point for a protein is the pH of a protein solution at which the net charge of the protein becomes zero. A higher pH means a protein becomes negatively charged and vice versa. The general trend for this parameter seems to favour a lower pI (Mehlin *et al.* 2006; White *et al.* 2007), although there does not seem to be hard evidence as to why this is the case.

The percentage of aromatic residues also seems to be negatively correlated with high levels of expression of proteins in yeast. The same observation can be made for the percentage of protein included in transmembrane domains. It was calculated using the sequence of each protein (Figure 3.1).

Overall, these parameters tend to show both proteins match very well all the optimal requirements for expression in *P. pastoris*. They may both be slightly large, but they have few enough transmembrane domains and are not too hydrophobic to be expressed correctly.

A.

MSAKPADASRPRAGDPKKVHIADTAITRQNWYKHVNWLNVFLIIGIPLYGCIQAFWVPLQ
LKTAIWAVVYYFFTGLGITAGYHRLWAHCSYSARLPLRIWLAAVGGGAVEGSIRWWARDH
RAHHRYTDTDKDPYSVRKGLLYSHIGWMVMKQNPKRIGRTDITDLNEDPVVVWQHRNYLK
VVLVMGLVVPMLVAGLGWGDWFGGFIYAGILRIFFVQQATFCVNSLAHWLGDQPFDDRNS
PRDHVITALVTLGEGYHNFHHEFPSDYRNAIEWHQYDPTKWTIWIWKQLGLAYDLKQFRA
NEIEKGRIQQLQKKIDQKRAKLDWGIPLDQLPVMEWDDYVEQAKNGRGLIAIAGVVHDVT
DFIKDHPGGKAMINSGIGKDATAMFNGGVYNHSNAAHNLLSTMRVGVIRGGCEVEIWKRA
QKESGEYVRDESGQRIIRAGQQVTKIPDPIPTADAAALEQKLISEEDLNSAVDHHHHHH

B.

MHHHHHHSSGLVPRGSGMKETAAAKFERQHMDSPDLGTDDDDKMVANSTSLAWKSAGLRARAVPSLRC
SHRSSVLHRQAAFQQHGAVRHASSTTSEAAEAVKEAPKKAGRGLKRTVYGTSLVLAALVGYVYATDTR
ASIHRYAVVPLVRTLYPDAEEAHHIGVEALKTLYKYGLHPRERGNQDGDGVLATEVFGYTLNNPIGIS
GGLDKHAEIPDPLFAIGPAIVEVGGTTPLPQEGNPRPRVFRLPSQKAMINRYGLNSLGADHMAAILER
RVRDFAYANGFGLHDEAEQRVLDGEAGVPPGSLQPGRLLAVQIAKNKATPDSDIEAIKRDYVYCVDRL
AKYADILVVNVSSPNTPGLRDLQATAPLTAILKAVVSAAKGVDRKTKPYVMVKVSPDEDSDEQVSGIC
DAVWHSGVDGVIVGNTTNRRPAPLPHGFTLPPKEQSTLKETGGYSGPQLFDRTAALVARYRALLDAPP
TPASDANETDQAKELAAAVTRAEPDVENVPAVEPPTPANRPARKVIFASGGITNGKQAQAVLDAGASV
AMMYTAVTYGGIGTVTRVKQELREEKKNRQ

Figure 3.1: Amino-acid sequences of SdeA (A.) and DHODH (B.). *Transmembrane domains are highlighted in grey. They were determined using transmembrane domain prediction softwares (detailed in figure 3.5 and 3.6) with hydrophobic residues within those in bold and polar residues underlined. Aromatic residues throughout the sequence are in italic. His-tags are positioned at different ends because SdeA was integrated in a vector containing the tag on its C-terminal end, while DHODH was provided by our industrial partner with a series of tags that were present on the N-terminal end, which we kept.*

3.2 Yeast transformation

Transformation of the SdeA plasmid into *P. pastoris* X-33 yeast was performed using either electroporation or chemical transformation. This strain was chosen because the protein of interest had already been successfully expressed in this host previously. The plasmid used for this transformation (Figure 3.2) could be performed using either circular or linear plasmid but linear plasmid was favoured for several reasons: first it required a much lower amount of plasmid (10 times less). Second, transformation with linear plasmid favoured homologous recombination in the genome, which was the desired transformation process. Another possibility when transforming yeast cells is to use episomal plasmids, where homologous recombination does not happen. While this method has been successfully used in *S. cerevisiae* (Chen *et al*. 2012), it has not been used much in *P. pastoris* (Dilworth *et al*. 2018),

despite some promoters being available (Sasagawa *et al.* 2011). Moreover, the plasmids that have been traditionally used in the lab (pPIC) do not present an origin of replication for yeast, making them unsuitable for this method. Episomal plasmids can also be less stable over time compared to recombination in the genome (Hohnholz, Pohlmann, and Achstetter 2017).

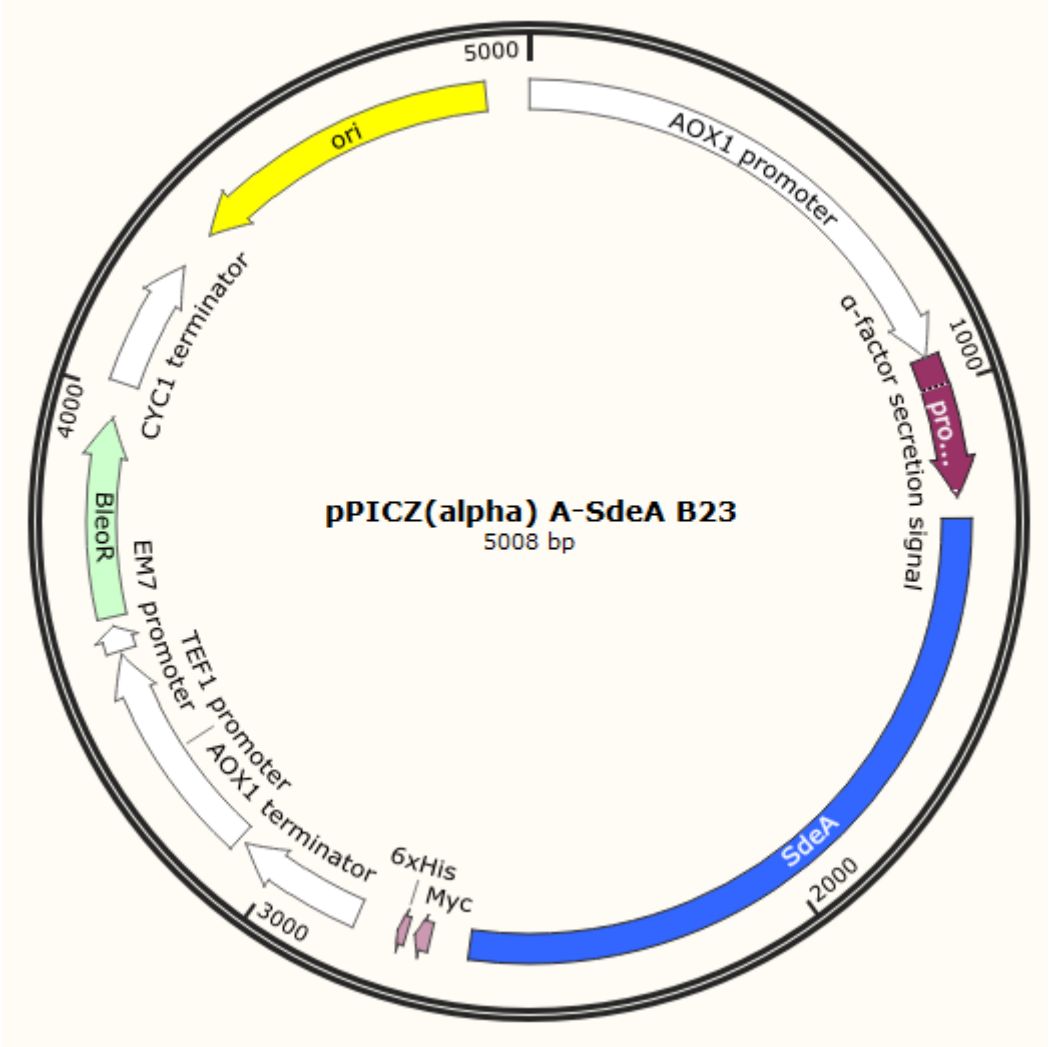

Figure 3.2: Plasmid map used for transformation of SdeA into* P. pastoris *cells. *The vector used is a pPICZ(alpha) A containing an origin of replication for plasmid production in bacteria, an AOX1 promoter and terminator for double homologous recombination, an α-factor secretion signal traditionally used for secreted proteins, but that seemed to show better results for membrane protein production according to other researchers in our lab. Finally, the SdeA sequence (blue) contained two tags on the C-terminal part of the sequence: a 6xHis-tag and a Myc-tag. It also contained a 3' extra region between the protein sequence and the tags, which was showing better protein production properties according to another researcher in our lab (Sarah Routledge, personal communication) who had worked on this protein earlier. The his-tag was positioned in the C-terminal part of the gene so that it would be the furthest away possible from the membrane segments, thus making it more available for purification purposes.*

The minimum size of homology between the plasmid and the genome for correct homologous recombination can be quite variable according to the system used, but it makes sense that the longer this sequence is, the less likely incorrect recombinations may happen. A homology of 100 bp or longer can be a good starting point for expecting correct recombination (Kuzminov 2011).

Chemical transformation was the preferred method due to technical issues encountered with the electroporation machine. After the cells were streaked onto YPD plates with a zeocin concentration of 100 µg/mL, a dozen colonies were put into liquid culture and checked under a microscope (Figure 3.3). The cells were looking healthy, with many of them seen budding, which is the way *P. pastoris* cells replicate. In order to select colonies further, each of the cultures were streaked again on a YPD plate containing 10 times more zeocin (1000 µg/mL). From this plate, only two colonies grew well, but one of them was much faster than the other, thus this one was selected for protein production.

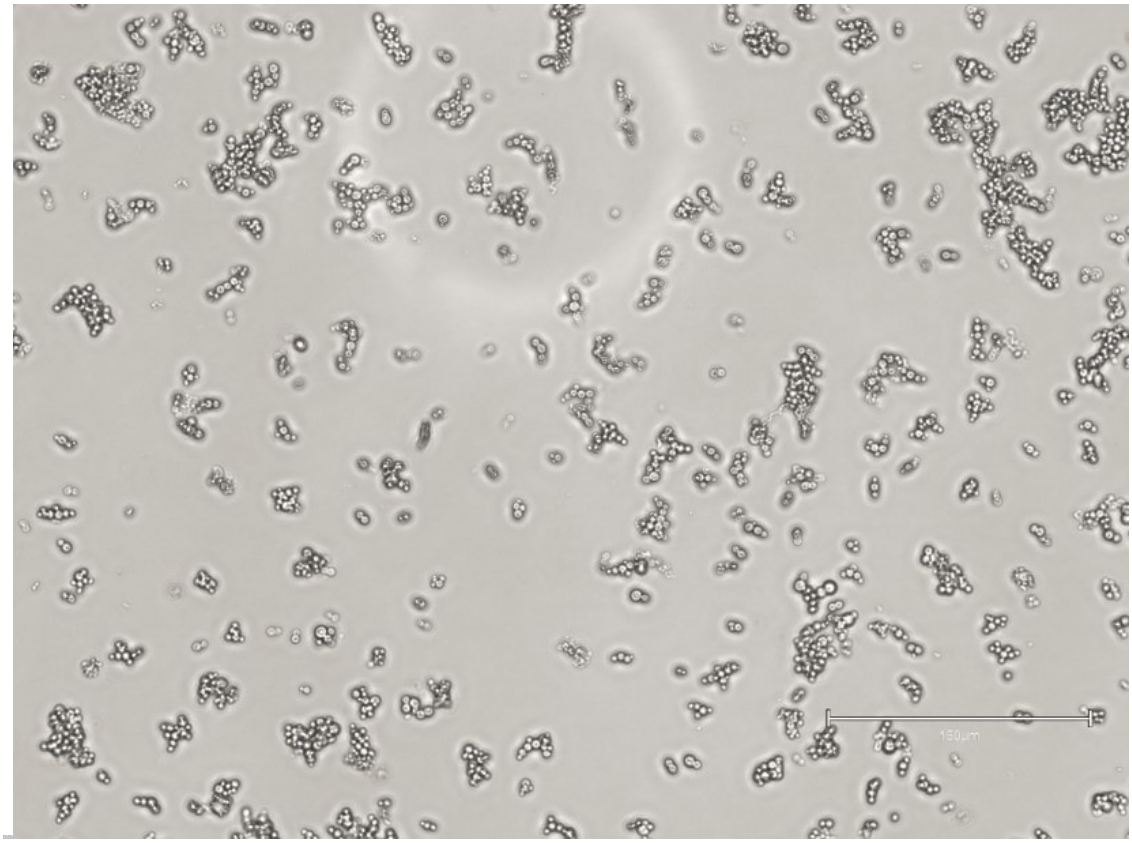

Figure 3.3: Microscope visualisation of one of the* P. pastoris X-33 *yeast cultures using microscope Evos m5000 from Invitrogen. *Scale bar in the bottom right hand corner represents 150 µm.*

3.3 Culture of SdeA-expressing *P. pastoris*

Using the same method as previously described, one culture showed some growth after an incubation time that was longer than expected during phase 1 (Incubation of a single colony into 50 mL BMGY), so further cultures were performed altering various parameters during the first phase of incubation. One of them was set up with half the amount of media traditionally used. A second one was set up without zeocin during phase 1. The last one was left incubated for 48h instead of 24h. After 24h of incubation at 30 ˚C and 200 rpm, there was no growth observed in the two first cultures, whereas the last one showed a nice cloudy media after 48h of incubation. If the first two cultures were left 48h instead of the usual 24, they did also show some growth. It was resuspended in larger amounts of BMMY and still showed a nice growth. The cell pellets were weighed and then broken using either glass beads, French press or an Emulsiflex-C3. The amount of membranes obtained was finally weighed following ultracentrifugation.

This culture procedure was repeated several times, with the OD_{600} measured throughout one of the cultures in order to check the growth pace of the culture (Figure 3.4). During the first part of the culture, the lag phase lasted approximately 10 hours before the growth phase started. The stationary phase was reached after around 30 hours. Then, a small volume of this first culture was diluted into a larger culture in order to reach a higher number of cells. The same logarithmic growth curve appeared, but there was no lag phase this time, probably due to the different initial cell concentration. Finally, after the second stationary phase was reached, another small volume of the culture was diluted into a different medium (with methanol) in order to induce the protein expression, since methanol induces the protein expression while glycerol represses it. After this experiment, the following cultures were grown each time with 36 to 48h incubation during phase 1 of the cell culture. The obtained yields for each of them are summarised in table 3.2.

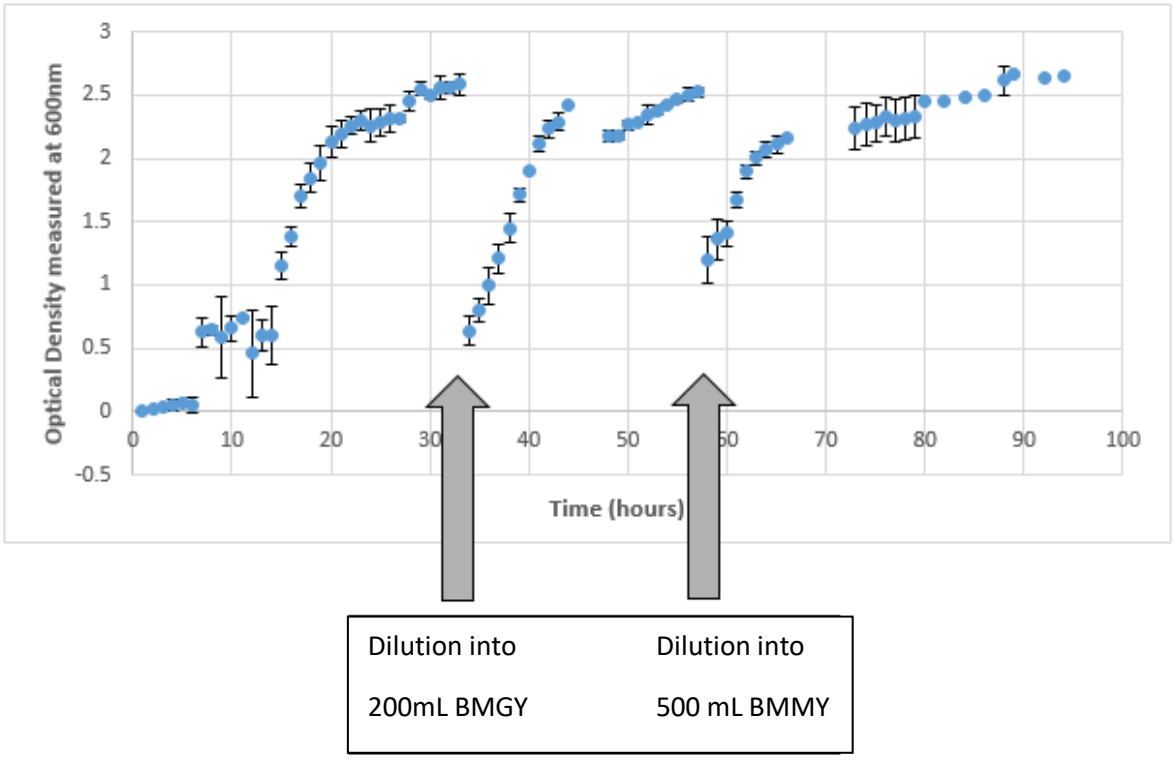

Figure 3.4: OD_{600} monitoring* P. pastoris *cell culture. *The cells were cultured in baffled flasks, first in 50 mL BMGY, before 5 mL of this culture were resuspended into 200 mL of the same media, which represses protein expression. They were then centrifuged and resuspended into 500 mL BMMY to induce protein expression. The OD_{600} was monitored every hour using a spectrophotometer.*

Experiment number	Total mass of cells obtained (g)	Mass of membranes obtained (g)	Ratio membranes / cells	Total volume of the culture (L)	Mass of membranes per litre of culture (g/L)
1	5.50	0.66	0.12	0.75	0.88
2	22.96	2.0	0.09	2	1.0
3	56.54	10.12	0.18	5	2.02
4	22.9	2.39	0.10	1.5	1.59
5	19.0	3.36	0.18	1.5	2.24

Table 3.2: Comparison of the yields of membranes containing SdeA obtained in each cell culture experiment. *The ratio of membranes / cells is calculated as well as the yield of membranes per litre of culture.*

The OD_{600} was measured at the end of experiments 4 and 5, just before cell harvesting. It was 2.30 for experiment 4 and 2.51 for experiment 5. The lower yields obtained in the first experiments are reflective of improved cell culture technique throughout the thesis.

The membranes were eventually resuspended at a concentration of 180 mg/mL by measuring the weight of the membranes collected and resuspending them in resuspension buffer, before freezing them at -80 ˚C.

3.4 Protein purification

After the membranes were collected from the cultures, they were diluted to 90 mg/mL in purification buffer and solubilised using 2.5 % (w/v) SMA2000 for an hour at room temperature. Following ultracentrifugation to harvest the solubilised proteins, SdeA was then purified by affinity chromatography using Ni-NTA resin, and eluted with imidazole. The protein content for each step of the procedure was then visualised on SDS-PAGE gels and on a western blot (Figure 3.5).

As can be observed on the first gel, SMA effectively solubilised a number of membrane proteins, but there are still quite a lot that remained in the insoluble pellet. The majority of these solubilised proteins did not bind to the resin but went directly to the flow-through instead. The lanes corresponding to the washings are essentially clear, meaning the resin did not contain any leftover protein that was not properly bound to it. Upon the addition of a higher amount of imidazole on the elution lanes, bands corresponding to proteins at a size of approximately 60 kDa can be observed coming out of the column.

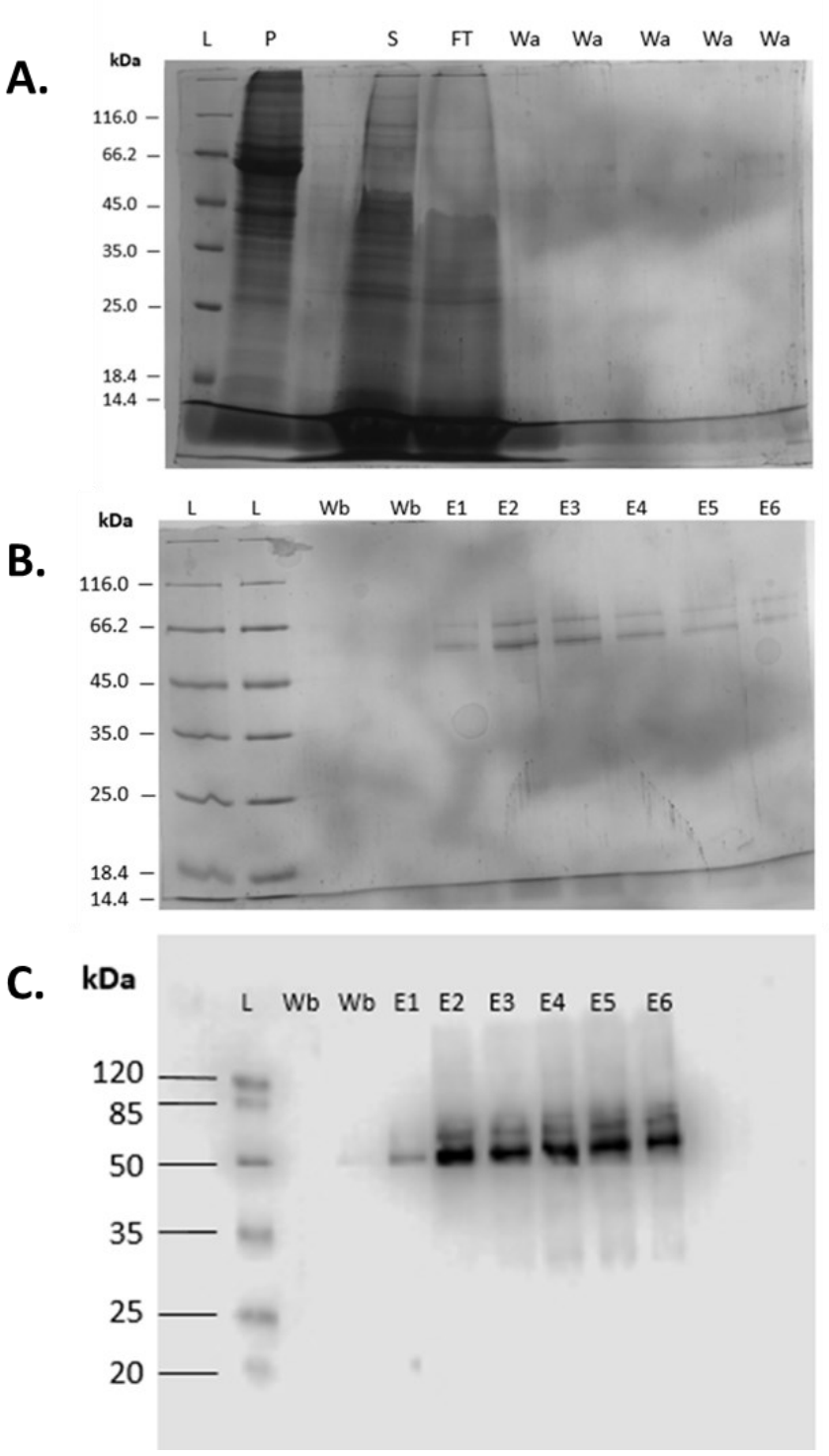

Figure 3.5: SDS-PAGE gels (A. and B.) and western blot membrane (C.) for SdeA*. Membranes were solubilised at a concentration of 90 mg/mL for one hour at room temperature with SMA2000, and the soluble fraction was harvested after an ultracentrifugation of 100,000 xg for 20 minutes at 4 ˚C. A and B are SDS-PAGE gels made with 12% polyacrylamide after purification via Ni-affinity chromatography, using 1 mL of nickel resin. C is a western blot experiment performed on a PVDF membrane with a mouse anti-His primary antibody and an anti-mouse HRP-linked secondary antibody. In each part of the figure, L stands for ladder, P and S stand for pellet (non-soluble membranes) and supernatant (soluble membranes) respectively. Wa are the washings performed with 50 mL of 20 mM imidazole in purification buffer. Wb are the washings performed with 20 mL of 40 mM imidazole in purification buffer, while E1 to E6 are the elutions performed with an imidazole concentration of 200 mM. SDS-PAGE were stained with InstantBlue and visualised on a GelDoc (BioRad). The western blot was visualised by chemiluminescence on a Li-Cor C-Digit.*

Surprisingly, all of the SDS gels and western blots performed showed at least two, if not more, bands during the elutions. One of them was usually at around 55 to 60 kDa and the second one a bit higher around 65 kDa. The lower size band would match the expected size for SdeA, while the larger one would be slightly too large. The lower size band seemed to be relatively more intense than the larger band.

These different bands were first checked on a western blot using an anti-his primary antibody directed against SdeA's 6xHis-tag, followed by a secondary anti-mouse HRP antibody. Again, the same two bands were observed, with the same relative intensity. These two bands have been checked on mass spectrometry by another researcher in our lab group, who found they both corresponded to SdeA (David Hardy, personal communication).

Another important feature from these gels is that there is a massive band in the pellet column, corresponding to the same size as the protein of interest. If it was indeed SdeA, this could mean that the solubilisation is not very efficient, leaving a huge amount of the produced protein behind. However, as none of the protein seems to be found in the flow-through, nor seemingly any other protein than SdeA in the elution lanes, the purification with the resin worked very well.

3.5 Investigation on the multiplicity of bands

In order to understand the multiplicity of bands that was observed, a first hypothesis was investigated, that the protein may be glycosylated. To begin investigating if there were any potential glycosylation sites in SdeA, the first step was to look at the topology of the protein, the location of the transmembrane regions and the connecting loops. The crystal structure of the protein in the membrane is not clearly elucidated, but transmembrane regions can be predicted from the sequences using a range of different softwares. First, a transmembrane (TM) domain prediction was performed using the software TMHMM (Figure 3.6a).

Three TM domains were clearly identified by TMHMM (in red on the figure), as they reached 1 on the vertical axis, which is the highest probability. Other potential TM domains could be spotted but they are considered much less likely to actually be present in the protein. The blue and pink lines respectively show the cytosolic and luminal parts of the protein. However, this conformation did not match the expected conformation proposed by the partner company F2G (Figure 3.6b), in which four TM domains were shown.

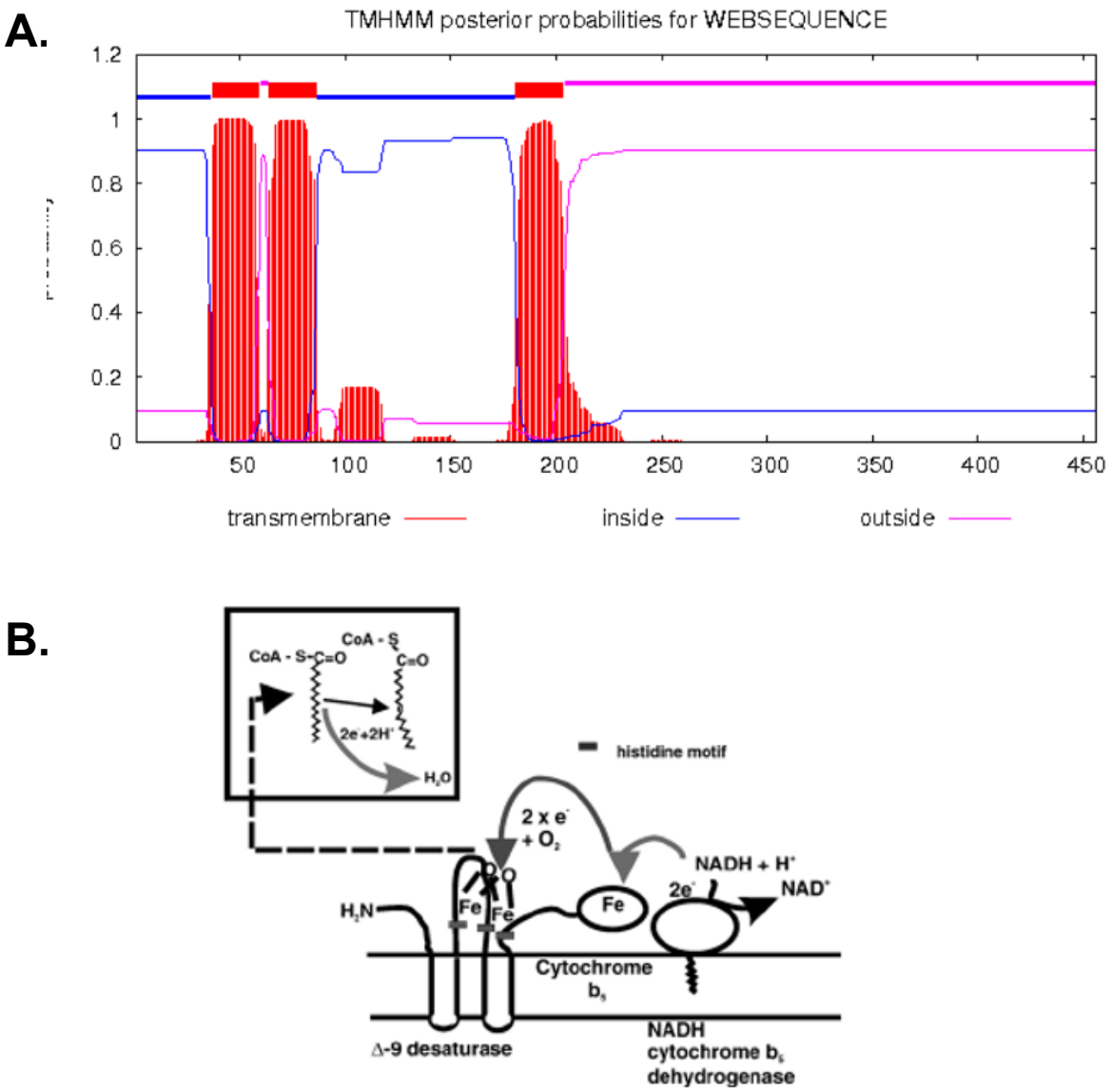

Figure 3.6: Investigation on SdeA's membrane conformation. *a. Conformation of SdeA in the ER membrane according to TMHMM. Three TM domains are identified (red). b. Proposed schematic of SdeA (Δ-9 desaturase) provided by F2G. Four TM domains are illustrated.*

Therefore, several other TM prediction softwares were used (Figure 3.7). Although there is some variation between them, there does seem to be a relative accordance about the presence of the fourth TM domain, which would be found immediately after the third one. This also agrees with the structure found for the human version of SdeA, called SCD1 (Figure 3.8), for which the crystal structure was quite recently elucidated (Wang, Klein, *et al.* 2015).

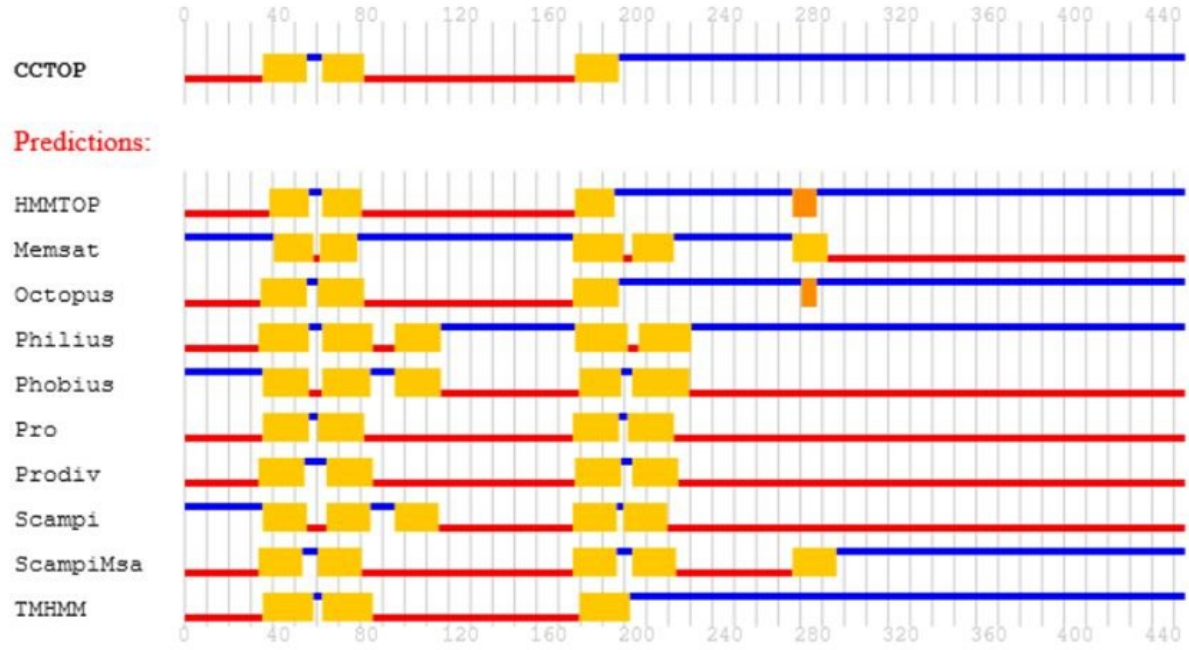

Figure 3.7: TM domain predictions according to several softwares*. TM domains are represented with yellow rectangles, while red and blue lines correspond respectively to luminal and cytosolic sides of the protein. Three of these domains are clearly identified in all of them, but they differ on the presence of the fourth one. It appears it is most likely to be found right after the third domain. Data gathered from the CCTOP TM domain prediction website (Link: http://cctop.ttk.hu/).*

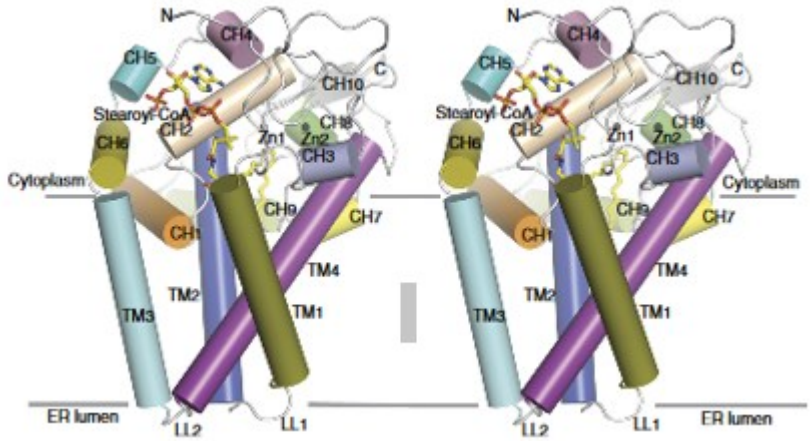

Figure 3.8: TM domains found in SCD1, the human version of SdeA. *They show four TM domains, with two very small sequences in the ER lumen and the active part of the protein on the cytoplasmic side (Wang, Klein, et al. 2015) (PDB code 4ZYO).*

A.

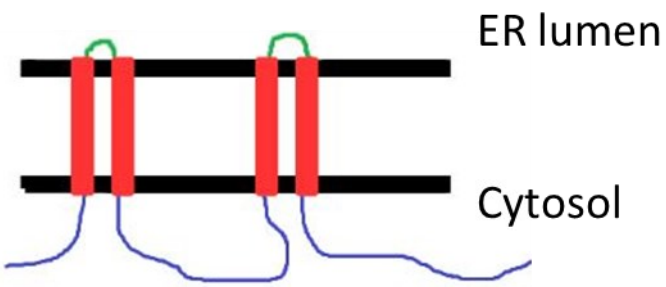

B.

NW Score	Identities	Positives	Gaps
334	123/498(25%)	188/498(37%)	181/498(36%)

```
Query   1    MSAK------------------PADASRPRAGDPKK---VHIAD------------TAI  26
             M A                    P        GD  +   +++ D             T
Sbjct   1    MPAHLLQDDISSSYTTTTTITAPPSRVLQNGGDKLETMPLYLEDDIRPDIKDDIYDPTYK  60

Query   27   TRQNWYKHVN--WLNVFLIIGIPLYGCIQAFWVPL-QLKTAIWAVVYYFFTGLGITAGYH  83
              ++     V   W N+ L+  + L          +P  +  T +W + YYF + LGITAG H
Sbjct   61   DKEGPSPKVCYVWRNIILMSLLHLGALYGITLIPTCKFYTWLWGVFYYFVSALGITAGAH  120

Query   84   RLWAHCSYSARLPLRIWLAAVGGGAVEGSIRWWARDHRAHHRYTDTDKDPYSVRKGLLYS  143
             RLW+H SY ARLPLR++L      A +  +  WARDHRAHH++++T  DP++ R+G  +S
Sbjct   121  RLWSHRSYKARLPLRLFLIIANTMAFQNDVYEWARDHRAHHKFSETHADPHNSRRGFFFS  180

Query   144  HIGWMVMKQNP--KRIGRT-DITDLNEDPVVVWQHRNYIKVVLVMGLVVPMLVAGLGWGD  200
             H+GW++++++P  K  G T D++DL  + +V++Q R Y   +L+M  ++P LV   WG+
Sbjct   181  HVGWLLVRKHPAVKEKGSTLDLSDLEAEKLVMFQRRYYKPGLLMMCFILPTLVPWYFWGE  240

Query   201  WFGGFIYAGILRIFFVQQATFCVNSLAHWLGDQPFDDRNSPRDHVITALVTIGEGYHNF  259
              F   ++ A  R  V  +T+ VNS AH  G +P+D   SPR+++ +L  +GEG+HN+
Sbjct   241  TFQNSVRATFLRYAVVLNATWLVNSAAHLFGYRPYDKNISPRENILVSLGAVGEGFHNY  300

Query   260  HHEFPSDYR-NAIEWHQYDPTKWTIWIWKQLGLAYDLKQFRANEIEKGRIQQLQKKIDQK  318
             HH FP DY  +   WH  + T + I     LGLAYD                +KK+
Sbjct   301  HHSFPYDYSASEYRWH-INFTTFFIDCMAALGLAYD----------------RKKVS--  340

Query   319  RAKLDWGIPLDQLPVMEWDDYVEQAKNGRGLIAIAGVVHDVTDFIKDHPGGKAMINSGIG  378
                                                          KA I + I
Sbjct   341  ----------------------------------------------KAAILARIK  349

Query   379  KDATAMFNGGVYNHSNAAHNLLSTMRVGVIRGGCEVEIWKRAQKESGEYVRDESGQRIIR  438
             +     +  G
Sbjct   350  RTGDGNYKSG                                                  359

Query   439  AGQQVTKIPDPIPTADAA  456
```

Figure 3.9: a. Representation of the most probable conformation of SdeA in the ER membrane. b. Comparison of the sequences of SdeA (Query) and SCD1 (Sbjct) on BLAST. *The TM domains are circled in red. The conserved area (green) is the fatty acid binding conserved region. It orientates the protein, with the C and N extremities being on the cytoplasmic side and the small sequences between TM domains being in the ER lumen.*

A sequence alignment of SdeA with the human SCD1 was undertaken (Figure 3.9b). It can be seen that the TM regions from the SCD1 structure align well with the four predicted TM regions for SdeA, Also importantly, the conserved fatty acid binding site is aligned.

Taken together, this data appears to show that the fungal version of the enzyme follows a very similar structure that of the human version (Figure 3.9a).

During the completion of this thesis, a new tool was made available for researchers to determine the 3D structure of proteins, called AlphaFold. This tool allows to predict with very interesting confidence scores the three-dimensional structure of a protein (Figure 3.10). Again, the data collected from this tool strongly suggests the presence of four transmembrane domains, with a very small luminal area and a predominantly cytosolic presence of this membrane protein.

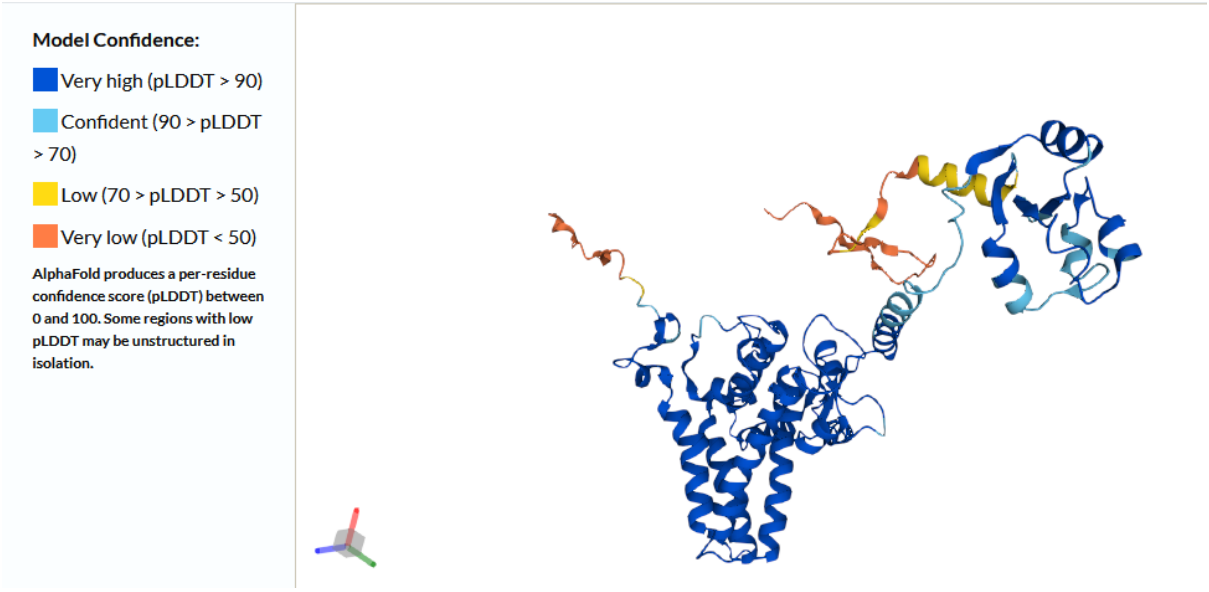

Figure 3.10: AlphaFold model predicted for SdeA. *Again, four transmembrane domains are very easily observable at the bottom part of this representation, with a very high confidence. Data collected from Uniprot website (https://www.uniprot.org/uniprotkb/Q4WGR1/entry#structure).*

Glycosylation sites were then investigated on the luminal side of the protein since they are normally present on the non-cytosolic side of membrane proteins. As this side is very small, only one site appears as a potential O-glycosylated site: Threonine 63 between TM1 and 2 (Figure 3.8b). Thus, it looks like glycosylation can be quite unlikely to be the reason for this double band issue, considering the presence of only one glycosylation site on the size-limited lumenal side of the protein, but remains a possibility.

3.6 Solubilisation optimisation

3.6.1 Solubilisation efficiency calculation

Despite the fact that some of the protein has been successfully purified, there was a concern that a large amount of the expressed SdeA was being lost during the solubilisation step.

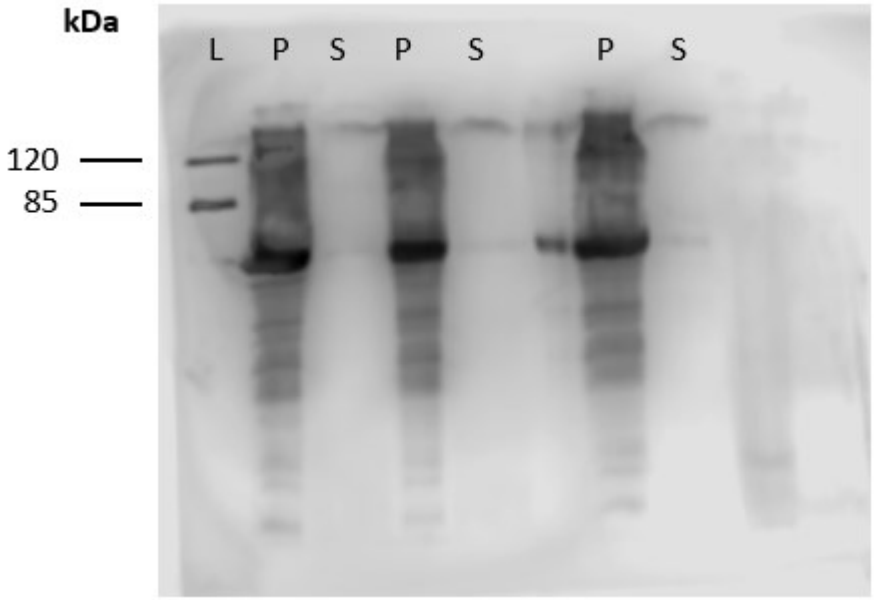

Figure 3.11: Western blot performed in order to measure SdeA's solubilisation efficiency with SMA2000. *P stands for pellet (insoluble part) and S for supernatant (soluble part). Membranes were solubilised at a concentration of 90 mg/mL during one hour at room temperature, with 2.5 % (w/v) SMA2000 polymer. A 100,000 xg centrifugation step was performed for 20 minutes at 4 ˚C to separate soluble and insoluble parts. A primary mouse anti-his antibody was used, followed by a secondary anti-mouse HRP antibody.*

A western blot was performed in order to quantify the solubilisation efficiency (Figure 3.11). Using an anti-his antibody, the solubilisation efficiency was calculated through densitometry on ImageJ. An average solubilisation efficiency value of 5.3% was measured with a standard deviation of 0.012 using this method. Considering this really low value, it was thought adjustments could be made to the solubilisation procedure in order to improve this issue. However, it is possible that this large amount of unsolubilised protein could correspond to aggregated protein that would be difficult to reach and solubilise.

3.6.2 Solubilisation improvement attempts with SMA2000

Several attempts were made to try to improve this solubilisation efficiency. Different temperatures (4 or 37 ˚C) and incubation times (4h or overnight) were tested without offering

any improvement. A sonication of membranes before or during solubilisation was also tested with no improvement. Different pH values for the buffer ranging from 7 to 9 were also tested (Figure 3.12). As SMA polymers are quite sensitive to low pH values, due to the maleic acid moiety getting protonated and losing its solubilisation properties, the pH values tested were not lower than 7.0. Unfortunately, this SDS-PAGE did not seem to show any significant improvement in the solubilisation efficiency for this protein, and the vast majority of SdeA looked like it was still in the pellet. No western blot experiment was performed on these samples due to the results looking already quite clear on this SDS-PAGE.

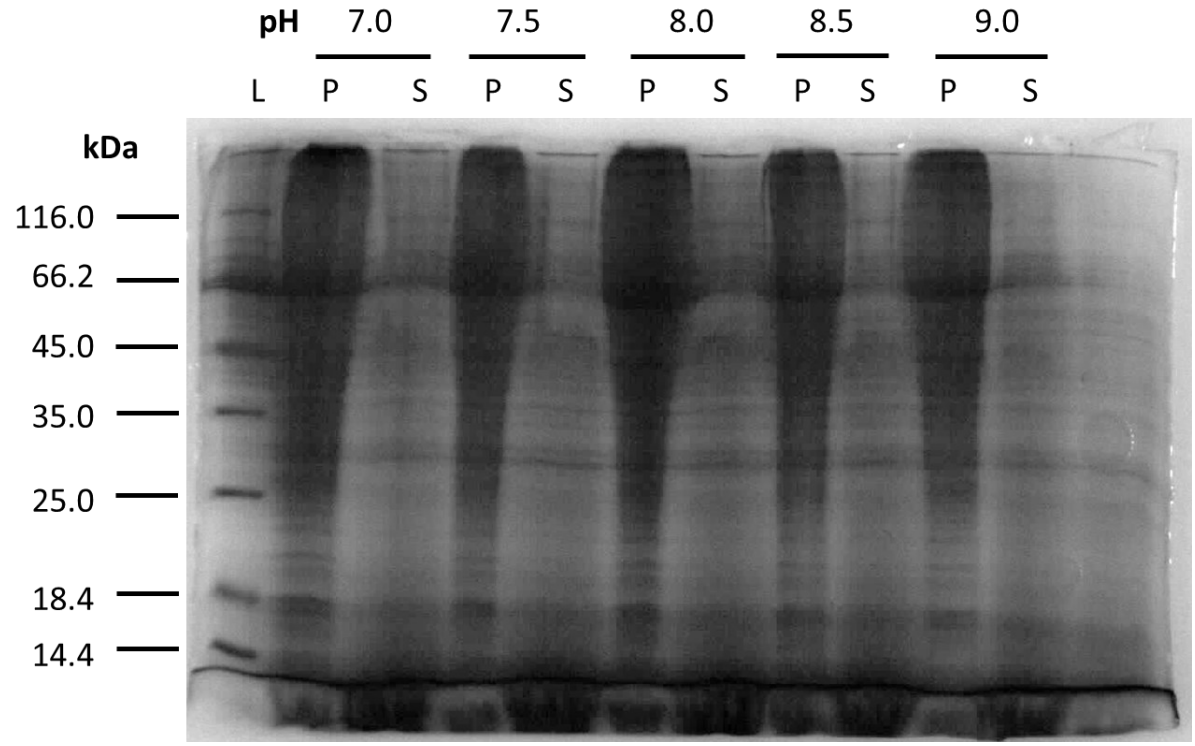

Figure 3.12: SDS-PAGE gel performed after different pH values were tested during the solubilisation step with SMA2000. *P stands for pellet (insoluble part) and S for supernatant (soluble part). Membranes were solubilised at a concentration of 90 mg/mL during one hour at room temperature, with 2.5 % (w/v) SMA2000 polymer. A 100,000 xg centrifugation step was performed for 20 minutes at 4 ˚C to separate soluble and insoluble parts.*

3.6.3 Use of different polymers

Another possibility to improve solubilisation efficiency was to try different SMA polymers. Several SMA polymer variants provided by Orbiscope were tested, namely SMALP200, SMALP300 and SMALP502E (Figure 3.13). They exhibit subtle different properties, most importantly in their S:MA ratio varying from 1.5:1 to 3:1 (Table 3.3). Furthermore, SMA502E is esterified on one of the carboxyl groups in the maleic acid with an aliphatic structure.

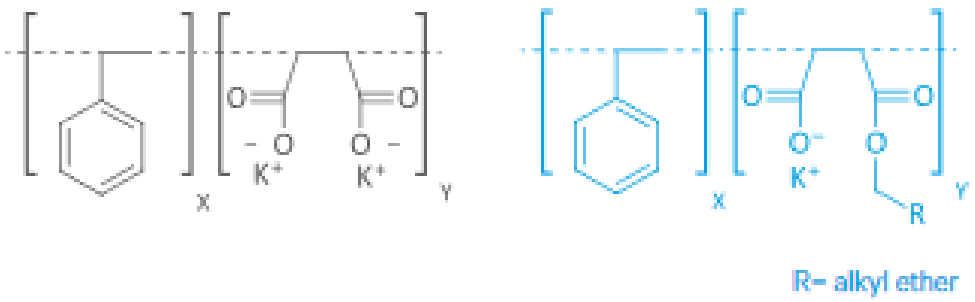

Figure 3.13: Chemical structures of the polymers used during solubilisation assays. *SMALP 200, 300 and 2000 are reprensented in black on the left-hand side. The esterified SMALP 502E is represented in blue on the right-hand side. Structures taken from Orbiscope's website.*

Polymer	SMALP200	SMALP300	SMALP502E	SMA2000
S:MA ratio	2:1	3:1	1.5:1	2:1
Molecular weight M_w (kDa)	6.5	10.0	7.0	7.5

Table 3.3: Comparison of properties of the different polymers tested. *Data gathered from Orbiscope's website for SMALP 200, 300 and 502E, or from Cray Valley for SMA2000 (Morrison* et al. *2016).*

While polymers SMALP200 and SMALP300 were quite viscous, hence more difficult to manipulate, SMALP502E was quite soluble and easier to work with, just like SMA2000. This is most likely due to the fact that the Orbiscope polymers were provided as concentrated solutions while SMA2000 was used as a powder. The explanation for SMALP502E being soluble could reside in its slightly different hydrophobicity profile, although we did not have access to its exact composition. After solubilisation with each of these polymers and purification on an affinity column, SDS-gels were performed to compare them. Again, none of them showed better results than the traditionally used method, with viscous SMALP300 polymer barely yielding any purified protein at all (Figure 3.14). As SMALP300 seems to be the least successful polymer, it can be assumed that the S:MA ratio needs to be as close as possible to 2:1, while the molecular weight should be around 7 kDa.

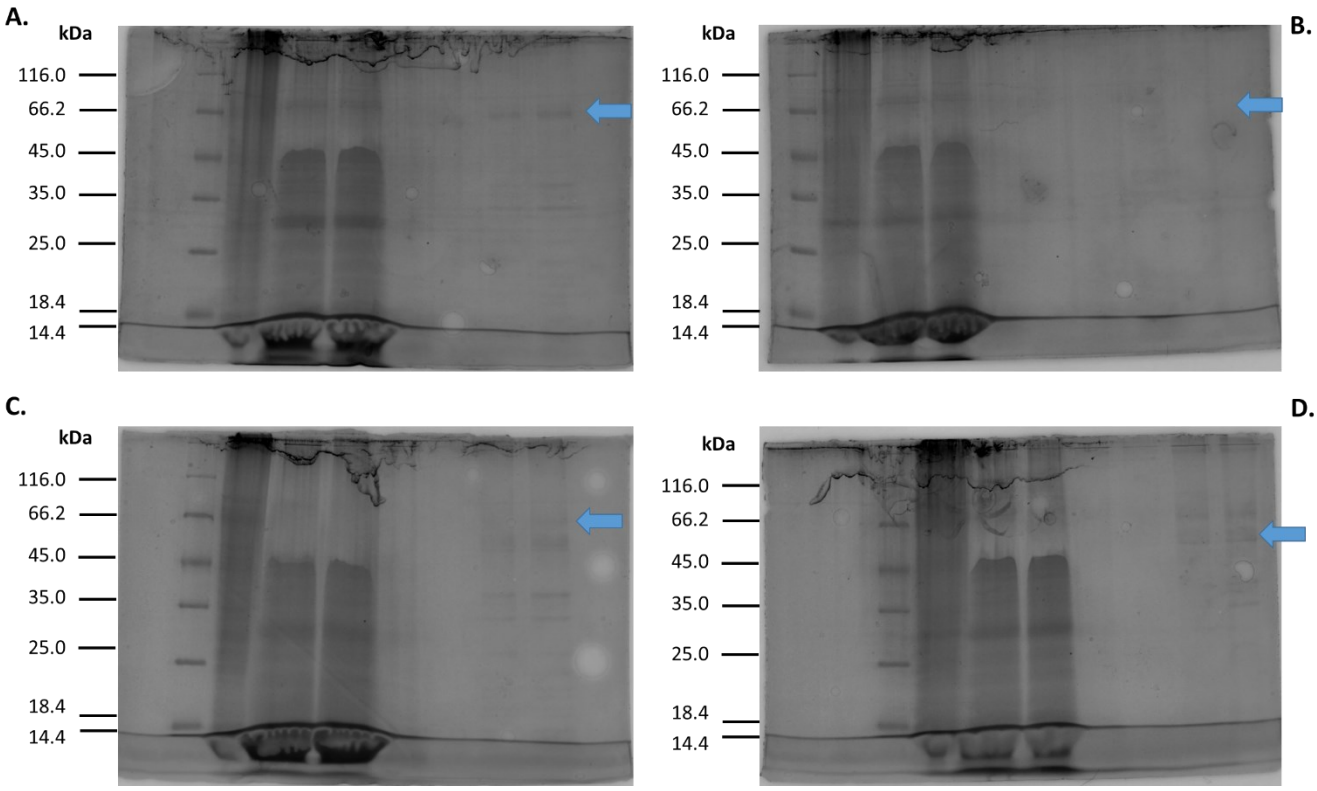

Figure 3.14: SDS-PAGE gels from the different solubilisations performed with each polymer. *A. SMALP200. B. SMALP300. C. SMALP502E. D. SMA2000. Each solubilisation has been carried out the same way, with membranes being solubilised at a concentration of 90 mg/mL during one hour at room temperature, with 2.5 % (w/v) of polymer. The soluble part was then purified by Ni-affinity chromatography and the protein was eluted with 200 mM imidazole. Each fraction was then loaded on SDS-PAGE. Bands corresponding to SdeA's size are highlighted with blue arrows.*

Interestingly, it can be observed that while SMALP 502E and SMA2000 are showing the same sort of double band as what has previously been observed. SMALP200 seems to be showing only one of them.

3.6.4 Use of detergents

Alternatively, since solubilisation with SMA polymers did not seem to show any improvement with different conditions, another method was investigated, relying on the use of detergents. They would be expected to show better solubilisation efficiencies due to the membrane getting fully broken up. Different detergents (DDM, DG, OG, LMNG and SDS as a positive control) were used, which present different properties (Table 3.4). SDS was used as a positive control due to its ionic feature, denaturing the protein and therefore much better at

solubilising. The CMC parameter is especially important because the concentration of detergent used must be above this concentration in order for the detergent to be able to form micelles (concentrations below the CMC would show monomeric detergent, incapable of solubilising membrane proteins). The general rule for working with membrane proteins and detergents is to keep a detergent concentration above twice the CMC and a detergent:protein weight-to-weight ratio of minimum 4:1 (Values from Anatrace detergents and membrane proteins workbook).

	DDM	**OG**	**DG**	**LMNG**
CMC	0.15 mM	25 mM	0.19 mM	0.01 mM
Molecular weight	510.6 g/mol	292.4 g/mol	348.5 g/mol	1005.2 g/mol
Minimum mass concentration	153.18 µg/mL	14.6 mg/mL	132.4 µg/mL	20.1 µg/mL

Table 3.4: Properties of the different detergents used for membrane protein solubilisation.

Each detergent was used at mass concentration of 1 %, corresponding to 10 mg/mL, except for OG which was used at 2 %, corresponding to 20 mg/mL, due to its high CMC. They were left rotating with 90 mg/mL SdeA membranes for two hours at 4 ˚C and centrifuged at 100,000 xg for 20 minutes to collect the soluble fraction, which was thereafter run on a western blot experiment alongside the insoluble part for each detergent (Figure 3.15).

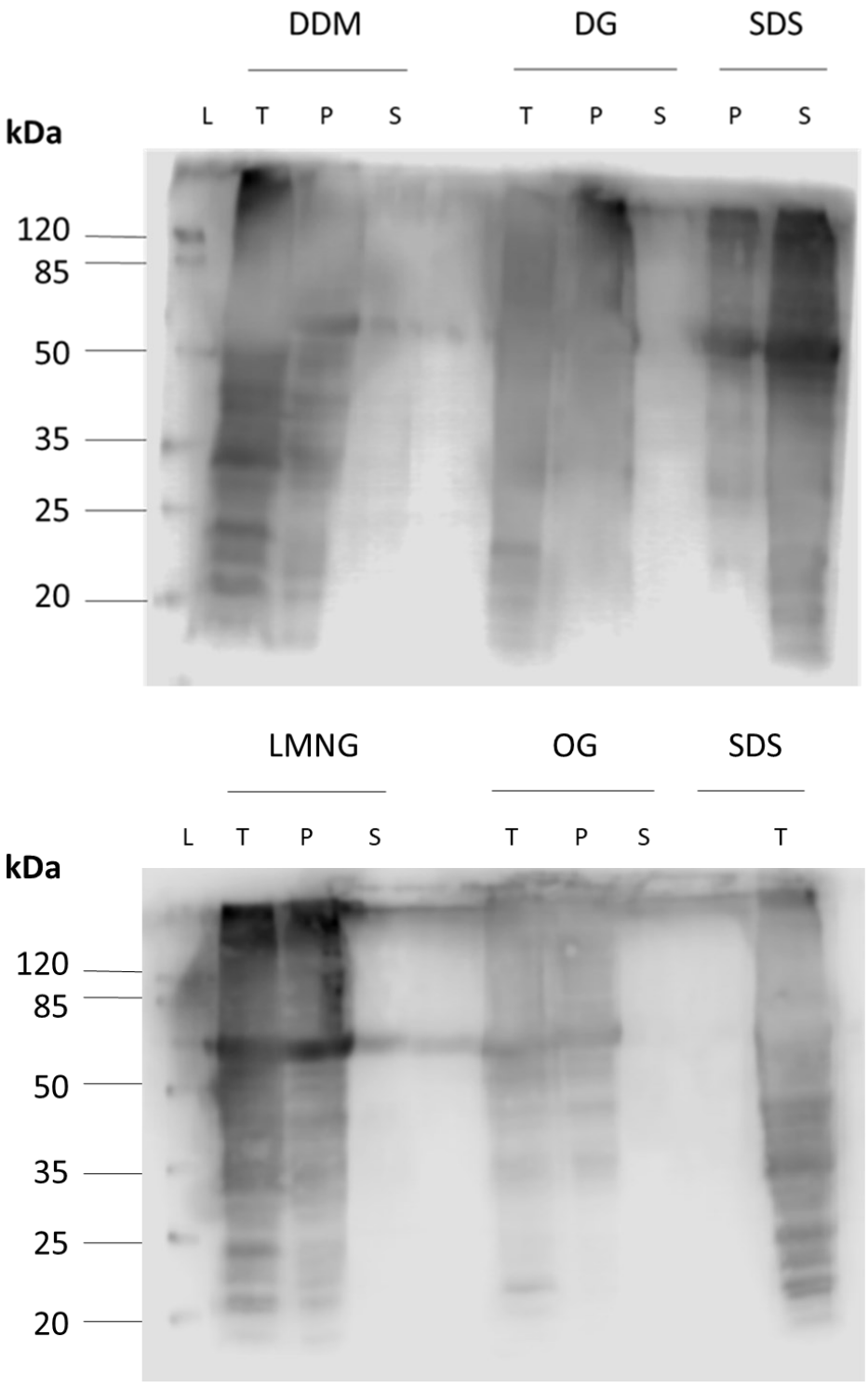

Figure 3.15: Western blot experiment performed after detergent solubilisation. *After two hours of solubilisation at 4 ˚C and centrifugation at 100,000 xg for 20 minutes, a fraction was taken from the total extract before solubilisation (T), from the insoluble pellet after the centrifugation (P) and from the soluble part (S) for each detergent.*

It can be a bit difficult to calculate solubilisation efficiencies for each of these detergents because some of them seem not to show any protein in the total extract (especially DDM

and SDS). It is however easy to notice there is barely any solubilisation at all for both glucoside detergents (OG and DG) considering the absence of observable band in the soluble fraction. The protein is obtainable in the soluble part after treatment with detergent, despite it being completely denatured and unfolded, considering the large band observable in the soluble column of SDS. However, this control is so destructive for the protein's native features that it is not the best positive control. LMNG and DDM look like they can extract at least a part of the protein from the membrane, but the band remains almost negligible compared to the size of the band in the insoluble column. Therefore, detergents do not seem to provide any substantial improvement in solubilisation efficiency compared to SMA.

3.7 Protein quantification

The amount of purified protein was calculated using densitometric analysis of a SDS-PAGE gel with a series of BSA standards run alongside SdeA (Figure 3.16). Densitometry, unlike many colourimetric assays, does not suffer from interference from lipids, SMA or imidazole (Morrison *et al.* 2016), which is why it was preferred. From the standard curve generated from the BSA samples, the amount of purified SdeA could be calculated.

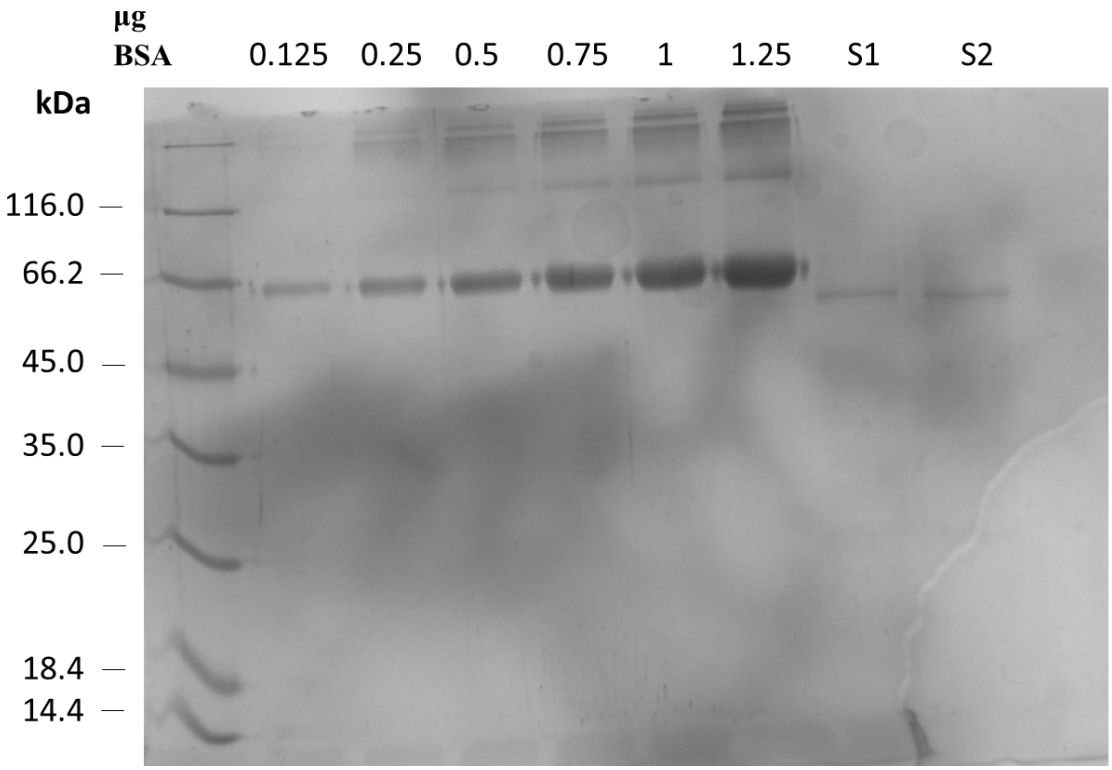

Figure 3.16: Quantification of purified SdeA using BSA standards. *The SDS-PAGE was loaded with standard amounts of BSA diluted in distilled water. S1 and S2 are duplicate of the same sample.*

The sample lanes on the right of the gel showed clear bands, however they are not very strong and fall out of the range of the curve. The protein's concentration was therefore not high enough for it to be calculated with this range of standards.

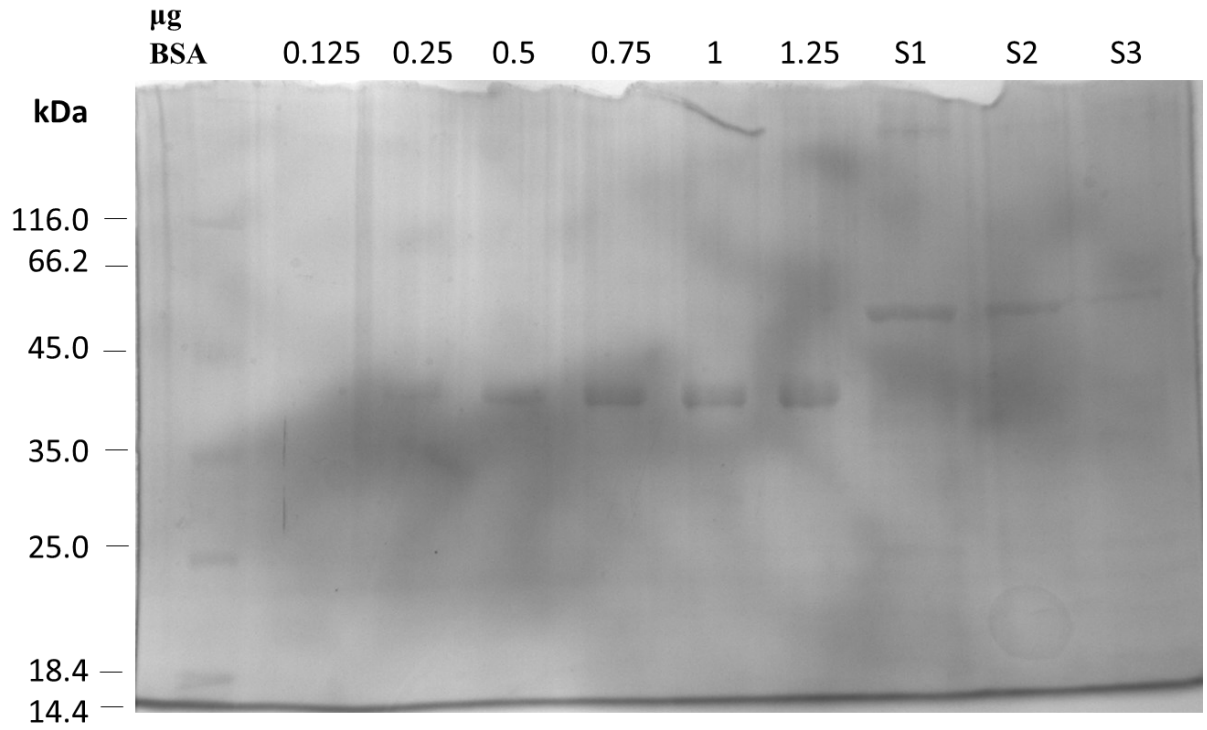

	S1	S2	S3
Protein amount (µg) per 15µL concentrated sample	0.98	0.63	0.43
Protein concentration (µg/mL)	65.5	41.8	28.5
Protein concentration before TCA precipitation (µg/mL)	9.82	6.27	4.28

***Figure 3.17: Protein quantification experiment with concentration samples**. A TCA precipitation was performed on 100 µL three different purified protein samples (labelled S1 to S3), by adding 10 µL of DOC, followed by 10 µL of 72 % TCA and a 10 minutes 16,000 xg centrifugation. After resuspension in 15 µL of resuspension buffer, each sample was fully loaded on SDS-PAGE alongside BSA standards ranging from 0.125 to 1.25 µg.*

As lower concentrations of BSA standards would become difficult to visualise on SDS-PAGE gel, an attempt to increase amount of SdeA sample loaded on the gel was carried out. To do

this, larger volumes of purified SdeA were TCA precipitated and resuspended in a smaller volume. After the TCA precipitation, they were run on SDS-PAGE alongside the BSA standards (Figure 3.17). This time, all three samples were in the range of the standard curve. The protein concentration was measured for all three samples, ranging from 28.5 to 65.5 µg/mL. However, the TCA precipitation meant that the equivalent of 100 µL of each sample had been loaded on the gel. Therefore, the concentrations must be divided by the initial concentration factor (which was 100/15), which gave results ranging from 4.28 to 9.82 µg/mL.

Another quantification method that could be used relied on BCA quantification. This method was compatible with SMA, which is why it could be used. However, it quantified any protein in the sample indiscriminately, meaning that if there were any protein contaminant in the purified protein sample, it would be accounted for by the experiment as well. The results obtained were quite consistent between the different elutions, but very different between the different dilutions (Table 3.5). While elution 1 was clearly less concentrated than elutions 2 and 3, the dilutions made it look like they were up to 8.4 times more concentrated. Furthermore, the standard curve did not look exactly straight and did not seem very reliable. Therefore, this method of quantification was discounted.

	E1	**E1 / 10**	**E2**	**E2 / 10**	**E3**	**E3 / 10**
Absorbance 562 nm	0.099	0.051	0.134	0.113	0.151	0.103
Concentration (µg/mL)	14.37	6.80	19.87	16.65	22.58	15.06
Multiplied by dilution factor	14.37	68.0	19.87	166.5	22.58	150.6

Table 3.5: Quantification of purified SdeA elutions using a micro-BCA assay. *The kit was obtained from Thermofisher and used according to the manufacturer's guidelines. Standards of BSA were ranging from 0.5 to 200 µg/mL. Elutions were measured at their normal concentration or diluted 10 times.*

3.8 Conclusion

SdeA was successfully expressed in *P. pastoris* X-33 cells. However, several issues have been encountered during the purification and characterisation of the protein:

- The solubilisation efficiency of the protein was very low when it was done using SMALP polymers, but also not much better when using detergents. None of the different conditions performed could improve this issue.
- Because of this first problem, the levels of purified protein found after purification were also very low.
- Several bands were identified on the elutions, which seemed to correspond both to SdeA. This must be confirmed by a mass spectrometry analysis.

4. Removal of stubborn contaminant

4.1.1 mADH identification

The protein of interest, called SdeA, together with its 6x His-tag, could be successfully expressed in *P. pastoris* X-33, extracted with SMA polymer and purified using the His-tag present in the C-terminal part of the protein sequence, via Ni-affinity chromatography. However, the purified protein was frequently quite impure, with several additional protein bands in the elution fractions (Figure 4.1). This became worrying as the exact same procedures had been followed throughout the whole process, from cell culture to purification. The same glycerol stocks of cell lines were also used.

Figure 4.1A shows the two main bands (around 55-60 kDa) which are always obtained in the elution fractions when expressing and purifying SdeA. It was hypothesised that the band at 55 kDa was SdeA based upon its size and that this band dominates on the western blot (Figure 4.1C). However, increasingly over time, the purifications were not as clean as this, with other contaminants being present. Figure 4.1B shows the same two bands at 55-60 kDa but there are more bands present too, including an intense band at around 40 kDa.

This 40 kDa band was particularly concerning because it was frequently more intense than the SdeA band itself. It clearly co-purified with the protein of interest, meaning it potentially had an affinity for the resin or for SdeA itself. It was however never found on the western blots (Figure 4.1C), meaning it most likely did not contain a His-tag.

In order to find out more about what it was, a mass spectrometry analysis was performed to identify the mystery contaminant. In-gel trypsin digestion was performed both on a single elution fraction and on a sample where several elution fractions were pooled together and concentrated using a filter concentrator, before being loaded on a SDS-PAGE (Figure 4.2).

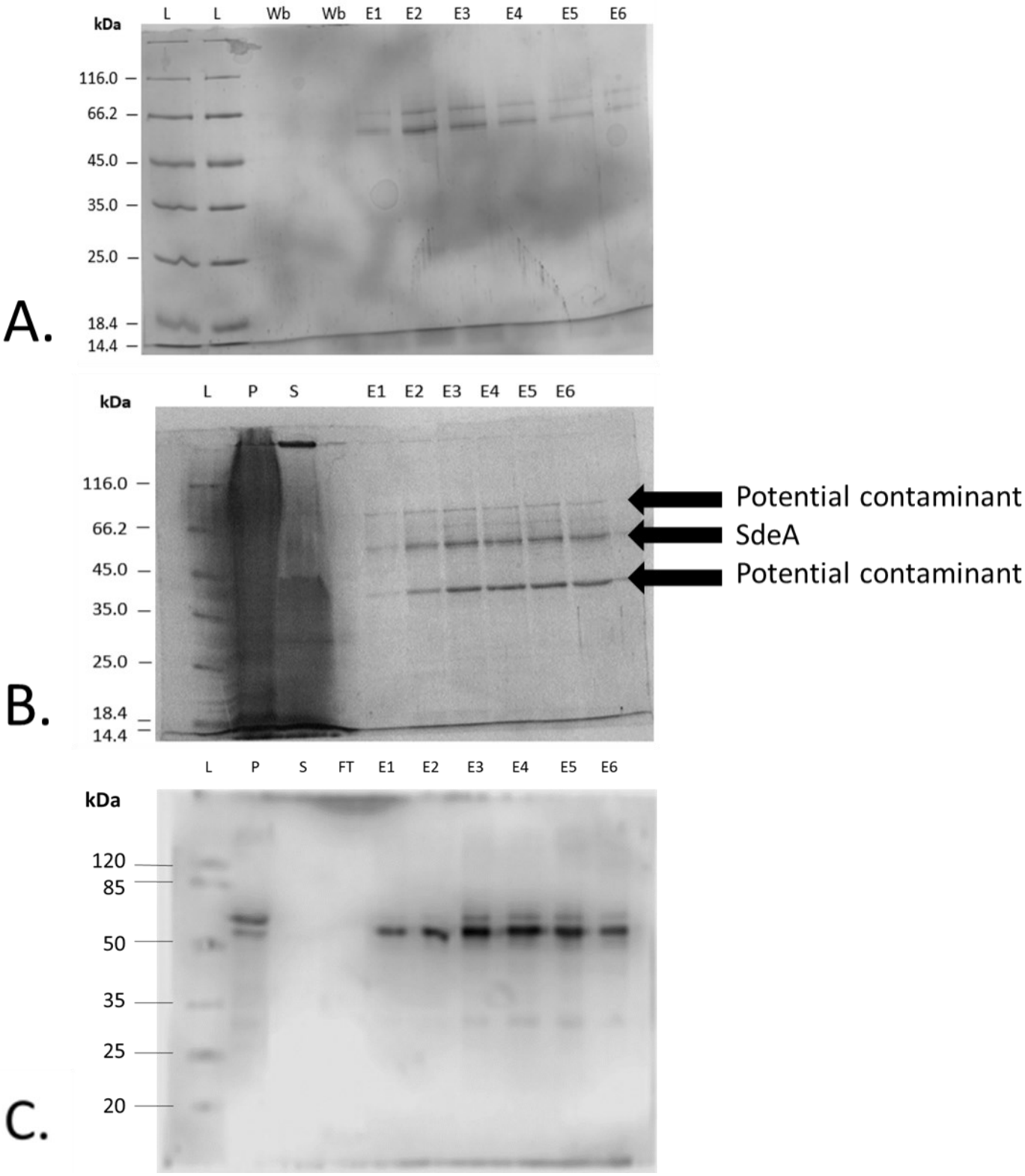

Figure 4.1: Characterisation of SdeA with and without contaminants*. A and B are SDS-PAGE gels made with 12% polyacrylamide after affinity chromatography. C is a western blot experiment performed on a PVDF membrane with an anti-His primary antibody. In each part of the figure, L stands for ladder, P and S stand for pellet (non-soluble membranes) and supernatant (soluble membranes) respectively. FT is the flow-through collected during the first step of the purification, Wb are the washings at an imidazole concentration of 40 mM performed during the affinity chromatography, while E1 to E6 are the elutions performed with an imidazole concentration of 200 mM.*

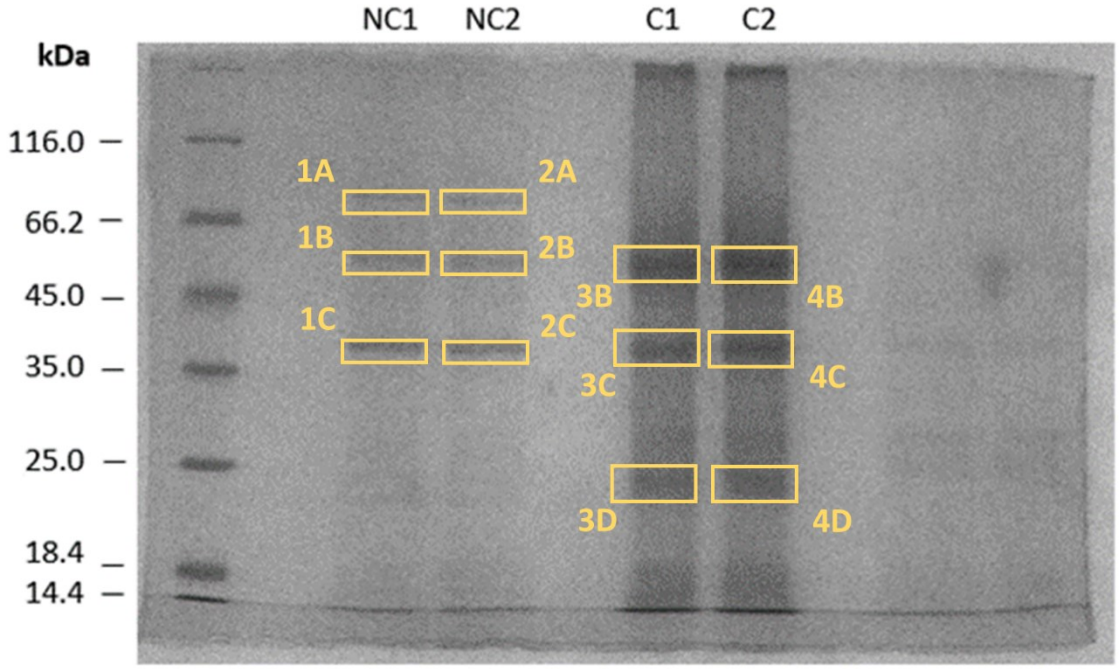

Figure 4.2: SDS-PAGE gel used for the in-gel trypsin digestion prior to mass spectrometry analysis. *NC stands for non-concentrated and C for concentrated sample, where several elutions from different purifications were pooled together and concentrated using a filter concentrator. Bands outlined in yellow were manually cut out of the gel and subjected to trypsin digestion.*

While the non-concentrated sample gave the same banding pattern as seen in Figure 4.1B, the concentrated sample did not show the band A, corresponding to the approximately 60 kDa band, but showed another band labelled D at about 20kDa. Only lanes NC1 and C1 were analysed.

After the LC-MS analysis, the results were compared to a database using a Mascot Daemon software, and a PDB database. Three different parameters can confirm or disprove the presence of a protein in the sample. These would be the ions score, which can be compared to an overall confidence score, the sequence coverage, which shows how many of the peptides composing the protein after trypsin digestion were picked up, and the total protein size that can be compared to the expected size of the protein to check if they match. The sequence coverage does not have to be very high as some small (< 5 amino acids) or large peptides (> 30 amino acids) are usually not picked up. Membrane proteins are also well known to show poor coverage in the transmembrane regions. However, it is important that the sequences detected be spread out across the whole sequence and not only in one part.

Ions scores were calculated and compared with the sequences from different organisms in the database, and the sequence coverage for each sample was given by the software (Figure 4.3). The protein size could be verified using the specific protein link associated with each ions score.

The band corresponding to the expected size of SdeA at around 55 kDa (1B and 3B) was confirmed as the protein of interest. The confidence was relatively low for the low concentrated sample, but much higher – both in ions score and sequence coverage – for the more concentrated sample (Figure 4.3a). This latter gel band showed an ions score for the protein of interest four to five times higher than the second hit, another protein from the same family. All the other important hits were coming from the host organism, which can let one think they could be co-purified proteins. SdeA is correctly identified as coming from *Aspergillus fumigatus*. The code given by the software (XP_748918.1) lead to the protein sequence and a weight of 52 kDa. The protein observed on this gel is slightly larger because of the amino acids added at the end of the sequence for the His-tag. The calculated weight for this modified protein is 56.66 kDa, which matches the expected size.

For the band corresponding to the 40kDa contaminant (1C and 3C), the higher concentrated sample did not give better results this time, but both samples gave similar results. The sequence coverage was good at 62 to 72%, spread out across the whole sequence. The ions scores showed a very clear first hit for mitochondrial alcohol dehydrogenase (mADH) from *Komagataella phaffii*, another name for *Pichia pastoris* (Figure 4.3b). The protein code (XP_002491382.1) can lead to the sequence of the protein, which has a calculated weight of 37 kDa. This matches the data observed on the gel.

This contaminant enzyme would thus be a co-purified enzyme from the host organism.

The highest band (1A) corresponding to the top contaminant showed a low sequence coverage (30%) spread out across the sequence, but a good ions score identifying it as another co-purified protein from the host called transketolase.

Finally, the last band from the concentrated sample (3D) seemed to identify mADH again with a lower ions score and sequence coverage than the band 3C. Moreover, the size of this band does not correspond to the size of mADH, perhaps meaning it was a breakdown product of mADH.

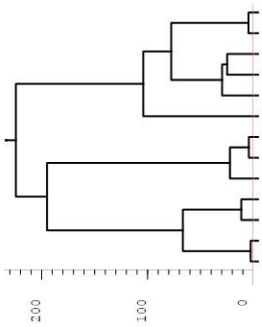

▸1	1	XP_748918.1	13723	stearic acid desaturase (SdeA), putative [Aspergillus fumigatus Af293]
	7	XP_018693198.1	1750	acyl-CoA desaturase [Fonsecaea erecta]
	2	XP_013284763.1	3038	acyl-CoA desaturase [Fonsecaea pedrosoi CBS 271.37]
	10	EMG45680.1	475	Fatty acid desaturase, putative [Candida maltosa Xu316]
	8	OLN83104.1	1425	Acyl-CoA desaturase 2 [Colletotrichum chlorophyti]
	5	CDM28398.1	2349	Delta-9 acyl-CoA desaturase, haem/steroid binding domain-containing [Penicillium roqueforti FM164]
	4	KND93200.1	2808	Acyl-CoA desaturase [Tolypocladium ophioglossoides CBS 100239]
	11	KHN94219.1	362	delta-9 fatty acid desaturase [Metarhizium album ARSEF 1941]
	9	XP_007822554.1	872	acyl-CoA desaturase 1 [Metarhizium robertsii ARSEF 23]
	3	EOD43414.1	2877	putative acyl- desaturase protein [Neofusicoccum parvum UCRNP2]
	12	EIT77130.1	294	fatty acid desaturase [Aspergillus oryzae 3.042]
	6	XP_024724224.1	1916	hypothetical protein M430DRAFT_134230 [Amorphotheca resinae ATCC 22711]
	13	XP_018191565.1	167	cytochrome b5-like Heme/Steroid binding domain-containing protein [Xylona heveae TC161]
▸2		CCA37662.1	2312	Heat shock protein with chaperone activity [Komagataella phaffii CBS 7435]
▸3		XP_002492074.1	1407	hypothetical protein PAS_chr2-2_0462 [Komagataella phaffii GS115]
▸4	1	XP_002493063.1	1370	Transketolase, similar to Tkl2p [Komagataella phaffii GS115]
	3	XP_013936414.1	84	Dihydroxyacetone synthase [Ogataea parapolymorpha DL-1]
	2	CCA39318.1	1143	Dihydroxyacetone synthase variant 2 [Komagataella phaffii CBS 7435]
▸5		XP_002494175.1	1122	Flavoprotein subunit of succinate dehydrogenase (Sdh1p, Sdh2p, Sdh3p, Sdh4p) [Komagataella phaffii GS115]
▸6		XP_002491382.1	738	Mitochondrial alcohol dehydrogenase isozyme III [Komagataella phaffii GS115]
▸7		AAQ99151.1	678	alcohol oxidase AOX1 [Ogataea pini]
▸8		XP_002491218.1	645	Calnexin [Komagataella phaffii GS115]
▸9		ANZ73348.1	547	BA75_01560T0 [Komagataella pastoris]
▸10		XP_002493047.1	451	Protein of unknown function involved in vacuolar protein sorting [Komagataella phaffii GS115]

A.

Protein sequence coverage: 55%

Matched peptides shown in ***bold red***.

```
  1 MSAKPADASR PRAGDPKKVH IADTAITRQN WYKHVNWLNV FLIIGIPLYG
 51 CIQAFWVPLQ LKTAIWAVVY YFFTGLGITA GYHRLWAHCS YSARLPLRIW
101 LAAVGGGAVE GSIRWWARDH RAHHRYTDTD KDPYSVRKGL LYSHIGWMVM
151 KQNPKRIGRT DITDLNEDPV VVWQHRNYLK VVLVMGLVVP MLVAGLGWGD
201 WFGGFIYAGI LRIFFVQQAT FCVNSLAHWL GDQPFDDRNS PRDHVITALV
251 TLGEGYHNFH HEFPSDYRNA IEWHQYDPTK WTIWIWKQLG LAYDLKQFRA
301 NEIEKGRIQQ LQKKIDQKRA KLDWGIPLDQ LPVMEWDDYV EQAKNGRGLI
351 AIAGVVHDVT DFIKDHPGGK AMINSGIGKD ATAMFNGGVY NHSNAAHNLL
401 STMRVGVIRG GCEVEIWKRA QKESGEYVRD ESGQRIIRAG QQVTKIPDPI
451 PTADAA
```

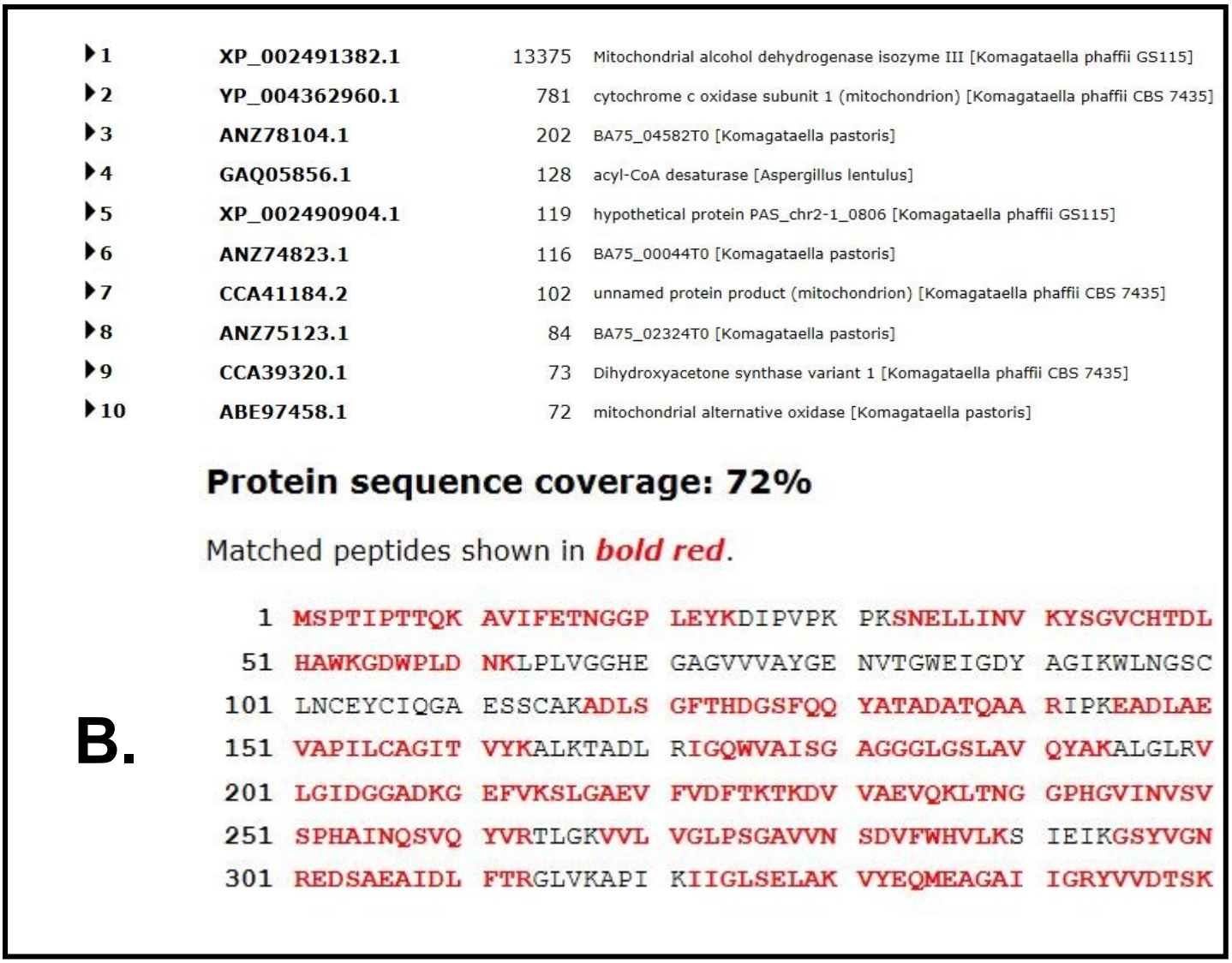

1	XP_002491382.1	13375	Mitochondrial alcohol dehydrogenase isozyme III [Komagataella phaffii GS115]
2	YP_004362960.1	781	cytochrome c oxidase subunit 1 (mitochondrion) [Komagataella phaffii CBS 7435]
3	ANZ78104.1	202	BA75_04582T0 [Komagataella pastoris]
4	GAQ05856.1	128	acyl-CoA desaturase [Aspergillus lentulus]
5	XP_002490904.1	119	hypothetical protein PAS_chr2-1_0806 [Komagataella phaffii GS115]
6	ANZ74823.1	116	BA75_00044T0 [Komagataella pastoris]
7	CCA41184.2	102	unnamed protein product (mitochondrion) [Komagataella phaffii CBS 7435]
8	ANZ75123.1	84	BA75_02324T0 [Komagataella pastoris]
9	CCA39320.1	73	Dihydroxyacetone synthase variant 1 [Komagataella phaffii CBS 7435]
10	ABE97458.1	72	mitochondrial alternative oxidase [Komagataella pastoris]

Figure 4.3: Mass spectrometry results from gel extracts. *A. Ions scores and sequence coverage for the band corresponding to SdeA, from the concentrated sample. B. Ions scores and sequence coverage for the band corresponding to mADH, from the non-concentrated sample.*

The presence of these contaminants was potentially problematic for the next stage of the study where a functional assay for SdeA was to be established. SdeA uses NADH,H^+ as a substrate to form NAD^+, it is put in a reaction with a cytochrome b_5 dehydrogenase, and it was proposed to monitor the decrease of the concentration of NADH spectrophotometrically, by the decrease of the OD_{340nm}, which is the wavelength at which NADH, H^+ absorbs, while NAD^+ does not.

However, mADH uses NAD^+ as a substrate, producing NADH, H^+ in response (Zhang *et al.* 2018). The presence of the mADH contaminant can therefore lead to an imbalance of the ratio of these two molecules, which can be used for this functional assay later on. On the other hand, transketolase is not involved in a reaction using NADH, H^+ and is therefore not so problematic (Zhang *et al.* 2018).

Moreover, the intensity for transketolase is small while the band intensity for mADH is

sometimes even larger than the one corresponding to SdeA. Thus, it was decided that mADH would have to be removed from the purified protein sample in order to carry on with the functional assay.

4.1.2 Initial steps for elimination of contaminant

The amino-acid sequence for mADH contains few histidines, none of them being next to the other, meaning it was unlikely that mADH's affinity for the nickel resin was as high as SdeA's, with its C-terminal 6xHis-tag. Therefore, during the Ni-affinity purification, as washings of 20 and 40 mM imidazole were not enough to elute the contaminant protein, but the elutions at 200 mM did remove both SdeA and mADH from the column, a gradient of increasing imidazole concentration washings was performed. This was done in order to try to elute the contaminant with a lower concentration of imidazole and separate it from SdeA. Regular washings at 20 and 40 mM were performed before running extra washings at 70, 100 and 150 mM, followed by elutions at 200 mM (Figure 4.4).

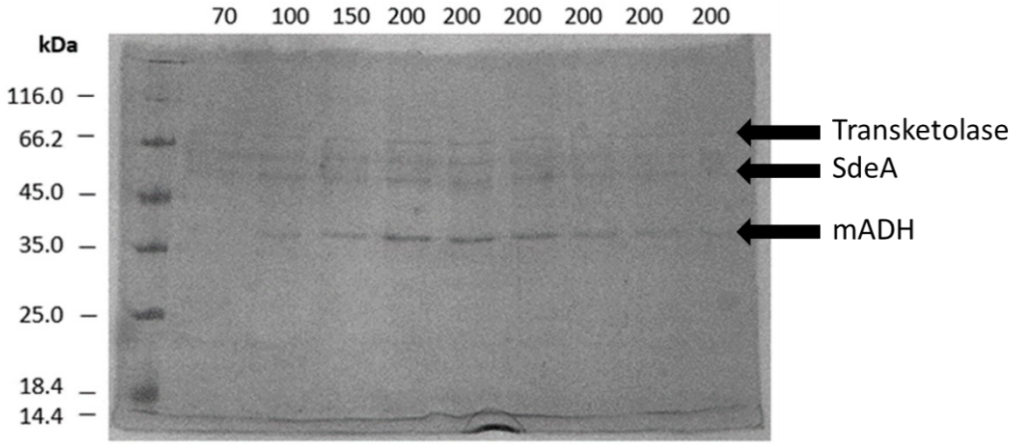

Figure 4.4: Imidazole gradient washings to try to remove mADH. *SDS-PAGE gel (12 % polyacrylamide) showing fractions obtained from imidazole gradient (70-200mM) washings carried out during Ni-NTA affinity chromatography. Gel was stained with InstantBlue.*

This SDS-PAGE shows that neither mADH nor SdeA were eluted at 70 mM, but both of them started to come out from 100 mM imidazole onwards. This was quite surprising as the affinity of mADH for the resin was expected to be lower than for SdeA, but they seem to be quite similar. The same thing can be observed for the transketolase band. Moreover, other methods such as increasing the NaCl concentration in the purification buffer from 150 to 500 mM, or adding glycerol up to 20%, two methods that are known to decrease unspecific binding to the resin via reducing ionic interactions (Bornhorst and Falke 2011), did not show any better results. One possible explanation for the contaminants' affinity for the resin could be explained by a three-dimensional folding that would place several histidine residues next

to each other. Another option could be that mADH was not binding to the resin but to SdeA itself, explaining why they could not be separated on the imidazole gradient purification experiment. mADH is typically a soluble protein and was not expected to be present in the membrane preparation from which the purification was done. This is the reason why it was thought that it could have been binding peripherally via an interaction with SdeA. In order to test this second hypothesis, a membrane washing experiment was carried out, in which the SdeA-containing membranes were washed several times before solubilisation in order to remove the contaminant that could potentially stick to the membrane or SdeA itself. The washings performed were urea/alkali washings, as it was shown to be able to remove peripheral proteins from membranes (Hasler *et al.* 1998; Karlsson *et al.* 2003; Fotiadis *et al.* 2001). The first washing consisted of urea-EGTA, followed by two NaOH washes and a final one with Tris-NaCl, each step followed by sedimentation. While the membranes were resuspended every time, the supernatants were kept to be run on a SDS-PAGE to see if the contaminant could be collected during the washings. The membranes did not resuspend very well following the first washing containing urea, but much better in the two following ones containing NaOH. Notably, the pellet obtained after centrifugation was of expected size after the urea washing but much smaller after the NaOH washing. The membrane's integrity might have been lost because of the NaOH. During the last washing, the remaining pellet resuspended fine and the pellet recovered was comparable in size to the previous step. SDS-PAGE analysis of the supernatant and pellet from each stage was carried out as well as on the remaining membranes, after having solubilised them. Each sample was purified using a Ni-affinity column before being run on the gel (Figure 4.5).

It is difficult to make any conclusions about SdeA from this experiment because it was not easily observed on any of the gels. One conclusion that could be made is that the NaOH may have indeed disrupted the membrane stability, leading to some of the SdeA being lost in the gel C corresponding to the first NaOH washing. It is easy to observe that mADH has not been washed away by this experiment, even after SdeA was lost. This means it is unlikely that it is attached to the protein of interest, and more generally that it is not a peripheral protein. One of the possible solutions that has been raised before would reside in the presence of large amounts of histidine, tryptophan and cysteine residues at the surface of the protein (Chen *et al.* 2014). These residues have been shown to facilitate the protein binding to Ni-affinity resins, through their electron-donating imidazole and thiol groups (Chivers and Sauer 2002; Wolfram and Bauerfeind 2002). Therefore, it seemed that separation of SdeA from mADH prior to or during Ni-NTA affinity chromatography was not going to be straightforward. This was particularly problematic because the proposed functional assay for SdeA involves monitoring NADH spectroscopically, and mADH also utilises NAD^+/NADH, H^+, as said previously.

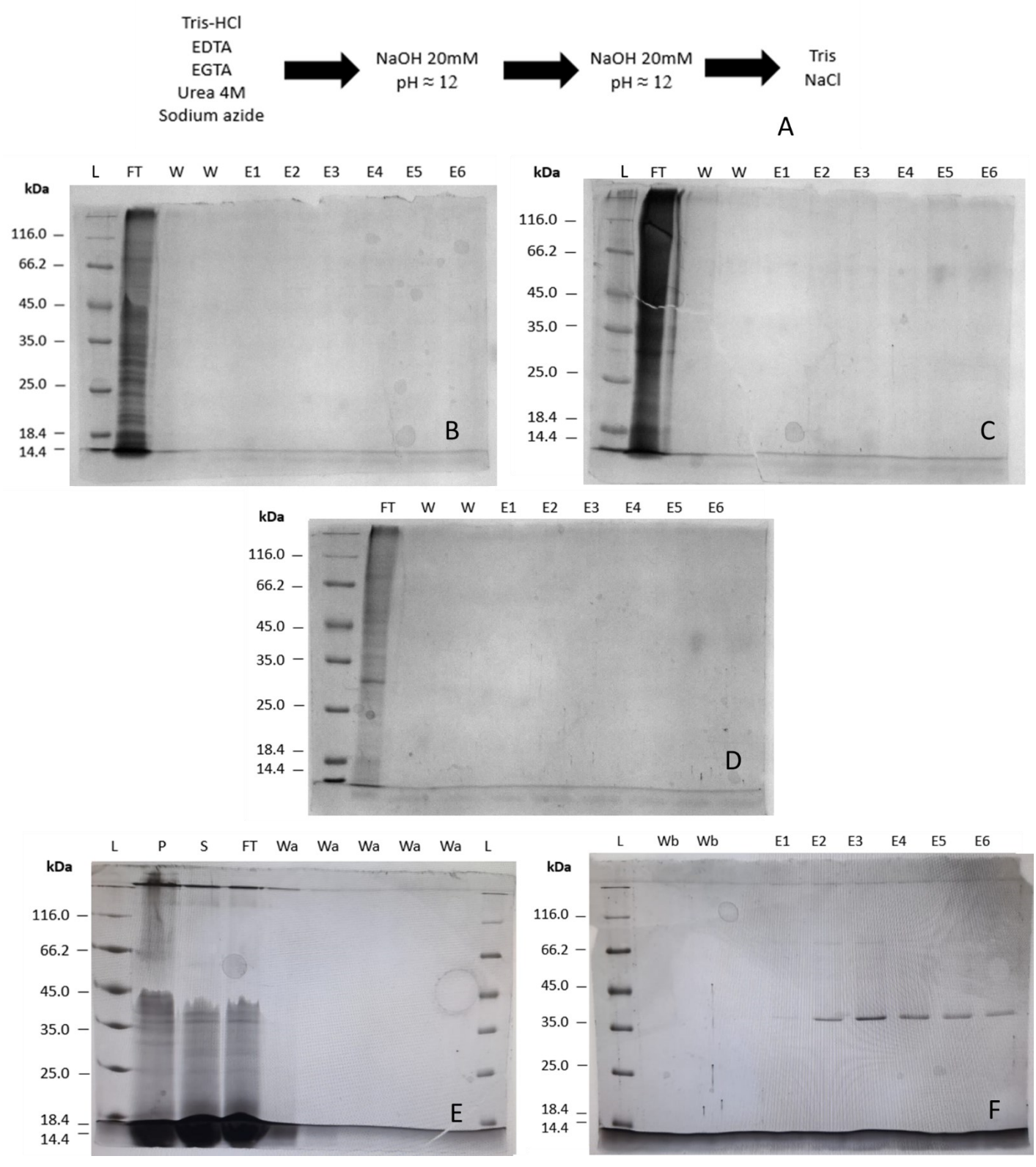

Figure 4.5: Washing membranes to try to remove mADH was not successful. *A. Experimental procedure followed during the urea/alkali membrane washings. B-F. SDS-PAGE gels (12 % polyacrylamide) run after each washing step and purification. A solubilisation step was also performed on the pellet recovered from the last washing. B corresponds to the first washing performed with urea. C and D correspond to the subsequent washings performed with NaOH. E and F correspond to the final solubilisation and purification performed on the pellet obtained after the last washing. In each gel, L stands for ladder, FT for flow-through, P for pellet and S for supernatant, W, Wa and Wb stand for various low imidazole concentrations used to wash the resin during purification and E1 to E6 are the elutions performed with high imidazole concentration.*

Two final attempts at separating SdeA from its contaminants was tested using size exclusion chromatography (SEC) and myc-tag purification. This was also unsuccessful, most likely due to the protein concentration being too small for proper detection by the SEC system, and to the presence of Tween-20 in the buffer used, which could have a destabilisation effect on the SMALP.

4.1.3 Construct design for knock out of mADH

Since none of the attempts for removing the contaminant seemed to work, another approach was hypothesised, where the gene coding for mADH could be knocked out in order to prevent its expression. This idea had already been explored previously and seemed to have shown interesting results (Chen *et al.* 2014). In this paper, they integrated the gene corresponding to mADH in a vector before digesting this gene in the middle and integrating a zeocin resistance gene inside. While this approach seemed convenient, the introduction of zeocin resistance in this new strain would prove problematic for the later transformation with the SdeA plasmid. Instead of using another antibiotic, a different approach was chosen, using the strain *P. pastoris* GS115. This strain is very similar to X-33, except that it does not contain a His4 gene, necessary for the bioproduction of histidine. Therefore, nutrient selection could be used in a histidine-depleted medium without having to use antibiotics. The resulting strain would be comparable to X-33, with the absence of a functioning mADH gene. In order to perform this, the mADH gene was integrated in a pGEX-2T bacterial vector, before being digested with restriction enzymes (which would remove approximately 240 bp), followed by the integration of the His4 gene in the middle (Figure 4.6). The resulting plasmid would then be added into GS115 cells in order to knockout mADH.

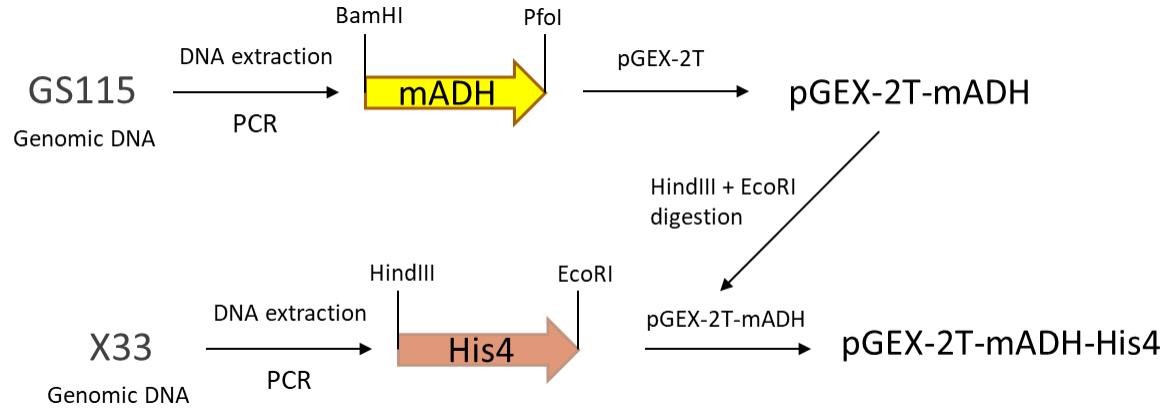

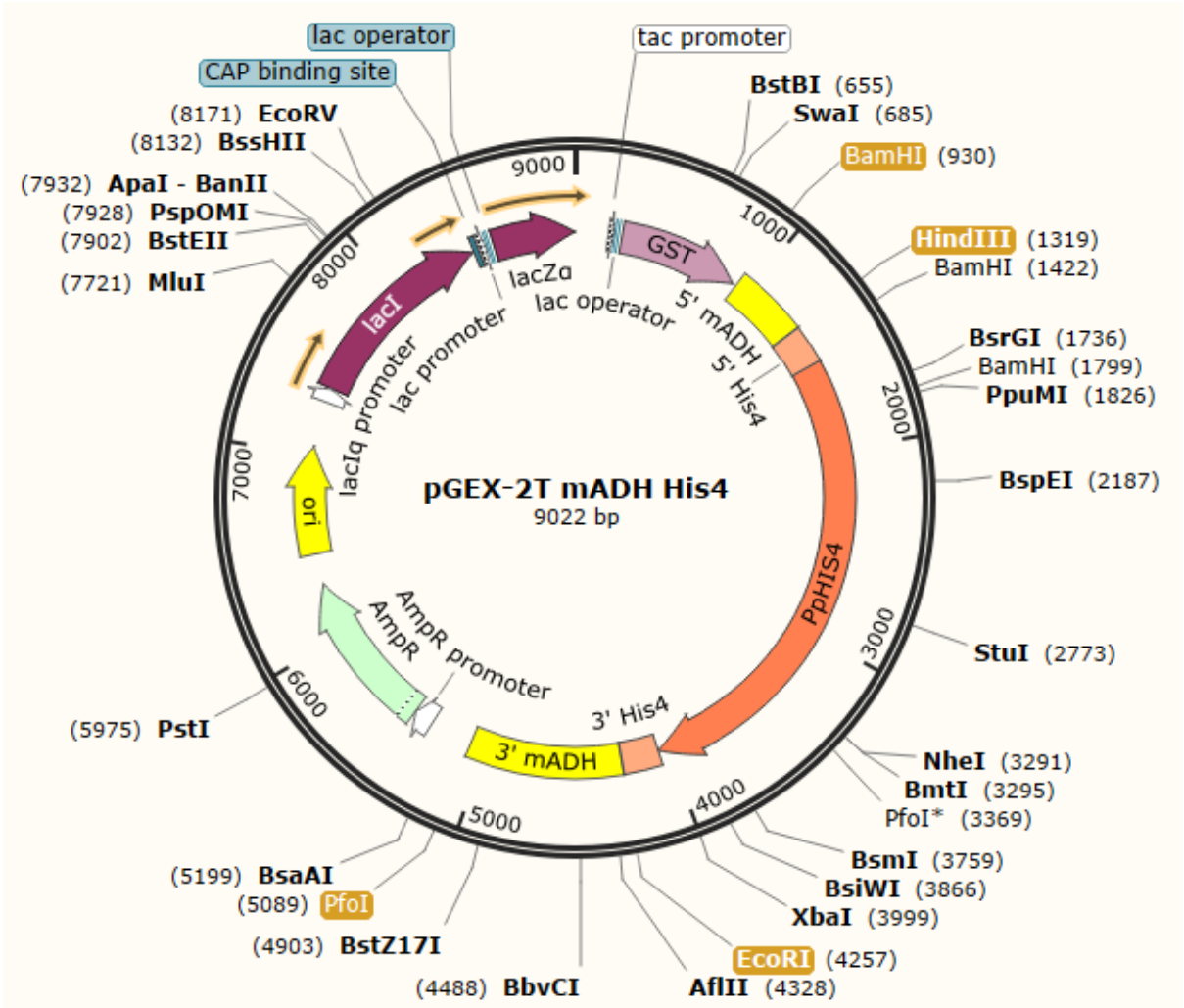

Figure 4.6: Experimental procedure used for the preparation of the plasmid, and the final plasmid obtained and used for the transformation of* P. pastoris *cells. *Restriction sites used for the integration of the genes are highlighted.*

When this plasmid is introduced into GS115 cells, it is capable of performing a homologous recombination on the mADH locus, leading to the knock out of the gene and the integration of the His4 gene (Figure 4.7).

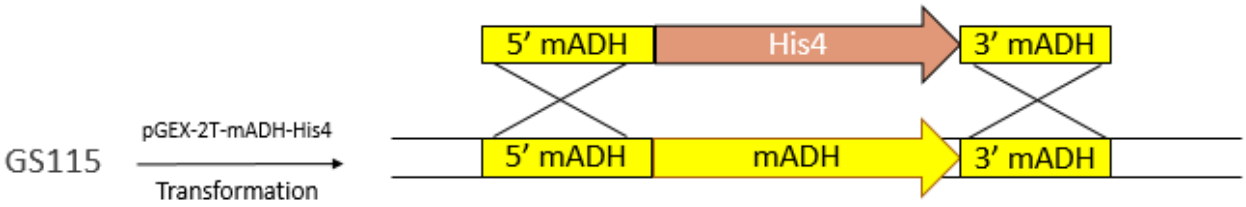

Figure 4.7: Homologous recombination of His4 on the mADH locus.

4.1.4 Gene and plasmid preparation

The His4 gene was extracted from *Pichia pastoris* X-33 genomic DNA and integrated in the middle of a mADH gene, itself extracted from *Pichia pastoris* GS115 genomic DNA via a DNA extraction kit using zymolyase. The extraction was followed by a PCR on each mADH and His4 genes with primers corresponding to each end of the gene, plus an area of 200 nucleotides upwards and downwards in order to include the promoter and the ribosome disassembly regions. The PCR results were run on an agarose gel to check the presence of a band at the correct size. Initial PCR conditions produced no bands of amplified DNA, so modifications were brought to the PCR protocol: for mADH, annealing temperature was working for several different temperatures (Figure 4.8A) but the amount of DNA template added to the mixture had to be low (Figure 4.8B). For His4, the annealing temperature only worked between 64.4 and 65.2°C (Figure 4.9A) while the amount of DNA template added to the mixture also had to be very low (Figure 4.9B).

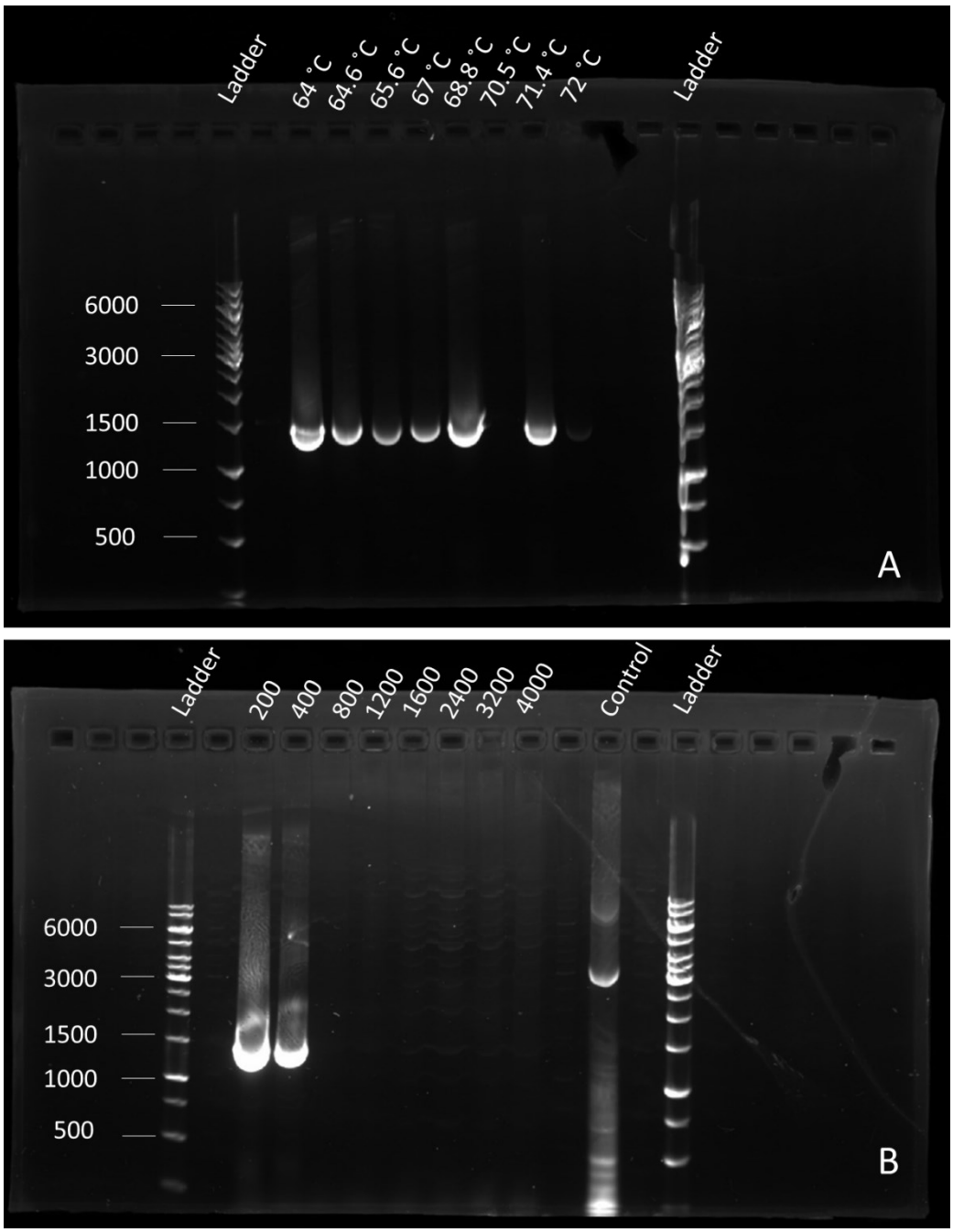

Figure 4.8: Agarose gels for the optimisation of PCR conditions on mADH*. Gels were prepared with 1% agarose and TAE buffer. A. Annealing temperature gradient experiment where different annealing temperatures were tested in order to find the optimal one. B. DNA template gradient experiment where the different amounts of DNA were added before the PCR to determine the optimal amount of template to add.*

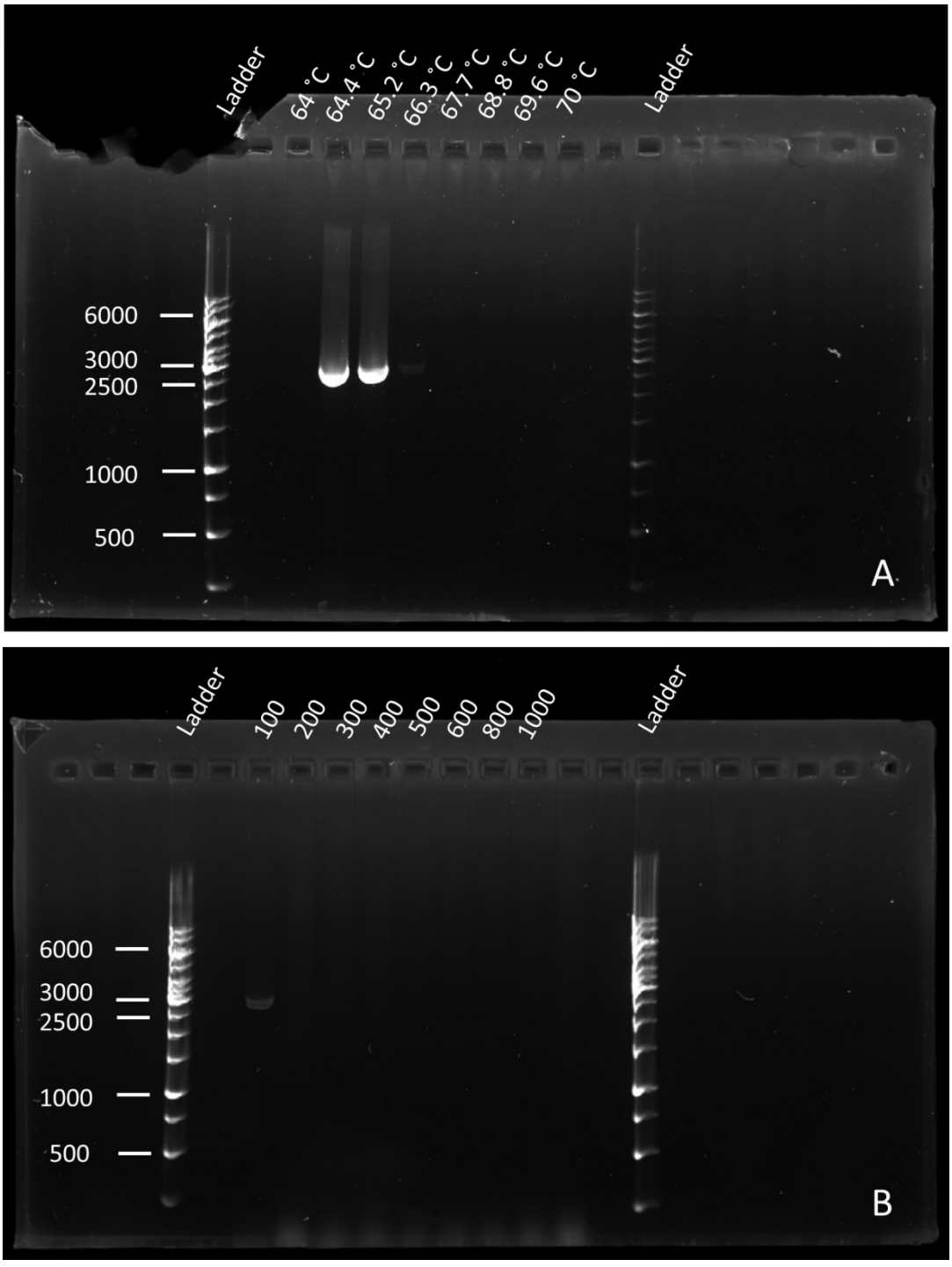

Figure 4.9: Agarose gels for the optimisation of PCR conditions on His4. *Gels were prepared with 1% agarose and TAE buffer. A. Annealing temperature gradient experiment where different annealing temperatures were tested in order to find the optimal one. B. DNA template gradient experiment where the different amounts of DNA were added before the PCR to determine the optimal amount of template to add.*

The DNA fragments obtained after PCR were expected to weigh 1.4 kb for mADH gene and 2.9 kb for His4. The agarose gels performed match the expected sizes in both cases.

After optimising the PCR conditions, each of them was run on an agarose gel with larger wells to separate it from other DNA fragments and extracted using a gel extraction kit. The concentration of DNA was then measured using a Nanodrop (Figure 4.10). The values appear to be high enough, although they tend to be higher for mADH than for His4. The 260/280 ratio seem to be in the correct range but the 260/230 ratios are quite low for both genes, emphasizing a high absorbance at 230 nm. Every single gel extraction performed since has shown a similar high absorbance at this wavelength, potentially because one of the buffers used during the gel extraction contains a compound strongly absorbing at this wavelength, such as EDTA or guanidine-HCl.

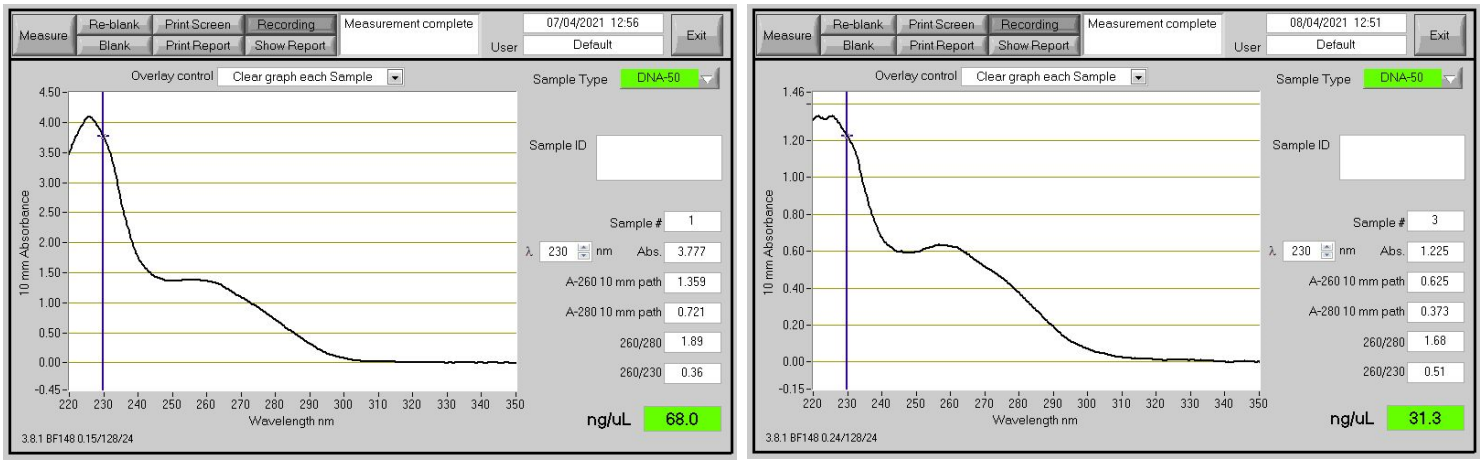

Figure 4.10: Nanodrop measurements for mADH gene (left) and His4 gene (right), obtained after an agarose gel extraction. *The DNA concentration is given, along with the measurement of the 260/280 and 260/230 ratios.*

The vector pGEX-2T used in this experiment was already present in the lab, and was thus cultured in DH5α *E. coli* cells in order to increase the available amount. A miniprep was then performed and the concentration of plasmid was measured by Nanodrop (Figure 4.11).

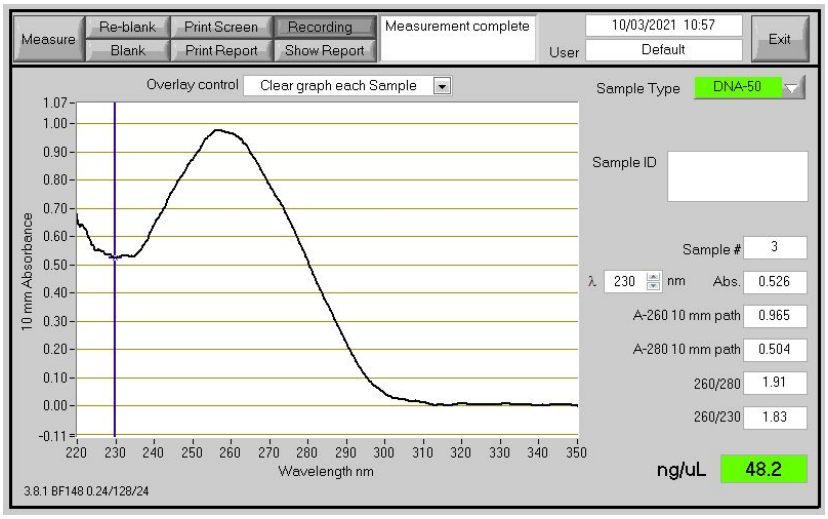

Figure 4.11: Nanodrop measurement of the concentration of pGEX-2T plasmid obtained after miniprep on a DH5α culture.

When sufficient amounts of DNA were obtained for both genes and the plasmid, they were digested with restriction enzymes in order to leave cohesive ends, using *Bam*HI and *Pfo*I for the integration of mADH, and *Hind*III and *Eco*RI for the integration of His4. During the mADH digestion, the major issue here was that the two enzymes were coming from a different supplier and there was no way of knowing if they were working correctly with each other's buffer. In order to test this, a single digestion was performed on the vector with *Pfo*I in *Bam*HI's buffer on one side, and with *Bam*HI in *Pfo*I's buffer on the other side. They were both compared to the undigested circular vector (Figure 4.12).

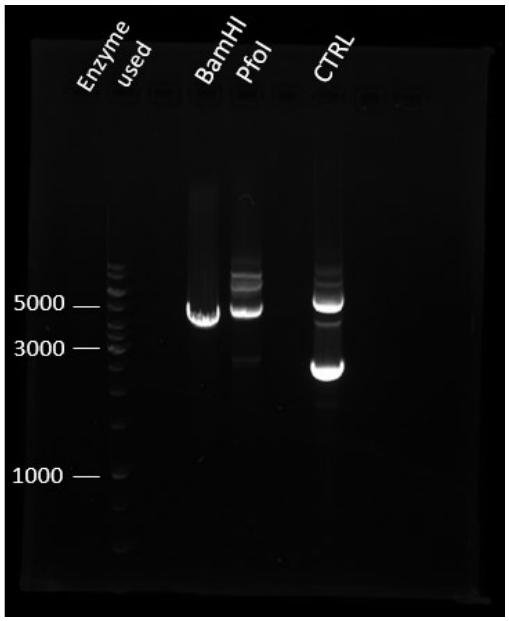

Figure 4.12: Agarose gel of pGEX-2T vector digested with* Bam*HI in* Pfo*I buffer (first lane), with* Pfo*I in* Bam*HI buffer (second lane) or undigested.

The first digestion seems to be leaving a cleaner result, with a single band observed on the lane, while the *Pfo*I digestion is showing several bands, possibly meaning that the digestion was not complete and that this enzyme does not work very well in *Bam*HI buffer. Therefore, *Pfo*I buffer was used from then on. The plasmid size is 4,948 bp, which seems to correspond to what can be observed although there seems to be a slight difference in band size between the two digestions. The control lane consists of undigested plasmid, and shows two brighter bands, characteristic of circular plasmids.
Following this step, a double digestion was performed with both enzymes in *Pfo*I buffer (Figure 4.13).

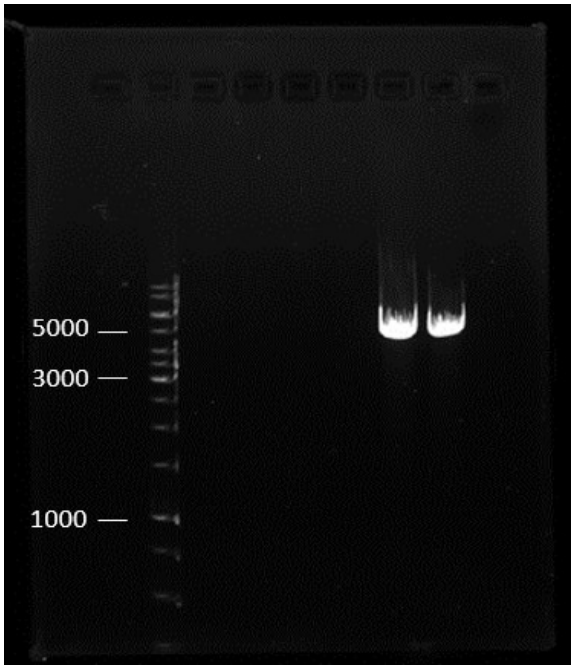

Figure 4.13: Double digestion of pGEX-2T with* Pfo*I and* Bam*HI in* Pfo*I buffer *(in duplicates).*

The distance between the two restrictions sites is 85 bp, meaning that the total size of the digested plasmid is 4,863 bp. The bands observed on the gel match this size, although it would be difficult to see a difference with a single digested plasmid for example.
The mADH amplified insert was also digested with these enzymes in order to leave only the area that is supposed to be integrated in the plasmid, with sticky ends.
After both plasmid and insert were digested with the restriction enzymes *Bam*HI and *Pfo*I, they were all run on an agarose gel and the relevant bands extracted (Figure 4.14).

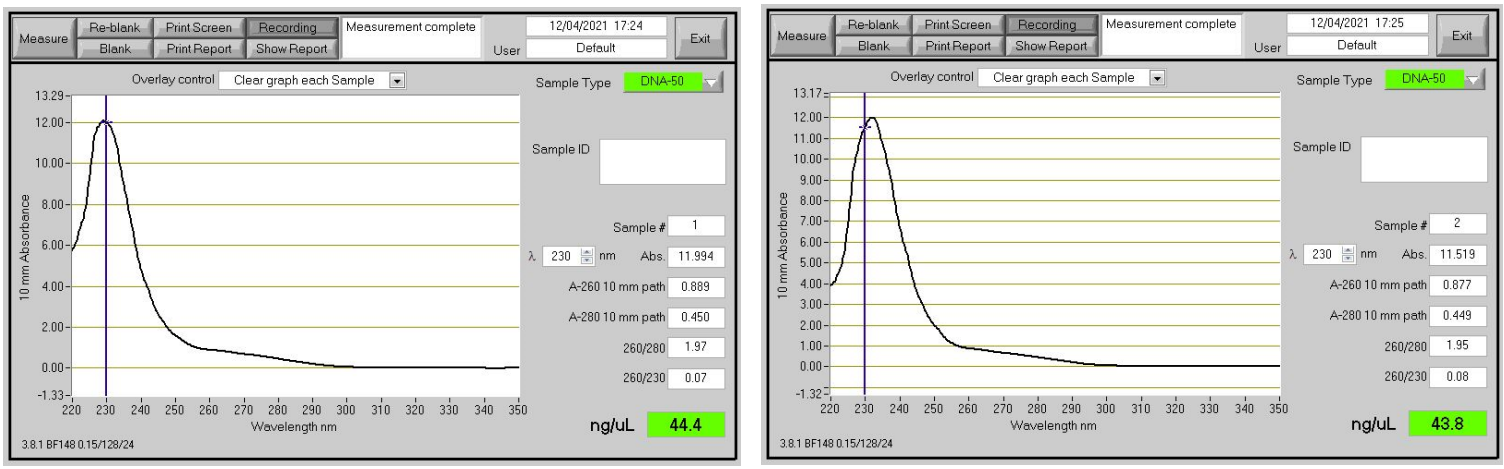

Figure 4.14: DNA concentration measurements on Nanodrop for digested pGEXT-2T (left) and digested mADH (right).

Again, the 260/280 ratios looked good but the 260/230 was low for both vector pGEX-2T (left) and mADH gene (right), also observable via the high absorbance at 230 nm on the graph, suggesting the presence of another molecule possibly absorbing strongly at this wavelength. The concentration for both DNA samples was quite low but an attempt at ligation was carried out.

4.1.5 Integration of double gene in plasmid

Once the vector and both genes had all been double digested and purified, the mADH gene had to be integrated in the vector first, before the His4 gene was inserted inside the first one, to cut it in half and inactivate it. In order to do so, a ligation experiment was performed with pGEX-2T and mADH, using a T4 ligase to combine them together. The first ligation attempt was unsuccessful, so different condition changes were tested to improve the results: the incubation was changed to 16 °C overnight rather than 10 minutes at room temperature. Different amounts of plasmid were added during the transformation (2 to 5 µL, which corresponds to $1/10^{th}$ to $1/4^{th}$ of the initial amount of plasmid added). While the amount of plasmid added did not make a significant difference in the transformation's successfulness, the incubation parameters did have an influence on the outcome, as the incubation at 16 °C overnight showed more colonies on the plates cultivated afterwards (Figure 4.15). The ligated plasmid was then cultivated in *E. coli* DH5α and a miniprep was performed on it (Figure 4.16).

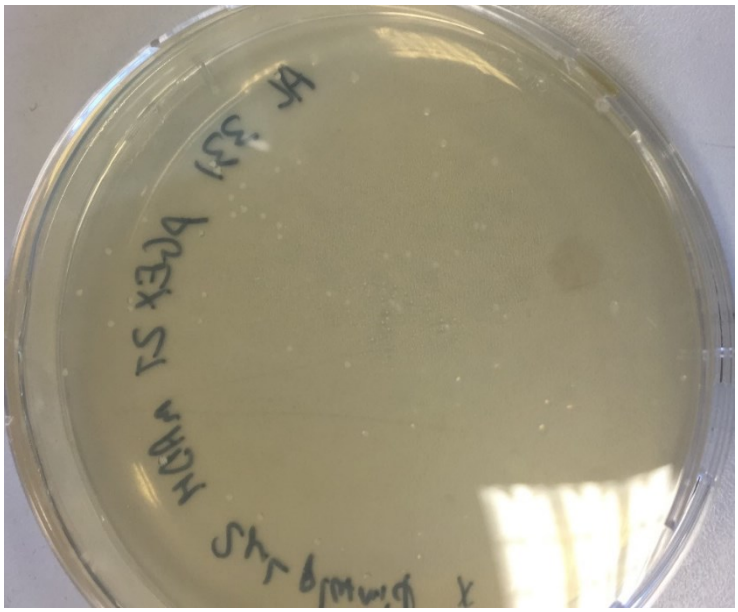

Figure 4.15: Transformation result of a ligated pGEX-2T-mADH plasmid into DH5α cells*. The ligation experiment was performed at 16 ˚C overnight, with 2 µL of plasmid added. Colonies are growing after a day of incubation at 37 ˚C.*

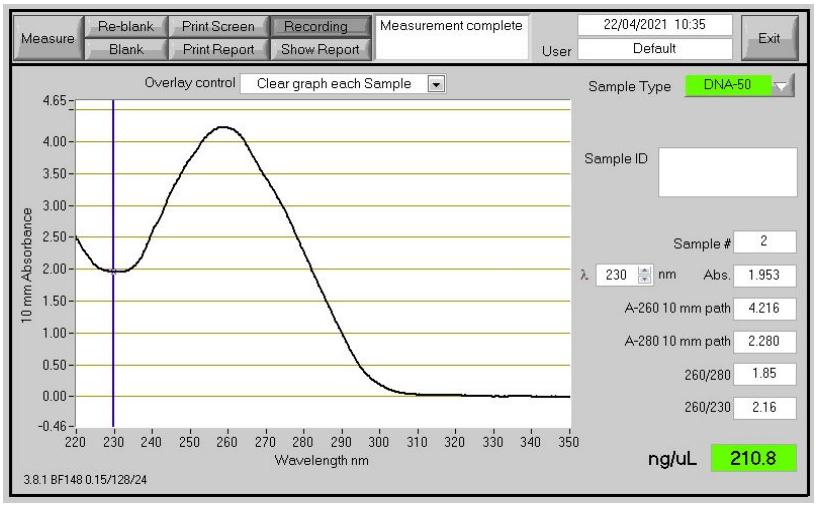

Figure 4.16: Nanodrop measurement of the plasmid concentration of pGEX-2T-mADH after miniprep in* E. coli *cultures. *The concentration is quite high, with excellent 260/280 and 260/230 ratios.*

After pGEX-2T-mADH was prepared, the second part of this approach was to integrate His4 inside the mADH gene. Both pGEX-2T-mADH and His4 were digested with the restriction enzymes *Hind*III and *Eco*RI, before being purified via gel extraction.

Different conditions were tested for the digestion of the vector pGEX-2T-mADH: with one or two of the enzymes and with three different types of buffer (Figure 4.17).

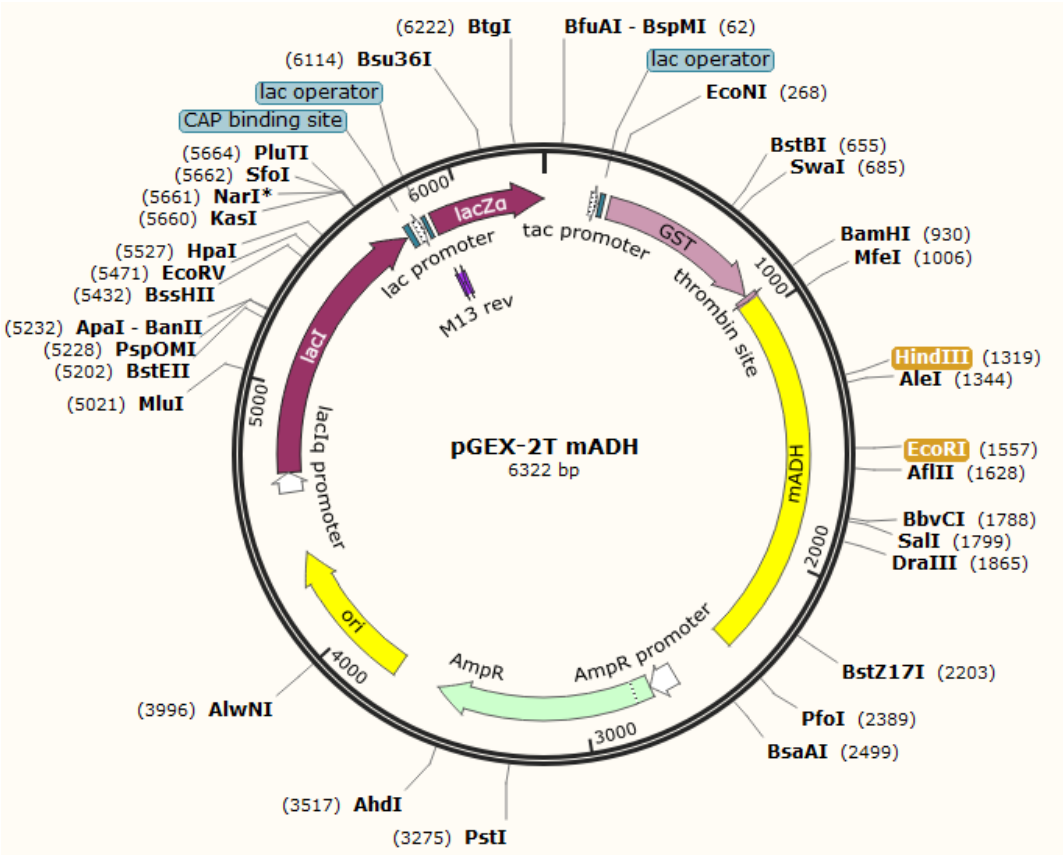

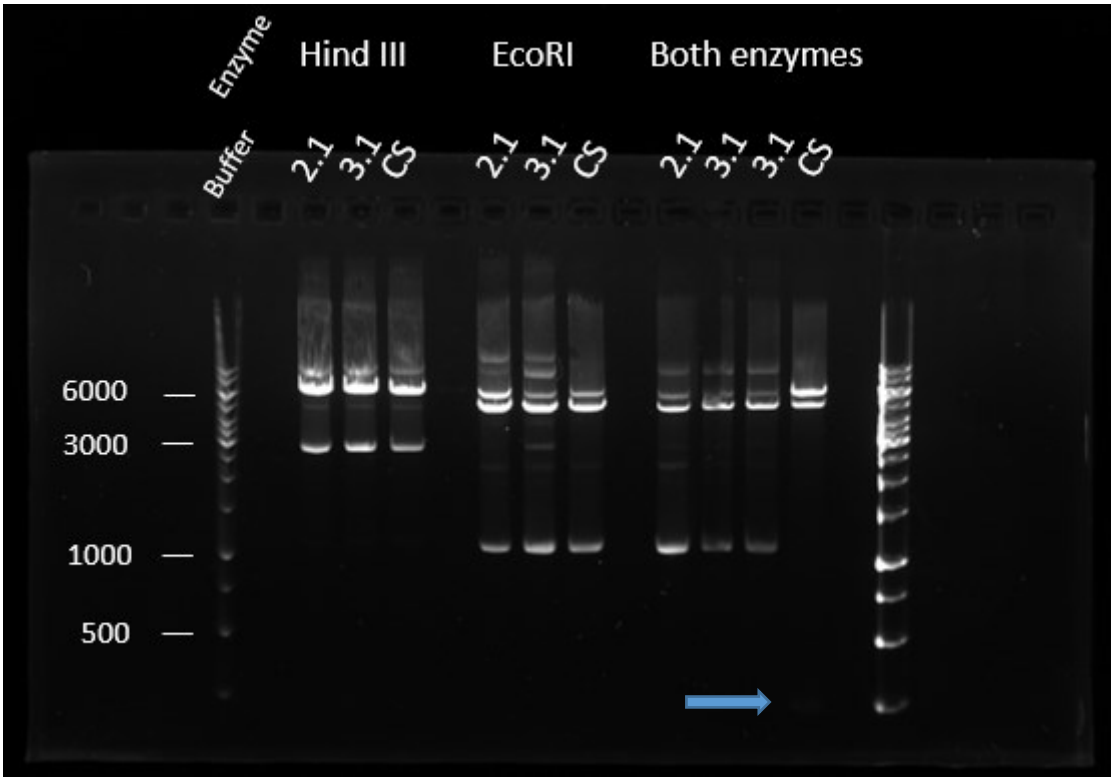

Figure 4.17: Comparison of the digestion efficiency between single and double digestion with* Hind*III and/or* Eco*RI, and between buffers 2.1, 3.1 and CutSmart (CS). *The plasmid map is also provided for more clarity. A small fraction of the mADH gene, between the two restriction sites, is removed during the process.*

Both enzymes show unexpected extra fragments at 3 kb for *Hind*III and at 1 kb for *Eco*RI. The *Eco*RI fragments can also be found in the double digested samples, only in buffers 2.1 and 3.1. There is no significant difference observed between the different buffers in single digested samples, but the extra bands are not found in the CutSmart buffer sample anymore. Moreover, a single tiny band can be observed in the CutSmart double digestion lane at around 250 bp (blue arrow) that could be the result of the fragment released by the double digestion. It is hardly observable because the lower parts of the gel usually have a lower concentration of stain and the diffusion of the DNA can be more important in this area. Thus, the double digestion was performed in CutSmart buffer in the following experiments. Both pGEX-2T-mADH and His4 were double digested and purified using agarose gel extraction (Figure 4.18).

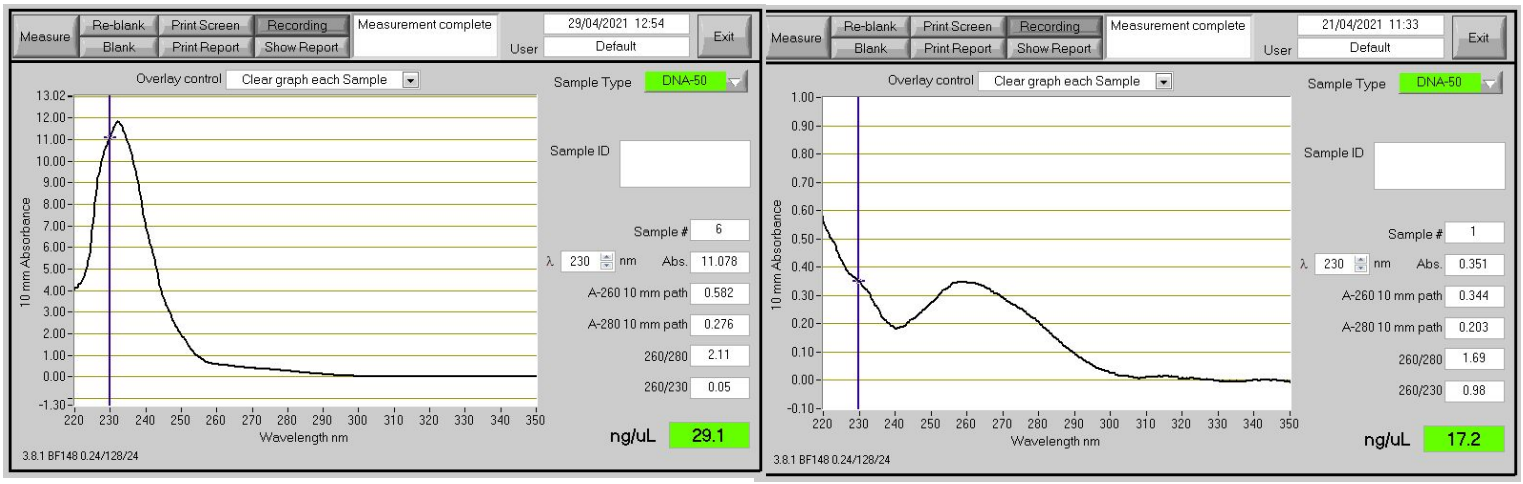

Figure 4.18: Nanodrop measurement of the gel extraction samples obtained from digested pGEX-2T-mADH (left) and from digested His4 (right). *While both 260/280 ratios seem acceptable, the 260/230 is a bit too low for His4 and extremely low for the vector, as a consequence of the very high absorbance observed at 230 nm.*

The obtained samples were then used in a ligation experiment, again with a T4 ligase at 16°C for 6 hours, and added into *E. coli* DH5α cells with ampicillin. Colonies were observed and a miniprep was performed on precultures (Figure 4.19).

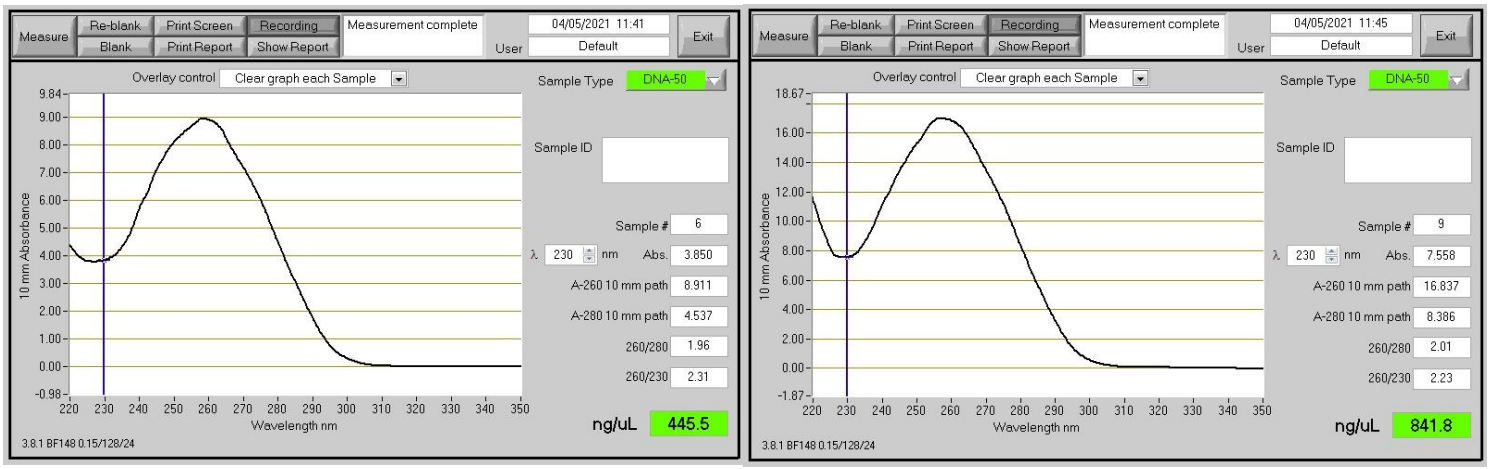

Figure 4.19: Nanodrop measurements of minipreps performed on the ligated pGEX-2T-mADH-His4 plasmid.

The concentrations for the miniprep samples were good, with also very good 260/280 and 260/230 ratios. Now that the plasmid had been synthesized fully, it was checked to see if its sequence matched the desired sequence.

4.1.6 Plasmid control

4.1.6.1 Digestion controls

The first plasmid control performed was done through several types of digestions with restriction enzymes that were expected to give bands at specific sizes (Figure 4.20).

Both *Bam*HI digestions show the same fragments, regardless of the amount of enzyme added. Small fragments corresponding to the 377 and 492 bp expected fragments can be observed (blue arrows), with a large fragment of 8.1 kb also possibly present, although there is an unexplained extra band slightly below it. *Hind*III digestion also does not show any major difference with extra enzyme added, and is showing a linearized 9 kb fragment that seems correct (slightly higher than the 8.1 kb from *Bam*HI).

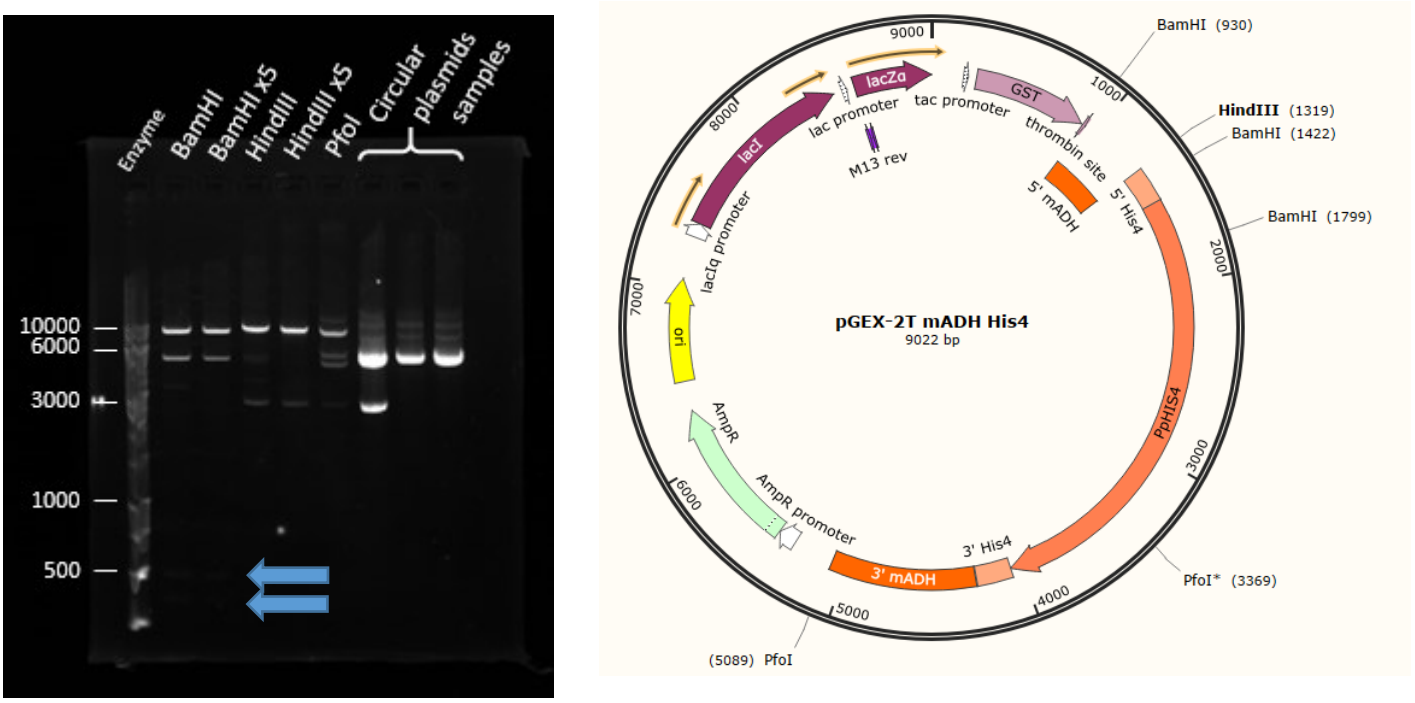

Figure 4.20: (Left) Agarose gel results for the control of plasmid size**. Digestion was performed with several enzymes and the different band sizes were checked. They were also compared with the same experiment with higher amounts of enzyme (5 times). **(Right) Full plasmid showing the different restriction sites used in this experiment.

Finally, *Pfo*I does not show the expected fragment at 1.7 kb, despite repeating the experiment several times. As there are two *Pfo*I restriction sites in the full plasmid, two fragments were expected, but we can only see one corresponding approximately to the plasmid at full size. The *Pfo*I restriction site is 5' - TCCNGGA - 3'. Although the middle nucleotide is supposed to be any of the four, some studies have found that *Pfo*I can sometimes be less effective at digesting 5' – TCC(A/T)GGA - 3' compared to 5' – TCC(C/G)GGA - 3' fragments, and sometimes not (Gaigalas *et al.* 2002). In this situation, the first *Pfo*I site that has been worked with earlier was a 5' – TCCCGGA - 3' fragment while the second one is a 5' – TCCAGGA - 3' fragment. It can be safe to assume that the *Pfo*I activity was not as successful on the second restriction site as it had originally been on the first one.

The digestion seems to confirm the presence of the His4 gene inside the vector, as shown by the two small fragments in the *Bam*HI lanes, results of the three restriction sites present in the plasmid. Both *Bam*HI and *Hind*III seem to linearize the plasmid correctly. However, there are still unexplained extra bands in every sample. The incomplete digestion of the plasmid (resulting in leftover circular plasmid) could have explained them but the increase of enzyme concentration did not improve it. An increase in incubation time could be tried to

improve this.

4.1.6.2 Plasmid sequencing

The obtained plasmid was sent for sequencing with a series of primers at Eurofins. The sequencing results showed that both mADH and His4 genes had been integrated in the locus of interest. A BLAST alignment was performed between the sequencing results and the His4 gene sequence obtained from the KEGG website, which showed a 100% homology between the sequences (Figure 4.21). The same homology was found for both the 5' mADH region and the 3' mADH region.

NW Score	Identities	Gaps	Strand
5064	2532/2532(100%)	0/2532(0%)	Plus/Plus

Figure 4.21: BLAST alignment results between the sequence of His4 obtained in KEGG and the sequencing results from Eurofins.

4.1.7 Transformation

Transformation was performed on *P. pastoris* GS115 strain using electroporation method, which is traditionally more efficient than chemical transformation. As the selection marker was the His4 gene, a histidine-depleted medium was used, without antibiotic, for growth of transformed cells onto plates. Volumes of 25, 50, 100, 200 and 500 µL were added on the plates before incubation at 30 °C, against a negative control containing non-transformed cells. After three days, some colonies started to appear, and the plates were left in the incubator for two more days. Unfortunately, after these two days, all the plates started to show contamination, in the form of round pink moist colonies or of mould. In any case, the small colonies that were first observed could not be cultured in liquid minimal medium afterwards. Extra care must be brought to the plating step in order to prevent contamination as no antibiotic is used during this culture.

During the second try, instead of using a full linearized plasmid, a PCR was performed on the plasmid, with the primers corresponding the mADH gene. Therefore, only the part containing the mADH-His4 was amplified and, after a PCR clean up, was introduced into the GS115 cells.

Several colonies appeared on the plates, which were then cultured into MGY medium, not containing any histidine. A colony PCR was performed on each of them, with either mADH or His4 primers (Figure 4.22).

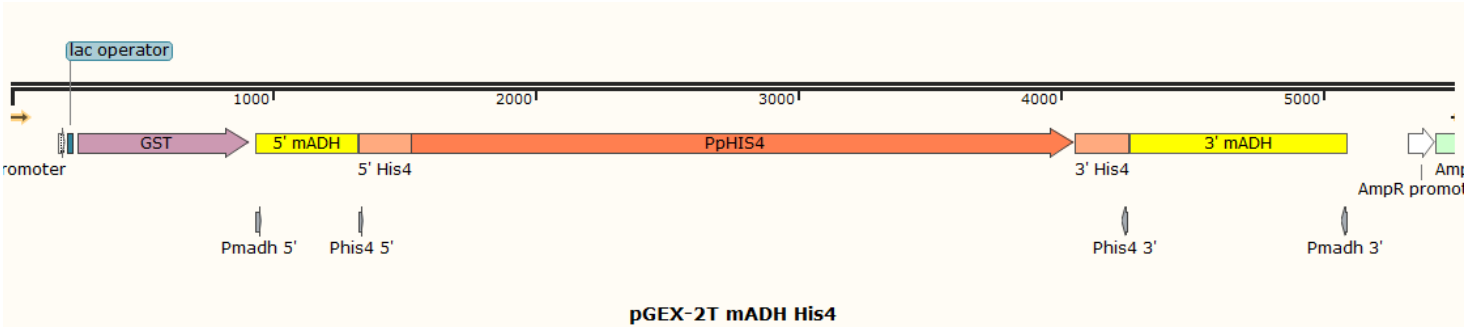

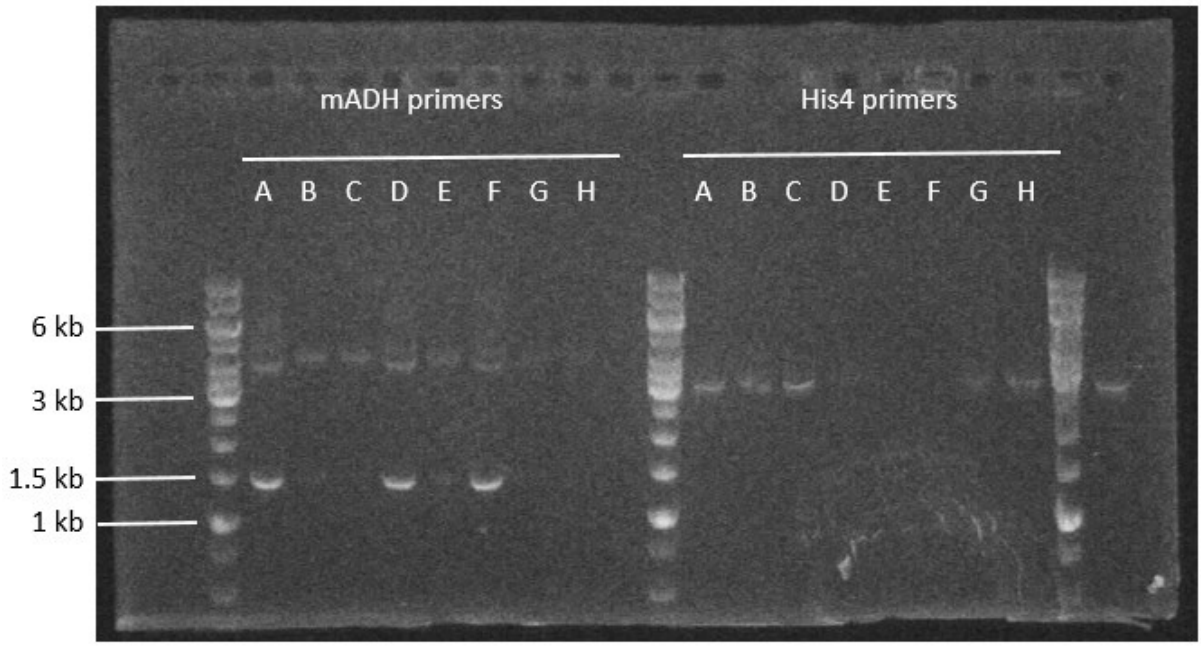

Figure 4.22: Agarose gel on the PCR results from the 8 different colonies (A-H) tested. *mADH (left) or His4 (right) primers were used. A map showing the different annealing loci for both mADH and His4 primers is also added. The mADH gene alone is represented in figure 4.17 and measures approximately 1450 bp.*

The expected size for the mADH-His4 gene is approximately 4.2 kb, while mADH on its own is 1.5 kb and His4 is 3 kb, these colonies show that A, D and F still have the unmodified mADH gene and are therefore not usable. Furthermore, colonies G and H are not exhibiting the 4.2 kb band expected to be observed. Finally, colonies D, E and F are not showing the His4 band at 3 kb. Therefore, only colonies B and C are showing the correct properties that would have been expected after this experiment and were the only two ones that were put into liquid culture in order to make glycerol stocks.

4.1.8 Growth curve

The growth pace of the newly engineered strain was compared to a wild-type *P. pastoris* X-33 in order to make sure the cell growth was not impaired by the knockout previously performed (Figure 4.23). This could be particularly important because mADH seems to be involved in the usage of alcohol, including methanol, which is the primary carbon source during the culture. The cultures were performed in BMMY, in order to be able to evaluate the different methanol usage pace. While the new strain seemed to grow a bit slower than the wild-type, they both went to reach the same optical density eventually.

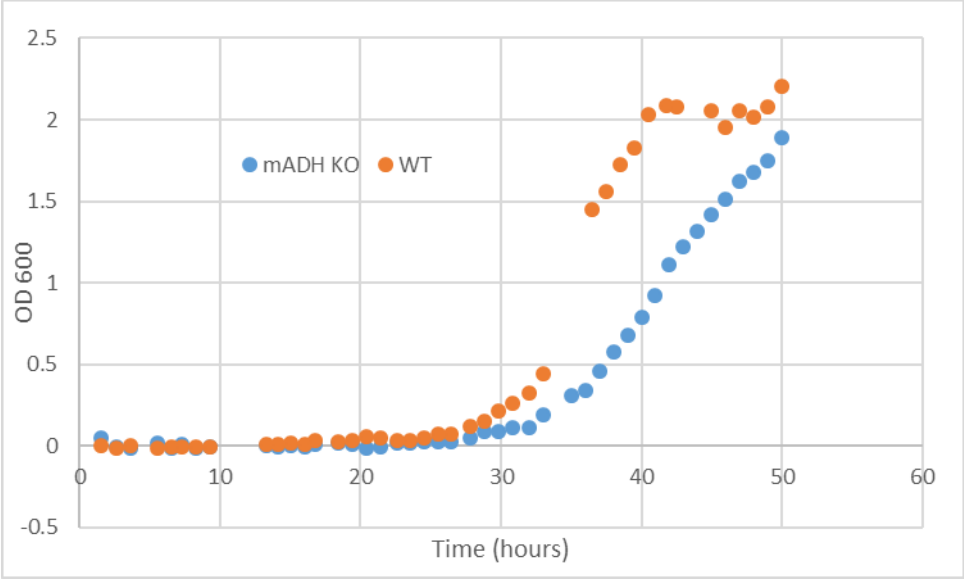

Figure 4.23: Growth curve of* P. pastoris *GS115 with the mADH gene knocked out compared to X-33 wild-type cells. *The culture was performed in 50 mL BMMY at 30 °C with the colony B from figure 4.22, and the optical density at 600 nm was measured every hour on a spectrophotometer.*

4.1.9 Expression test

The successful integration of the plasmid could also be confirmed via a test for mADH expression, where cultures of the knocked out and wild-type strains were compared to measure mADH appearance when methanol was in the culture medium.

Colonies A and B, as well as wild-type X-33 cells were put into MGY culture before being resuspended in BMMY in order to induce mADH expression. Colony A was added to this experiment as another control. Regular samples were taken from the culture in order to run them on a SDS-PAGE gel (Figure 4.24).

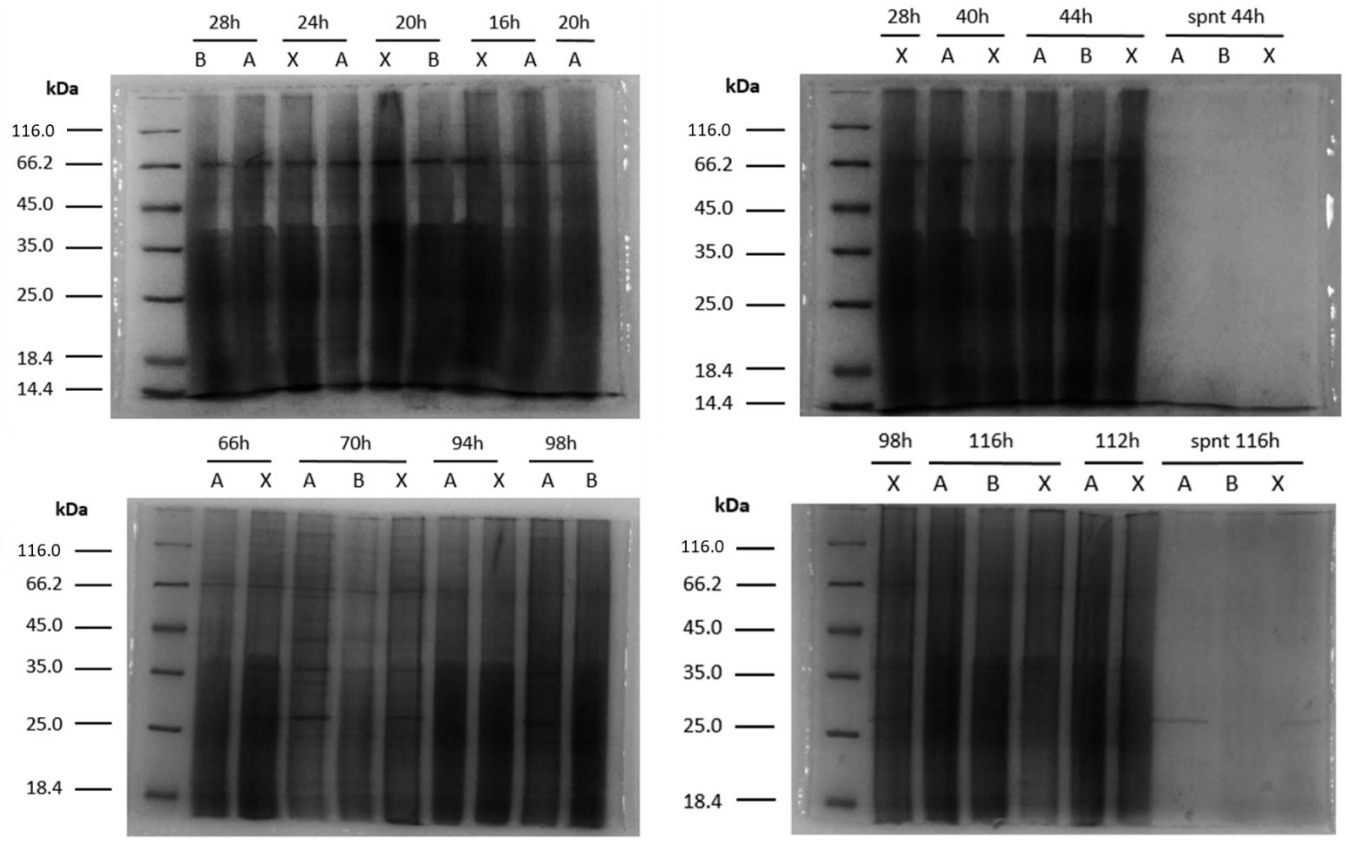

Figure 4.24: SDS-PAGE gels run from the three cell cultures at different time points after methanol induction. *A and B stand for the colonies A and B from the corresponding colonies from the previous PCRs. X stands for X-33, the wild-type strain. Supernatants (spnt) were also analysed at 44 and 116h.*

As the SDS-PAGE gels were run on total cell lysates, the results are difficult to interpret, and mADH cannot be specifically observed. There are no apparent differences between the knockout strain B and the control A or the wild-type strains.

As the expression test was inconclusive, a solubilisation of the membranes, followed by a 'purification' by affinity chromatography, using the same parameters as previously, was performed, in order to try to isolate mADH. Unfortunately, mADH could not be observed in the KO strains A and B nor in the control wild-type X-33. This result could mean that the over-expression of SdeA could be essential for the over-expression of mADH to occur.

4.1.10 Conclusion

After the strain was made ready, a transformation attempt was carried out with an SdeA plasmid on both normal X-33 strain and one with the knockout, followed by a medium-scale protein expression (same conditions as previous SdeA expression in order to verify if any potential difference was due to the gene knockout) in order to see if the contaminant's expression was indeed impaired.

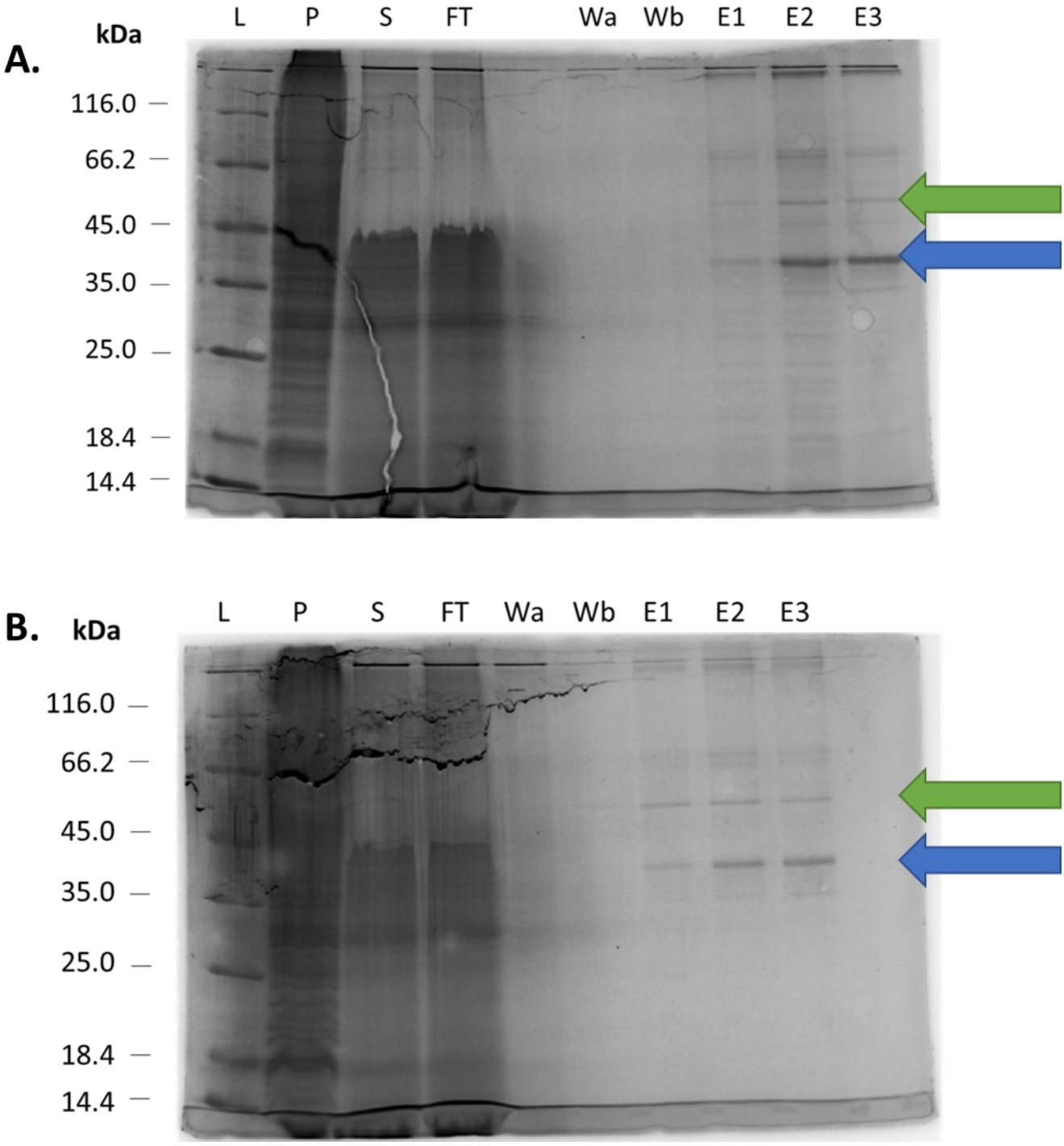

Figure 4.25: Production of SdeA from the wild-type strain (A.) or from the mADH knockout strain (B.) visualised on SDS-PAGE. *L = ladder, P = Pellet (non-solubilised membranes), S = Supernatant (solubilised membranes), FT = Flow-through, W = 40 mM imidazole washings, E1-3 = elutions with 200 mM imidazole. Each solubilisation has been carried out with membranes being solubilised at a concentration of 90 mg/mL during one hour at room temperature, with 2.5 % (w/v) of SMA2000 polymer. The soluble part was then purified by Ni-affinity chromatography and the protein was eluted with 200 mM imidazole. Each fraction was then loaded on SDS-PAGE.*

The SDS-PAGE gels that were performed (Figure 4.25) both showed bands corresponding to SdeA's size (green arrows), but also at the same size as mADH (blue arrows). A western blot was also carried out with anti-his antibody and HRP secondary antibody, which did show the right bands for SdeA at the correct size (Figure 4.26).

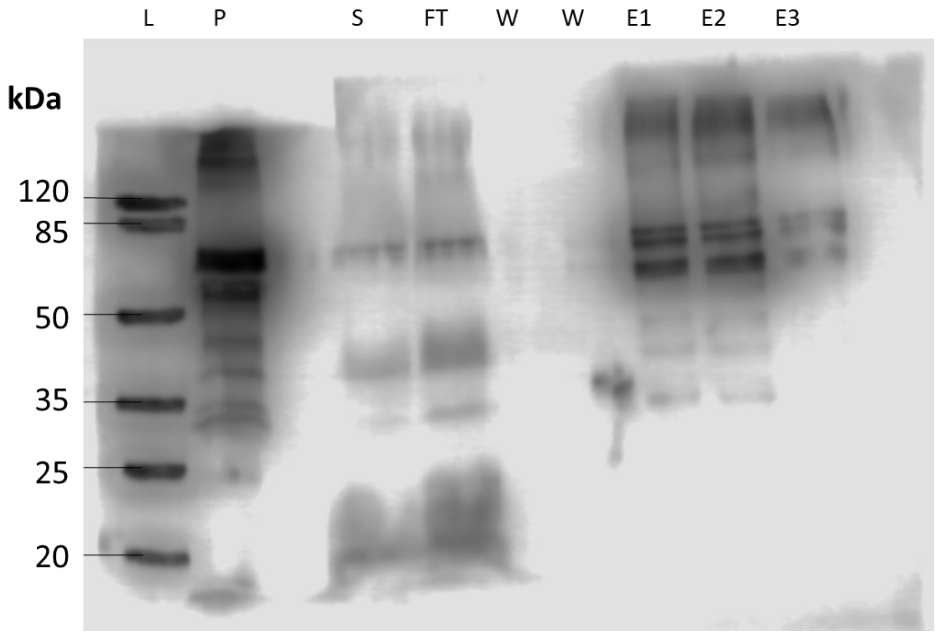

Figure 4.26: Western blot performed after SdeA production from the mADH-KO strain, with anti-his mouse primary antibody and anti-mouse HRP secondary antibody. *L = ladder, P = Pellet (non-solubilised membranes), S = Supernatant (solubilised membranes), FT = Flow-through, W = 40 mM imidazole washings, E1-3 = elutions with 200 mM imidazole.*

Therefore, the preparation of the plasmid worked correctly, with the sequencing confirming the correct presence of both mADH and His4. Another confirmation was brought by PCR, with the presence of the mADH-His4 construct detected in the new strain.

While it cannot be 100% ascertained the contaminating band from the new strain is mADH still, it would seem likely given the size. Therefore, it would seem the gene knockout was not completely efficient at removing the contaminant. Interestingly the band corresponding to mADH does seem to be somewhat fainter on the knockout strain compared to the wild type.

5. Activity assays

SdeA works with an associated protein called cytochrome b5 dehydrogenase (cytb5R). Several cofactors (NADH,H^+ and FAD) are also involved in the reaction that produces unsaturated fatty acids (Figure 5.1).

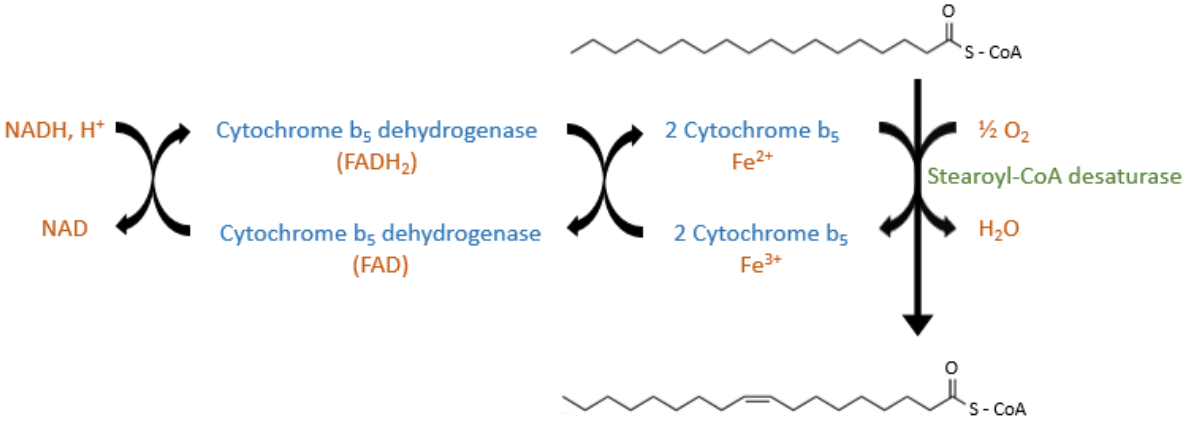

Figure 5.1: Chemical reaction leading to the desaturation of fatty acids using stearoyl-CoA desaturase (SdeA) as the enzyme. *The oxidation of NADH,H^+ provides electrons that are transported to the enzyme via an iron ion. Saturated acyl-CoA (most importantly stearoyl-CoA) are transformed into the corresponding monounsaturated acyl-CoA (most importantly oleyl-CoA).*

Therefore, in order to test SdeA's activity, its associated protein cytochrome b5 dehydrogenase had to be expressed as well so the two proteins could be assayed together. It was also important to characterise both expressed proteins with absorbance spectra in order to confirm the correct structure of the target. Finally, the functional assay was an essential step to firmly assess the protein's activity in order to be able to inhibit this activity with an inhibitor.

5.1 Production of cytochrome b5 dehydrogenase

F2G provided plasmid pET30-CBR coding for a truncated version of cytochrome b5 dehydrogenase (cytb$_5$R) protein, missing 40 amino acids in N-ter corresponding to the membrane anchor. The resulting gene coding for a soluble protein was introduced into DH5α *E. coli* cells (Figure 5.2). The obtained colonies were numerous, yet quite small. They were precultured in LB-kanamycin and a plasmid preparation was performed on them. Two different preparations gave concentrations of 67.7 and 52.6 µg/mL of purified plasmid DNA.

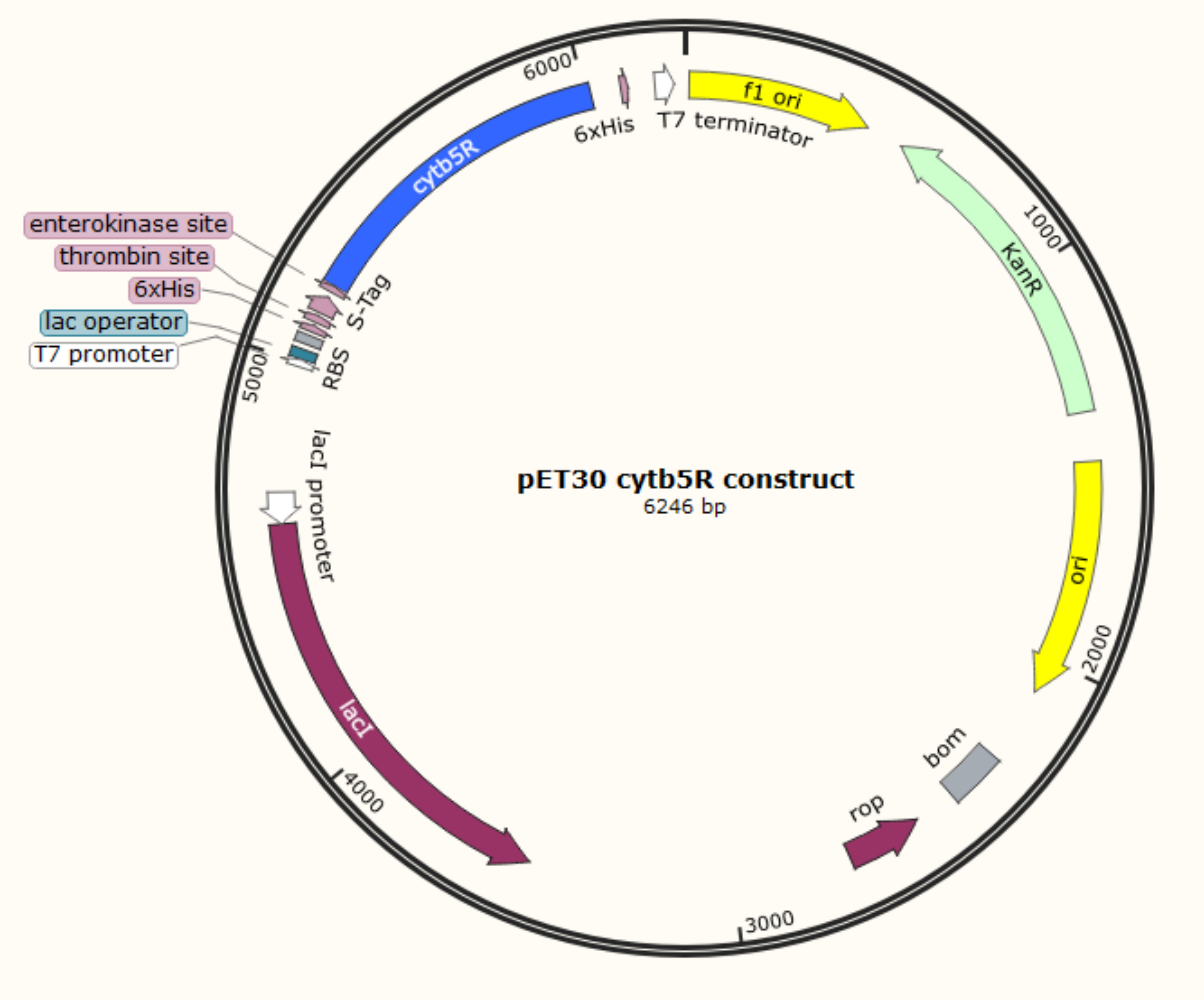

Figure 5.2: Plasmid map used for transformation of cytb5R into* E.coli *BL21 (DE3) cells. *The vector used contains a* lacI *gene (dark purple), responsible for the production of LacI, which itself is going to bind to the lac operator present on the plasmid, repressing the expression of the gene of interest, and on the operator present before the T7 RNA polymerase gene present in the host. Upon addition of IPTG, this repression is lifted, leading to the production of T7 RNA polymerase, in turn producing the protein of interest. The* cytb5R *gene (blue) is associated to a T7 promoter for its expression, two tags (one 6xHis and one S-tag) and two cleavage sites (one enterokinase and one thrombin). The antibiotic resistance gene is for kanamycin.*

The plasmid was then introduced into BL21(DE3) *E. coli* cells. These cells were precultured in LB-kanamycin before making glycerol stocks. Large cultures (1L) were then set up, with IPTG induction once the OD_{600} had reached 0.6.

The cells were harvested and sonicated to break them open. They were centrifuged to obtain the cytosolic components before the protein was purified with a Ni-NTA affinity chromatography. A SDS-PAGE was later performed in order to check the production and purification's efficiency (Figure 5.3). Single bands were observed in the elution columns that could correspond to the protein's expected migration at 34.4 kDa. The bands were very large, meaning that the protein was expressed and purified in high amounts. Same size

bands were observed in the washings, meaning that the amount of protein was high enough to be eluted from the column with small amounts of imidazole, and even in the flow-through, possibly suggesting higher volumes of Ni-NTA should be used in the future. Finally, other bands were observed in the elution columns, at a higher molecular weight than the protein of interest. These may be dimers (as they match the double of the size of cytb5R on the gel) or contaminants, but the amount of them compared to the target protein is very small.

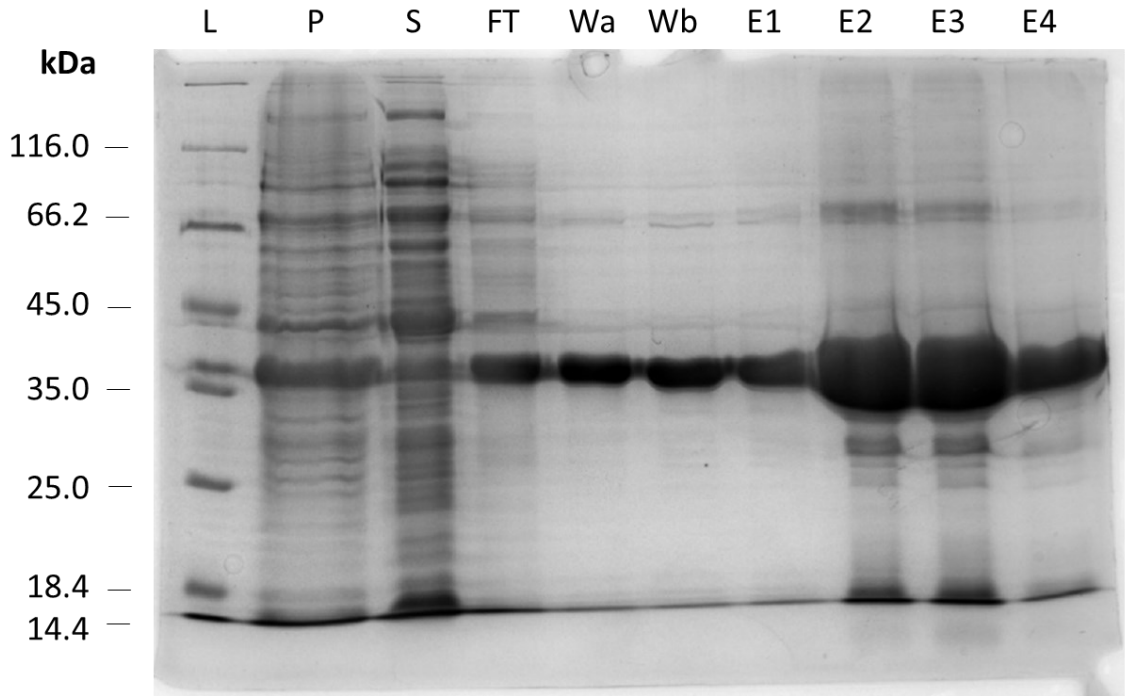

Figure 5.3: SDS-PAGE gels for cytochrome b5 dehydrogenase. *The protein was expressed in* E. coli *(BL21(DE3)). The cells were broken using sonication and the soluble protein was harvested by centrifugation at 43,667 xg for 20 min at 4 °C. The supernatant was then added onto 1 mL of Ni-resin for Ni-affinity chromatography. Fractions were then loaded on a SDS-PAGE for visualisation. L = ladder; P = pellet containing cell debris after 43,667 xg centrifugation; S = supernatant containing soluble fraction; FT = flow through; Wa = washing with 20 mM imidazole; Wb = washing with 40 mM imidazole; E1 to E4 = elutions with 200 mM imidazole.*

A colourimetric DC protein assay (from BioRad) was performed in order to evaluate the amount of purified protein produced. The first production of cytb5R yielded 5.5 mg/mL of protein. A second repeat of this expression yielded approximately 2.0 mg/mL and a final one gave 4.8 mg/mL. They were therefore all in the same range of yield.

5.2 Absorbance spectra

With both SdeA and cytb5R successfully expressed and purified, their absorbance spectra were measured without and upon reduction with sodium dithionite (Figure 5.4), as performed according to the literature (Wahl *et al.* 2010). As SdeA contains a cytochrome b5 group, its absorbance spectrum could be expected to be similar to what can be found in the literature for proteins with the same feature. An absorbance peak, called Soret peak, can be observed at approximately 410 nm. It shifts upon reduction to 420 nm. When zooming on the 450 nm area, minor peaks were also observed upon reduction. This confirms that at least the cytochrome b5 part of SdeA is correctly folded and should be functional. If any doubt was raised concerning the rest of the protein during the functional assay, it could be checked with a circular dichroism spectroscopy experiment.

A.

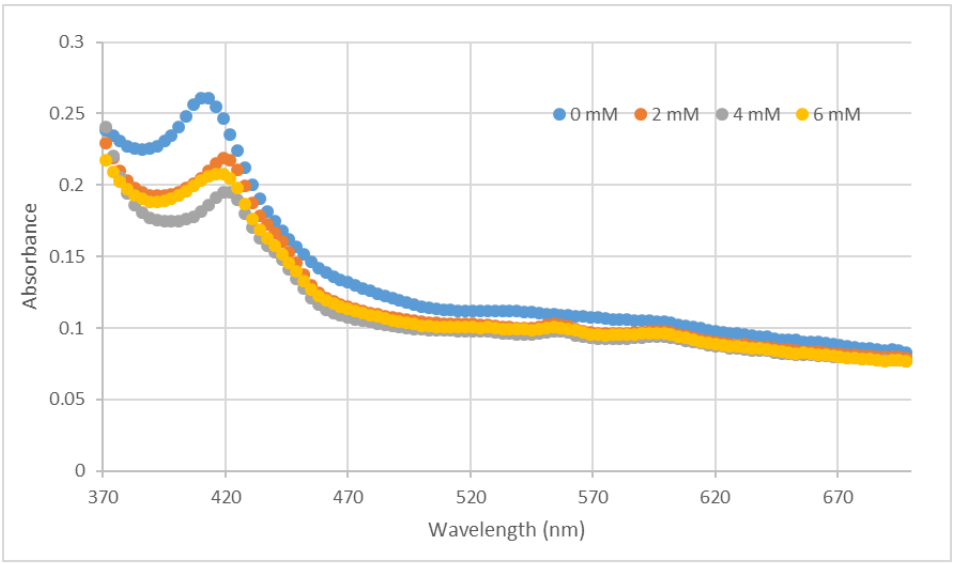

B.

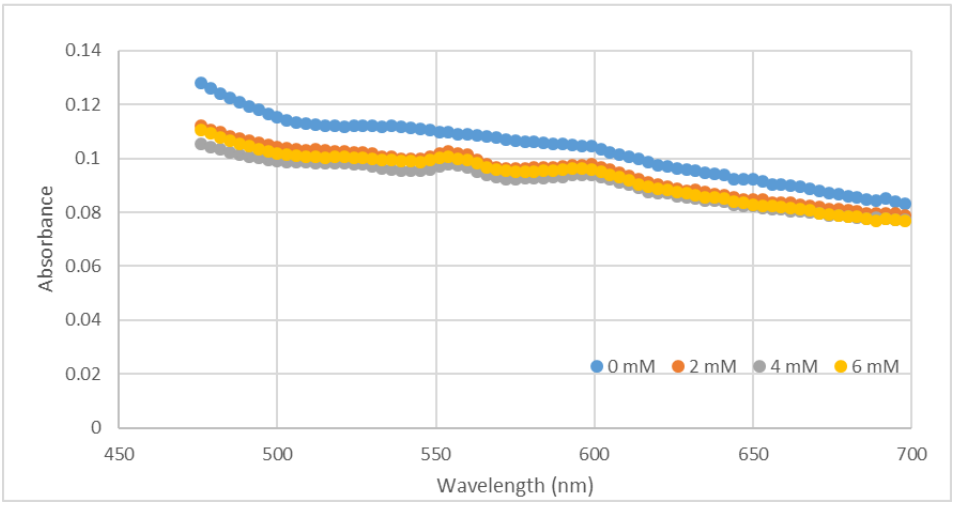

C.

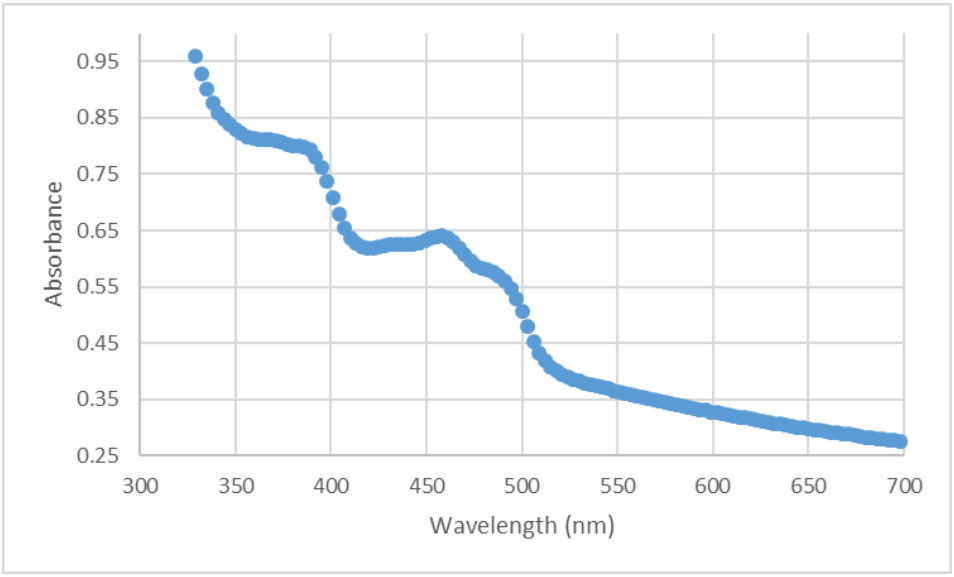

Figure 5.4: Absorbance spectra of both SdeA and cytochrome b5 reductase proteins*. A. Absorbance spectrum of SdeA upon reduction with sodium dithionite (2, 4 or 6 mM) The sample used for this spectrum did not contain the mADH contaminant. B. Zoom on the 550 nm area of the SdeA spectrum. C. Absorbance spectrum of cytb5R.*

For cytb5R, major peaks can be seen at approximately 390 and 460 nm. The latter is accompanied by a shoulder up to 480 nm. The sample also absorbs strongly in the UV area, which tends to slightly hide the peaks. As this absorbance was not removed when using a UV-compatible cuvette for the spectroscopic measurement, this absorbance can possibly be due to the presence of imidazole in the purified sample, but it does not prevent from observing the peaks.
This data is in accordance with what was found in the literature.

5.3 Functional assay

The activity of SdeA, together with cytb5R, was investigated using an enzymatic assay, where the consumption of NADH,H^+ was measured over a period of time of approximately 75 minutes (Figure 5.5). It is important to note that the SdeA used in these assays was from one of the early productions of SdeA, which did not contain the mADH contaminant.

SdeA, the substrate stearoyl-CoA, and co-factors NADH, H^+ and FAD were mixed together in a cuvette and the reaction was started by the addition of cytb$_5$R.

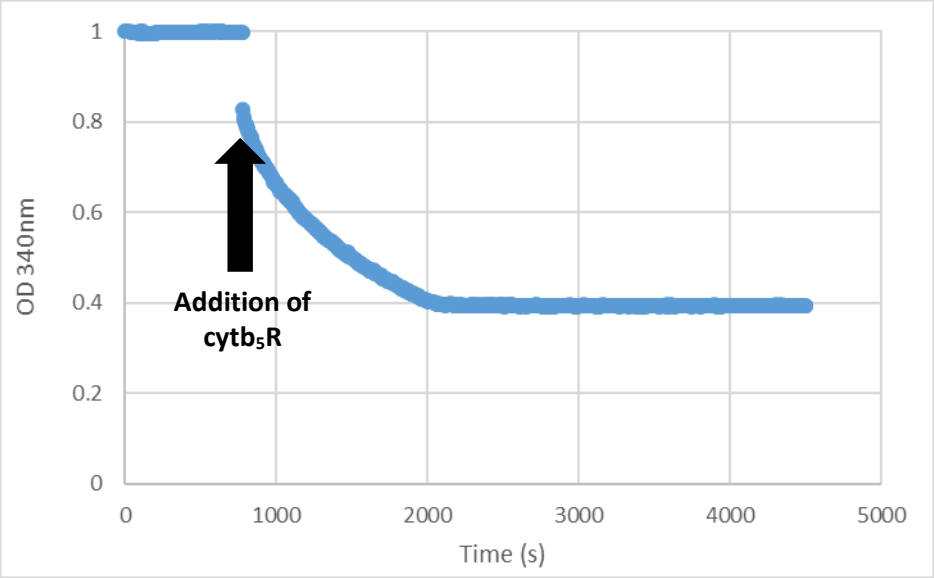

Figure 5.5: Functional assay of SdeA, together with cofactors FAD and NADH,H^+, the substrate stearoyl-CoA and the second protein cytochrome b_5 reductase. *The absorbance measurement at 340 nm was started and the latter component was added after approximately 800 seconds. The results were normalised using 1 as the starting value of absorbance.*

Cytb5R was only added after the reaction had started so that we could make sure the decrease of absorbance that would be observed would be due to the reaction taking place rather than other factors. For example, we were suspecting that a decrease of $NADH,H^+$ absorbance could be due to it being naturally oxidised through contact with the oxygen in the air. As we observed that the absorbance was quite stable over time before addition of the second protein, we could conclude this was not the case. The initial rapid drop in absorbance observed upon the addition of cytb5R is due to the dilution of the reaction mixture, as approximately 200 µL were added in order to make a final volume of 1 mL, which is in accordance with the approximate drop of 20 % of absorbance observed.

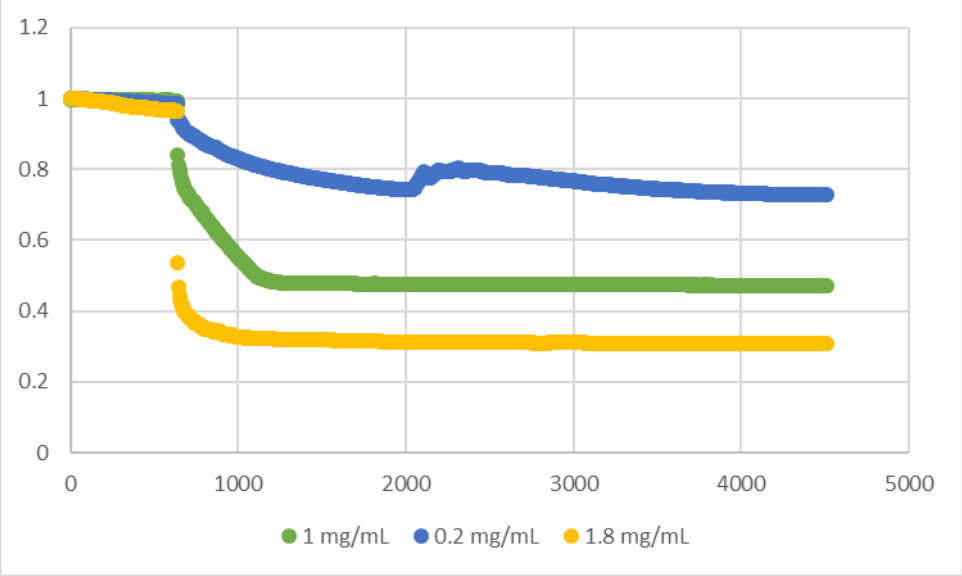

Figure 5.6: Evolution of the absorbance measured at 340 nm during the functional assay with varying concentrations of cytb5R.

The ratio of some of the components in the reaction could be modified in order to change some of the reaction parameters. For example, the higher the final concentration of cytb5R, the faster the reaction took place (Figure 5.6). Several concentration parameters were tested in order to find the optimal speed for the reaction. The final concentration of cytb5R chosen for the following experiments was 1 mg/mL, or 10 mM.

Another parameter that could be changed was the initial concentration of $NADH,H^+$, which was influencing the initial absorbance of the mixture. Finally, an excess concentration of stearoyl-CoA was initially used, but as it is a quite expensive reagent, lower concentrations of this substrate were tested in order to save it (Figure 5.7). Dividing the concentration of stearoyl-CoA by 4 did not affect the successfulness of the reaction.

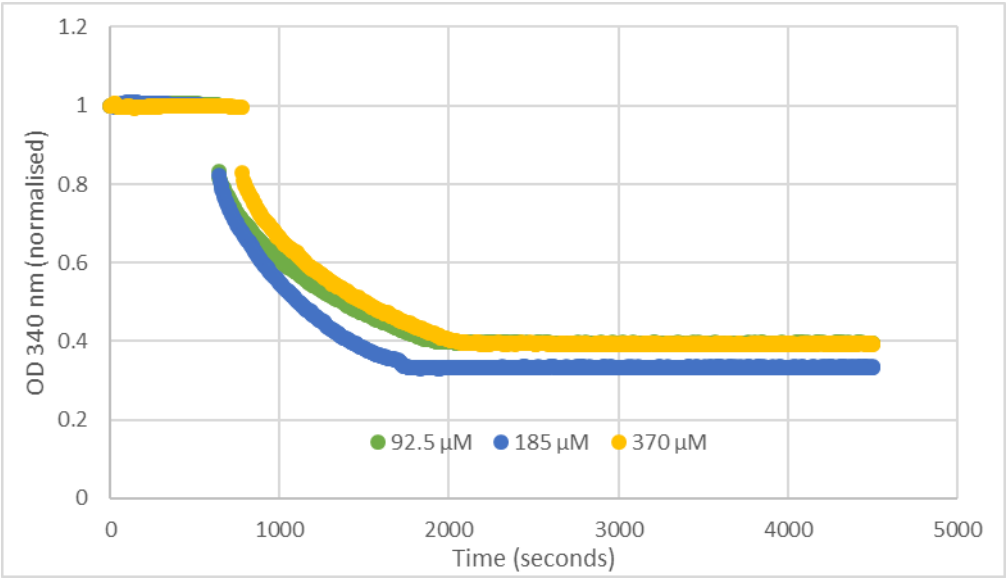

Figure 5.7: Use of different concentrations of stearoyl-CoA during the functional assay.

Furthermore, in order to make sure the decrease measured was really representative of the reaction, several controls were performed, where the reaction was set up normally except for one component missing, therefore preventing the reaction to take place. The missing component was replaced with purification buffer in order to keep the same final reaction volume. Controls were performed with either FAD, cytb5R or stearoyl-CoA missing (Figure 5.8).

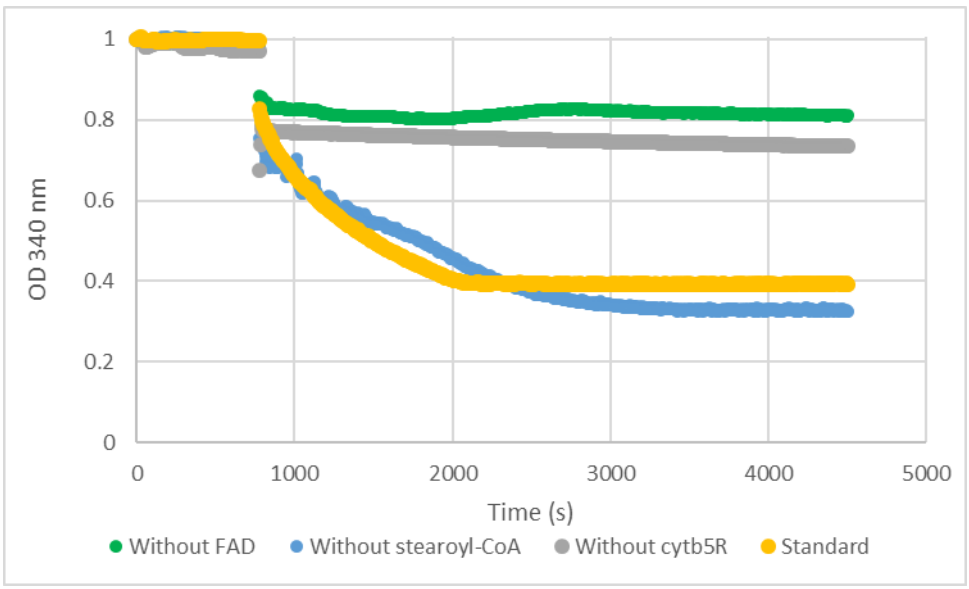

Figure 5.8: Controls performed on the functional assay with one component missing. *The different controls were performed using the exact same parameters as the standard reaction, except that the missing component was replaced by purification buffer.*

While the reactions that did not contain FAD or cytb5R did show that the reaction was not taking place anymore, it is not the case for the reaction without stearoyl-CoA, which surprisingly showed similar decreasing absorbance properties as per the standard reaction. It could be easy to conclude that two of the controls were successful in showing that the standard functional assay was working correctly, but one can wonder how the reaction was able to take place without its substrate. Our main hypothesis to explain this would reside in the presence of lipids in the SMALP, which could be used as an alternative substrate for the reaction to take place. As the membrane lipids contain phospholipids, themselves containing hydrophobic tails including stearic acid equivalents, we could easily think of them as being used by the enzyme in the absence of a substrate. One good way of (dis)proving this theory would be to solubilise the membrane protein with a solubilisation tool that does not engulf the lipids surrounding the membrane protein. Notably, the protein's activity would have to be checked by performing a normal function assay at first to make sure it is working correctly, before performing the substrate-lacking control.

5.4 Testing of antifungal compound

An antifungal compound named F900742, belonging to the F6 series developed by the industrial partner F2G was provided. The minimum inhibitory concentration (MIC) against *Aspergillus spp.* was measured by F2G at 0.8 µg/mL on the whole fungal organism. Therefore, larger amounts of the compound were first tested, to see if the inhibition of the reaction was taking place, before reducing the inhibitor's reaction towards the range of the MIC (Figure 5.9), in order to be able to observe a dose-dependant response.

While the reaction was inhibited as expected with large concentrations of 20 to 50 µg/mL of inhibitor (25 to 60 times the MIC), with the final reached OD of approximately 70 to 80 %, the inhibition stopped taking place with concentrations lower than 20 µg/mL. Indeed, with tested concentrations of 5 and 10 µg/mL, the final OD went down to approximately 40 % of the initial absorbance measurement, which corresponds to what was observed with the normal reaction taking place. Therefore, it can be assumed that the measured inhibition value in these conditions, which corresponds to the IC50, was approximately 20 times higher than the MIC. This can come as a surprising result as one could expect that concentrations *in vivo* would require higher values to be effective, due to the level of complexity of the environment leading to the drug interacting with other elements of the target organism. One possible explanation for this mechanism could rely on the protein concentration, potentially higher in the *in vitro* test. The amount of SdeA naturally present in *A. fumigatus* would be required in order to perform a test with an equivalent concentration.

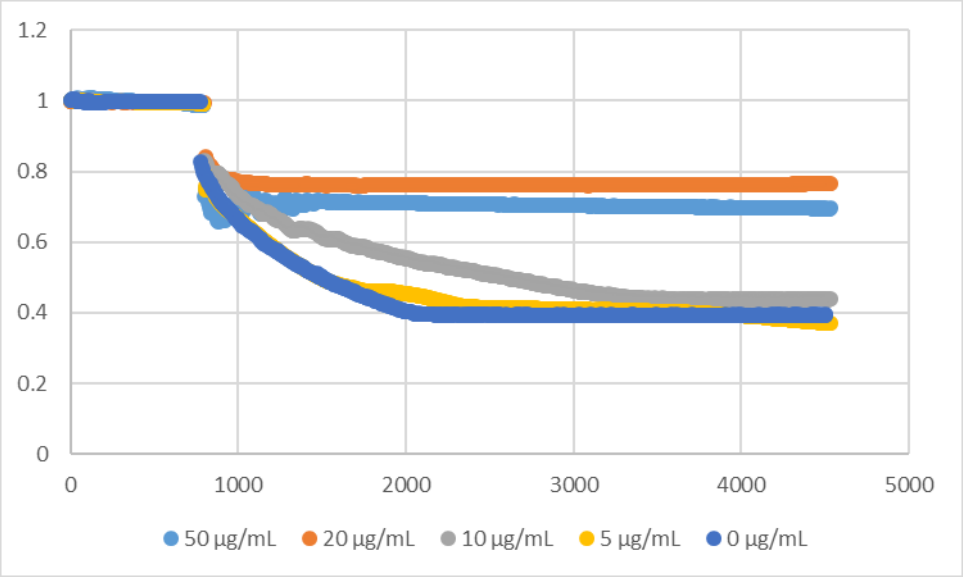

Figure 5.9: Evolution of OD measurement at 340 nm, with decreasing concentrations of inhibitor F900742. *The same parameters were used as during the functional assay, with the addition of different concentrations of the inhibitor.*

Overall, despite the low SdeA concentration that was obtained after purification, the functional assay worked very well. The $NADH,H^+$ absorbance can be very well seen decreasing over time, meaning its electrons were used for the reaction. A basal absorbance was always observed at the end of the functional assay, which could be explained by the absorbance observed at 340 nm for both SdeA and cytb5R. The controls performed were very successful as well, with the reaction being prevented every time one of the components of the reaction was missing. Furthermore, the inhibitor F900742 provided by F2G was successful at inhibiting the desaturation reaction down to 20 µg/mL. The reaction is also slowed down at 10 µg/mL but not completely inhibited. The reaction takes place normally with concentrations of 5 µg/mL of inhibitor, as the curve corresponding to this concentration almost fully matches the one without inhibitor, meaning that the reaction takes place normally in this range of concentration. This was more of a surprise as the MIC calculated by F2G on whole fungal organisms was 0.8 µg/mL.

6. DHODH

The other potential target developed by F2G is dihydroorotate dehydrogenase, another membrane protein from the inner mitochondrial membrane involved in the process of pyrimidine biosynthesis (Figure 1.6). This flavin-dependent target already has a drug candidate called olorofim, currently under clinical trials.

F2G Ltd has already expressed a truncated version of this target as a soluble protein, missing the membrane anchor, which has been used so far for the drug screening processes (Oliver *et al.* 2016). However, a better test sample would be the full-length protein including the transmembrane region. It would particularly be of interest to see if the transmembrane location had any impact on the protein function and/or interaction with the drug olorofim. This part of this project therefore focusses on the production of both the full length (DHODH-FL) and the truncated (DHODH-TR) versions of the protein in order to test potential differences between them.

6.1 DHODH-TR

6.1.1 Production and purification

The truncated version of DHODH was expressed in *E.coli*. The plasmid provided by F2G contained a NusA protein sequence fused to the DHODH-TR sequence. NusA is a protein capable of inhibiting the Rho-dependent transcription termination in *E. coli*, thus preventing unwanted terminations (Qayyum, Dey, and Sen 2016). This plasmid was first introduced into *E.coli* DH5α cells before performing a miniprep on them. 300 µg/mL of purified plasmid were obtained from a 20 µL elution sample, which gives a total of 6 µg of DNA. 2 µL of this plasmid sample were added into *E. coli* BL21(DE3) cells for expression. After induction with IPTG and cell harvesting, the cells were broken using sonication and the contents were collected for purification on a Ni-affinity column.

Fractions of each elution from the purification were run on SDS-PAGE (Figure 6.2).

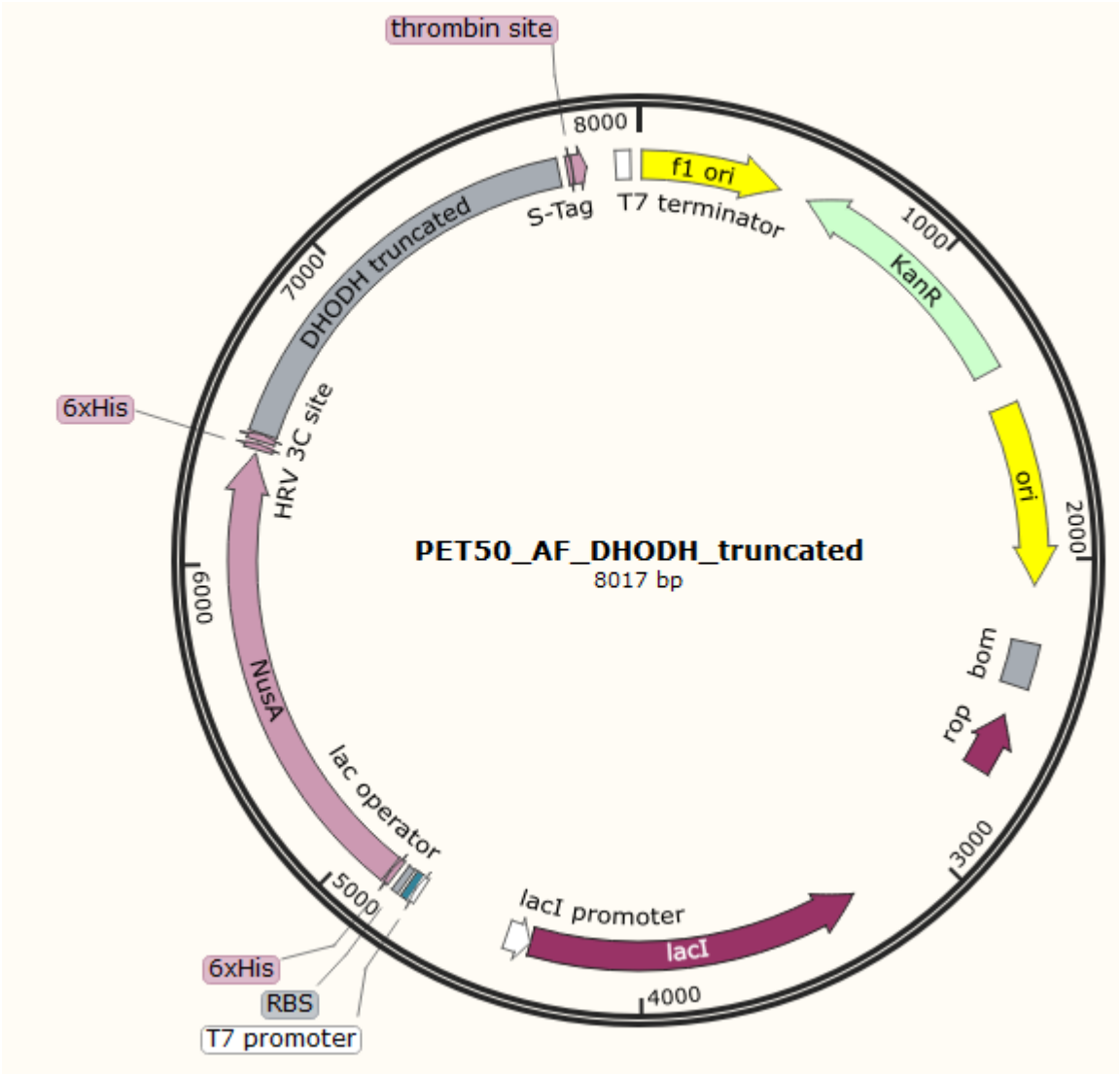

Figure 6.1: Plasmid map used for transformation of DHODH-TR into* E.coli *BL21(DE3) cells. *The vector used contains a* lacI *gene (dark purple), responsible for the production of LacI, which itself is going to bind to the lac operator present on the plasmid, repressing the expression of the gene of interest, and on the operator present before the T7 RNA polymerase gene present in the host. Upon addition of IPTG, this repression is lifted, leading to the production of T7 RNA polymerase, in turn producing the protein of interest. The* DHODH-TR *gene (grey) is associated to a T7 promoter for its expression, two 6xHis tags) and one cleavage site (HRV 3C). The antibiotic resistance gene is for kanamycin.*

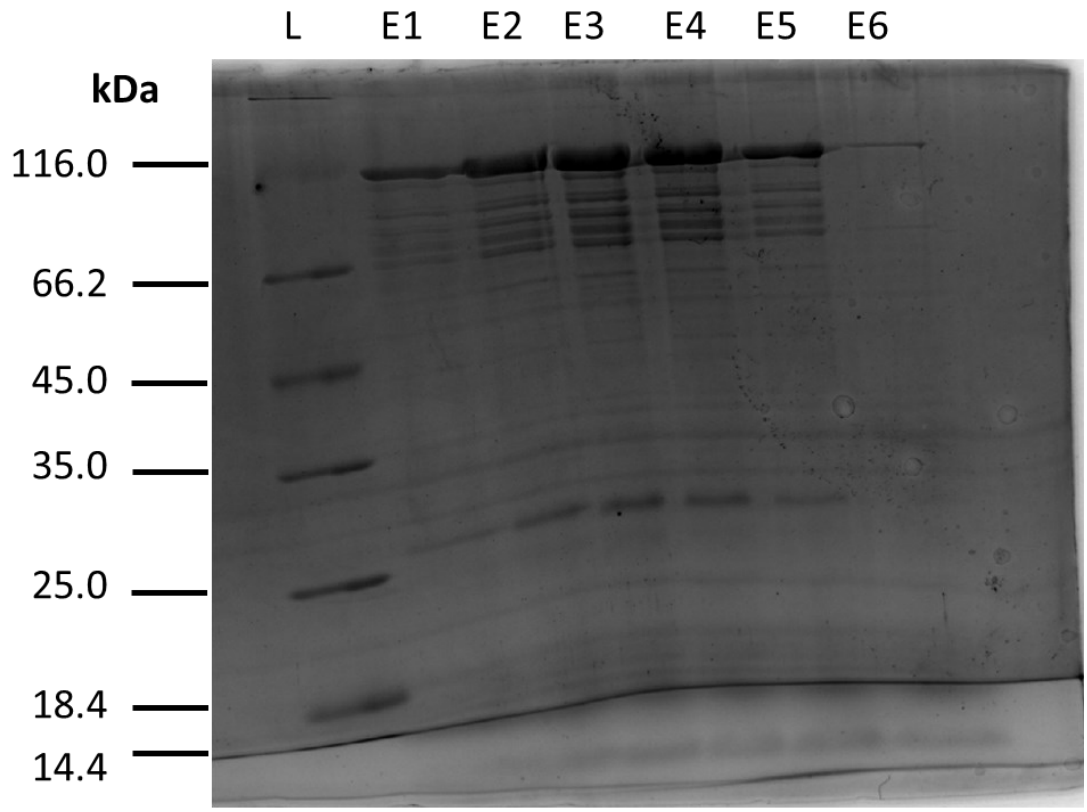

Figure 6.2: SDS-PAGE gel of DHODH-TR purified protein*. Purification was performed after harvesting 1 L of* E. coli *BL21(DE3) and breaking it with sonication. Purification was performed via Ni-affinity chromatography. L= ladder, E1 to E6 = elutions with 200 mM imidazole*

As can be observed on the gel, there are many bands showing very different size. A band of relatively high intensity can be observed at the expected migration (105 kDa), corresponding to the expressed construct. The other bands could correspond to contamination or protein degradation. The use of protease inhibitors is supposed to prevent such degradation but it is not always successful. Several more attempts were performed for protein production and purification, which showed the same degradation, even despite using double the concentration of protease inhibitor. Moreover, there were also more bands observed on top of the gel (Figure 6.3). They could correspond to aggregation, despite the presence of the NusA fusion protein partner, which is supposed to prevent this from happening.

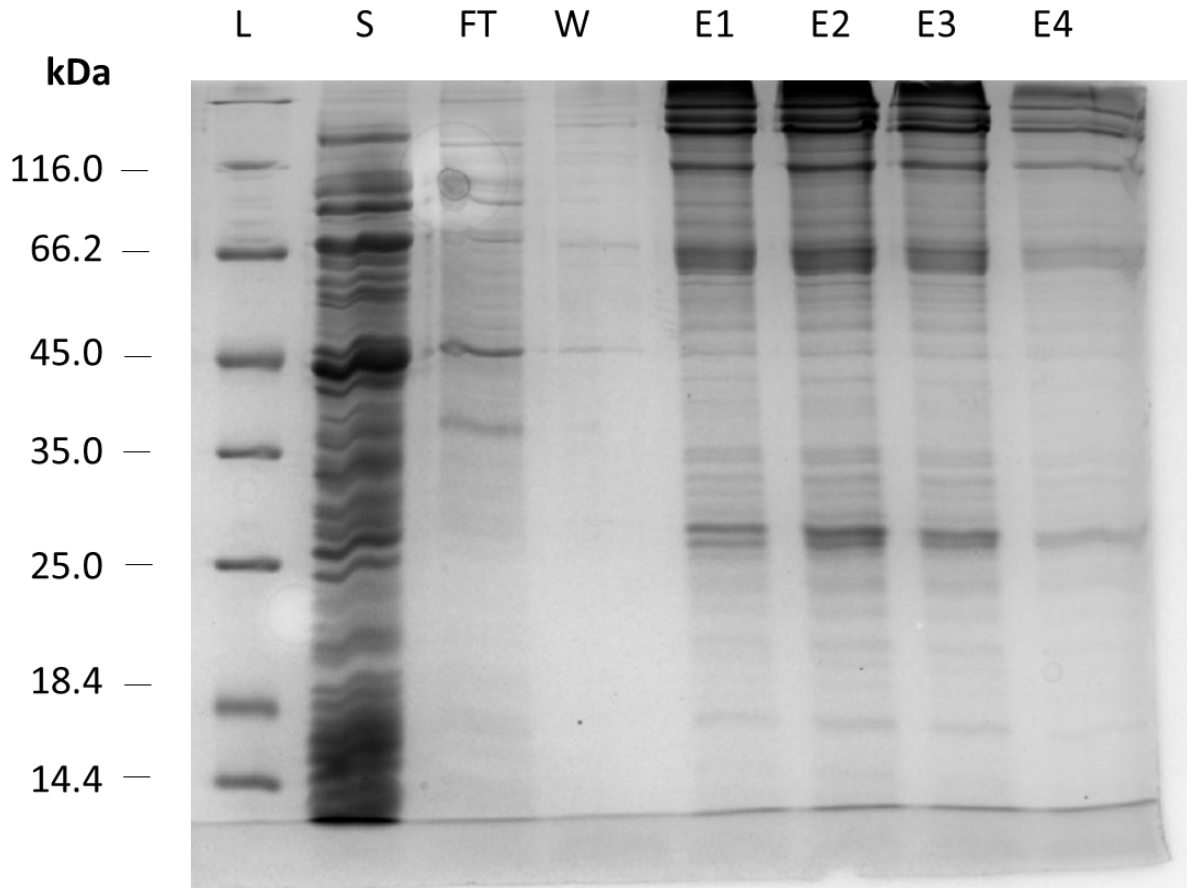

Figure 6.3: SDS-PAGE for a second DHODH-TR production. *The same methods were used as for the previous one. L= Ladder, S = soluble part, FT = flow-through, W = Washing with 40 mM imidazole, E1 to E4 = elutions performed with 200 mM imidazole during Ni-affinity chromatography.*

Again, there could be a band that correspond to the expected size of the protein at 105 kDa, but there are more importantly a lot of other bands below and especially above the right size. After having performed a western blot analysis on the purified protein sample, it turns out the same bands are found again (Figure 6.4). This came as a surprise, but could confirm the hypothesis of protein degradation for the lower size bands and potentially aggregation for the higher size bands. Since this entire protein sample seemed to correspond to the protein of interest, a quantification experiment was performed using a micro-BCA assay (Table 6.1). A concentration of protein of up to 175 µg/mL was found for elution 2.

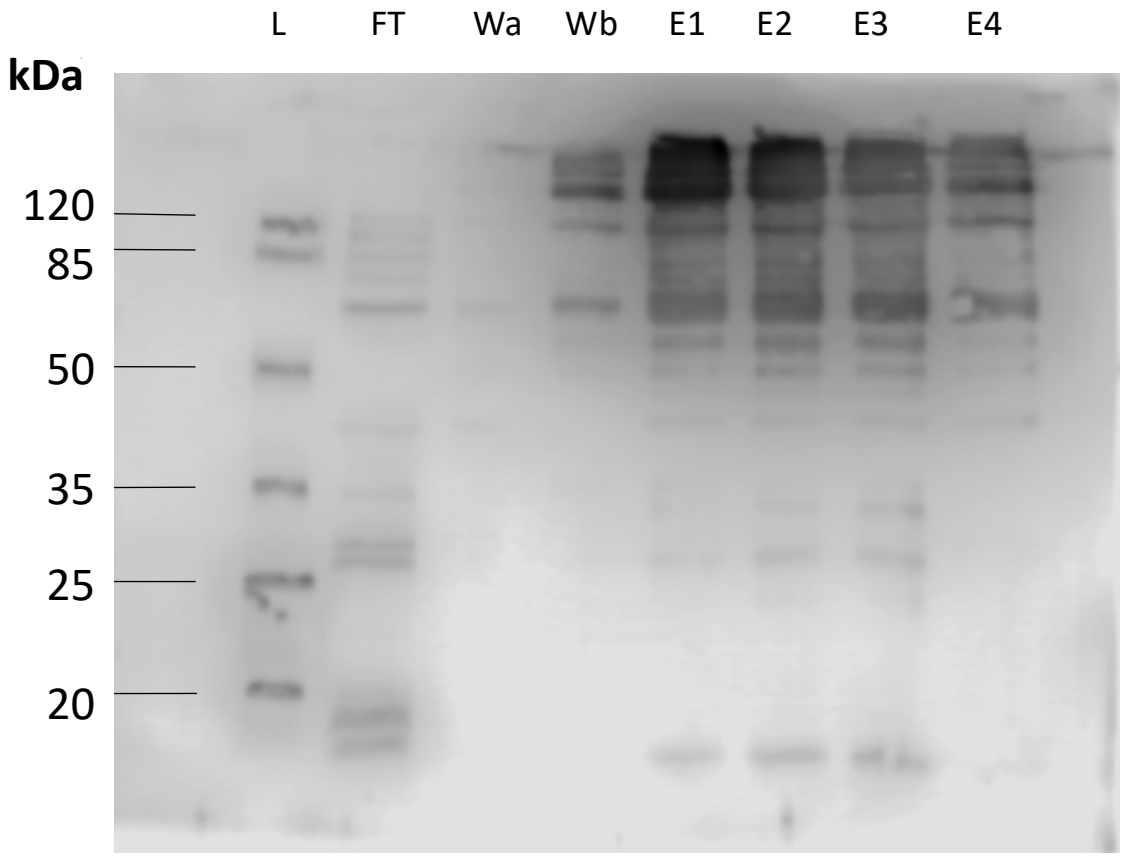

Figure 6.4: Western blot analysis for purified DHODH-TR protein. *The antibody used is an anti-his mouse antibody, coupled to an anti-mouse HRP secondary antibody.*

	OD 562 nm	Concentration (µg/mL)
E1	1.118333	155.3619
E2	1.253333	174.6476
E3	0.888667	122.5524
E4	0.556	75.02857

Table 6.1: Quantification of purified DHODH-TR protein using a micro-BCA assay. *This quantification was performed on the second protein production, with extra bands for protein degradation and aggregation.*

6.2 DHODH-FL

6.2.1 Transformation in *P. pastoris*

A bacterial expression plasmid containing the DHODH full-length gene was provided by F2G Ltd. F2G had previously attempted to express the full-length protein in *E. coli* without success, but given it is a fungal protein, it was considered that *Pichia pastoris* would be a better choice of host. The successfulness of this membrane protein expression in yeast was predicted (Table 3.1)((White *et al.* 2007), with all the optimal parameters being met, except the protein size being slightly too large. The single transmembrane domain makes the protein simple enough to be able to be confident about the expression in a yeast host. The gene could not easily be transferred from the bacterial vector into a yeast vector. Instead, the gene was ordered from Genscript in the yeast expression vector pPICZα A (Figure 6.5).

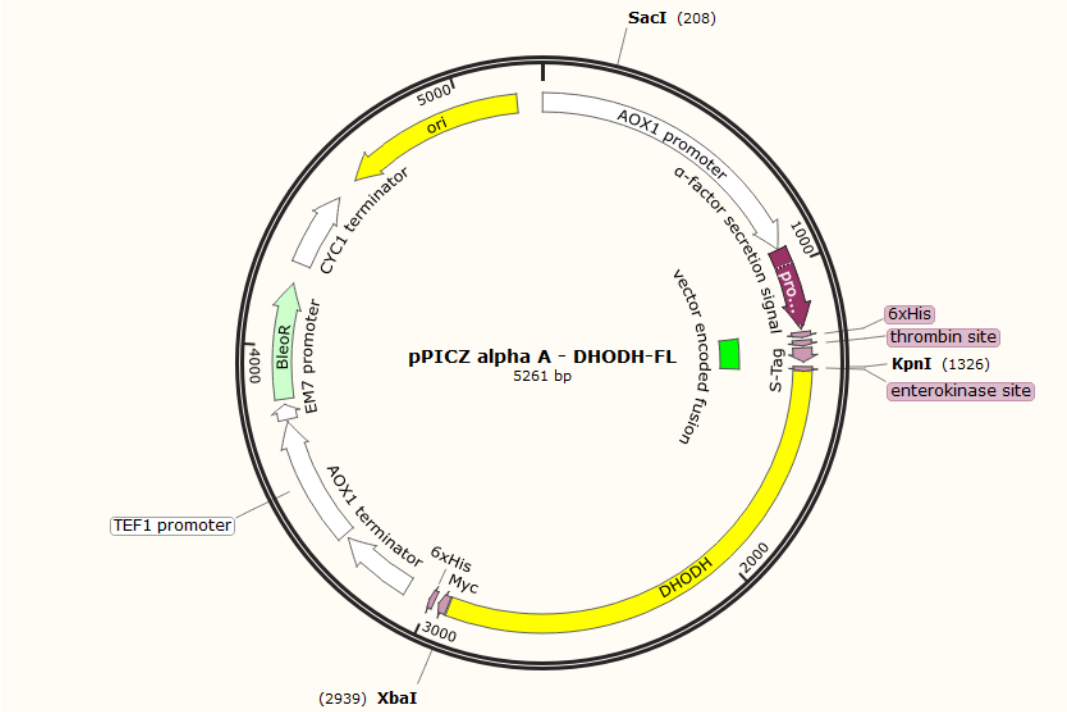

***Figure 6.5: Map of the plasmid used for the transformation of the DHODH-FL gene in* P. pastoris**. *The gene was cloned in the vector using KpnI and XbaI restriction sites. The plasmid was linearised prior to transformation using the SacI restriction site in the AOX1 promoter. The vector used is a pPICZ(alpha) A containing an AOX1 promoter and terminator for double homologous recombination, an α-factor secretion signal traditionally used for secreted proteins, but that seemed to show better results for membrane protein production according to other researchers in our lab. Finally, the DHODH sequence (yellow) contained two tags on the C-terminal part of the sequence: a 6xHis-tag and a Myc-tag.*

Transformation of DHODH-FL plasmid was performed in *P. pastoris* X-33 cells. Several trials were performed with both electroporation and chemical methods before the latter finally yielded several dozens of colonies. These were put into liquid YPD culture with 100 µg/mL of zeocin, before being streaked again on high (1000 µg/mL) antibiotic-containing YPD plates. They were also checked under the microscope (Figure 6.6). Quite a few colonies were still growing in this environment, but the three showing fastest growth were selected for protein production.

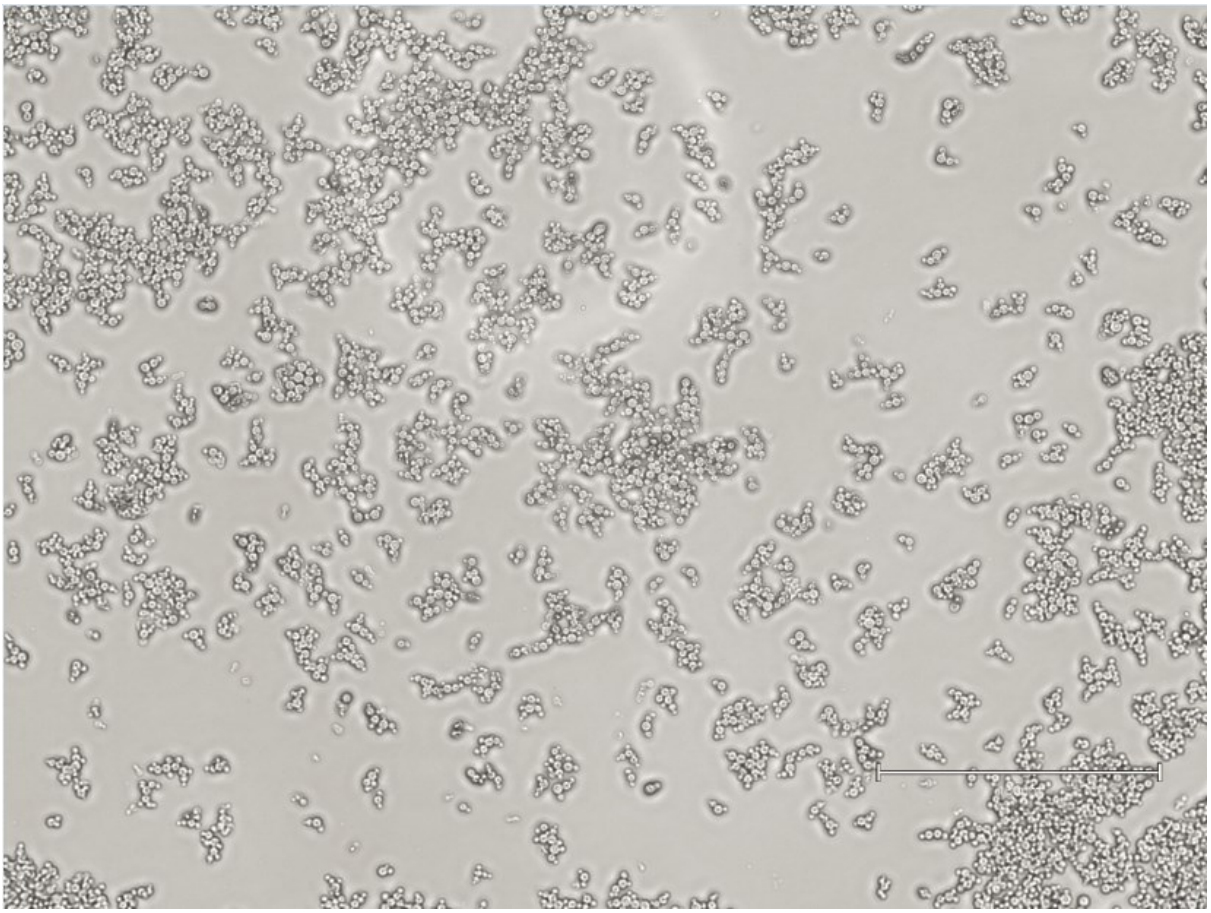

Figure 6.6: Microscope visualisation of one of the DHODH-FL-transformed yeast cultures using microscope Evos m5000 from Invitrogen. *Scale bar in the bottom right hand corner represents 150 µm.*

6.2.2 Protein production and purification

Medium-scale cultures were prepared with protein production in 500 mL BMMY. Cells were broken with each method at least once (C3, French Press, glass beads), with C3 being again the most efficient method for large enough samples. Two of the cultures used with C3 as the cell breaking method have been summed up in table 6.2. The OD_{600} was also measured at the end of the culture, just before cell harvesting, and showed 2.10 for experiment 1 and 2.37 for experiment 2.

Experiment number	Total mass of cells obtained (g)	Mass of membranes obtained (g)	Ratio membranes / cells	Total volume of the culture (L)	Mass of membranes per litre of culture (g/L)
1	42.1	4.41	0.10	2	2.21
2	24.2	2.71	0.11	1.5	1.81

Table 6.2: Comparison of the yields of membranes containing DHODH-FL obtained in each cell culture experiment. *The ratio of membranes / cells is calculated as well as the yield of membranes per litre of culture. The membranes collected were eventually resuspended in resuspension buffer at around 180 mg/mL.*

Membranes were then solubilised using SMA2000 and purified with Ni-affinity chromatography.

6.2.3 Characterisation

Fractions from the purification were loaded on a 12% polyacrylamide gel (Figure 6.7). A very faint band seems to appear at the expected size for DHODH of approximately 60 kDa. However, the mADH contaminant seems to be present once again at around 40 kDa.

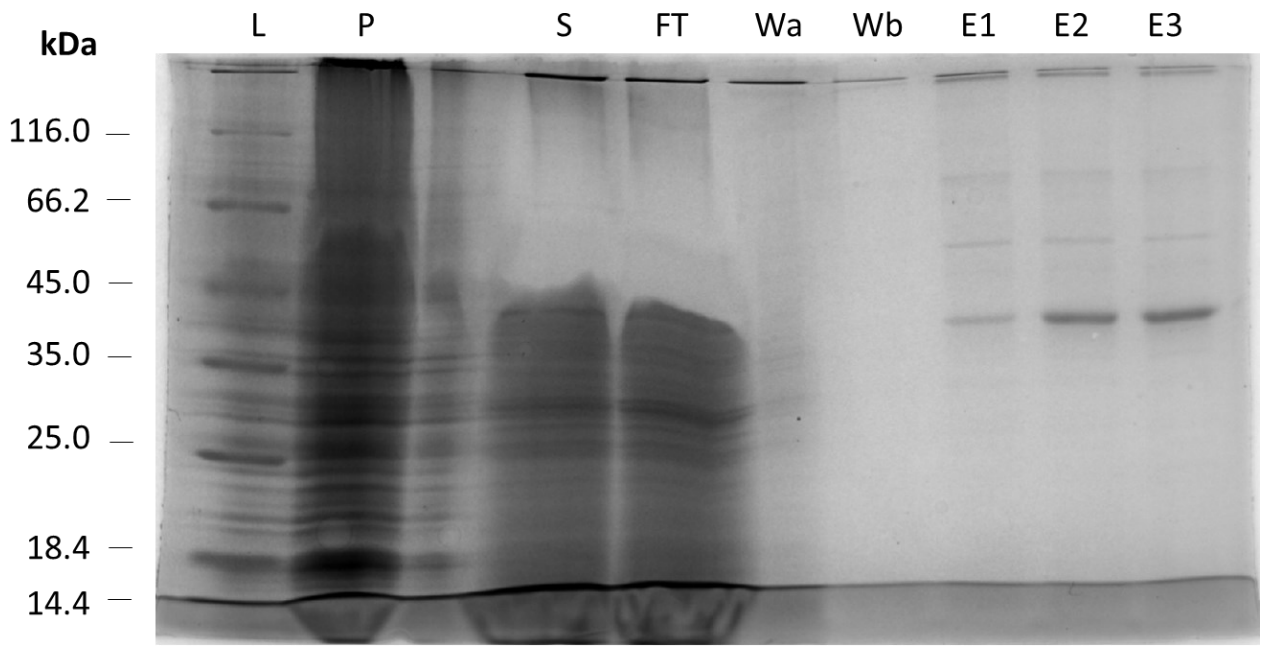

Figure 6.7: SDS-PAGE gel of DHODH-FL purified protein*. Cells were harvested after a culture in BMGY followed by BMMY. They were broken using a C3. Purification was performed by Ni-affinity chromatography. L = ladder, P = Pellet (non-solubilised membranes), S = Supernatant (solubilised membranes), FT = Flow-through, Wa = 20 mM imidazole washings, Wb = 40 mM imidazole washings, E1-3 = elutions with 200 mM imidazole.*

In conclusion, DHODH could be successfully expressed both in its truncated and full-length version. These productions are still quite preliminary results and would need further investigation with western blot analysis, potentially absorbance spectra and mass spectrometry analysis to confirm they were correctly expressed. Several issues regarding protein aggregation or degradation are still present for the truncated protein, while the full-length one is showing an extra band that looks like the same contaminant found with the SdeA production. Transformation of the DHODH-FL plasmid could be performed in the mADH-KO *P. pastoris* strain in order to see if this issue can be improved.

7. Discussion

7.1 SdeA production and purification

7.1.1 Optimisation of the transformation protocol

While the transformation using electroporation was successful during the preparation of the mADH-KO *P. pastoris* strain, it did not work so well when transforming the SdeA or the DHODH plasmid due to technical issues with the equipment. Chemical transformation was therefore the preferred method although it was coming with its setbacks as well. While it is generally admitted electroporation is a more efficient method (Kawai, Hashimoto, and Murata 2010; Wu and Letchworth 2004), it is also much faster and easier than the chemical one, which requires more time and reagents. One of the biggest issues encountered was the fact that the experiment was generally started early in the morning, only to be finished approximately 14 hours later, quite late in the evening. The main reason for this was that the cells had to be left to incubate at 30 ˚C for approximately 6 hours to go from OD_{600} 0.1 to 0.8-1, in order for them to be actively dividing, before the actual transformation process could be started. In order to improve this, the cells were instead left to incubate overnight at a lower temperature, in order to be able to start the transformation protocol early in the morning. The temperature used varied between 20 and 25 ˚C, but the transformations were eventually not very successful. Instead, a much lower volume of the preculture was added into the 50 mL of YPD (10 µL instead of 300). This time, the transformation worked much better with high number of colonies growing on plates, meaning that the cells most likely had to be actively dividing at their optimal temperature for the experiment to be successful. This method was also tested by other researchers with high efficiency (Fitzgerald, Rodriguez, and Lewis 2022). The same researchers also showed that better transformation efficiencies are obtained when DMSO is used at a final concentration of 10 to 15 %, which is not something that was tested during this project but could be an improvement opportunity. DTT has also been successfully used in the same kind of protocol (Tripp *et al.* 2013). This chemical is believed to promote the destabilisation of the cell wall. They also emphasized the importance of using relatively fresh salmon carrier DNA, as older batches tend to show a reduction in size that dramatically decreases the transformation efficiency. During this project, better transformations were indeed performed upon using a fresh carrier DNA sample.

Furthermore, the transformation that worked the best contained only 6 µg of linearised plasmid, meaning that it is not necessary to add 10 µg every time. Finally, the linearised plasmid was either cleaned up after the digestion experiment, removing the buffer and nuclease, or not. No difference in the successfulness of the experiment was observed, meaning that the presence of the enzyme and the buffer were not issues for this experiment (The enzyme was however heat inactivated every time to avoid further unwanted digestion).

More methods for transformation of yeast species have been developed, including physical methods using shockwaves, vacuum infiltration or biolisitics although they have not always been applied to *P. pastoris* yet (Rivera *et al.* 2014; Kawai, Hashimoto, and Murata 2010).

7.1.2 Optimisation of the production protocol

We chose to use shaker flasks as SdeA had already been produced and purified successfully by another research using this method. Although some studies showed that yields were typically higher using bioreactors (Matthews *et al.* 2018; Cregg *et al.* 2000), it did not work so well for other proteins (Ayub *et al.* 2022). As it is a very protein-dependent process, bioreactors remain a possible idea for optimisation that can be investigated, because they offer a strict control over oxygen, pH and feeding levels, allowing for optimal growth conditions. It is of course much more difficult to control these parameters with shaker flasks. For example, continuous control over feeding decreases the likelihood of cell lysis in the culture due to nutrient starvation or overdosing caused by intermittent manual feeding (Werten *et al.* 2019). This is especially the case for the regular additions of methanol on the later culture stages. Moreover, the pH in the culture can have a dramatic impact on proteolysis of secreted recombinant proteins produced in *P. pastoris* (Sinha *et al.* 2005).

The protocol that was used for the production of a protein in *P. pastoris* normally includes 24 hours of incubation during the first phase of the culture. It is believed that cells in growth phase are actively dividing, while cells in stationary phase develop a wider resistance to environmental stresses (Herman 2002). During the experiments performed, several dilution times were tested, including cells in growth phase (24 h), late growth phase (30 hours) or stationary phase (48 h). As shown in figure 3.3, the cells do not reach the stationary phase before at least 30 hours of culture with the initial inoculation. While the first experiment did not show growth, the two others worked fine. Therefore, we suggest cells need to reach a certain level of concentration before being diluted into larger culture volumes. However, they do not seem to need to be actively dividing to be able to divide again upon dilution.

7.1.3 Solubilisation of the protein from the membrane

Unfortunately, as it is easy to notice on the SDS-PAGE gel of figure 3.4, most of the SdeA protein production was lost in the pellet during the solubilisation. Only a small part remained to be purified. This was confirmed by western blot on figure 3.9, where solubilisation efficiencies measured remained around 5%. The reason for this disappointing result is yet to be identified, but it can be something quite protein-specific. Different studies have had varying levels of solubilisation efficiencies, with some barely finding any solubilisation at all (Voskoboynikova *et al.* 2021) while others were more successful in this regard (Ayub *et al.* 2020; Jamshad *et al.* 2015; Smirnova *et al.* 2016). The ones that did manage to perform a nice extraction of their respective membranes proteins tend to have used longer solubilisation times (of up to 20 hours at room temperature), which may seem a bit concerning in regards to protein stability, but could be worth a try nevertheless. Other studies had more mixed results according to the different types of membrane proteins or polymer used (Skaar *et al.* 2015), which would indicate that this could be quite a protein-dependent process. The fact that most of successful solubilisation studies used *Saccharomyces cerevisiae* instead of *Pichia pastoris* can also be an indicator that membrane lipid composition could have a role in solubilisation efficiency, especially considering the differences in lipid composition between these two organisms. Indeed, *P. pastoris* lipid droplets seem to show higher preponderance of triacylglycerols, unsaturated fatty acids and ergosterol precursors than *S. cerevisiae* (Ivashov *et al.* 2013). Similar conclusions were reached upon analysis of microsomal membranes (Klug *et al.* 2014).

Lipidomic studies have been showing SMA's propensity to solubilise different lipids from yeast cells, showing that ergosterol seems to be depleted from SMALPs compared to its overall presence in the yeast plasma membrane by 6-fold, while phosphatidylserine is two to three times more present in SMALPs than in the overall plasma membrane *(*van 't Klooster *et al.* 2020). This would suggest that the presence of ergosterol around the membrane protein that is supposed to be solubilised from the plasma membrane would be detrimental for its proper extraction, thus decreasing solubilisation efficiency. Humanised cell lines have been engineered for yeast, including the presence of cholesterol instead of ergosterol on their membranes, mostly in order to express human proteins but it should be also considered to verify SMA's efficiency at solubilising membrane proteins (Emmerstorfer-Augustin *et al.* 2019; Hirz *et al.* 2013). On the other hand, it has already been shown that *P. pastoris* membranes contain 8 times less ergosterol than *S. cerevisiae* (Grillitsch *et al.* 2014), which would tend to disculpate ergosterol's responsibility in low solubilisation efficiency. Since there seems to be better solubilisation efficiencies using *S. cerevisiae*, more lipidomic studies comparing the organism's lipid compositions could be helpful to try to understand

why *P. pastoris* seems so resistant to solubilisation with SMA polymers, using thin layer chromatography for example and possibly mass spectrometry analysis. While the poor solubilisation efficiency also observed with detergent would tend to support the idea of SdeA preferentially locating in lipid rafts, containing higher levels of ergosterol, SdeA's native location in the ER means that we are not sure about its propensity to localize in lipid rafts when being overexpressed, and therefore if this could have an influence on the solubilisation experiments performed.

Another option for SMA's lack of efficiency towards solubilising membranes from yeast could stem from the cell wall. Despite it being theoretically removed during membrane preparation, there could still be remnants of the cell wall that would impair SMA's activity on membrane proteins. Investigating this by making protoplasts before breaking the cell, by using zymolyase treatment for example, could represent a way of improving membrane proteins' solubility in yeast. Short induction times could also be tested in order to harvest cells presenting a smaller cell wall.

Finally, a last hypothesis explaining low levels of membrane protein solubilisation could rely on the protein of interest forming big oligomeric aggregates in the membrane. There is evidence that this issue would lead to SMA not being able to extract the protein from the membrane correctly (Gulati *et al.* 2014; Bell, Frankel, and Bricker 2015).

The levels of production for SdeA were high enough for the low solubilisation efficiency not to be a problem, but it could become a problem for membrane proteins expressed at lower levels. Studies have tried to solubilise proteins directly from cells rather than from membrane preparations, which would tend to decrease the rate of aggregated and misfolded proteins (Hartmann *et al.* 2017). However, for yeast this requires pre-treatment with zymolyase in order to remove the cell wall and make protoplasts.

In any case, several options have been investigated in order to improve this solubilisation without success. Different temperatures, incubation times, pH or polymers have not shown any improvement of solubilisation efficiency. Sonication of membranes prior to solubilisation was expected to further destabilize the constituents of the membrane, making the protein more available as has been shown previously (Gulati *et al.* 2014). pH was also an interesting option because it has been shown to have an influence on solubilisation efficiency in yeast and *E. coli* membranes (Kopf *et al*. 2020). Unfortunately, these ideas did not lead to improved solubilisation efficiency.

The use of detergents did not bring any significant improvement to this efficiency, with solubilisation rates still very low. There seems to be acceptable solubilisation rates for DDM and LMNG, both of which could be used to purify SdeA in sufficient amounts to test the

antifungal compound on a purified protein without the presence of lipids. The activity of the protein would however need to be verified in a functional assay first.

Two last options that remain to be tested relied on the use of different concentrations of SMA during solubilisation, or on expression optimisation. Studies have been showing variations in extraction of proteins from membranes using differential SMA concentrations and this could be an interesting option (Kopf *et al.* 2020). It is also likely that optimising expression conditions in order to favour thinner cell wall, by avoiding stationary phase during the different culture steps for example, could also lead to the protein being more available for solubilisation.

7.1.4 Purification using Ni-affinity chromatography

Despite the co-purification of mADH, Ni-affinity purification was quite successful at binding the protein of interest, especially considering the very low amounts that could be solubilised. What was more of an issue however was that it was surprisingly not possible to separate SdeA and its contaminant by imidazole gradient during the chromatography. It was expected for SdeA to bind more strongly to the resin thanks to its 6xHis-tag, which mADH did not possess. One of the explanations for this could reside in the SMALP, which, because of its size, could prevent the protein from properly going through the resin's pores and binding to the nickel ions. It would however be surprising as the contaminant has been observed by Chen *et al.* without using SMA polymers. Another possibility would be that the His-tag, despite being located far from the transmembrane region in the sequence, might find itself too close to the membrane in the three dimensional structure, thus being less accessible for binding the resin. It could have been interesting to test a different tag that contained more histidine residues (10 or 12 for example) in order to test harsher washing steps and make a difference with the mADH contaminant's potential affinity for the resin.

7.1.5 Yield of purified protein

The yields of purified protein obtained were quite disappointing for SdeA, with quantification estimations ranging from a few µg/mL to approximately 200 µg/mL, with the lowest estimations seemingly closer to the truth considering the different quantification experiments performed. This is most likely in line with the poor solubilisation rates measured, affecting the final concentration of purified protein *in fine*. It also seems to be less abundant that what

can be found in the literature, although it is quite rare to find studies that actually put final concentrations of purified proteins, especially for enzymes.

During protein quantification, the concentration was too low to be calculated with the BSA standards usually used. Therefore, going forward three options have been considered: loading a larger amount of protein by concentrating the protein sample using the TCA precipitation method, using a smaller volume for the elution steps or recycling the elution fractions back through the column to increase protein concentration without increasing volume. The first option was tested as there were purified protein samples available and worked out well on the different samples. Unfortunately, the bands corresponding to SdeA were not looking as good as usual. Concentrating the sample by using centrifugation concentrators (Amicon 30K from Merck) was also tested without success, due to the protein of interest not being visible on SDS-PAGE afterwards (while the contaminant was still there).

SMALP was also said to be compatible with BCA quantification, which was also performed. Again, the results were not very convincing, with concentrations varying a lot between the non-diluted sample and the 10 times diluted one.

7.2 mADH contamination

As mADH can use methanol as a substrate (as well as formaldehyde), it can be understandable that using the methylotrophic properties of *Pichia pastoris* via the addition of methanol in the culture media, thus leading to the activation of the mADH gene, can lead to the overexpression of this contaminant (Sakai *et al.* 1995). Methanol can be used as a carbon source, but also as an activator of the *AOX1* promoter region, a strong promoter often used for the expression of heterologous proteins. It is not clear however why mADH was not a problem in the initial rounds of expression, but began to be a challenge at a later date. Perhaps some seemingly minor change in one of the media components or a different supplier helped induce mADH overexpression, but preliminary investigations into this showed nothing obvious. However, it is notable that several other students working on different membrane proteins also developed a problem with mADH contamination (Thanos Kesidis, Philip Kitchen, Lucas Unger, Idoia Company-Marin, personal communication). It was considered for some time that the cell line that was used during each of the transformations may have been faulty in some way. However, this hypothesis no longer stands against the new ‘knocked out’ strain that has been engineered during this thesis since the cell line used was GS115 and not X-33. Another possibility that was considered was that the protocol that was used favoured the presence of mADH. This hypothesis does not seem to stand either

when considering the fact that this protocol has been used by some people in our lab who have not seen this kind of issue. Moreover, the mentioned protocol is largely inspired by the Pichia expression manual, which would make us think more people using *P. pastoris* would have been encountered this issue around the world.

While the preparation of the plasmid to facilitate the mADH knockout worked successfully, the transformation into yeast cells was found to be more challenging. Several issues were encountered during this process but one of them was a regular contamination of the plates, which could be attributed to the absence of antibiotic due to the different selection method used (auxotrophy). This method shows several important advantages such as the limitation of the use of antibiotics to repress the development of resistant strains in the environment, or the limitation of the use of antibiotic-resistance genes, which spread in the environment could also have very negative consequences (Mignon, Sodoyer, and Werle 2015). However, it also means that any contaminant finding its way into the culture, and, in this case, already capable of producing its own histidine, could grow without a problem. A selection through an antibiotic, with the integration of an antibiotic resistance gene, could have been more successful in regards to contamination of the plates, but there is a very limited pool of antibiotics that can be used in yeast cell cultures, consisting mostly of zeocin and phleomycin, and for which the resistance gene is the same. Introducing the resistance gene for the knocking out of the mADH gene, as done by Chen *et al.* would have meant we would not have been able to use it for the subsequent heterologous protein production that was to be performed on the newly created strain. Other antibiotics could have also been used such as hygromycin or nourseothricin but they were not chemicals that were traditionally used in our lab (Yang, Nie, *et al.* 2014).

Another antibiotic that can be used in *P. pastoris* is called geneticin, or G418, which resistance gene is the same as the kanamycin one. This could provide an interesting alternative to zeocin.

It was important to be able to remove this contaminant for the proper running of a functional assay, but also because we could not let it interfere in any way with potential drug affinity studies that would be carried out later on.

The transformation ended up working after having solved the few technical issues that were encountered during the process and the plasmid was successfully integrated in the genome of GS115.

Following transformation of the new ‘knockout’ strain with SdeA, production and purification of SdeA, it appeared that the mADH contaminant was still present. While it has not been confirmed this band did correspond to the contaminant (via mass spectrometry for example), it is very likely to correspond to it. This was despite the fact that the PCR analysis of the

strain suggested it was successful (Figure 4.22). How can this be explained? Perhaps the double homologous recombination that was designed is not always what happens during the integration of a gene in the genome in *P. pastoris*. Indeed, there is an enormous variability during transformation, where single homologous recombination is a possibility. In this case, only one of the recognition sites is used for the integration, which means the integrated gene is not substituting the gene that should be knocked out, but instead is added next to it, so that both genes are still in the genome (Figure 7.1).

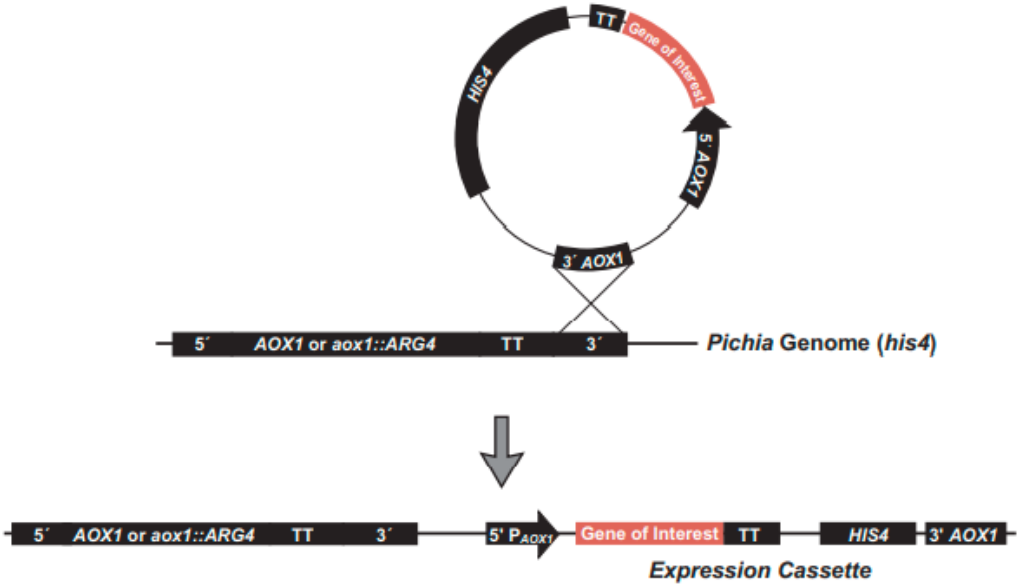

***Figure 7.1: Representation of the mechanism of a single homologous recombination event in* P. pastoris.** *Only the 3' area of the AOX1 is recognised, which leads to the addition of the gene of interest next to the gene corresponding to AOX1, still active. Figure taken from Pichia expression kit manual from Invitrogen.*

This is the same phenomenon as what happens with Mut^s versus Mut^+ *P. pastoris* phenotypes, where the AOX1 gene is respectively knocked out or still active. If it is still active, the cell will have a faster rate of utilization (or metabolism) of methanol, which means it has a faster growth rate but it is more difficult to maintain a constant activation of the pAOX1 promoter (Schwarzhans *et al.* 2016). This is also the same thing that happens when multiple copies of the gene of interest are integrated in the genome, for higher rate of production of the protein of interest (Figure 7.2).

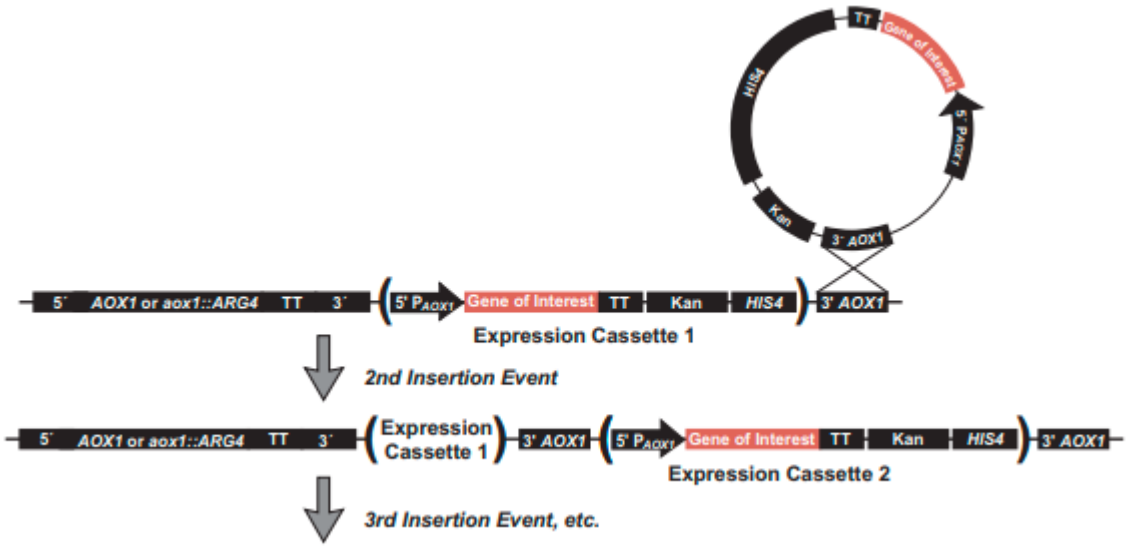

***Figure 7.2: Representation of the integration of several copies of the gene of interest in* P. pastoris.** *A single homologous recombination event is necessary for the addition of each copy of the gene. Figure taken from* Pichia *expression kit manual from Invitrogen.*

For this knockout of mADH, if a single homologous recombination happens, the mADH gene would therefore not be removed and could still be active, while the selection with His4 still works fine. This is probably why some bands can still be observed at the size of mADH alone when the PCR was performed with mADH primers (Figure 4.22) on transformed colonies A, D and F.

Many different events can happen during transformation such as relocation of the locus targeted for replacement to another chromosome or disruption of untargeted genes affecting colony morphology, which are important to understand in order to control cloning in yeast (Schwarzhans *et al.* 2016).

Revisiting the results of the PCR analysis of the new strain (Figure 4.22), there could be a very faint band possibly observable on strain B, which could explain why the mADH protein was still found on the SDS-PAGE gel (Figure 4.25). It would be interesting to test strain C in order to see if the same results are observed, as it really does not look like there is a band corresponding to mADH in the PCR results for strain C.

One other possible alternative that has not yet been investigated consisted in the isolation of mitochondria from the yeast cells, first by making spheroplasts with zymolyase treatment, followed by a mechanical disruption, and finally by isolating the mitochondria by differential centrifugation (Daum, Bohni, and Schatz 1982; Kopf *et al.* 2020). This method should be able to remove the mitochondria and therefore their contents from the rest of the cell, and as mADH is a mitochondrial protein, it should be a possibility for separating it from the rest of

the sample.

It could also be possible to test the influence of the methanol concentration on the production of mADH. Since methanol can be used as a substrate by this protein, changing the methanol concentration during cell culture could have an impact on the presence of this contaminant at the end of the culture. Furthermore, it could also be interesting to measure the apparition rate of mADH during the induction phase in order to see if the contaminant production would be induced only in later stages of the induction phase for example.

Moreover, performing the myc-tag purification again without using Tween could also be an idea to investigate, as well as the use of other possible tags.

Finally, a last investigation possibility would rely on the solubilisation method, where the appearance of the contaminant could be linked to the use of SMA during solubilisation. Trying to solubilise and purify SdeA with a detergent such as DDM or LMNG would be a good start. This hypothesis would be very surprising considering Chen *et al.* did not observe this contaminant using SMA. They do insist however on the fact that this issue seems to stem from the use of affinity chromatography. Another purification method would therefore be welcome.

This contaminant has been quite worrisome for members of our lab and other labs around us. It has been observed on most protein productions that have been performed by people trying to express recombinant membrane proteins in *P. pastoris* using the same cell line.

7.3 SdeA glycosylation

So far, the potential glycosylation site has not yet been proven to carry actual glycosydic residues. In order to investigate it further, several options can be assessed. A first option consists in a deglycosylation experiment using an enzyme that would remove the potential glycosidic residues from the protein. The deglycosylated SdeA would then be run on another SDS-PAGE gel in order to verify the absence of the previously observed multiplicity of bands. Several enzymes have been identified as likely to be able to remove the glycosylation including endo-β-n-acetylglucosaminidase or α-mannosidase (Neubert *et al.*

2016), as yeast are known to usually present high-mannose glycosylation patterns. These patterns seem to be found in both N- and O-glycosylation (Neubert *et al.* 2016; Wildt and Gerngross 2005).

A second option would rely on a mass spectrometry analysis of the different bands found on the gel. This has already been done previously to show the different bands all corresponded to SdeA, but it has not yet been performed for the analysis of the presence of glycosidic residues on the membrane protein.

A third option would rely on the oxidative release of natural glycans (ORNG) (Banazadeh *et al.* 2017), which consists in the removal of glycosidic residues using sodium hypochlorite (NaClO). This compound selectively liberates glycans, including O-glycans. The products can then be analysed using MALDI-TOF-MS. This option is very similar to the first one but would not need to use expensive enzymes.

Finally, a last option that could be considered uses lectin-glycan interactions to identify glycosidic residues on a protein sample. Again, this possibility removes the need for enzymes.

This glycosylation hypothesis will therefore need further analysis before it can be accepted or disproved.

7.4 Production and purification of soluble proteins

7.4.1 Cytochrome b5 dehydrogenase

The overexpression and purification of cytochrome b5 dehydrogenase was simple and effective, giving a purified protein concentration of up to 5.5 mg/mL. This concentration was measured from a 3 mL sample (6 x 0.5 mL elutions) after protein purification, which means 16.5 mg of purified protein were harvested from the 1 L culture. The second production of the protein was a bit less efficient but the last one looked even more effective. Indeed, during the purification, the protein sample was quite yellow, meaning it was quite concentrated. Therefore, more washings were performed on the purification column (5 * 20 mM and 4 * 40 mM imidazole) and more elutions as well (8 * 1 mL for a total elution volume of 8 mL instead of 3). Still, the concentration was similar to the first production (4.8 mg/mL), meaning the total mass of purified protein was 38.4 mg from the same kind of 1 L culture as during the first production.

As can be observed on the SDS-PAGE gels performed for this protein (Figure 5.3), the yield is high enough for the protein to be washed out of the column during washings, with limited

amounts of imidazole. We also see a second band on the gel that could correspond to the protein dimer, emphasizing the important concentration of the protein in the sample. It is difficult to compare this yield with other yields from different papers because they often use different conditions, whether the strain, the culture conditions or the protein are completely different. Still, some studies have been working on protein production optimisation in *E. coli*, and some of them have shown they were able to routinely produce several hundreds of milligrams of protein per litre of culture on average, using a few optimisations and high cell-density cultures (Sivashanmugam *et al.* 2009). Another study expressing a human version of a duodenal cytochrome b protein in *E. coli* obtained a yield of approximately 26 mg of purified protein per litre of culture (Liu *et al.* 2011). Finally, the production of a bovine microsomal cytochrome b5 protein, still in *E. coli*, with the transmembrane domain truncated, yielded approximately 20 mg of protein per litre of culture (Hewson, Newbold, and Whitford 1993). Considering these different results and the fact that the production of cytochrome b5 dehydrogenase was very classical, without any particular modification to the protocol, the obtained yield can be satisfactory.

The extra band observed that corresponds to double the size of cytb5R has not been confirmed as a dimer of the protein, but a DLS (Dynamic light scattering) experiment could be performed to verify this hypothesis.

7.4.2 DHODH-TR

The expression of DHODH-TR was not as easy however. This is a bit surprising considering it was a soluble protein just as Cytb5R, using the same host and the same expression conditions. One of the main reasons for this contrast could reside in the size difference between the two proteins, as DHODH-TR is expressed with a NusA protein attached to it, making it three times larger than the reductase (105 vs 35 kDa). Large proteins are inherently more difficult to produce in high yields, due to the cell processing machinery being busier with them. Large portions of hydrophobic amino acids can also be a factor for increased levels of aggregation in a non-lipid containing environment (Thoring *et al.* 2017). For this reason, the average amino acid composition was compared between DHODH-TR and what could be found in the literature (Figure 7.3) (Trinquier and Sanejouand 1998).

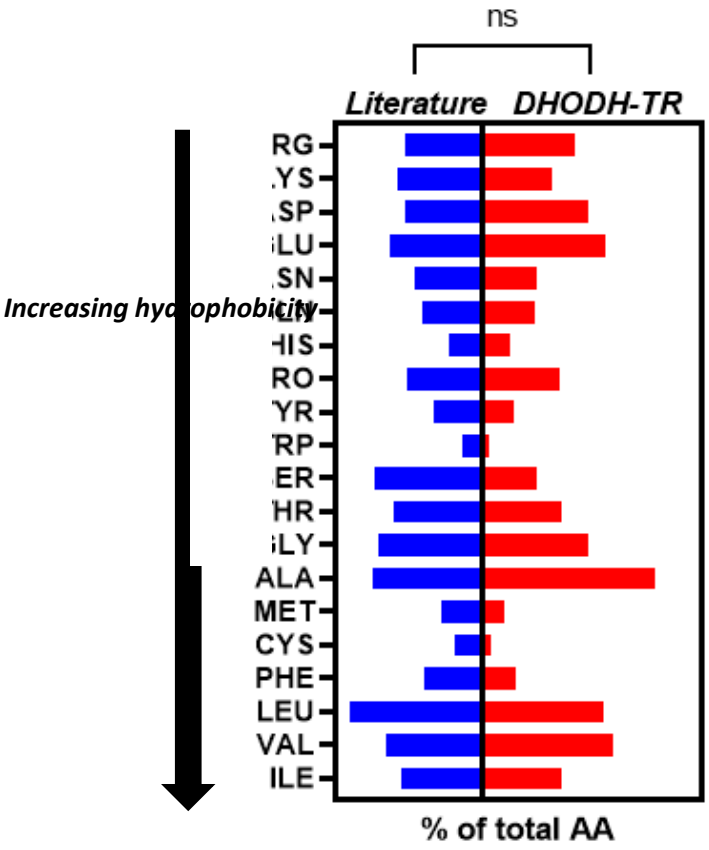

Figure 7.3: Comparison of the amino-acid composition of DHODH-TR with what can be found in the literature for average protein composition. *There is no significant difference between their compositions. Statistical test used: unpaired t test (p value = 0.96).*

Amino acids are ranked by their hydropathy index, according to Kyte-Doolittle scale. A statistical t test was performed on DHODH-TR's data in order to see if it was significantly different from the average value found in the literature. It appeared there was no significant difference, despite some minor differences in their composition. For example, Alanine seemed to be more present in DHODH-TR's sequence, as well as Valine to a lesser extent, but this was compensated by a lower amount of Cysteine, Leucine, Phenylalanine and Methionine. If considering the values for hydrophobic amino acids (between Isoleucine and Glycine included), the sum for the literature data is 44.2 %, versus 46.37 % for DHODH-TR. The hydrophobic composition of the protein is therefore not likely to be the reason for this tendency to aggregate. More studies about the aggregation rate of this protein could have been performed, including a Dynamic Light Scattering (DLS) experiment.

This NusA protein is known to be one of the most efficient ways to prevent aggregation of soluble proteins expressed in *E. coli*, as it is a highly soluble protein. As hydrophobic

proteins tend to have an increased tendency to aggregate, the presence of this fusion partner thus decreases the likelihood of this problem. However, despite this, there still seems to be a large portion of it that has aggregated anyway (Figure 6.3 and 6.4). It is still unclear why the first production that was performed did not show any sign of aggregation whereas the two following ones showed a large portion of it that looked aggregated. In order to make sure if those bands correspond to aggregated DHODH-TR, several experiments could be considered such as dynamic light scattering, size exclusion chromatography or a native electrophoresis.

7.5 Absorbance spectra

The absorbance spectra measured were quite comparable to what was found in the literature. The same absorbance peaks were observed in each case and a nice absorbance shift was observed for the cytochrome b5-containing SdeA upon reduction with sodium dithionite. Thus, we could confirm with confidence we were dealing with the right protein here. Cytochrome b5 dehydrogenase worked differently however, as the spectrum observed did match the literature, but the reduction of the protein did not have that much of an impact on the curve. Because this spectrum did look similar to a mix between the oxidised and the reduced version of the spectra, an oxidation attempt was also carried out using hydrogen peroxide without any significant difference observed.

7.6 Functional assay

The functional assay ended up working nicely, showing the desired decrease of absorbance at 340nm. Since the second protein (cytb5R) was added after a couple of minutes, we can say that the decrease observed upon addition was indeed due to the reaction taking place. The controls with one of the components missing did show an absence of reaction as expected. Two things that were observed remain unverified to this day.

First of all, the decrease of absorbance always went down to approximately 40% of its initial value, sometimes even down to 30%, but there seemed to have been some kind of baseline value for the absorbance at this wavelength. One of the compounds for the reaction could potentially absorb in the area, thus preventing the value from reaching zero. After having verified the absorbance spectra for the different compounds, it would seem FAD would be the favourite candidate for this baseline absorbance value. First, it would make sense as it has some structural similarities with NAD. Second, controls without FAD usually seemed to

have lower initial absorbance values, which could be in line with the absorbance base value observed in the standard functional assay. However, both proteins used in this experiment also showed some minimal absorbance at 340 nm and should not be ruled out. It is likely that a combination of basal absorbance from each of these compounds is responsible for this basal absorbance observed.

Another interesting feature of this functional assay resides in some of the controls not showing what was expected to be observed. We have already discussed the reaction still taking place in the results part during the control without stearoyl-CoA and hypothesize that lipids such as stearic acid present in SMALPs could be used as a substrate by the enzyme SdeA. We are still unsure what the exact underlying mechanism is here, but several experiments could be performed in order to verify if the SMALP lipids are actually responsible for this. One easy way to do this would have been to perform the functional assay with an SdeA sample that was not purified in SMA. Using detergent-purified protein, on the condition that SdeA would still be functional without native lateral interactions, could be a simple enough way to verify this. If this was not possible, other solubilisation tools could be used, mimicking the membrane environment without using lipids should be considered, such as previously mentioned amphipols.

7.7 Antifungal compound test

As previously discussed in the results, the MIC observed during this inhibition was higher than expected (between 10 and 20 µg/mL instead of the 0.8 µg/mL expected according to our industrial partner). It was not confirmed that the drug was indeed sequestered in SMALP, but the fact that this molecule is most likely a lipophilic compound presenting amphiphilic properties (due to its solubility in water) would make it a suitable candidate for being sequestered in SMALP, as this has already been observed before (Gulamhussein *et al.* 2020). The easiest option would be for it to be integrated in the lipids surrounding SdeA, but this would in term increase the local concentration, having the opposite effect to what has been observed experimentally with the increase of the MIC. Furthermore, we have observed that the reaction was still taking place with the absence of the substrate stearoyl-CoA, and have hypothesised that the presence of stearic acid in SMALPs could lead to the reaction still taking place. If that was the case, the sequestering of the drug in SMALPs should not prevent it from performing the inhibition. Another option could reside in the drug being sequestered by the SMA polymer rather than the lipids, through its amphiphilic properties as well. This would mean that the inhibitor would be sequestered too far from the protein, in an

environment potentially less fluid that what would be found in membrane lipids, thus decreasing its effective concentration.

This test is a good first approach to verifying the inhibition reaction, but it would also need to be miniaturised in order to allow for drug screening of multiple candidates that would present different chemical variations. It would also enable the use of multiple concentrations for each of these variants in order to find the best working conditions.

Finally, alternative assay methods have been developed in order to verify further the inhibition reaction taking place. Instead of measuring the absorbance of NADH,H^+, these other methods use the ratio of substrate and product of the reaction. While the former is saturated, the latter is unsaturated, meaning that they could be differentiated by a lipid mass spectrometry analysis (Quehenberger, Armando, and Dennis 2011). A second method that could be used is known as iodine value assay, where lipid unsaturations can form dihalogenated single bonds upon addition of iodine monochloride (ICl) (Figure 7.4). The remaining ICl can then react with potassium iodine (KI) in order to form diiodine, which absorbance can then be read at 450 nm. This assay could not yet be used as it was being developed while this project took place, but it can represent an interesting future alternative.

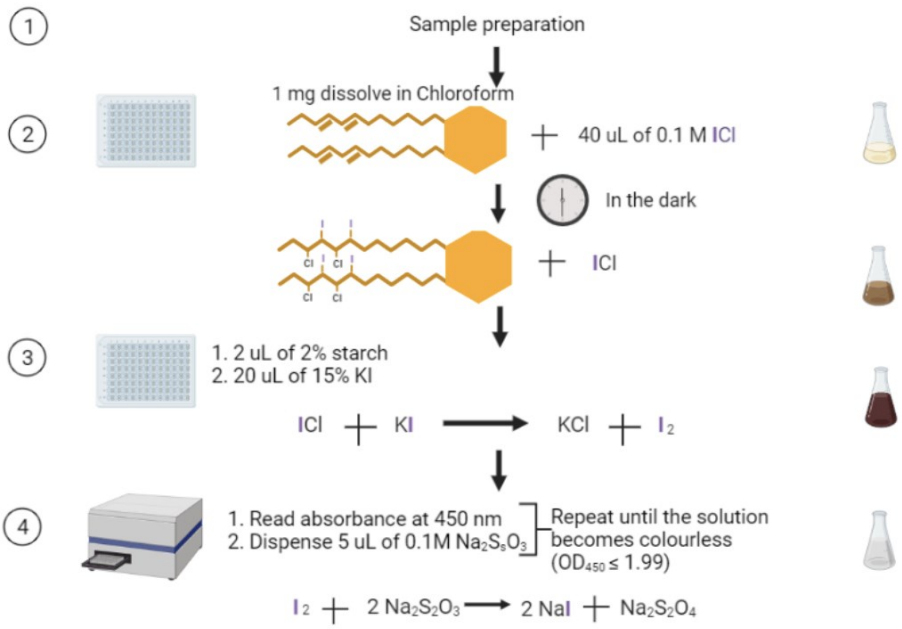

Figure 7.4: Representation of the iodine value assay. *It was developed by lab colleague Monserrat Román Lara, who also kindly provided this figure.*

8. Future work

SCD1, the human version of SdeA, could be expressed and purified in order to perform secondary screens for drug specificity, but also because the human SCD1 can be used as a drug target in its own, especially for lipid related diseases, including some cancers were lipid metabolism pathways are deregulated (Du *et al.* 2022; Galbraith, Leung, and Ahmad 2018). It could be useful to find a way to express it easily for potential human therapies.

The development of a functional assay for DHODH would be highly desirable, using both its full-length and truncated versions to verify the protein's correct function, before testing the drug's potency on both versions of this protein. It could be particularly interesting to check if the presence of the transmembrane domain has any kind of impact on the protein structure, function, or its ability to bind the drug efficiently. Moreover, biophysical characterization of the DHODH/olorofim complex could also be performed.

Finally, target 3 could be expressed and purified, with the development of a functional assay. Target 3 is a large multispanning transmembrane protein that has not yet been expressed by F2G Ltd before, which is why it would have to be analysed in order to identify a suitable host. As for the two previous targets, a functional assay and an inhibition assay would be desirable for this new target in order to see if it can become an interesting new antifungal drug target.

9. References

Abad, A., J. V. Fernandez-Molina, J. Bikandi, A. Ramirez, J. Margareto, J. Sendino, F. L. Hernando, J. Ponton, J. Garaizar, and A. Rementeria. 2010. 'What makes Aspergillus fumigatus a successful pathogen? Genes and molecules involved in invasive aspergillosis', *Rev Iberoam Micol*, 27: 155-82.

Arnold, T., and D. Linke. 2008. 'The use of detergents to purify membrane proteins', *Curr Protoc Protein Sci*, Chapter 4: Unit 4 8 1-4 8 30.

Ayub, H., M. Clare, L. Broadbent, J. Simms, A. D. Goddard, A. J. Rothnie, and R. M. Bill. 2022. 'Membrane Protein Production in the Yeast P. pastoris', *Methods Mol Biol*, 2507: 187-99.

Ayub, H., M. Clare, I. Milic, N. P. Chmel, H. Boning, A. Devitt, T. Krey, R. M. Bill, and A. J. Rothnie. 2020. 'CD81 extracted in SMALP nanodiscs comprises two distinct protein populations within a lipid environment enriched with negatively charged headgroups', *Biochim Biophys Acta Biomembr*, 1862: 183419.

Banazadeh, A., L. Veillon, K. M. Wooding, M. Zabet-Moghaddam, and Y. Mechref. 2017. 'Recent advances in mass spectrometric analysis of glycoproteins', *Electrophoresis*, 38: 162-89.

Barratt, G., and S. Bretagne. 2007. 'Optimizing efficacy of Amphotericin B through nanomodification', *Int J Nanomedicine*, 2: 301-13.

Barrett-Bee, K., L. Newboult, and P. Pinder. 1991. 'Biochemical changes associated with the antifungal action of the triazole ICI 153,066 on Candida albicans and Trichophyton quinckeanum', *FEMS Microbiol Lett*, 63: 127-31.

Beauvais, A., and J. P. Latge. 2001. 'Membrane and cell wall targets in Aspergillus fumigatus', *Drug Resist Updat*, 4: 38-49.

Bell, A. J., L. K. Frankel, and T. M. Bricker. 2015. 'High Yield Non-detergent Isolation of Photosystem I-Light-harvesting Chlorophyll II Membranes from Spinach Thylakoids: IMPLICATIONS FOR THE ORGANIZATION OF THE PS I ANTENNAE IN HIGHER PLANTS', *J Biol Chem*, 290: 18429-37.

Berman, J., and D. J. Krysan. 2020. 'Drug resistance and tolerance in fungi', *Nat Rev Microbiol*, 18: 319-31.

Bill, R. M. 2012. *Recombinant protein production in yeast*.

Bongomin, F., S. Gago, R. O. Oladele, and D. W. Denning. 2017. 'Global and Multi-National Prevalence of Fungal Diseases-Estimate Precision', *J Fungi (Basel)*, 3.

Bornhorst, B. J., and J. J. Falke. 2011. 'Reprint of: Purification of Proteins Using Polyhistidine Affinity Tags', *Protein Expr Purif*.

Brady, J. R., C. A. Whittaker, M. C. Tan, D. L. Kristensen, 2nd, D. Ma, N. C. Dalvie, K. R. Love, and J. C. Love. 2020. 'Comparative genome-scale analysis of Pichia pastoris variants informs selection of an optimal base strain', *Biotechnol Bioeng*, 117: 543-55.

Brajtburg, J., S. Elberg, J. Bolard, G. S. Kobayashi, R. A. Levy, R. E. Ostlund, Jr., D. Schlessinger, and G. Medoff. 1984. 'Interaction of plasma proteins and lipoproteins with amphotericin B', *J Infect Dis*, 149: 986-97.

Brakhage, A. A., and B. Liebmann. 2005. 'Aspergillus fumigatus conidial pigment and cAMP signal transduction: significance for virulence', *Med Mycol*, 43 Suppl 1: S75-82.

Breedveld, F. C., and J. M. Dayer. 2000. 'Leflunomide: mode of action in the treatment of rheumatoid arthritis', *Ann Rheum Dis*, 59: 841-9.

Broadbent, L., P. Depping, A. Lode, A. Vaitsopoulou, D. Hardy, H. Ayub, J. Mitchell-White, I. D. Kerr, A. D. Goddard, R. M. Bill, and A. J. Rothnie. 2022. 'Detergent-Free Membrane Protein Purification Using SMA Polymer', *Methods Mol Biol*, 2507: 389-404.

Brown, G. D., D. W. Denning, N. A. Gow, S. M. Levitz, M. G. Netea, and T. C. White. 2012. 'Hidden killers: human fungal infections', *Sci Transl Med*, 4: 165rv13.

Bruns, S., M. Seidler, D. Albrecht, S. Salvenmoser, N. Remme, C. Hertweck, A. A. Brakhage, O. Kniemeyer, and F. M. Muller. 2010. 'Functional genomic profiling of Aspergillus fumigatus biofilm reveals enhanced production of the mycotoxin gliotoxin', *Proteomics*, 10: 3097-107.

Brunton, L., J. Lazo, and K. Parker. 2005. *Goodman & Gilman's The Pharmacological Basis of Therapeutics, Eleventh Edition* (McGraw-Hill Education).
Burns, C., R. Geraghty, C. Neville, A. Murphy, K. Kavanagh, and S. Doyle. 2005. 'Identification, cloning, and functional expression of three glutathione transferase genes from Aspergillus fumigatus', *Fungal Genet Biol*, 42: 319-27.
Byrne, B. 2015. 'Pichia pastoris as an expression host for membrane protein structural biology', *Curr Opin Struct Biol*, 32: 9-17.
Calvo, A. M., L. L. Hinze, H. W. Gardner, and N. P. Keller. 1999. 'Sporogenic effect of polyunsaturated fatty acids on development of Aspergillus spp', *Appl Environ Microbiol*, 65: 3668-73.
Calvo, A. M., R. A. Wilson, J. W. Bok, and N. P. Keller. 2002. 'Relationship between secondary metabolism and fungal development', *Microbiol Mol Biol Rev*, 66: 447-59, table of contents.
CDC. Accessed 19/05/2022. https://www.cdc.gov/fungal/antifungal-resistance.html.
Cereghino, G. P., J. L. Cereghino, C. Ilgen, and J. M. Cregg. 2002. 'Production of recombinant proteins in fermenter cultures of the yeast Pichia pastoris', *Curr Opin Biotechnol*, 13: 329-32.
Chamilos, G., and D. P. Kontoyiannis. 2005. 'Update on antifungal drug resistance mechanisms of Aspergillus fumigatus', *Drug Resist Updat*, 8: 344-58.
Chang, C. C., M. A. Slavin, and S. C. Chen. 2017. 'New developments and directions in the clinical application of the echinocandins', *Arch Toxicol*, 91: 1613-21.
Chanumolu, S. K., C. Rout, and R. S. Chauhan. 2012. 'UniDrug-target: a computational tool to identify unique drug targets in pathogenic bacteria', *PLoS One*, 7: e32833.
Chaudhuri, T. K., and S. Paul. 2006. 'Protein-misfolding diseases and chaperone-based therapeutic approaches', *FEBS J*, 273: 1331-49.
Chen, S., T. Getter, D. Salom, D. Wu, D. Quetschlich, D. S. Chorev, K. Palczewski, and C. V. Robinson. 2022. 'Capturing a rhodopsin receptor signalling cascade across a native membrane', *Nature*, 604: 384-90.
Chen, Y., Y. Li, P. Liu, Q. Sun, and Z. Liu. 2014. 'Optimized expression in Pichia pastoris eliminates common protein contaminants from subsequent His-tag purification', *Biotechnol Lett*, 36: 711-8.
Chen, Y., S. Partow, G. Scalcinati, V. Siewers, and J. Nielsen. 2012. 'Enhancing the copy number of episomal plasmids in Saccharomyces cerevisiae for improved protein production', *FEMS Yeast Res*, 12: 598-607.
Chia, J. K., and E. J. McManus. 1990. 'In vitro tumor necrosis factor induction assay for analysis of febrile toxicity associated with amphotericin B preparations', *Antimicrob Agents Chemother*, 34: 906-8.
Chivers, P. T., and R. T. Sauer. 2002. 'NikR repressor: high-affinity nickel binding to the C-terminal domain regulates binding to operator DNA', *Chem Biol*, 9: 1141-8.
Christian, S., C. Merz, L. Evans, S. Gradl, H. Seidel, A. Friberg, A. Eheim, P. Lejeune, K. Brzezinka, K. Zimmermann, S. Ferrara, H. Meyer, R. Lesche, D. Stoeckigt, M. Bauser, A. Haegebarth, D. B. Sykes, D. T. Scadden, J. A. Losman, and A. Janzer. 2019. 'The novel dihydroorotate dehydrogenase (DHODH) inhibitor BAY 2402234 triggers differentiation and is effective in the treatment of myeloid malignancies', *Leukemia*, 33: 2403-15.
Cowen, L. E., D. Sanglard, S. J. Howard, P. D. Rogers, and D. S. Perlin. 2014. 'Mechanisms of Antifungal Drug Resistance', *Cold Spring Harb Perspect Med*, 5: a019752.
Cregg, J. M., J. L. Cereghino, J. Shi, and D. R. Higgins. 2000. 'Recombinant protein expression in Pichia pastoris', *Mol Biotechnol*, 16: 23-52.
Cuevas Arenas, R., J. Klingler, C. Vargas, and S. Keller. 2016. 'Influence of lipid bilayer properties on nanodisc formation mediated by styrene/maleic acid copolymers', *Nanoscale*, 8: 15016-26.
Cui, C. B., H. Kakeya, and H. Osada. 1996. 'Spirotryprostatin B, a novel mammalian cell cycle inhibitor produced by Aspergillus fumigatus', *J Antibiot (Tokyo)*, 49: 832-5.

Cybulska, B., M. Herve, E. Borowski, and C. M. Gary-Bobo. 1986. 'Effect of the polar head structure of polyene macrolide antifungal antibiotics on the mode of permeabilization of ergosterol- and cholesterol-containing lipidic vesicles studied by 31P-NMR', *Mol Pharmacol*, 29: 293-8.

Cymer, F., G. von Heijne, and S. H. White. 2015. 'Mechanisms of integral membrane protein insertion and folding', *J Mol Biol*, 427: 999-1022.

D'Enfert, C., M. Diaquin, A. Delit, N. Wuscher, J. P. Debeaupuis, M. Huerre, and J. P. Latge. 1996. 'Attenuated virulence of uridine-uracil auxotrophs of Aspergillus fumigatus', *Infect Immun*, 64: 4401-5.

Daum, G., P. C. Bohni, and G. Schatz. 1982. 'Import of proteins into mitochondria. Cytochrome b2 and cytochrome c peroxidase are located in the intermembrane space of yeast mitochondria', *J Biol Chem*, 257: 13028-33.

de Gontijo, F. A., R. C. Pascon, L. Fernandes, J. Machado, Jr., J. A. Alspaugh, and M. A. Vallim. 2014. 'The role of the de novo pyrimidine biosynthetic pathway in Cryptococcus neoformans high temperature growth and virulence', *Fungal Genet Biol*, 70: 12-23.

Debono, M., and R. S. Gordee. 1994. 'Antibiotics that inhibit fungal cell wall development', *Annu Rev Microbiol*, 48: 471-97.

Delliere, S., E. Dudoignon, S. Fodil, S. Voicu, M. Collet, P. A. Oillic, M. Salmona, F. Depret, T. Ghelfenstein-Ferreira, B. Plaud, B. Chousterman, S. Bretagne, E. Azoulay, A. Mebazaa, B. Megarbane, and A. Alanio. 2020. 'Risk factors associated with COVID-19-associated pulmonary aspergillosis in ICU patients: a French multicentric retrospective cohort', *Clin Microbiol Infect*.

Denker, S. P., and D. L. Barber. 2002. 'Ion transport proteins anchor and regulate the cytoskeleton', *Curr Opin Cell Biol*, 14: 214-20.

Denning, D. W. 1998. 'Invasive aspergillosis', *Clin Infect Dis*, 26: 781-803; quiz 04-5.

Denning, D. W., and M. J. Bromley. 2015. 'Infectious Disease. How to bolster the antifungal pipeline', *Science*, 347: 1414-6.

Desai, J. V., A. P. Mitchell, and D. R. Andes. 2014. 'Fungal biofilms, drug resistance, and recurrent infection', *Cold Spring Harb Perspect Med*, 4.

Dilworth, M. V., M. S. Piel, K. E. Bettaney, P. Ma, J. Luo, D. Sharples, D. R. Poyner, S. R. Gross, K. Moncoq, P. J. F. Henderson, B. Miroux, and R. M. Bill. 2018. 'Microbial expression systems for membrane proteins', *Methods*, 147: 3-39.

Dominguez Pardo, J. J., J. M. Dorr, A. Iyer, R. C. Cox, S. Scheidelaar, M. C. Koorengevel, V. Subramaniam, and J. A. Killian. 2017. 'Solubilization of lipids and lipid phases by the styrene-maleic acid copolymer', *Eur Biophys J*, 46: 91-101.

Dominguez Pardo, J. J., M. C. Koorengevel, N. Uwugiaren, J. Weijers, A. H. Kopf, H. Jahn, C. A. van Walree, M. J. van Steenbergen, and J. A. Killian. 2018. 'Membrane Solubilization by Styrene-Maleic Acid Copolymers: Delineating the Role of Polymer Length', *Biophys J*, 115: 129-38.

Dorr, J. M., S. Scheidelaar, M. C. Koorengevel, J. J. Dominguez, M. Schafer, C. A. van Walree, and J. A. Killian. 2016. 'The styrene-maleic acid copolymer: a versatile tool in membrane research', *Eur Biophys J*, 45: 3-21.

Dorr, J. M., M. H. van Coevorden-Hameete, C. C. Hoogenraad, and J. A. Killian. 2017. 'Solubilization of human cells by the styrene-maleic acid copolymer: Insights from fluorescence microscopy', *Biochim Biophys Acta Biomembr*, 1859: 2155-60.

Du, D., C. Liu, M. Qin, X. Zhang, T. Xi, S. Yuan, H. Hao, and J. Xiong. 2022. 'Metabolic dysregulation and emerging therapeutical targets for hepatocellular carcinoma', *Acta Pharm Sin B*, 12: 558-80.

du Pre, S., N. Beckmann, M. C. Almeida, G. E. M. Sibley, D. Law, A. C. Brand, M. Birch, N. D. Read, and J. D. Oliver. 2018. 'Effect of the Novel Antifungal Drug F901318 (Olorofim) on Growth and Viability of Aspergillus fumigatus', *Antimicrob Agents Chemother*, 62.

Emmerstorfer-Augustin, A., T. Wriessnegger, M. Hirz, G. Zellnig, and H. Pichler. 2019. 'Membrane Protein Production in Yeast: Modification of Yeast Membranes for Human Membrane Protein Production', *Methods Mol Biol*, 1923: 265-85.

Fang, W., and J. P. Latge. 2018. 'Microbe Profile: Aspergillus fumigatus: a saprotrophic and opportunistic fungal pathogen', *Microbiology*, 164: 1009-11.

Fisher, M. C., A. Alastruey-Izquierdo, J. Berman, T. Bicanic, E. M. Bignell, P. Bowyer, M. Bromley, R. Bruggemann, G. Garber, O. A. Cornely, S. J. Gurr, T. S. Harrison, E. Kuijper, J. Rhodes, D. C. Sheppard, A. Warris, P. L. White, J. Xu, B. Zwaan, and P. E. Verweij. 2022. 'Tackling the emerging threat of antifungal resistance to human health', *Nat Rev Microbiol*, 20: 557-71.

Fitzgerald, O. R., N. D. Rodriguez, and L. K. Lewis. 2022. 'High-Efficiency Plasmid DNA Transformation in Yeast', *Methods Mol Biol*, 2513: 15-22.

Fotiadis, D., P. Jeno, T. Mini, S. Wirtz, S. A. Muller, L. Fraysse, P. Kjellbom, and A. Engel. 2001. 'Structural characterization of two aquaporins isolated from native spinach leaf plasma membranes', *J Biol Chem*, 276: 1707-14.

Gaigalas, M., Z. Maneliene, R. Kazlauskiene, M. Petrusyte, and A. Janulaitis. 2002. 'PfoI, a unique type II restriction endonuclease that recognises the sequence 5'-T downward arrow CCNGGA-3'', *Nucleic Acids Res*, 30: e98.

Galbraith, L., H. Y. Leung, and I. Ahmad. 2018. 'Lipid pathway deregulation in advanced prostate cancer', *Pharmacol Res*, 131: 177-84.

Gardiner, D. M., P. Waring, and B. J. Howlett. 2005. 'The epipolythiodioxopiperazine (ETP) class of fungal toxins: distribution, mode of action, functions and biosynthesis', *Microbiology*, 151: 1021-32.

Georgacopoulos, O., N. S. Nunnally, E. M. Ransom, D. Law, M. Birch, S. R. Lockhart, and E. L. Berkow. 2021. 'In Vitro Activity of Novel Antifungal Olorofim against Filamentous Fungi and Comparison to Eight Other Antifungal Agents', *J Fungi (Basel)*, 7.

Giaever, G., and C. Nislow. 2014. 'The yeast deletion collection: a decade of functional genomics', *Genetics*, 197: 451-65.

Goh, C. S., N. Lan, S. M. Douglas, B. Wu, N. Echols, A. Smith, D. Milburn, G. T. Montelione, H. Zhao, and M. Gerstein. 2004. 'Mining the structural genomics pipeline: identification of protein properties that affect high-throughput experimental analysis', *J Mol Biol*, 336: 115-30.

Grau, S., M. Salavert, J. Carlos Pozo Laderas, M. Garcia Vargas, J. A. Barrueta, and N. Mir. 2013. 'Cost-effectiveness of anidulafungin in confirmed candidaemia and other invasive Candida infections in Spain', *J Mycol Med*, 23: 155-63.

Grillitsch, K., P. Tarazona, L. Klug, T. Wriessnegger, G. Zellnig, E. Leitner, I. Feussner, and G. Daum. 2014. 'Isolation and characterization of the plasma membrane from the yeast Pichia pastoris', *Biochim Biophys Acta*, 1838: 1889-97.

Gruszecki, W. I., M. Gagos, M. Herec, and P. Kernen. 2003. 'Organization of antibiotic amphotericin B in model lipid membranes. A mini review', *Cell Mol Biol Lett*, 8: 161-70.

Gsaller, F., P. Hortschansky, T. Furukawa, P. D. Carr, B. Rash, J. Capilla, C. Muller, F. Bracher, P. Bowyer, H. Haas, A. A. Brakhage, and M. J. Bromley. 2016. 'Sterol Biosynthesis and Azole Tolerance Is Governed by the Opposing Actions of SrbA and the CCAAT Binding Complex', *PLoS Pathog*, 12: e1005775.

Gulamhussein, A. A., R. Uddin, B. J. Tighe, D. R. Poyner, and A. J. Rothnie. 2020. 'A comparison of SMA (styrene maleic acid) and DIBMA (di-isobutylene maleic acid) for membrane protein purification', *Biochim Biophys Acta Biomembr*, 1862: 183281.

Gulati, S., M. Jamshad, T. J. Knowles, K. A. Morrison, R. Downing, N. Cant, R. Collins, J. B. Koenderink, R. C. Ford, M. Overduin, I. D. Kerr, T. R. Dafforn, and A. J. Rothnie. 2014. 'Detergent-free purification of ABC (ATP-binding-cassette) transporters', *Biochem J*, 461: 269-78.

Gulezian, E., C. Crivello, J. Bednenko, C. Zafra, Y. Zhang, P. Colussi, and S. Hussain. 2021. 'Membrane protein production and formulation for drug discovery', *Trends Pharmacol Sci*, 42: 657-74.

Hagiwara, D., A. Watanabe, and K. Kamei. 2016. 'Sensitisation of an Azole-Resistant Aspergillus fumigatus Strain containing the Cyp51A-Related Mutation by Deleting the SrbA Gene', *Sci Rep*, 6: 38833.
Hamill, R. J. 2013. 'Amphotericin B formulations: a comparative review of efficacy and toxicity', *Drugs*, 73: 919-34.
Harayama, T., and H. Riezman. 2018. 'Understanding the diversity of membrane lipid composition', *Nat Rev Mol Cell Biol*, 19: 281-96.
Hartmann, L., E. Metzger, N. Ottelard, and R. Wagner. 2017. 'Direct Extraction and Purification of Recombinant Membrane Proteins from Pichia pastoris Protoplasts', *Methods Mol Biol*, 1635: 45-56.
Hartner, F. S., and A. Glieder. 2006. 'Regulation of methanol utilisation pathway genes in yeasts', *Microb Cell Fact*, 5: 39.
Hasler, L., T. Walz, P. Tittmann, H. Gross, J. Kistler, and A. Engel. 1998. 'Purified lens major intrinsic protein (MIP) forms highly ordered tetragonal two-dimensional arrays by reconstitution', *J Mol Biol*, 279: 855-64.
Herman, P. K. 2002. 'Stationary phase in yeast', *Curr Opin Microbiol*, 5: 602-7.
Hewson, R., R. J. Newbold, and D. Whitford. 1993. 'The expression of bovine microsomal cytochrome b5 in Escherichia coli and a study of the solution structure and stability of variant proteins', *Protein Eng*, 6: 953-64.
Hirz, M., G. Richter, E. Leitner, T. Wriessnegger, and H. Pichler. 2013. 'A novel cholesterol-producing Pichia pastoris strain is an ideal host for functional expression of human Na,K-ATPase alpha3beta1 isoform', *Appl Microbiol Biotechnol*, 97: 9465-78.
Hitchcock, C. A. 1991. 'Cytochrome P-450-dependent 14 alpha-sterol demethylase of Candida albicans and its interaction with azole antifungals', *Biochem Soc Trans*, 19: 782-7.
Hoelz, L. V., F. A. Calil, M. C. Nonato, L. C. Pinheiro, and N. Boechat. 2018. 'Plasmodium falciparum dihydroorotate dehydrogenase: a drug target against malaria', *Future Med Chem*, 10: 1853-74.
Hoenigl, M., D. Seidel, A. Carvalho, S. M. Rudramurthy, A. Arastehfar, J. P. Gangneux, N. Nasir, A. Bonifaz, J. Araiza, N. Klimko, A. Serris, K. Lagrou, J. F. Meis, O. A. Cornely, J. R. Perfect, P. L. White, A. Chakrabarti, Ecmm, and Isham collaborators. 2022. 'The emergence of COVID-19 associated mucormycosis: a review of cases from 18 countries', *Lancet Microbe*.
Hof, H., and C. Kupfahl. 2009. 'Gliotoxin in Aspergillus fumigatus: an example that mycotoxins are potential virulence factors', *Mycotoxin Res*, 25: 123-31.
Hohnholz, R., K. J. Pohlmann, and T. Achstetter. 2017. 'Impact of plasmid architecture on stability and yEGFP3 reporter gene expression in a set of isomeric multicopy vectors in yeast', *Appl Microbiol Biotechnol*, 101: 8455-63.
Hope, W. W., L. Tabernero, D. W. Denning, and M. J. Anderson. 2004. 'Molecular mechanisms of primary resistance to flucytosine in Candida albicans', *Antimicrob Agents Chemother*, 48: 4377-86.
Hu, C., M. Zhou, W. Wang, X. Sun, O. Yarden, and S. Li. 2018. 'Abnormal Ergosterol Biosynthesis Activates Transcriptional Responses to Antifungal Azoles', *Front Microbiol*, 9: 9.
Ibrahim, K. A., O. M. Helmy, M. T. Kashef, T. R. Elkhamissy, and M. A. Ramadan. 2020. 'Identification of Potential Drug Targets in Helicobacter pylori Using In Silico Subtractive Proteomics Approaches and Their Possible Inhibition through Drug Repurposing', *Pathogens*, 9.
Ivashov, V. A., K. Grillitsch, H. Koefeler, E. Leitner, D. Baeumlisberger, M. Karas, and G. Daum. 2013. 'Lipidome and proteome of lipid droplets from the methylotrophic yeast Pichia pastoris', *Biochim Biophys Acta*, 1831: 282-90.
Jahic, M., F. Wallberg, M. Bollok, P. Garcia, and S. O. Enfors. 2003. 'Temperature limited fed-batch technique for control of proteolysis in Pichia pastoris bioreactor cultures', *Microb Cell Fact*, 2: 6.

Jahn, B., A. Koch, A. Schmidt, G. Wanner, H. Gehringer, S. Bhakdi, and A. A. Brakhage. 1997. 'Isolation and characterization of a pigmentless-conidium mutant of Aspergillus fumigatus with altered conidial surface and reduced virulence', *Infect Immun*, 65: 5110-7.

James, J. E., E. Lamping, J. Santhanam, and R. D. Cannon. 2021. 'PDR Transporter ABC1 Is Involved in the Innate Azole Resistance of the Human Fungal Pathogen Fusarium keratoplasticum', *Front Microbiol*, 12: 673206.

Jamshad, M., J. Charlton, Y. P. Lin, S. J. Routledge, Z. Bawa, T. J. Knowles, M. Overduin, N. Dekker, T. R. Dafforn, R. M. Bill, D. R. Poyner, and M. Wheatley. 2015. 'G-protein coupled receptor solubilization and purification for biophysical analysis and functional studies, in the total absence of detergent', *Biosci Rep*, 35.

Jamshad, M., and R. A. Darby. 2012. 'Disruption of yeast cells to isolate recombinant proteins', *Methods Mol Biol*, 866: 237-46.

Jamshad, M., Y. P. Lin, T. J. Knowles, R. A. Parslow, C. Harris, M. Wheatley, D. R. Poyner, R. M. Bill, O. R. Thomas, M. Overduin, and T. R. Dafforn. 2011. 'Surfactant-free purification of membrane proteins with intact native membrane environment', *Biochem Soc Trans*, 39: 813-8.

Jensen, H. L. 1931. 'The fungus flora of the soil', *Soil science*, 31: 123-58.

Karlsson, M., D. Fotiadis, S. Sjovall, I. Johansson, K. Hedfalk, A. Engel, and P. Kjellbom. 2003. 'Reconstitution of water channel function of an aquaporin overexpressed and purified from Pichia pastoris', *FEBS Lett*, 537: 68-72.

Kawai, S., W. Hashimoto, and K. Murata. 2010. 'Transformation of Saccharomyces cerevisiae and other fungi: methods and possible underlying mechanism', *Bioeng Bugs*, 1: 395-403.

Kellokumpu, S. 2019. 'Golgi pH, Ion and Redox Homeostasis: How Much Do They Really Matter?', *Front Cell Dev Biol*, 7: 93.

Kelly, S. L., D. C. Lamb, A. J. Corran, B. C. Baldwin, and D. E. Kelly. 1995. 'Mode of action and resistance to azole antifungals associated with the formation of 14 alpha-methylergosta-8,24(28)-dien-3 beta,6 alpha-diol', *Biochem Biophys Res Commun*, 207: 910-5.

Kesidis, A., P. Depping, A. Lode, A. Vaitsopoulou, R. M. Bill, A. D. Goddard, and A. J. Rothnie. 2020. 'Expression of eukaryotic membrane proteins in eukaryotic and prokaryotic hosts', *Methods*.

Klug, L., P. Tarazona, C. Gruber, K. Grillitsch, B. Gasser, M. Trotzmuller, H. Kofeler, E. Leitner, I. Feussner, D. Mattanovich, F. Altmann, and G. Daum. 2014. 'The lipidome and proteome of microsomes from the methylotrophic yeast Pichia pastoris', *Biochim Biophys Acta*, 1841: 215-26.

Knowles, T. J., R. Finka, C. Smith, Y. P. Lin, T. Dafforn, and M. Overduin. 2009. 'Membrane proteins solubilized intact in lipid containing nanoparticles bounded by styrene maleic acid copolymer', *J Am Chem Soc*, 131: 7484-5.

Kontoyiannis, D. P., and G. P. Bodey. 2002. 'Invasive aspergillosis in 2002: an update', *Eur J Clin Microbiol Infect Dis*, 21: 161-72.

Kontoyiannis, D. P., K. A. Marr, B. J. Park, B. D. Alexander, E. J. Anaissie, T. J. Walsh, J. Ito, D. R. Andes, J. W. Baddley, J. M. Brown, L. M. Brumble, A. G. Freifeld, S. Hadley, L. A. Herwaldt, C. A. Kauffman, K. Knapp, G. M. Lyon, V. A. Morrison, G. Papanicolaou, T. F. Patterson, T. M. Perl, M. G. Schuster, R. Walker, K. A. Wannemuehler, J. R. Wingard, T. M. Chiller, and P. G. Pappas. 2010. 'Prospective surveillance for invasive fungal infections in hematopoietic stem cell transplant recipients, 2001-2006: overview of the Transplant-Associated Infection Surveillance Network (TRANSNET) Database', *Clin Infect Dis*, 50: 1091-100.

Kopf, A. H., J. M. Dorr, M. C. Koorengevel, F. Antoniciello, H. Jahn, and J. A. Killian. 2020. 'Factors influencing the solubilization of membrane proteins from Escherichia coli membranes by styrene-maleic acid copolymers', *Biochim Biophys Acta Biomembr*, 1862: 183125.

Kopf, A. H., M. C. Koorengevel, C. A. van Walree, T. R. Dafforn, and J. A. Killian. 2019. 'A simple and convenient method for the hydrolysis of styrene-maleic anhydride copolymers to styrene-maleic acid copolymers', *Chem Phys Lipids*, 218: 85-90.

Kovalchuk, A., and A. J. Driessen. 2010. 'Phylogenetic analysis of fungal ABC transporters', *BMC Genomics*, 11: 177.
Kozakiewicz, Z., and D. Smith. 1994. 'Physiology of *Aspergillus*.' in J. E. Smith (ed.), *Aspergillus* (Springer, Boston, MA).
Kuzminov, A. 2011. 'Homologous Recombination-Experimental Systems, Analysis, and Significance', *EcoSal Plus*, 4.
Kwon-Chung, K. J., and J. A. Sugui. 2013. 'Aspergillus fumigatus--what makes the species a ubiquitous human fungal pathogen?', *PLoS Pathog*, 9: e1003743.
Lakhani, P., A. Patil, and S. Majumdar. 2019. 'Challenges in the Polyene- and Azole-Based Pharmacotherapy of Ocular Fungal Infections', *J Ocul Pharmacol Ther*, 35: 6-22.
Lamb, D. C., D. E. Kelly, T. C. White, and S. L. Kelly. 2000. 'The R467K amino acid substitution in Candida albicans sterol 14alpha-demethylase causes drug resistance through reduced affinity', *Antimicrob Agents Chemother*, 44: 63-7.
Lamping, E., P. V. Baret, A. R. Holmes, B. C. Monk, A. Goffeau, and R. D. Cannon. 2010. 'Fungal PDR transporters: Phylogeny, topology, motifs and function', *Fungal Genet Biol*, 47: 127-42.
Langfelder, K., B. Jahn, H. Gehringer, A. Schmidt, G. Wanner, and A. A. Brakhage. 1998. 'Identification of a polyketide synthase gene (pksP) of Aspergillus fumigatus involved in conidial pigment biosynthesis and virulence', *Med Microbiol Immunol*, 187: 79-89.
Langhans, S. A. 2018. 'Three-Dimensional in Vitro Cell Culture Models in Drug Discovery and Drug Repositioning', *Front Pharmacol*, 9: 6.
Latge, J. P. 1999. 'Aspergillus fumigatus and aspergillosis', *Clin Microbiol Rev*, 12: 310-50.
Ledoux, M. P., B. Guffroy, Y. Nivoix, C. Simand, and R. Herbrecht. 2020. 'Invasive Pulmonary Aspergillosis', *Semin Respir Crit Care Med*, 41: 80-98.
Lee, A. G. 2005. 'How lipids and proteins interact in a membrane: a molecular approach', *Mol Biosyst*, 1: 203-12.
Leonardelli, F., D. Macedo, C. Dudiuk, M. S. Cabeza, S. Gamarra, and G. Garcia-Effron. 2016. 'Aspergillus fumigatus Intrinsic Fluconazole Resistance Is Due to the Naturally Occurring T301I Substitution in Cyp51Ap', *Antimicrob Agents Chemother*, 60: 5420-6.
Lepesheva, G. I., and M. R. Waterman. 2007. 'Sterol 14alpha-demethylase cytochrome P450 (CYP51), a P450 in all biological kingdoms', *Biochim Biophys Acta*, 1770: 467-77.
Lin, A., C. Zeng, Q. Wang, W. Zhang, M. Li, M. Hanna, and W. Xiao. 2018. 'Utilization of a Strongly Inducible DDI2 Promoter to Control Gene Expression in Saccharomyces cerevisiae', *Front Microbiol*, 9: 2736.
Liu, W., G. Wu, A. L. Tsai, and R. J. Kulmacz. 2011. 'High-yield production, purification and characterization of functional human duodenal cytochrome b in an Escherichia coli system', *Protein Expr Purif*, 79: 115-21.
Lortholary, O., M. Desnos-Ollivier, K. Sitbon, A. Fontanet, S. Bretagne, F. Dromer, and Group French Mycosis Study. 2011. 'Recent exposure to caspofungin or fluconazole influences the epidemiology of candidemia: a prospective multicenter study involving 2,441 patients', *Antimicrob Agents Chemother*, 55: 532-8.
Macedo, D., F. Leonardelli, M. S. Cabeza, S. Gamarra, and G. Garcia-Effron. 2021. 'The natural occurring Y129F polymorphism in Rhizopus oryzae (R. arrhizus) Cyp51Ap accounts for its intrinsic voriconazole resistance', *Med Mycol*, 59: 1202-09.
Maharana, P. K., N. Sharma, R. Nagpal, V. Jhanji, S. Das, and R. B. Vajpayee. 2016. 'Recent advances in diagnosis and management of Mycotic Keratitis', *Indian J Ophthalmol*, 64: 346-57.
Marconnet, A., B. Michon, C. Le Bon, F. Giusti, C. Tribet, and M. Zoonens. 2020. 'Solubilization and Stabilization of Membrane Proteins by Cycloalkane-Modified Amphiphilic Polymers', *Biomacromolecules*, 21: 3459-67.
Mattanovich, D., B. Gasser, H. Hohenblum, and M. Sauer. 2004. 'Stress in recombinant protein producing yeasts', *J Biotechnol*, 113: 121-35.

Matthews, C. B., A. Kuo, K. R. Love, and J. C. Love. 2018. 'Development of a general defined medium for Pichia pastoris', *Biotechnol Bioeng*, 115: 103-13.
McCarthy, M. W., D. P. Kontoyiannis, O. A. Cornely, J. R. Perfect, and T. J. Walsh. 2017. 'Novel Agents and Drug Targets to Meet the Challenges of Resistant Fungi', *J Infect Dis*, 216: S474-S83.
Mehlin, C., E. Boni, F. S. Buckner, L. Engel, T. Feist, M. H. Gelb, L. Haji, D. Kim, C. Liu, N. Mueller, P. J. Myler, J. T. Reddy, J. N. Sampson, E. Subramanian, W. C. Van Voorhis, E. Worthey, F. Zucker, and W. G. Hol. 2006. 'Heterologous expression of proteins from Plasmodium falciparum: results from 1000 genes', *Mol Biochem Parasitol*, 148: 144-60.
Mignon, C., R. Sodoyer, and B. Werle. 2015. 'Antibiotic-free selection in biotherapeutics: now and forever', *Pathogens*, 4: 157-81.
Miller, A. E. 2017. 'Teriflunomide in multiple sclerosis: an update', *Neurodegener Dis Manag*, 7: 9-29.
Mitchell, K. F., R. Zarnowski, H. Sanchez, J. A. Edward, E. L. Reinicke, J. E. Nett, A. P. Mitchell, and D. R. Andes. 2015. 'Community participation in biofilm matrix assembly and function', *Proc Natl Acad Sci U S A*, 112: 4092-7.
Mora-Duarte, J., R. Betts, C. Rotstein, A. L. Colombo, L. Thompson-Moya, J. Smietana, R. Lupinacci, C. Sable, N. Kartsonis, J. Perfect, and Group Caspofungin Invasive Candidiasis Study. 2002. 'Comparison of caspofungin and amphotericin B for invasive candidiasis', *N Engl J Med*, 347: 2020-9.
Morris, M. I., and M. Villmann. 2006. 'Echinocandins in the management of invasive fungal infections, part 1', *Am J Health Syst Pharm*, 63: 1693-703.
Morrison, K. A., A. Akram, A. Mathews, Z. A. Khan, J. H. Patel, C. Zhou, D. J. Hardy, C. Moore-Kelly, R. Patel, V. Odiba, T. J. Knowles, M. U. Javed, N. P. Chmel, T. R. Dafforn, and A. J. Rothnie. 2016. 'Membrane protein extraction and purification using styrene-maleic acid (SMA) copolymer: effect of variations in polymer structure', *Biochem J*, 473: 4349-60.
Nascimento, A. M., G. H. Goldman, S. Park, S. A. Marras, G. Delmas, U. Oza, K. Lolans, M. N. Dudley, P. A. Mann, and D. S. Perlin. 2003. 'Multiple resistance mechanisms among Aspergillus fumigatus mutants with high-level resistance to itraconazole', *Antimicrob Agents Chemother*, 47: 1719-26.
Neoh, C. F., D. Liew, M. Slavin, D. Marriott, S. C. Chen, O. Morrissey, K. Stewart, and D. C. Kong. 2011. 'Cost-effectiveness analysis of anidulafungin versus fluconazole for the treatment of invasive candidiasis', *J Antimicrob Chemother*, 66: 1906-15.
Neoh, C. F., E. Senol, A. Kara, E. C. Dinleyici, S. J. Turner, and D. C. M. Kong. 2017. 'Cost-effectiveness analysis of anidulafungin vs fluconazole for the treatment of invasive candidiasis (IC) in Turkey', *Mycoses*, 60: 714-22.
Nes, W. D., G. G. Janssen, F. G. Crumley, M. Kalinowska, and T. Akihisa. 1993. 'The structural requirements of sterols for membrane function in Saccharomyces cerevisiae', *Arch Biochem Biophys*, 300: 724-33.
Neubert, P., A. Halim, M. Zauser, A. Essig, H. J. Joshi, E. Zatorska, I. S. Larsen, M. Loibl, J. Castells-Ballester, M. Aebi, H. Clausen, and S. Strahl. 2016. 'Mapping the O-Mannose Glycoproteome in Saccharomyces cerevisiae', *Mol Cell Proteomics*, 15: 1323-37.
Nevone, A., G. Merlini, and M. Nuvolone. 2020. 'Treating Protein Misfolding Diseases: Therapeutic Successes Against Systemic Amyloidoses', *Front Pharmacol*, 11: 1024.
Nierman, W. C., G. May, H. S. Kim, M. J. Anderson, D. Chen, and D. W. Denning. 2005. 'What the Aspergillus genomes have told us', *Med Mycol*, 43 Suppl 1: S3-5.
Noble, S. M., and A. D. Johnson. 2005. 'Strains and strategies for large-scale gene deletion studies of the diploid human fungal pathogen Candida albicans', *Eukaryot Cell*, 4: 298-309.
Noor, A., and C. V. Preuss. 2020. 'Antifungal Membrane Function Inhibitors (Amphotericin B).' in, *StatPearls* (Treasure Island (FL)).
Oliver, J. D., G. E. M. Sibley, N. Beckmann, K. S. Dobb, M. J. Slater, L. McEntee, S. du Pre, J. Livermore, M. J. Bromley, N. P. Wiederhold, W. W. Hope, A. J. Kennedy, D. Law, and M. Birch. 2016.

'F901318 represents a novel class of antifungal drug that inhibits dihydroorotate dehydrogenase', *Proc Natl Acad Sci U S A*, 113: 12809-14.
Oren, I., and N. Goldstein. 2002. 'Invasive pulmonary aspergillosis', *Curr Opin Pulm Med*, 8: 195-200.
Oren, I., and M. Paul. 2014. 'Up to date epidemiology, diagnosis and management of invasive fungal infections', *Clin Microbiol Infect*, 20 Suppl 6: 1-4.
Ostrosky-Zeichner, L., A. Casadevall, J. N. Galgiani, F. C. Odds, and J. H. Rex. 2010. 'An insight into the antifungal pipeline: selected new molecules and beyond', *Nat Rev Drug Discov*, 9: 719-27.
Ostrowsky, B., J. Greenko, E. Adams, M. Quinn, B. O'Brien, V. Chaturvedi, E. Berkow, S. Vallabhaneni, K. Forsberg, S. Chaturvedi, E. Lutterloh, D. Blog, and C. auris Investigation Work Group. 2020. 'Candida auris Isolates Resistant to Three Classes of Antifungal Medications - New York, 2019', *MMWR Morb Mortal Wkly Rep*, 69: 6-9.
Overington, J. P., B. Al-Lazikani, and A. L. Hopkins. 2006. 'How many drug targets are there?', *Nat Rev Drug Discov*, 5: 993-6.
Pagano, L., M. Caira, A. Candoni, M. Offidani, L. Fianchi, B. Martino, D. Pastore, M. Picardi, A. Bonini, A. Chierichini, R. Fanci, C. Caramatti, R. Invernizzi, D. Mattei, M. E. Mitra, L. Melillo, F. Aversa, M. T. Van Lint, P. Falcucci, C. G. Valentini, C. Girmenia, and A. Nosari. 2006. 'The epidemiology of fungal infections in patients with hematologic malignancies: the SEIFEM-2004 study', *Haematologica*, 91: 1068-75.
Pampaloni, F., E. G. Reynaud, and E. H. Stelzer. 2007. 'The third dimension bridges the gap between cell culture and live tissue', *Nat Rev Mol Cell Biol*, 8: 839-45.
Patil, A., and S. Majumdar. 2017. 'Echinocandins in antifungal pharmacotherapy', *J Pharm Pharmacol*, 69: 1635-60.
Postis, V., S. Rawson, J. K. Mitchell, S. C. Lee, R. A. Parslow, T. R. Dafforn, S. A. Baldwin, and S. P. Muench. 2015. 'The use of SMALPs as a novel membrane protein scaffold for structure study by negative stain electron microscopy', *Biochim Biophys Acta*, 1848: 496-501.
Qayyum, M. Z., D. Dey, and R. Sen. 2016. 'Transcription Elongation Factor NusA Is a General Antagonist of Rho-dependent Termination in Escherichia coli', *J Biol Chem*, 291: 8090-108.
Quehenberger, O., A. M. Armando, and E. A. Dennis. 2011. 'High sensitivity quantitative lipidomics analysis of fatty acids in biological samples by gas chromatography-mass spectrometry', *Biochim Biophys Acta*, 1811: 648-56.
Rask-Andersen, M., M. S. Almen, and H. B. Schioth. 2011. 'Trends in the exploitation of novel drug targets', *Nat Rev Drug Discov*, 10: 579-90.
Rask-Andersen, M., S. Masuram, and H. B. Schioth. 2014. 'The druggable genome: Evaluation of drug targets in clinical trials suggests major shifts in molecular class and indication', *Annu Rev Pharmacol Toxicol*, 54: 9-26.
Ravi, M., V. Paramesh, S. R. Kaviya, E. Anuradha, and F. D. Solomon. 2015. '3D cell culture systems: advantages and applications', *J Cell Physiol*, 230: 16-26.
Rementeria, A., N. Lopez-Molina, A. Ludwig, A. B. Vivanco, J. Bikandi, J. Ponton, and J. Garaizar. 2005. 'Genes and molecules involved in Aspergillus fumigatus virulence', *Rev Iberoam Micol*, 22: 1-23.
Retallack, D. M., E. L. Heinecke, R. Gibbons, G. S. Deepe, Jr., and J. P. Woods. 1999. 'The URA5 gene is necessary for histoplasma capsulatum growth during infection of mouse and human cells', *Infect Immun*, 67: 624-9.
Rhodes, J., and M. C. Fisher. 2019. 'Global epidemiology of emerging Candida auris', *Curr Opin Microbiol*, 52: 84-89.
Rivera, A. L., D. Magana-Ortiz, M. Gomez-Lim, F. Fernandez, and A. M. Loske. 2014. 'Physical methods for genetic transformation of fungi and yeast', *Phys Life Rev*, 11: 184-203.
Rocha, E. M., G. Garcia-Effron, S. Park, and D. S. Perlin. 2007. 'A Ser678Pro substitution in Fks1p confers resistance to echinocandin drugs in Aspergillus fumigatus', *Antimicrob Agents Chemother*, 51: 4174-6.

Rosenfeld, S. A. 1999. 'Use of Pichia pastoris for expression of recombinant proteins', *Methods Enzymol*, 306: 154-69.
Rothnie, A. J. 2016. 'Detergent-Free Membrane Protein Purification', *Methods Mol Biol*, 1432: 261-7.
Sakai, Y., A. P. Murdanoto, L. Sembiring, Y. Tani, and N. Kato. 1995. 'A novel formaldehyde oxidation pathway in methylotrophic yeasts: methylformate as a possible intermediate', *FEMS Microbiol Lett*, 127: 229-34.
Sander, C. L., A. E. Sears, A. F. M. Pinto, E. H. Choi, S. Kahremany, F. Gao, D. Salom, H. Jin, E. Pardon, S. Suh, Z. Dong, J. Steyaert, A. Saghatelian, D. Skowronska-Krawczyk, P. D. Kiser, and K. Palczewski. 2021. 'Nano-scale resolution of native retinal rod disk membranes reveals differences in lipid composition', *J Cell Biol*, 220.
Sanglard, D. 2016. 'Emerging Threats in Antifungal-Resistant Fungal Pathogens', *Front Med (Lausanne)*, 3: 11.
Sanglard, D., and A. T. Coste. 2016. 'Activity of Isavuconazole and Other Azoles against Candida Clinical Isolates and Yeast Model Systems with Known Azole Resistance Mechanisms', *Antimicrob Agents Chemother*, 60: 229-38.
Santos, R., O. Ursu, A. Gaulton, A. P. Bento, R. S. Donadi, C. G. Bologa, A. Karlsson, B. Al-Lazikani, A. Hersey, T. I. Oprea, and J. P. Overington. 2017. 'A comprehensive map of molecular drug targets', *Nat Rev Drug Discov*, 16: 19-34.
Sasagawa, T., M. Matsui, Y. Kobayashi, M. Otagiri, S. Moriya, Y. Sakamoto, Y. Ito, C. C. Lee, K. Kitamoto, and M. Arioka. 2011. 'High-throughput recombinant gene expression systems in Pichia pastoris using newly developed plasmid vectors', *Plasmid*, 65: 65-9.
Scheidelaar, S., M. C. Koorengevel, J. D. Pardo, J. D. Meeldijk, E. Breukink, and J. A. Killian. 2015. 'Molecular model for the solubilization of membranes into nanodisks by styrene maleic Acid copolymers', *Biophys J*, 108: 279-90.
Scheidelaar, S., M. C. Koorengevel, C. A. van Walree, J. J. Dominguez, J. M. Dorr, and J. A. Killian. 2016. 'Effect of Polymer Composition and pH on Membrane Solubilization by Styrene-Maleic Acid Copolymers', *Biophys J*, 111: 1974-86.
Schleicher, L., G. Fritz, J. Seifert, and J. Steuber. 2020. 'Anoxic cell rupture of Prevotella bryantii by high-pressure homogenization protects the Na(+)-translocating NADH:quinone oxidoreductase from oxidative damage', *Arch Microbiol*, 202: 1263-66.
Schroeder, R., E. London, and D. Brown. 1994. 'Interactions between saturated acyl chains confer detergent resistance on lipids and glycosylphosphatidylinositol (GPI)-anchored proteins: GPI-anchored proteins in liposomes and cells show similar behavior', *Proc Natl Acad Sci U S A*, 91: 12130-4.
Schwarzhans, J. P., D. Wibberg, A. Winkler, T. Luttermann, J. Kalinowski, and K. Friehs. 2016. 'Non-canonical integration events in Pichia pastoris encountered during standard transformation analysed with genome sequencing', *Sci Rep*, 6: 38952.
Seyedmousavi, S., W. J. Melchers, J. W. Mouton, and P. E. Verweij. 2013. 'Pharmacodynamics and dose-response relationships of liposomal amphotericin B against different azole-resistant Aspergillus fumigatus isolates in a murine model of disseminated aspergillosis', *Antimicrob Agents Chemother*, 57: 1866-71.
Shah, D. N., R. Yau, T. M. Lasco, J. Weston, M. Salazar, H. R. Palmer, and K. W. Garey. 2012. 'Impact of prior inappropriate fluconazole dosing on isolation of fluconazole-nonsusceptible Candida species in hospitalized patients with candidemia', *Antimicrob Agents Chemother*, 56: 3239-43.
Shen, H. H., T. Lithgow, and L. Martin. 2013. 'Reconstitution of membrane proteins into model membranes: seeking better ways to retain protein activities', *Int J Mol Sci*, 14: 1589-607.
Simons, K., and E. Ikonen. 1997. 'Functional rafts in cell membranes', *Nature*, 387: 569-72.
Sinha, J., B. A. Plantz, M. Inan, and M. M. Meagher. 2005. 'Causes of proteolytic degradation of secreted recombinant proteins produced in methylotrophic yeast Pichia pastoris: case study with recombinant ovine interferon-tau', *Biotechnol Bioeng*, 89: 102-12.

Sivashanmugam, A., V. Murray, C. Cui, Y. Zhang, J. Wang, and Q. Li. 2009. 'Practical protocols for production of very high yields of recombinant proteins using Escherichia coli', *Protein Sci*, 18: 936-48.

Skaar, K., H. J. Korza, M. Tarry, P. Sekyrova, and M. Hogbom. 2015. 'Expression and Subcellular Distribution of GFP-Tagged Human Tetraspanin Proteins in Saccharomyces cerevisiae', *PLoS One*, 10: e0134041.

Slaven, J. W., M. J. Anderson, D. Sanglard, G. K. Dixon, J. Bille, I. S. Roberts, and D. W. Denning. 2002. 'Increased expression of a novel Aspergillus fumigatus ABC transporter gene, atrF, in the presence of itraconazole in an itraconazole resistant clinical isolate', *Fungal Genet Biol*, 36: 199-206.

Smirnova, I. A., D. Sjostrand, F. Li, M. Bjorck, J. Schafer, H. Ostbye, M. Hogbom, C. von Ballmoos, G. C. Lander, P. Adelroth, and P. Brzezinski. 2016. 'Isolation of yeast complex IV in native lipid nanodiscs', *Biochim Biophys Acta*, 1858: 2984-92.

Snelders, E., W. J. Melchers, and P. E. Verweij. 2011. 'Azole resistance in Aspergillus fumigatus: a new challenge in the management of invasive aspergillosis?', *Future Microbiol*, 6: 335-47.

Snelders, E., H. A. van der Lee, J. Kuijpers, A. J. Rijs, J. Varga, R. A. Samson, E. Mellado, A. R. Donders, W. J. Melchers, and P. E. Verweij. 2008. 'Emergence of azole resistance in Aspergillus fumigatus and spread of a single resistance mechanism', *PLoS Med*, 5: e219.

Spitzer, M., N. Robbins, and G. D. Wright. 2017. 'Combinatorial strategies for combating invasive fungal infections', *Virulence*, 8: 169-85.

Stroud, Z., S. C. L. Hall, and T. R. Dafforn. 2018. 'Purification of membrane proteins free from conventional detergents: SMA, new polymers, new opportunities and new insights', *Methods*, 147: 106-17.

Sugui, J. A., J. Pardo, Y. C. Chang, K. A. Zarember, G. Nardone, E. M. Galvez, A. Mullbacher, J. I. Gallin, M. M. Simon, and K. J. Kwon-Chung. 2007. 'Gliotoxin is a virulence factor of Aspergillus fumigatus: gliP deletion attenuates virulence in mice immunosuppressed with hydrocortisone', *Eukaryot Cell*, 6: 1562-9.

Sun, C., S. Benlekbir, P. Venkatakrishnan, Y. Wang, S. Hong, J. Hosler, E. Tajkhorshid, J. L. Rubinstein, and R. B. Gennis. 2018. 'Structure of the alternative complex III in a supercomplex with cytochrome oxidase', *Nature*, 557: 123-26.

Swainsbury, D. J. K., S. Scheidelaar, N. Foster, R. van Grondelle, J. A. Killian, and M. R. Jones. 2017. 'The effectiveness of styrene-maleic acid (SMA) copolymers for solubilisation of integral membrane proteins from SMA-accessible and SMA-resistant membranes', *Biochim Biophys Acta Biomembr*, 1859: 2133-43.

Szary, J., E. Missol, and S. Szala. 1998. 'Characteristics of cytosine deaminase-5-fluorocytosine system. Enhancement of radiation cytotoxicity and bystander effect', *Adv Exp Med Biol*, 451: 121-3.

Teo, A. C. K., S. C. Lee, N. L. Pollock, Z. Stroud, S. Hall, A. Thakker, A. R. Pitt, T. R. Dafforn, C. M. Spickett, and D. I. Roper. 2019. 'Analysis of SMALP co-extracted phospholipids shows distinct membrane environments for three classes of bacterial membrane protein', *Sci Rep*, 9: 1813.

Thoring, L., S. K. Dondapati, M. Stech, D. A. Wustenhagen, and S. Kubick. 2017. 'High-yield production of "difficult-to-express" proteins in a continuous exchange cell-free system based on CHO cell lysates', *Sci Rep*, 7: 11710.

Tokuda, Y., M. Tsuji, M. Yamazaki, S. Kimura, S. Abe, and H. Yamaguchi. 1993. 'Augmentation of murine tumor necrosis factor production by amphotericin B in vitro and in vivo', *Antimicrob Agents Chemother*, 37: 2228-30.

Trinquier, G., and Y. H. Sanejouand. 1998. 'Which effective property of amino acids is best preserved by the genetic code?', *Protein Eng*, 11: 153-69.

Tripp, J. D., J. L. Lilley, W. N. Wood, and L. K. Lewis. 2013. 'Enhancement of plasmid DNA transformation efficiencies in early stationary-phase yeast cell cultures', *Yeast*, 30: 191-200.

Uhlen, M., L. Fagerberg, B. M. Hallstrom, C. Lindskog, P. Oksvold, A. Mardinoglu, A. Sivertsson, C. Kampf, E. Sjostedt, A. Asplund, I. Olsson, K. Edlund, E. Lundberg, S. Navani, C. A. Szigyarto, J. Odeberg, D. Djureinovic, J. O. Takanen, S. Hober, T. Alm, P. H. Edqvist, H. Berling, H. Tegel, J. Mulder, J. Rockberg, P. Nilsson, J. M. Schwenk, M. Hamsten, K. von Feilitzen, M. Forsberg, L. Persson, F. Johansson, M. Zwahlen, G. von Heijne, J. Nielsen, and F. Ponten. 2015. 'Proteomics. Tissue-based map of the human proteome', *Science*, 347: 1260419.

van 't Klooster, J. S., T. Y. Cheng, H. R. Sikkema, A. Jeucken, B. Moody, and B. Poolman. 2020. 'Periprotein lipidomes of Saccharomyces cerevisiae provide a flexible environment for conformational changes of membrane proteins', *Elife*, 9.

van Meer, G., D. R. Voelker, and G. W. Feigenson. 2008. 'Membrane lipids: where they are and how they behave', *Nat Rev Mol Cell Biol*, 9: 112-24.

Vermeulen, E., K. Lagrou, and P. E. Verweij. 2013. 'Azole resistance in Aspergillus fumigatus: a growing public health concern', *Curr Opin Infect Dis*, 26: 493-500.

Verrastro, I., K. Tveen-Jensen, C. M. Spickett, and A. R. Pitt. 2018. 'The effect of HOCl-induced modifications on phosphatase and tensin homologue (PTEN) structure and function', *Free Radic Res*, 52: 232-47.

Verweij, Paul E, John A Lucas, Maiken C Arendrup, Paul Bowyer, Arjen JF Brinkmann, David W Denning, Paul S Dyer, Matthew C Fisher, Petra L Geenen, and Ulrich Gisi. 2020. 'The one health problem of azole resistance in Aspergillus fumigatus: Current insights and future research agenda', *Fungal Biology Reviews*, 34: 202-14.

Voskoboynikova, N., M. Karlova, R. Kurre, A. Y. Mulkidjanian, K. V. Shaitan, O. S. Sokolova, H. J. Steinhoff, and J. J. Heinisch. 2021. 'A Three-Dimensional Model of the Yeast Transmembrane Sensor Wsc1 Obtained by SMA-Based Detergent-Free Purification and Transmission Electron Microscopy', *J Fungi (Basel)*, 7.

Wahl, B., D. Reichmann, D. Niks, N. Krompholz, A. Havemeyer, B. Clement, T. Messerschmidt, M. Rothkegel, H. Biester, R. Hille, R. R. Mendel, and F. Bittner. 2010. 'Biochemical and spectroscopic characterization of the human mitochondrial amidoxime reducing components hmARC-1 and hmARC-2 suggests the existence of a new molybdenum enzyme family in eukaryotes', *J Biol Chem*, 285: 37847-59.

Walker, L. A., N. A. Gow, and C. A. Munro. 2010. 'Fungal echinocandin resistance', *Fungal Genet Biol*, 47: 117-26.

Waller, D. G., Sampson, A. P. 2018. 'Chemotherapy of infections.' in, *Medical Pharmacology and Therapeutics*.

Wang, H., M. G. Klein, H. Zou, W. Lane, G. Snell, I. Levin, K. Li, and B. C. Sang. 2015. 'Crystal structure of human stearoyl-coenzyme A desaturase in complex with substrate', *Nat Struct Mol Biol*, 22: 581-5.

Wang, J. F., Y. Xue, X. B. Zhu, and H. Fan. 2015. 'Efficacy and safety of echinocandins versus triazoles for the prophylaxis and treatment of fungal infections: a meta-analysis of RCTs', *Eur J Clin Microbiol Infect Dis*, 34: 651-9.

Warrilow, A. G., N. Melo, C. M. Martel, J. E. Parker, W. D. Nes, S. L. Kelly, and D. E. Kelly. 2010. 'Expression, purification, and characterization of Aspergillus fumigatus sterol 14-alpha demethylase (CYP51) isoenzymes A and B', *Antimicrob Agents Chemother*, 54: 4225-34.

Wasylnka, J. A., M. I. Simmer, and M. M. Moore. 2001. 'Differences in sialic acid density in pathogenic and non-pathogenic Aspergillus species', *Microbiology*, 147: 869-77.

Werten, M. W. T., G. Eggink, M. A. Cohen Stuart, and F. A. de Wolf. 2019. 'Production of protein-based polymers in Pichia pastoris', *Biotechnol Adv*, 37: 642-66.

Whaley, S. G., Q. Zhang, K. E. Caudle, and P. D. Rogers. 2018. 'Relative Contribution of the ABC Transporters Cdr1, Pdh1, and Snq2 to Azole Resistance in Candida glabrata', *Antimicrob Agents Chemother*, 62.

White, M. A., K. M. Clark, E. J. Grayhack, and M. E. Dumont. 2007. 'Characteristics affecting expression and solubilization of yeast membrane proteins', *J Mol Biol*, 365: 621-36.

WHO. 2020. Accessed May 2020. https://www.who.int/features/qa/18/en/.
Wiederhold, N. P. 2020. 'Review of the Novel Investigational Antifungal Olorofim', *J Fungi (Basel)*, 6.
Wiederhold, N. P., and R. E. Lewis. 2003. 'The echinocandin antifungals: an overview of the pharmacology, spectrum and clinical efficacy', *Expert Opin Investig Drugs*, 12: 1313-33.
Wildt, S., and T. U. Gerngross. 2005. 'The humanization of N-glycosylation pathways in yeast', *Nat Rev Microbiol*, 3: 119-28.
Wilson, E., L. Thorson, and D. P. Speert. 1991. 'Enhancement of macrophage superoxide anion production by amphotericin B', *Antimicrob Agents Chemother*, 35: 796-800.
Wilson, R. A., A. M. Calvo, P. K. Chang, and N. P. Keller. 2004. 'Characterization of the Aspergillus parasiticus delta12-desaturase gene: a role for lipid metabolism in the Aspergillus-seed interaction', *Microbiology*, 150: 2881-88.
Woese, C. R. 2000. 'Interpreting the universal phylogenetic tree', *Proc Natl Acad Sci U S A*, 97: 8392-6.
Wolfram, L., and P. Bauerfeind. 2002. 'Conserved low-affinity nickel-binding amino acids are essential for the function of the nickel permease NixA of Helicobacter pylori', *J Bacteriol*, 184: 1438-43.
Wu, S., and G. J. Letchworth. 2004. 'High efficiency transformation by electroporation of Pichia pastoris pretreated with lithium acetate and dithiothreitol', *Biotechniques*, 36: 152-4.
Xu, P., S. Huang, H. Zhang, C. Mao, X. E. Zhou, X. Cheng, I. A. Simon, D. D. Shen, H. Y. Yen, C. V. Robinson, K. Harpsoe, B. Svensson, J. Guo, H. Jiang, D. E. Gloriam, K. Melcher, Y. Jiang, Y. Zhang, and H. E. Xu. 2021. 'Structural insights into the lipid and ligand regulation of serotonin receptors', *Nature*, 592: 469-73.
Yang, J., L. Nie, B. Chen, Y. Liu, Y. Kong, H. Wang, and L. Diao. 2014. 'Hygromycin-resistance vectors for gene expression in Pichia pastoris', *Yeast*, 31: 115-25.
Yang, N. J., and M. J. Hinner. 2015. 'Getting across the cell membrane: an overview for small molecules, peptides, and proteins', *Methods Mol Biol*, 1266: 29-53.
Yang, Z., C. Wang, Q. Zhou, J. An, E. Hildebrandt, L. A. Aleksandrov, J. C. Kappes, L. J. DeLucas, J. R. Riordan, I. L. Urbatsch, J. F. Hunt, and C. G. Brouillette. 2014. 'Membrane protein stability can be compromised by detergent interactions with the extramembranous soluble domains', *Protein Sci*, 23: 769-89.
Yu, A. Q., J. C. Zhu, B. Zhang, L. J. Xing, and M. C. Li. 2012. 'Knockout of fatty acid desaturase genes in Pichia pastoris GS115 and its effect on the fatty acid biosynthesis and physiological consequences', *Arch Microbiol*, 194: 1023-32.
Zhang, H., Q. Li, L. Wang, and Y. Chen. 2018. 'Investigation of structure and function of mitochondrial alcohol dehydrogenase isozyme III from Komagataella phaffii GS115', *Biochim Biophys Acta Gen Subj*, 1862: 1199-208.
Zhuang, J., R. Gutknecht, K. Flukiger, L. Hasler, B. Erni, and A. Engel. 1999. 'Purification and electron microscopic characterization of the membrane subunit (IICB(Glc)) of the Escherichia coli glucose transporter', *Arch Biochem Biophys*, 372: 89-96.
Zonios, D. I., and J. E. Bennett. 2008. 'Update on azole antifungals', *Semin Respir Crit Care Med*, 29: 198-210.